NASA Contractor Report 3558
Part 1

LSST (Hoop/Column) Maypole Antenna Development Program

Marvin R. Sullivan

CONTRACT NAS1-15763
JUNE 1982

NASA

LSST (Hoop/Column) Maypole Antenna Development Program

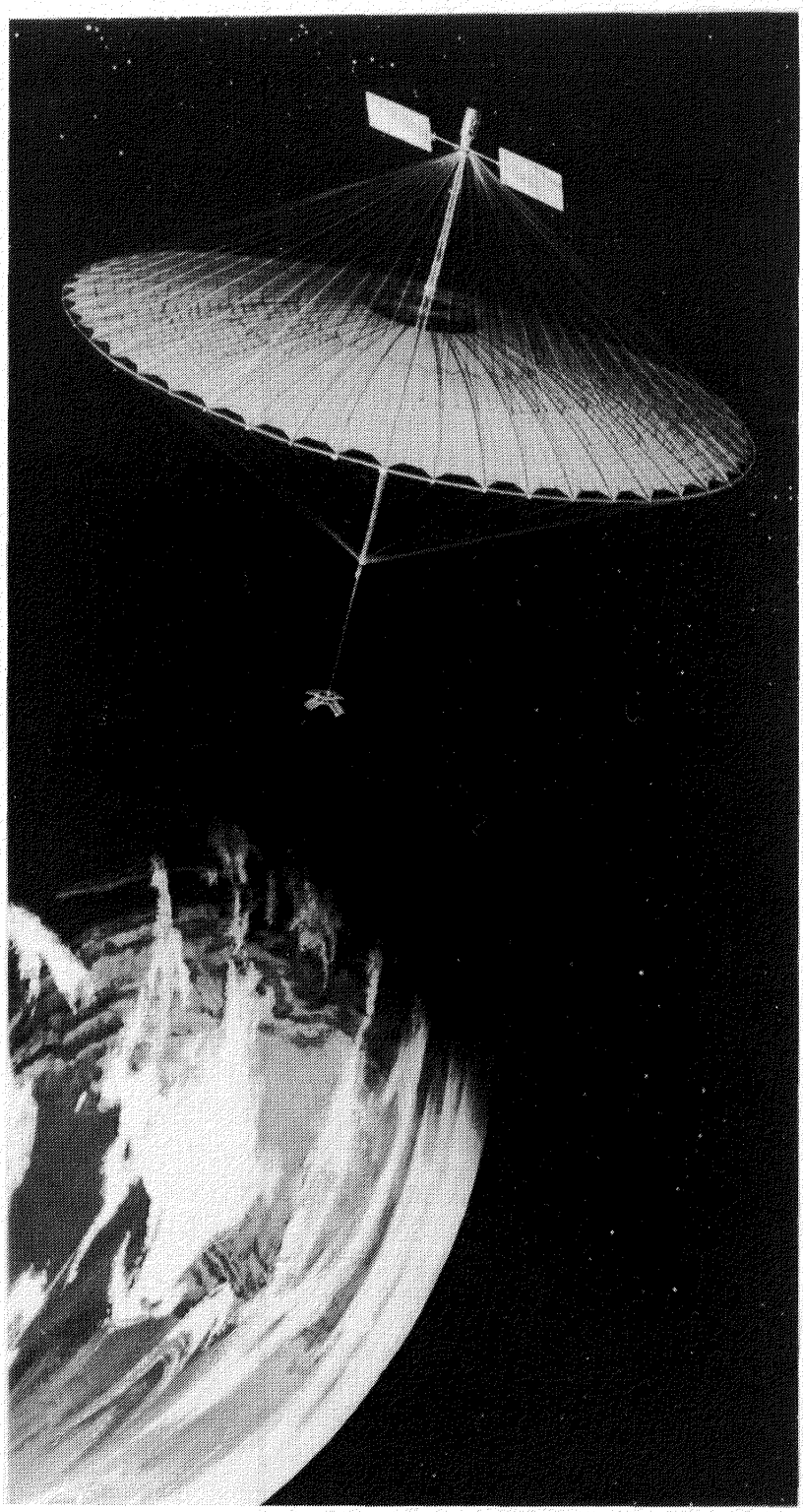

NASA Contractor Report 3558
Part 1

LSST (Hoop/Column) Maypole Antenna Development Program

Marvin R. Sullivan
Harris Corporation
Melbourne, Florida

Prepared for
Langley Research Center
under Contract NAS1-15763

National Aeronautics
and Space Administration

**Scientific and Technical
Information Office**

1982

Use of trade names or names of manufacturers in this report does not constitute an official endorsement of such products or manufacturers, either expressed or implied, by the National Aeronautics and Space Administration.

CONTENTS

Part 1

*Chapters 6 to 12 are published under separate cover.

1.0 INTRODUCTION

This report documents the Phase I activities and results under the "Development of the Maypole (Hoop/Column) Deployable Reflector Concept for Large Space Systems Applications" study program, for NASA Langley Research Center, Hampton, Virginia. The program is a part of the Large Space Systems Technology (LSST) Program which has as a primary objective the development of technology in many interrelated technical disciplines to support the development of cost-effective large area space systems. Since many of the space systems proposed for the future utilize large reflector antennas, the development of large, self-deployable reflectors has been identified as a major technology activity in the LSST program.

One of the leading structural concepts for such large reflector applications is the Maypole (Hoop/Column) concept. This concept is a cable-stiffened Hoop/Column structure that supports and contours a RF reflective mesh surface (see Figure 1.0-1). Under previous contracts, as part of the Advanced Applications Flight Experiments Program, the Maypole (Hoop/Column) design was originated. The objective of this program is to perform more detailed design and analyses to develop the technology needed to evaluate, design, fabricate, package, transport, and deploy the Maypole Hoop/Column Reflector.

The program consists of six tasks briefly described below:

Task 1. Preliminary Design and Performance Projections for the Maypole (Hoop/Column) Reflector Concept for Large Space Systems Applications - Develop Hoop/Column system performance requirements and specifications, conduct systems level analyses, trade-offs, and integrate subsystems and component designs. Also, identify, design, and analyze specific subsystems and components suitable for deploying, positioning, and controlling the antenna so as to meet established system level performance objectives. Conduct technical analyses using existing and extended analytical/computerized modeling techniques to predict the performance capabilities for the Maypole (Hoop/Column)

LSST POINT DESIGN – DEPLOYED

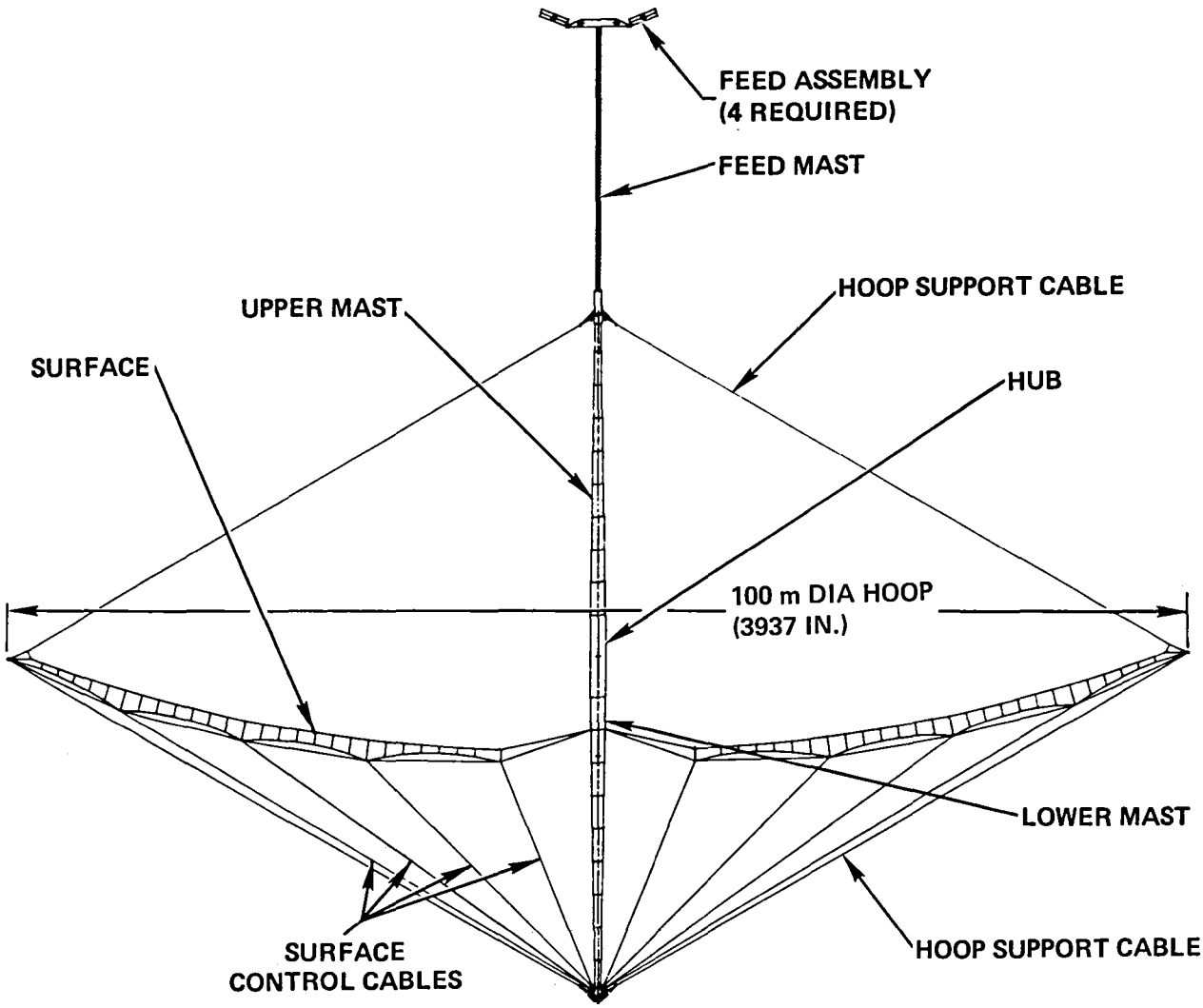

Figure 1.0-1. LSST Point Design - Deployed

concept for 30 to 100-meters in diameter. Analysis areas will include thermal, structural/deformation, materials requirements/specifications, dynamics, performance modeling, error budgeting, and the development of a software bank for predictive analysis.

Task 2. Materials Development - Identify unique materials necessary for the Hoop/Column Concept development based on applicable antenna requirements and specifications. Specific emphasis is to be placed on developing cable technology by defining the structural, thermal, and environmental requirements for the Hoop/Column cables, performing a data search on available cable materials and constructions, fabrication of samples of selected material/configuration combinations, obtaining cable structural and thermal properties by conducting appropriate tests, and through evaluation of all cable candidates, recommending a cable material/configuration to be used in the Hoop/Column Concept development.

Task 3. Advanced Concepts - Perform appropriate analyses and testing in technological areas that may not directly relate to the development of the Hoop/Column Concept, but study results may be used in the application of the Hoop/Column to a specific mission in the future. Examples of advanced concept studies are the investigation of aperture blockage effects of cables and feed support structure on RF performance in a microwave radiometer or communications application and the determination of the necessary reflector surface control techniques and surface quality for a microwave radiometer mission.

Task 4. Economic Assessment - Develop and validate a system economic model suitable for quantitatively evaluating program cost relationship and performing cost projections.

Task 5. Demonstration Models and Full Scale Elements - Provide Hoop/Column display models which satisfy focus mission configuration requirements, identify critical Hoop/Column components and fabricate full or partial scale verification

models, build an active surface control breadboard model capable of incorporating a surface accuracy measurement system, and provide a RF scaled model and necessary tests to investigate the performance of the Hoop/Column Concept when used in an offset feed/quadaperture antenna configuration for a possible communications application.

Task 6. 15-Meter Engineering Model - Design and build a 15-meter diameter model of the Hoop/Column antenna that will verify the 100-meter point design. More specifically, it will verify deployment kinematics, deployment reliability, failure modes investigation, surface interaction, manufacturing techniques, and scaling theory.

The above program tasks are accomplished in two phases. Phase I is completed and the activities are reported in this document. Phase II is initiated in FY 81 and completed in FY 84. The activities that are accomplished under each phase are summarized in Figure 1.0-2.

This report is organized in an order independent of the sequence of the program tasks described above. The report organization and associated task references are:

The requirement for the use of the International System of Units (SI) as the primary unit of measure has been waived for this report.

TASK	PHASE I (COMPLETED)	PHASE II (PLANNED)
1. ANTENNA DESIGN AND PERFORMANCE	• COMPLETED PRELIMINARY DESIGN AND ANALYSES OF 100 m POINT DESIGN.	• UPDATE AS REQUIRED BY VERIFICATION MODEL TESTING. • ANALYZE THE STRUCTURAL EFFECTS OF REPLACING THE FRONT GRAPHITE HOOP CONTROL CABLES WITH DIELECTRIC (QUARTZ) CABLES.
2. MATERIAL DEVELOPMENT	• SELECTED CABLE MATERIAL AND CONSTRUCTION.	• DEVELOP DIELECTRIC FRONT HOOP CONTROL CABLES. • DEVELOP STATISTICAL BASIS ALLOWABLES FOR CABLE PROPERTIES.
3. ADVANCED CONCEPTS	• COMPLETED.	• NO ACTIVITY PLANNED.
4. ECONOMIC ASSESSMENT	• COMPLETED.	• UPDATE MODELS AND RESULTS TO REFLECT COST DATA FROM VERIFICATION MODELS.
5. DEMONSTRATION MODELS	• BUILT DESK TOP MODEL OF QUADAPERATURE POINT DESIGN. • BUILT FULL SCALE HOOP JOINT ELEMENT MODEL. • BUILT 1/6 SCALE DEPLOYABLE MAST MODEL. • DESIGNED 50 METER SURFACE BREADBOARD MODEL. • DEVELOPED CONCEPT FOR RF VERIFICATION MODEL.	• BUILD AND TEST 50 METER SURFACE BREADBOARD MODEL. • BUILD AND TEST RF VERIFICATION MODEL.
6. 15 m ENGINEERING MODEL	• DEVELOPED CONCEPTUAL DESIGN.	• DESIGN, BUILD, AND TEST 15 METER DIAMETER ENGINEERING MODEL.

Figure 1.0-2. Phase I and II Activities

2.0 EXECUTIVE SUMMARY

This section briefly summarizes the activities and results under Phase I of the "Development of the Maypole (Hoop/Column) Deployable Reflector Concept for Large Space Systems Applications." The general areas covered are:

TASK DESCRIPTIONS AND PROGRAM OBJECTIVES

The Hoop/Column Antenna development program is divided into 6 Tasks. All support the main objective of the program which is the technology development necessary to evaluate, design, manufacture, package, transport and deploy the Hoop/Column reflector by means of a ground based test program.

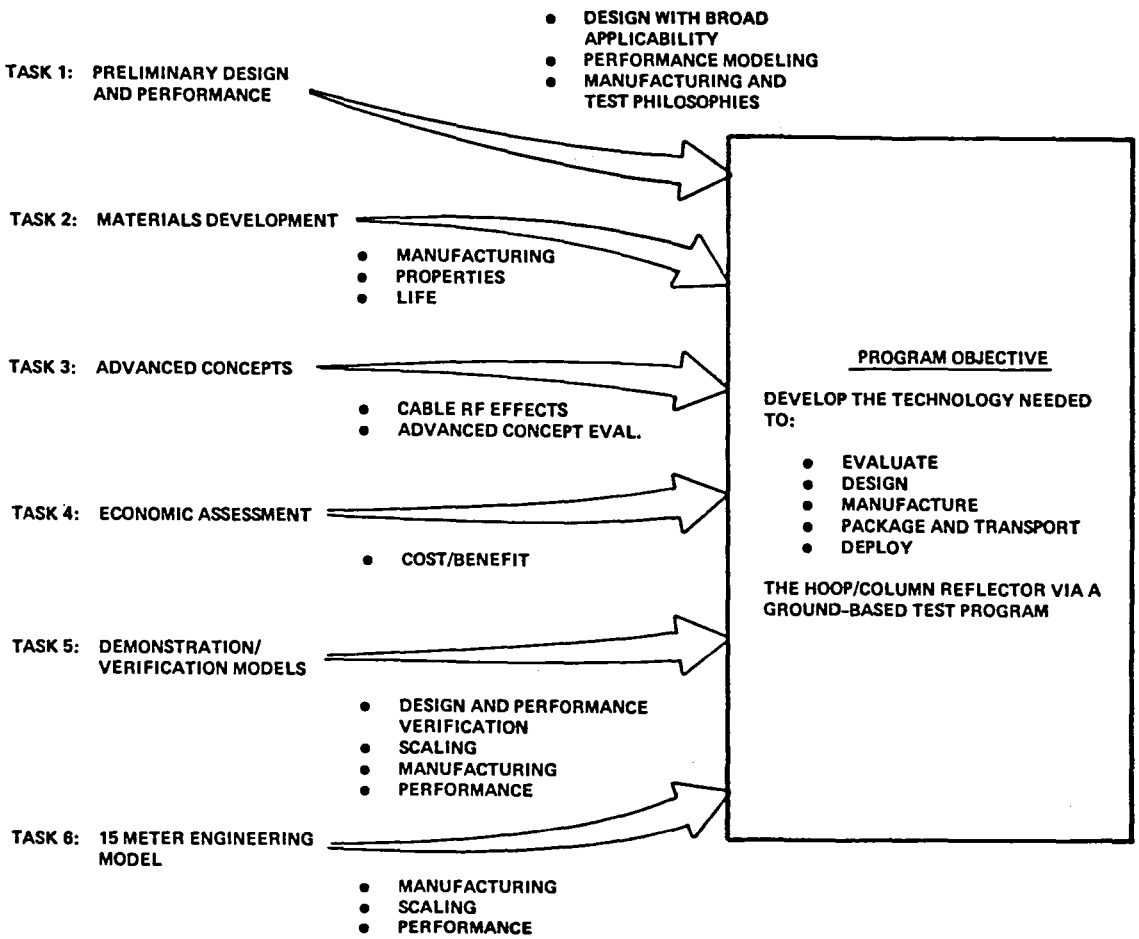

POINT DESIGN SELECTION

The program was initiated with a review of the NASA supplied mission scenarios for the communications, radiometry and radio astronomy missions. The study of these mission scenarios led to specific Hoop/Column antenna configurations for each mission. The mission configurations were then evaluated to identify specific technology items requiring further development. The compilation of these technology drivers resulted in a specification of a point design. All design and performance estimates for the program were made for the point design.

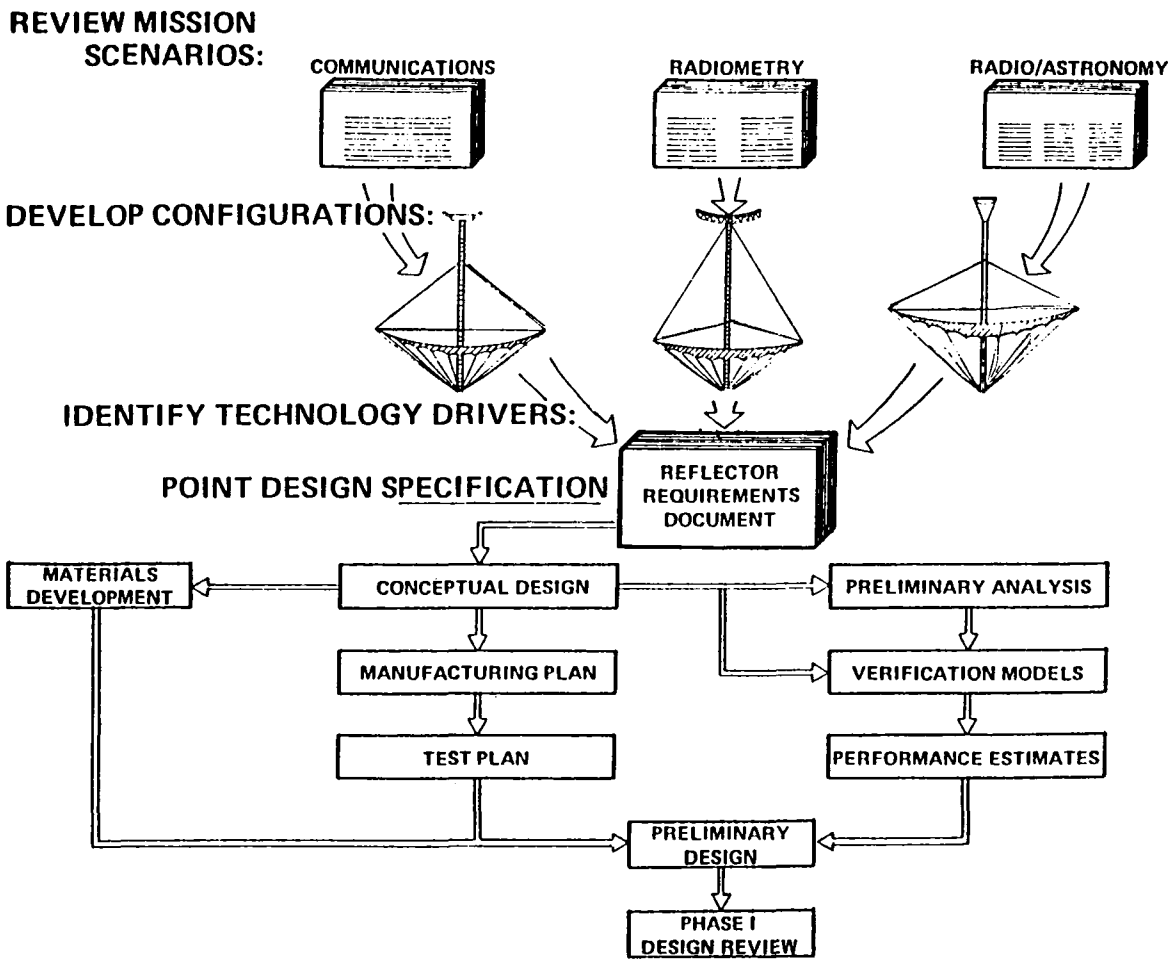

ANTENNA REQUIREMENTS SUMMARY

The following requirements goals were selected for the Point Design:

PARAMETER	REQUIREMENTS
• CONFIGURATION	• 100 METER DIAMETER QUAD-APERTURE
• f/D	• 1.53
• STOWED ENVELOPE	• MAXIMUM ALLOWABLE ENVELOPE IS – 4.56 METERS (15 FEET) DIAMETER – 12 METERS (30.4 FEET) LENGTH
• OPERATING FREQUENCY	• 2.0 GHz
• CONTOUR ACCURACY	• λ /20 MAXIMUM (7.5mm RMS)
• GAIN	• 55.4 dB
• NO. BEAMS	• 219 (55 BEAMS/APERTURE)
• HPBW	• 0.256^{o}
• BEAM-TO-BEAM ISOLATION	• 30 dB
• POINTING ACCURACY	• 0.03^{o}
• SURFACE ADJUSTMENT	• ADJUSTMENT CAPABILITY ON ORBIT
• DEPLOYMENT	• CONTROLLED, AUTOMATIC (NO EVA) • 60 MINUTES MAXIMUM • MICROSWITCHES FOR DEPLOYMENT VERIFICATION AND STOP
• RETRIEVABILITY	• AUTOMATIC, CONTROLLED • MICROSWITCHES TO STOP AND VERIFY STOWAGE • MESH SURFACE IS EXPENDABLE
• LAUNCH & LANDING LOADS	• COMPATIBLE WITH STS ENVIRONMENTS
• ORBITAL ENVIRONMENT	• COMPATIBLE WITH LEO AND GEO

POINT DESIGN DEPLOYED CONFIGURATION

The specific elements of the Hoop/Column are identified in the figure below. The main structural element of the antenna concept is the mast, which consists of a central hub and extendable portions called the upper and lower mast sections. The periphery of the reflector is a hoop made of rigid articulating segments. The hoop is controlled by a series of cables emanating from both the lower and upper mast ends and attached to each hoop joint. These cables serve to support and locate the hoop. The reflector surface is attached to both the hoop and a lower mast section and is shaped by a series of catenary cord elements which supports and contours the reflective mesh surface. The cord elements are high stiffness/low coefficient of thermal expansion graphite material which provide a very stable structure to which a gold-plated molybdenum reflective mesh is attached. Control cords are attached to the edges of each catenary element to provide adjustable points for in-orbit surface enhancement. The feed mast is a independent, expandable mast which supports the four separate feed array elements.

THE ENVIROMENTALLY STABLE DEPLOYED CONTOUR CAN BE ADJUSTED

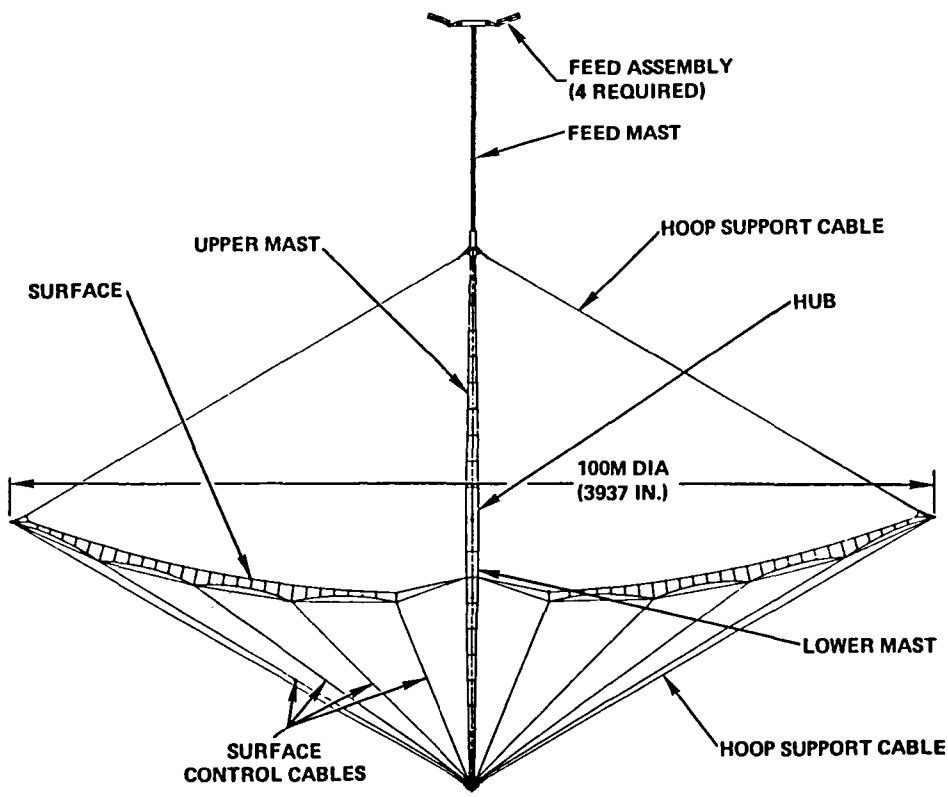

POINT DESIGN STOWED CONFIGURATION

The stowed Hoop/Column antenna packages vary efficiently within the constraints of the Shuttle bay. The configuration selected for the point design, which is a 100-meter diameter deployed reflector, utilizes 48 articulating hoop segments. This dictates the aspect ratio of length to diameter of the stowed package. The aspect ratio can be modified for any given deployed diameter by changing the number of hoop segments.

THE EFFICIENT STOWED PACKAGE CAN BE TAILORED TO A RANGE OF REQUIREMENTS

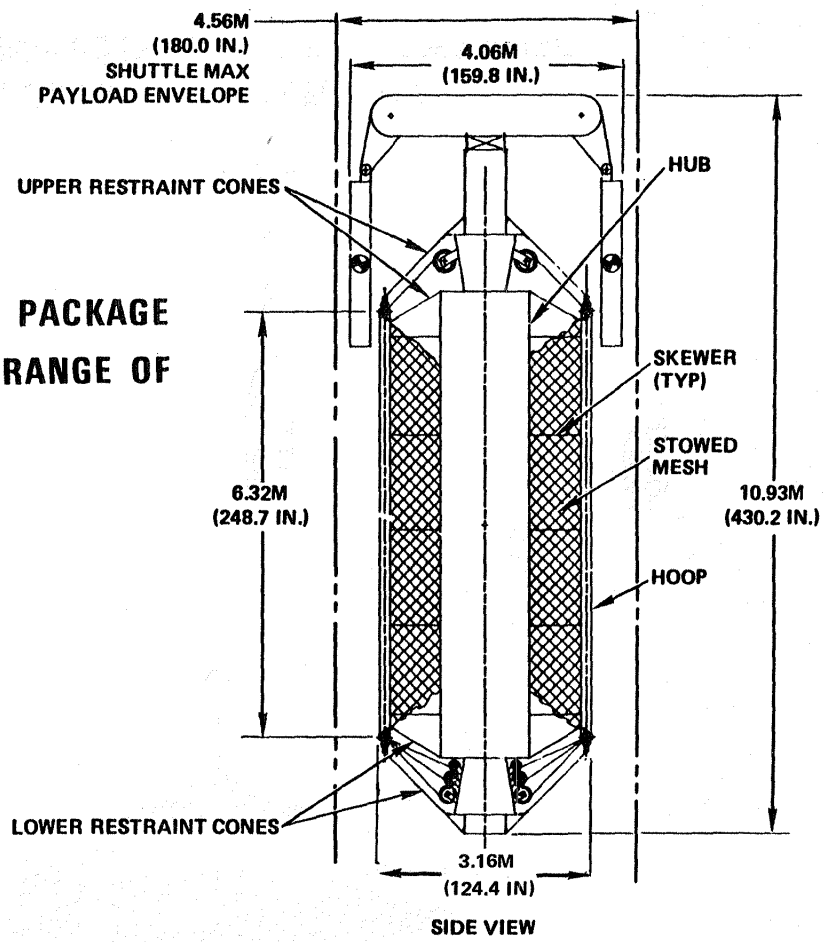

HOOP/COLUMN ANTENNA DEPLOYMENT SEQUENCE

The deployment sequence of the Hoop/Column antenna is initiated by the extension of both the feed mast and the main structural mast. Once this mast extension is completed, the hoop begins to deploy outward. The energy for deployment is provided by four separate drive units located on joints 90^{o} apart around the hoop. Once the hoop is deployed to its full circular approximation, a separate section of the mast called the preload section is deployed. This motion tensions all of the hoop support cables and thus preloads the system.

DEPLOYMENT IS CONTROLLED AND UNIT CAN BE AUTOMATICALLY RESTOWED

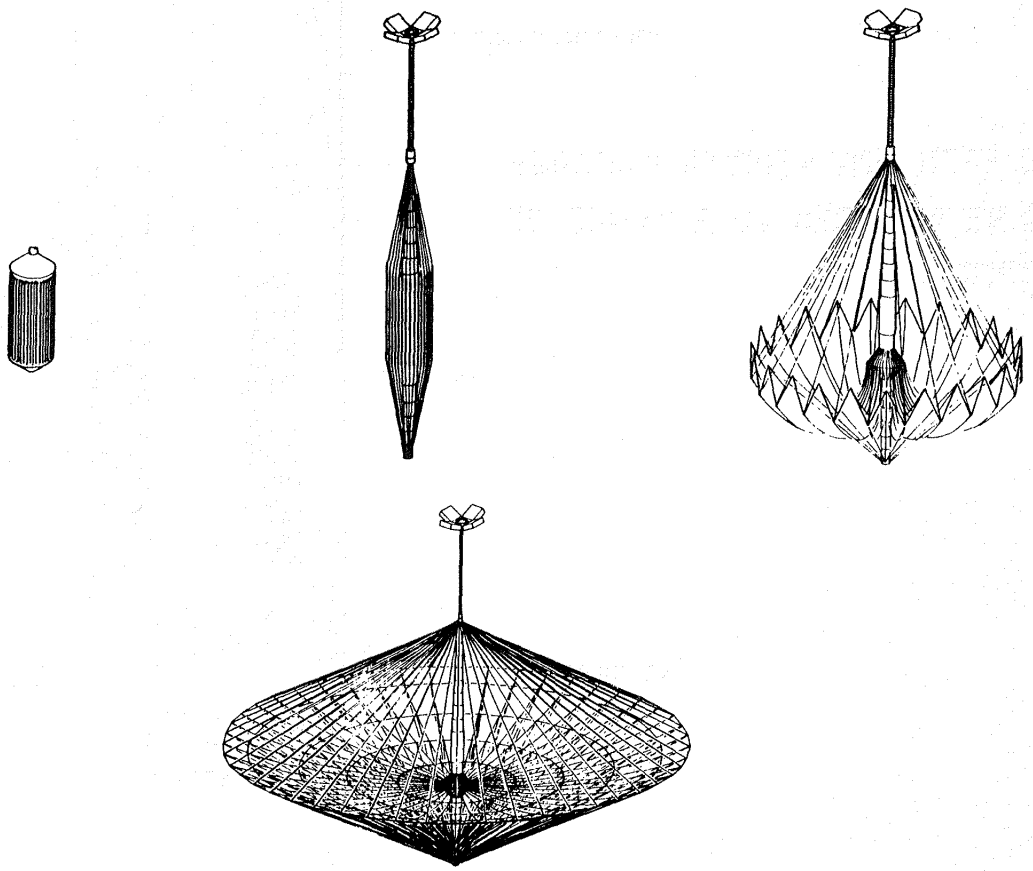

POINT DESIGN MISSION SCENARIO

The artist depiction represents the various stages of the mission for the point design. The first stage is orbit insertion by the STS and deployment out of the orbiter bay with the IUS attached. Second phase is a boost from LEO to geosynchronous orbit where deployment initiation takes place. Finally, the spacecraft is oriented Earth looking and the operational phase of the antenna begins.

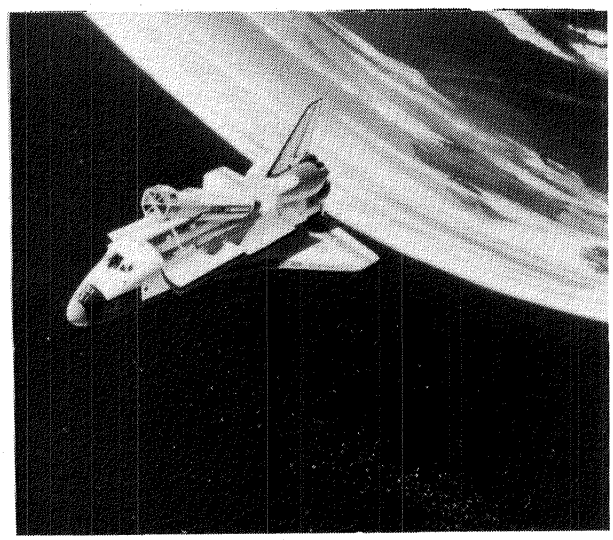

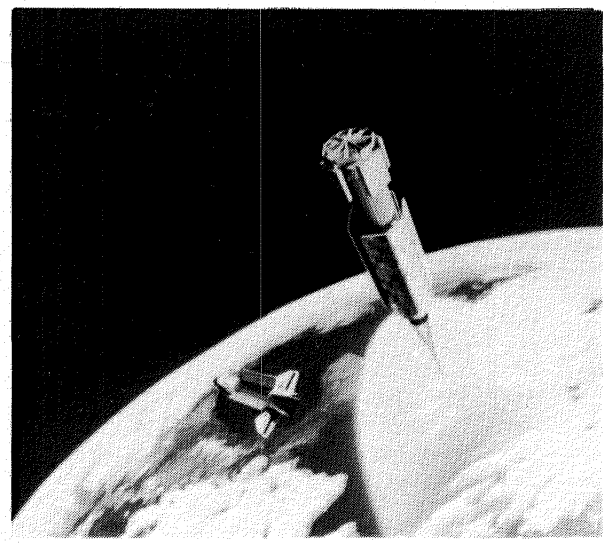

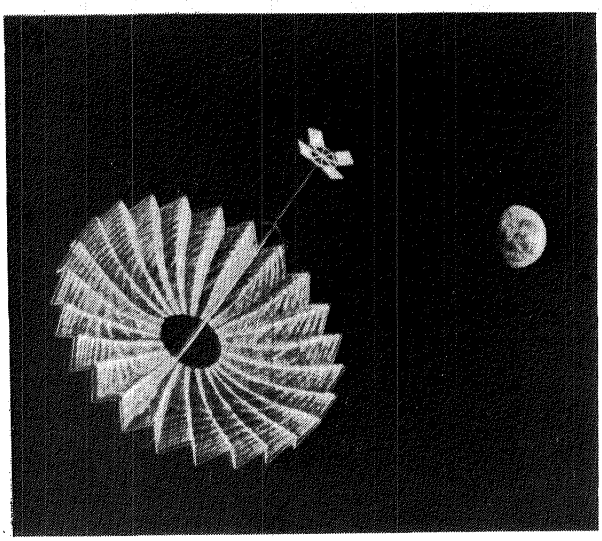

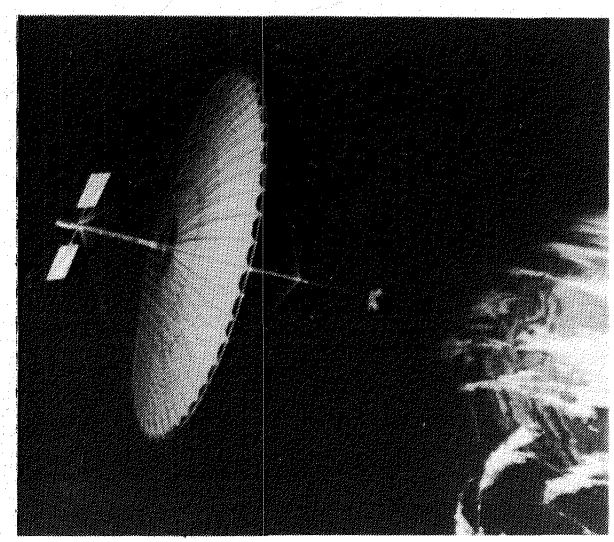

HOOP DEPLOYMENT SEQUENCE

The hoop deployment sequence is shown in the figure below. The approach developed utilizes a double hinge at each joint which permits rotation without any torsional wrap-up in the hoop members. The individual hoop segments simply rotate from vertical to horizontal about an axis through the center of each member.

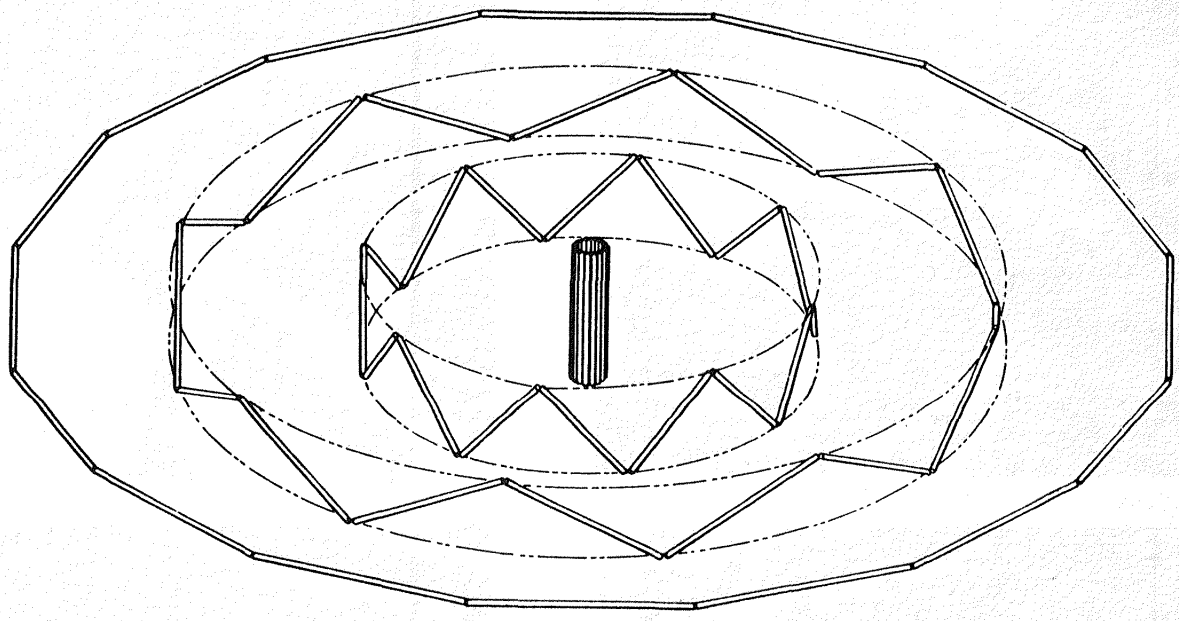

HOOP JOINT

This figure shows a side view of the hinge joint. The hinge platform is a truss structure which has high strength and stiffness efficiency. The tubular hoop segments are terminated with bonded fittings transitioning from a tubular section to a truss section which mates with the hinge platform. A pushrod is connected to adjacent hoop segments to transfer moment across the hinge. The synchronization strips transmit deployment energy to adjacent joints. Linear actuators are used to stow and deploy the hoop.

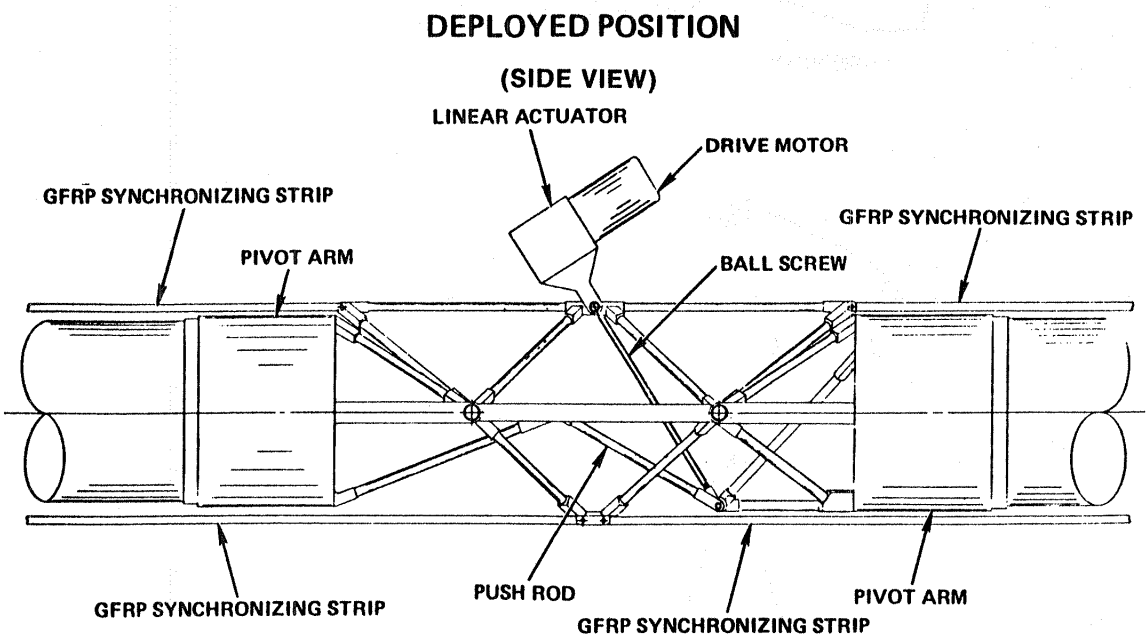

HOOP JOINT PUSHROD KINEMATICS

This figure shows a schematic of how one hoop segment is coupled to another in different stages of deployment. The hinge platform provides two hinge points for connecting adjacent segments. Movement is transferred across the hinge by means of a pushrod. Synchronization of the hoop joints is possible by keeping all hinge platforms parallel during deployment. This is illustrated on the next page.

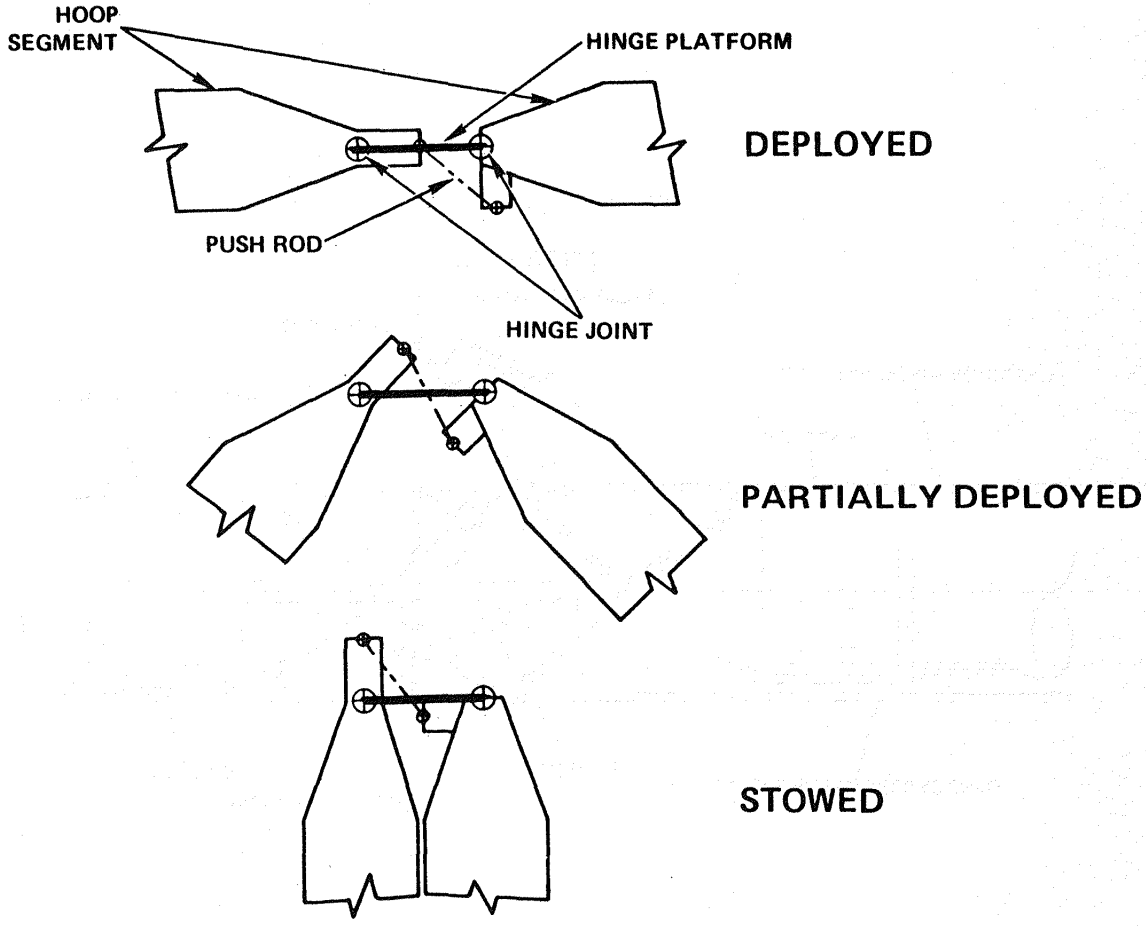

HOOP JOINT SYNCHRONIZATION

The hoop synchronization approach is one of pantograph or parallelogram type action. The philosophy of synchronization is that all hinge platforms remain parallel throughout the deployment motion, to provide uniform and controlled deployment.

HOOP SYNCHRONIZATION APPROACH

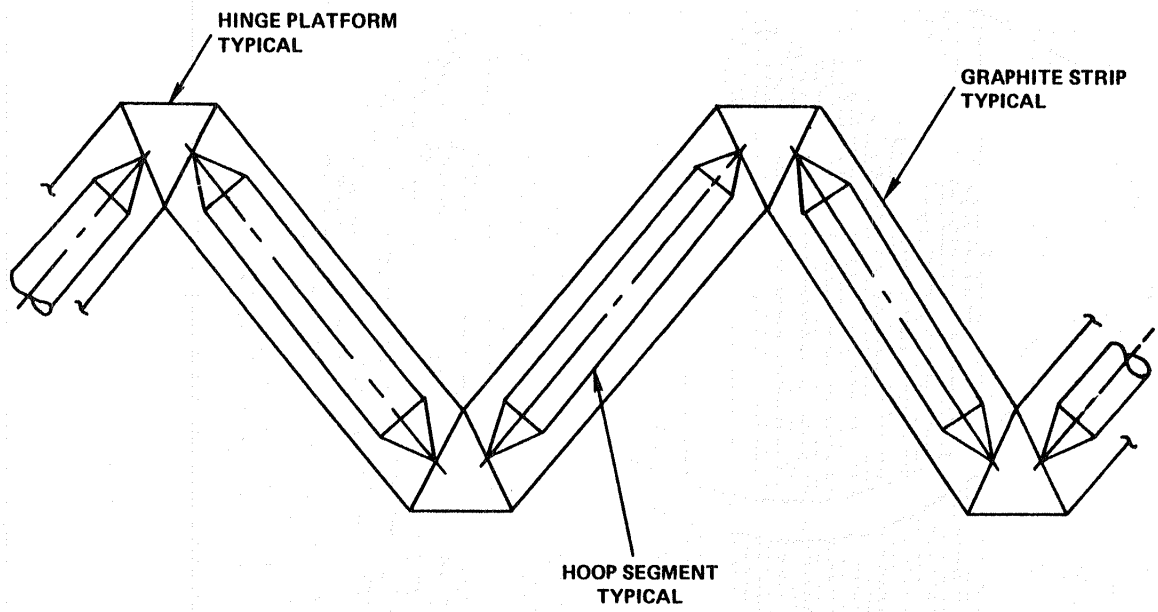

TELESCOPIC MAST

After many trade-off exercises, the cable driven telescopic mast was selected as the candidate approach which offered the most advantages. The deployment mechanism design consists of a cable that emanates from a drive spool and extends to the outer-most section of the mast. The cable runs over a pulley at the outer-most section, up the full length of the section, over a pulley at the top of that section and back down the adjacent section. It continues this path until it reaches the innermost section, at which time the cable crosses over to the opposite side and returns to the drive spool by an identical circuit to that just described. Deployment is initiated by activating the drive spool which takes up the cable and thus forces the sections to expand outward.

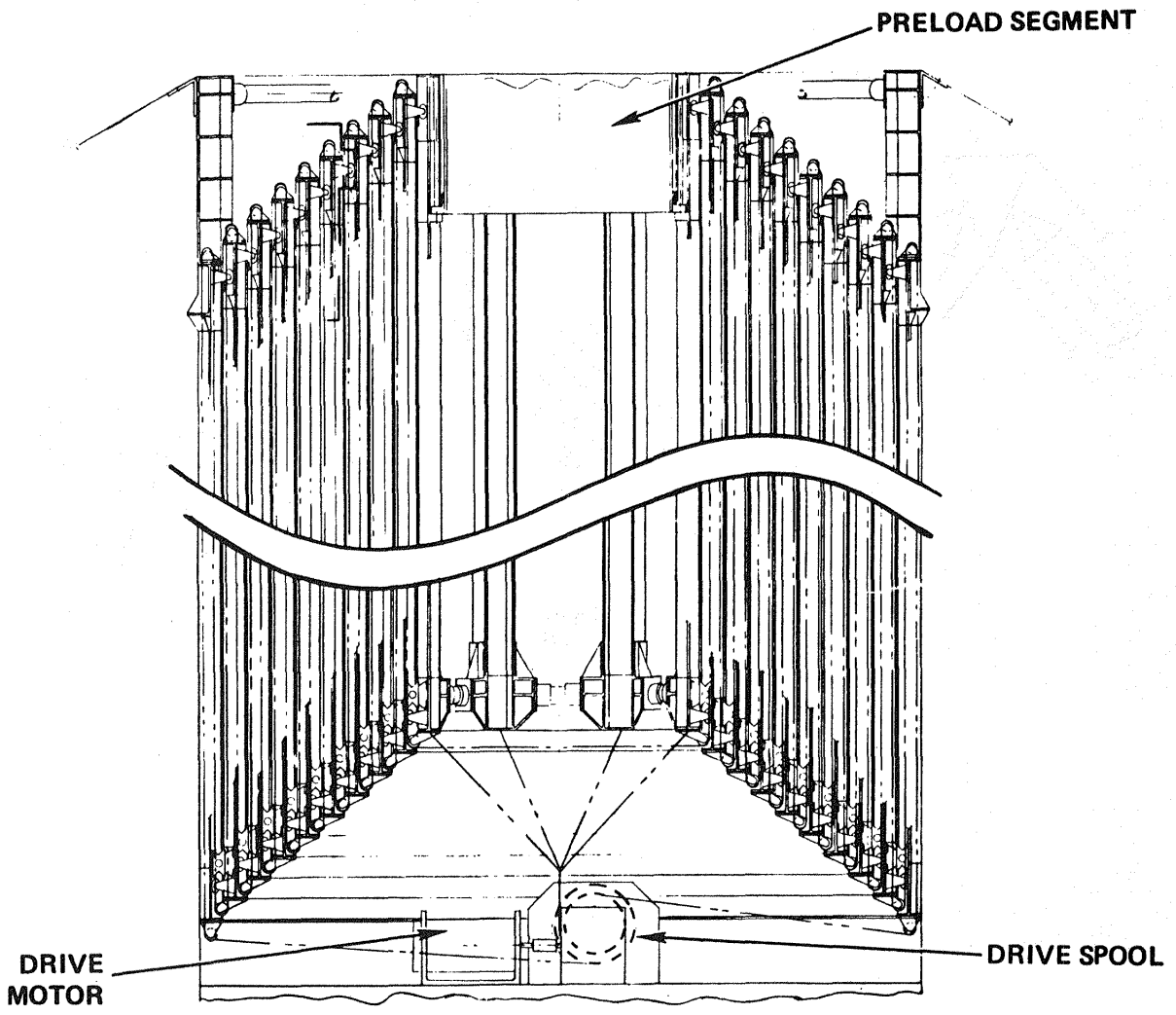

TYPICAL MAST SEGMENT

A typical mast section is shown in the figure below. The mast consists of an open lattice truss-type structure. This configuration was selected for high structural efficiency and low weight.

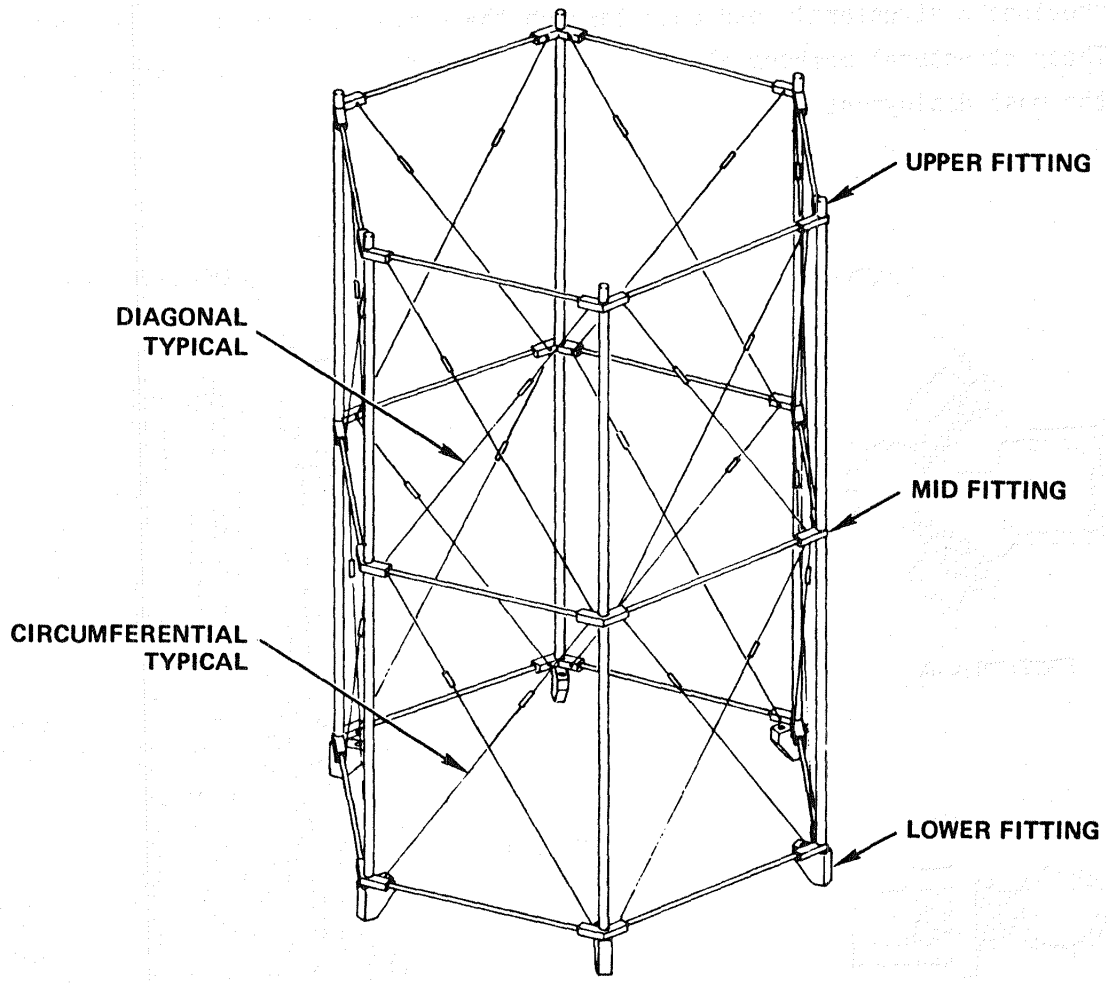

MAST RESTOWABILITY LATCH

One of the unique features of the mast is restowability. A latch design was developed which provides a means of reliably deploying and restowing the mast repeatedly without having to use electro-mechanical devices to deactuate the latch upon the restowed cycle. The latch shown is a simple ratchet type device that is triggered upon over-deployment of the mast. Once the mast is compressed, the latch engages against the adjacent fitting and provides a structural load path through the vertical elements of the mast. These structural members also serve as guides for rollers to ride on during the mast deployment.

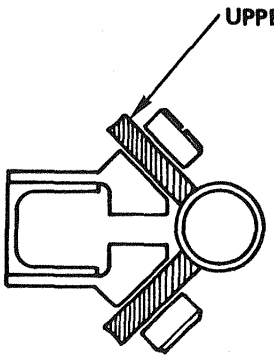

SECTION A–A

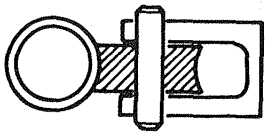

SECTION B–B

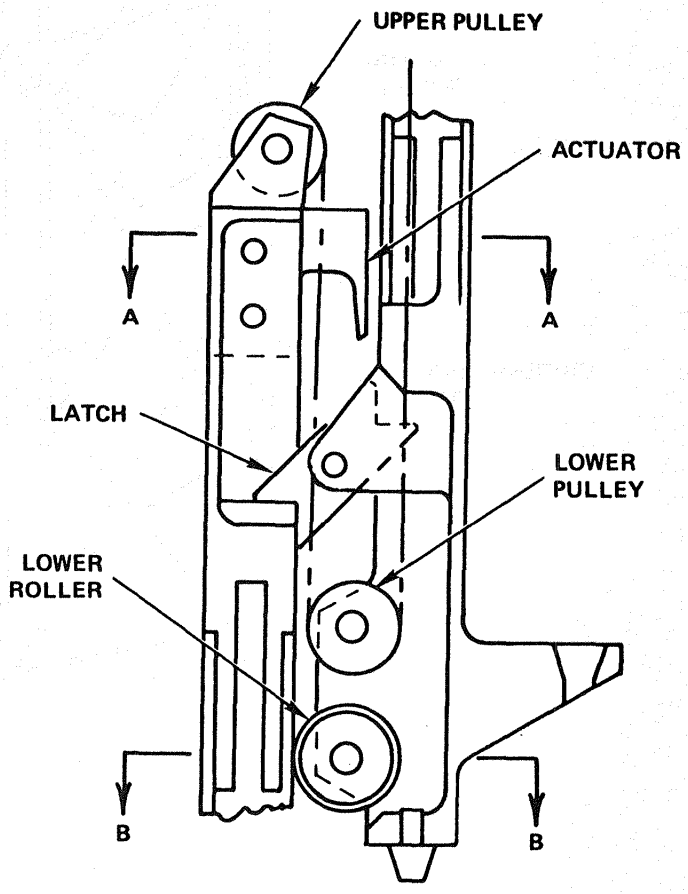

REFLECTOR SURFACE

The point design is a multiple beam/multiple quadrant offset reflector system. Four separate areas of illumination or aperture areas on the parent reflector are shown. The surface is shaped as if it were four offsets; thus the parent reflector is cusped.

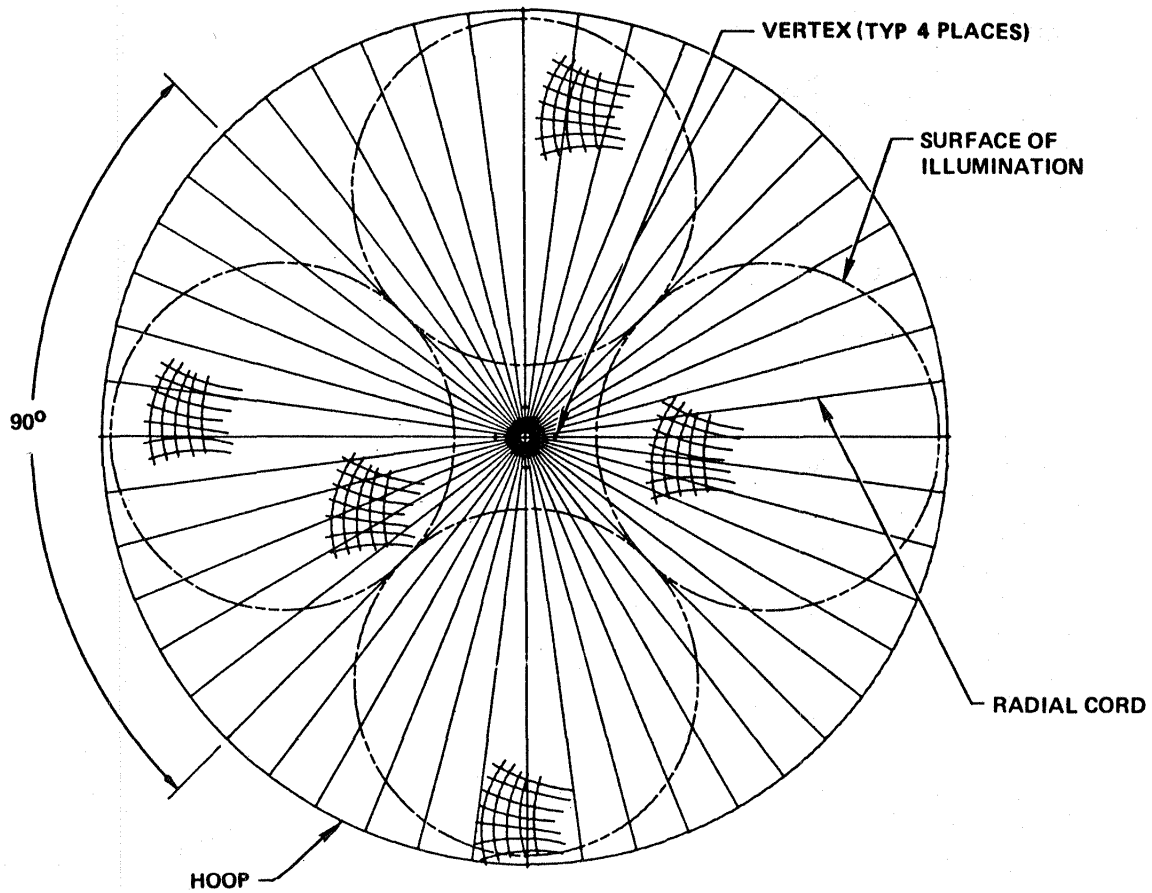

SURFACE ELEMENTS

This figure shows an isometric view of a one-half gore analytical model with the major elements of the design identified. The surface is shaped by catenary cords and tie members and a series of radial front cord elements. Diagonal ties are also used to position points on the surface between the edges of the gore.

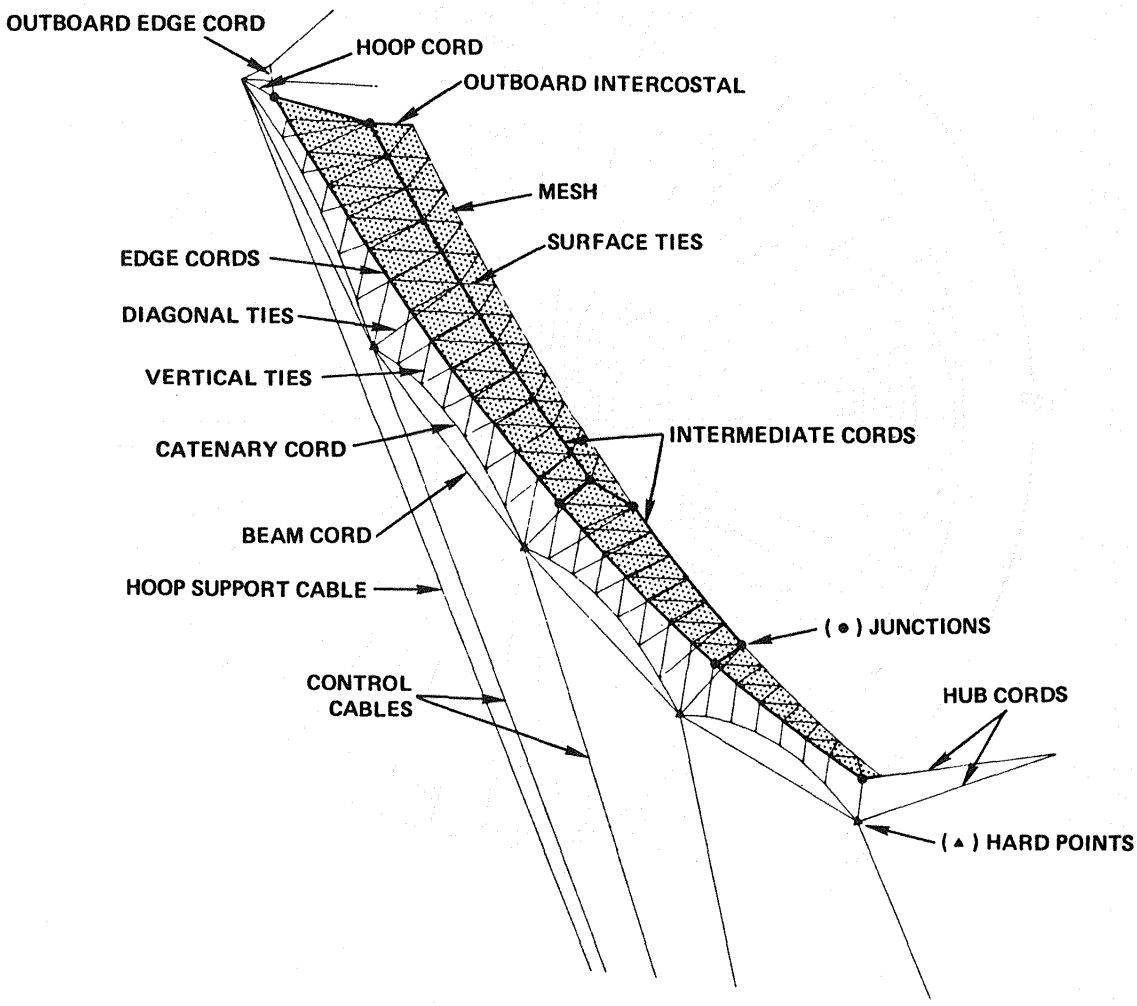

CONTOUR PERFORMANCE

The final contour performance budget shown below is improved from the initial contour by a biasing surface setting technique. On-orbit active surface control/adjustment capability provides improvement as noted in the footnote.

FINAL CONTOUR PERFORMANCE BUDGET

	△F + △Z (CM)	RMS (CM)
MANUFACTURING	-7.704 CM	0.455
PILLOWING	0.000	0.294
THERMAL ELASTIC ECLIPSE	-0.433	0.070
MATERIAL PROP. DEGR.	-0.112	0.120
UNCERTAINTIES	-8.116	0.076
TOTAL	-16.365 CM* (SUM) (-6.443 IN)	0.565 CM (RSS) (0.222 IN)

* △F + △Z MAY BE REDUCED TO 8.445 CM (3.329 IN) BY USING OPTIONAL ON-ORBIT ACTIVE SURFACE CONTROL/ADJUSTMENT CAPABILITY.

HOOP/COLUMN QUAD APERTURE RF GAIN

The quad aperture gain is calculated by a budget shown below. Gain loss mechanisms are tabulated and subtracted from the maximum projected area gain.

PROJECTED GAIN BUDGET

LOSS MECHANISM	LOSS (dB)
AMPLITUDE ILLUMINATION (20 dB TAPER)	1.27
PHASE EFFICIENCY	0.05
AMPLITUDE SPILLOVER	0.46
FEED BLOCKAGE	0.00
FEED OHMIC LOSS	0.15
FEED VSWR (1.2:1)	0.04
CABLE BLOCKAGE (CABLE DIA = 0.22 IN)	0.13
SURFACE REFLECTIVITY (MESH OPENING SIZE 0.25 IN)	0.20
REFLECTOR ROUGHNESS (RMS ϵ = 0.22 IN)	0.47
REFLECTOR CROSS POLARIZATION	0.01
DEFOCUS (ΔF = 6.82 IN)	0.08
SCAN LOSS (13 BEAMWIDTHS SCAN)	0.25
TOTAL LOSSES (dB)	3.1
ANTENNA EFFICIENCY	49%
100% GAIN (dBi)	58.6
NET GAIN (dBi)	55.5

WEIGHT

The total weight of the 100-meter point design in a flight configuration is 3942 pounds, and 4476 pounds with contingency weight. A weight breakdown by subassembly is given below:

Item No.	Group Description	Current Weight Pounds	Contingency Weight Pounds
001	Hoop Assembly	644	722
051	Hub Assembly	145	163
101	Mast Assembly	1180	1341
201	Feed Support Assembly	300	336
276	Long Restraint Assembly	156	175
301	Transverse Restraint Assembly	118	132
326	Surface Target Assembly	2	2
401	Feed Assembly	600	678
501	Mesh Stowage Assembly	21	25
551	Thermal Control Assembly	202	238
601	Wiring Cabling Assembly	249	294
701	Instrumentation Assembly	17	20
751	Optical Alignment	20	24
801	Reflector Surface Assembly	289	326
	Total	3942	4476

DYNAMIC PERFORMANCE

The Hoop/Column antenna normal dynamic modes were characterized for a range of antenna diameters using the NASTRAN[1] computer program. The results are given in the chart below:

VARIATION OF MODAL FREQUENCIES AS A FUNCTION OF RADIUS (RIGID HOOP AND MAST MODEL)

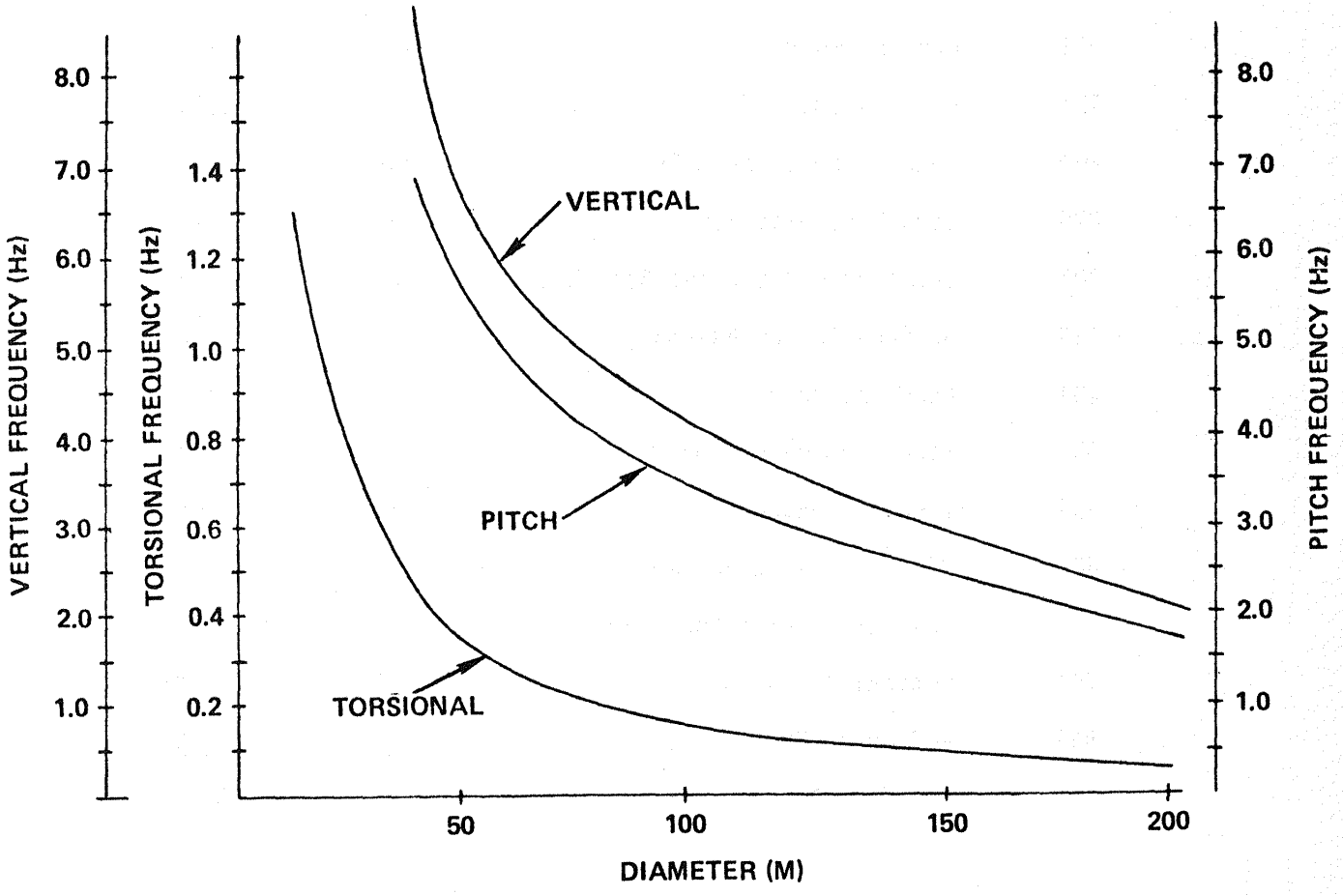

[1] NASTRAN: Registered trademark of the National Aeronautics and Space Administration.

MATERIALS DEVELOPMENT TASK

Because of the large number of cords and cable elements in the Hoop/Column concept, this task was devoted entirely to the development of key materials for the various cord applications. The objectives of the task are defined in the figure below:

OBJECTIVES

- **DEFINE CABLE REQUIREMENTS, STRUCTURAL, THERMAL, ENVIRONMENTAL**
- **PERFORM DATA RESEARCH**
- **EVALUATE CANDIDATE MATERIALS AND CONFIGURATIONS**
- **FABRICATE SAMPLES OF SELECTED CABLE MATERIAL/ CONFIGURATION COMBINATIONS**
- **DETERMINE MATERIAL PROPERTIES OF SELECT CONFIGURATIONS VIA APPROPRIATE TESTS**
- **PROVIDE DESIGN DATA AS INPUT TO OTHER TASKS**

MATERIAL DEVELOPMENT FLOW

The chart below shows the materials development task flow from its initiation to the completion of Phase I.

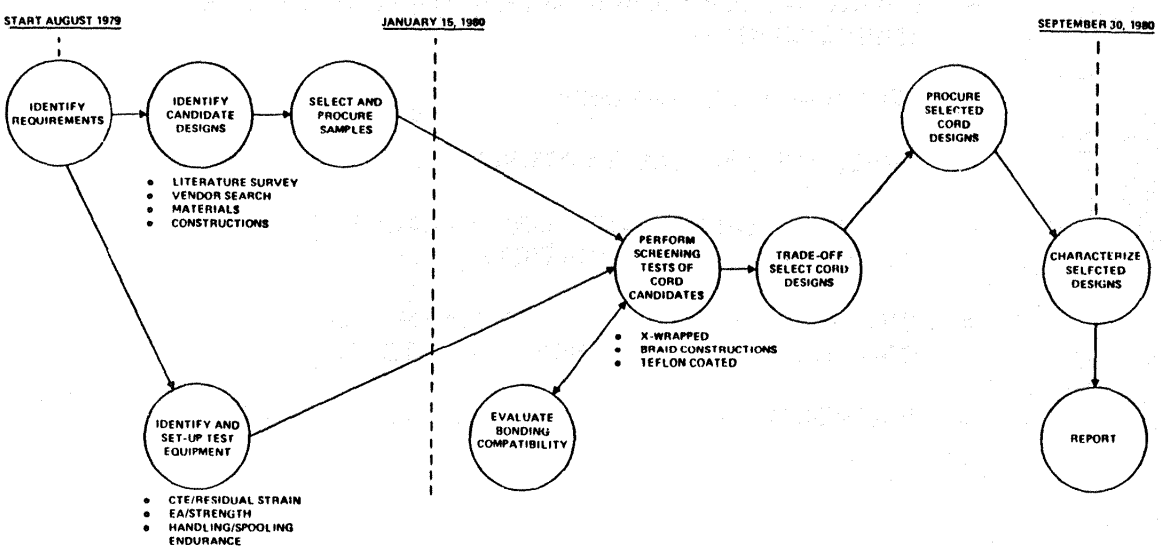

CANDIDATE CABLE MATERIALS

One of the critical parameters used to evaluate material under consideration was the coefficient of thermal expansion (CTE). In the chart below, values of CTE are plotted against specific modulus. The candidates that fall within a preferred range of $\pm 0.9 \times 10^{-6}$ cm/cm/^{o}C (graphite and quartz) have desirable thermal elastic properties. Graphite shows a significant advantage in terms of the specific modulus. This led to most of the evaluation work being performed on the CELION[2] graphite fiber.

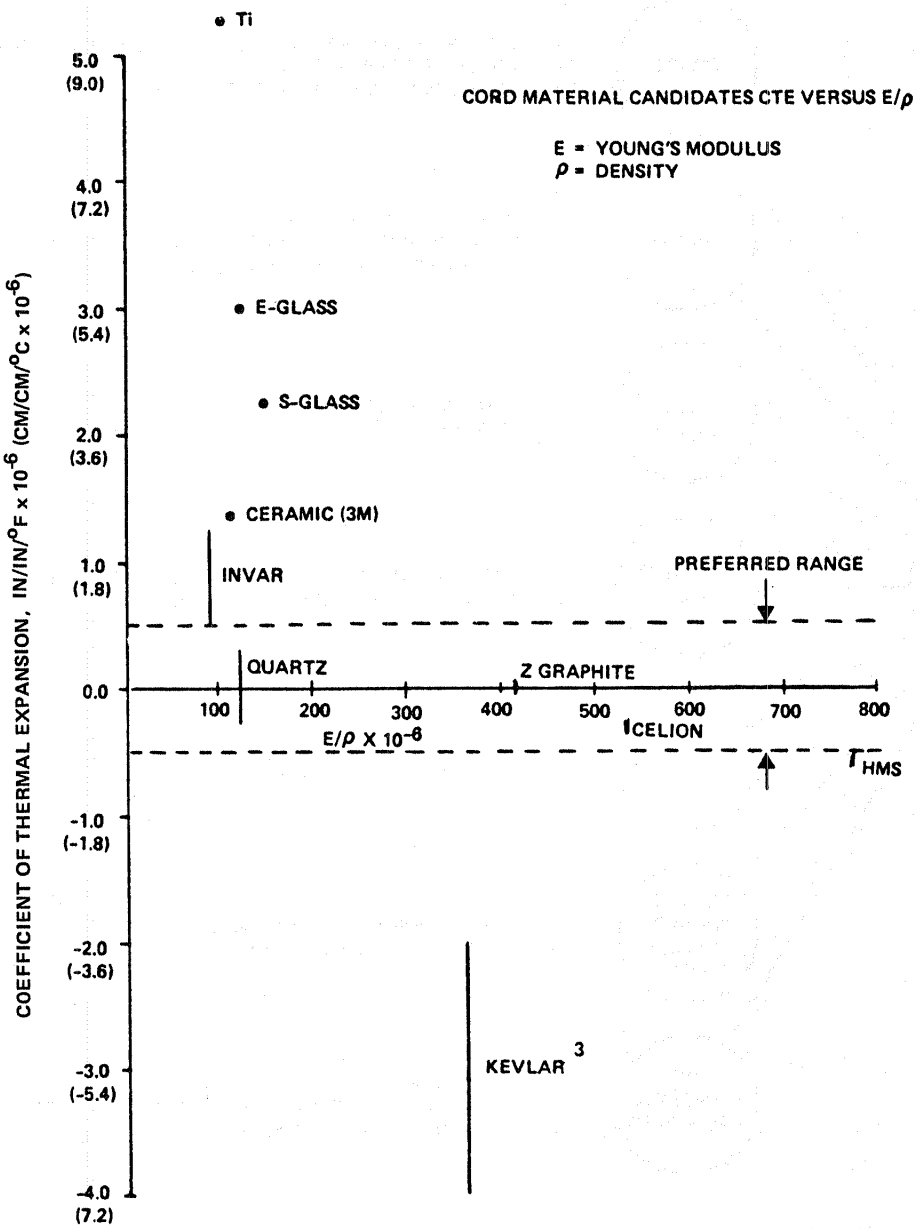

[2]CELION: Trademark of Celanese Corporation

[3]KEVLAR: Trademark of E.I. du Pont de Nemours & Co., Inc.

CABLE CONSTRUCTION METHODS

Various techniques were evaluated for making cables. The chart below describes the basic types that were considered and comments on each. For most of the Hoop/Column cord applications, the Teflon[4] impregnated cord offers the greatest promise.

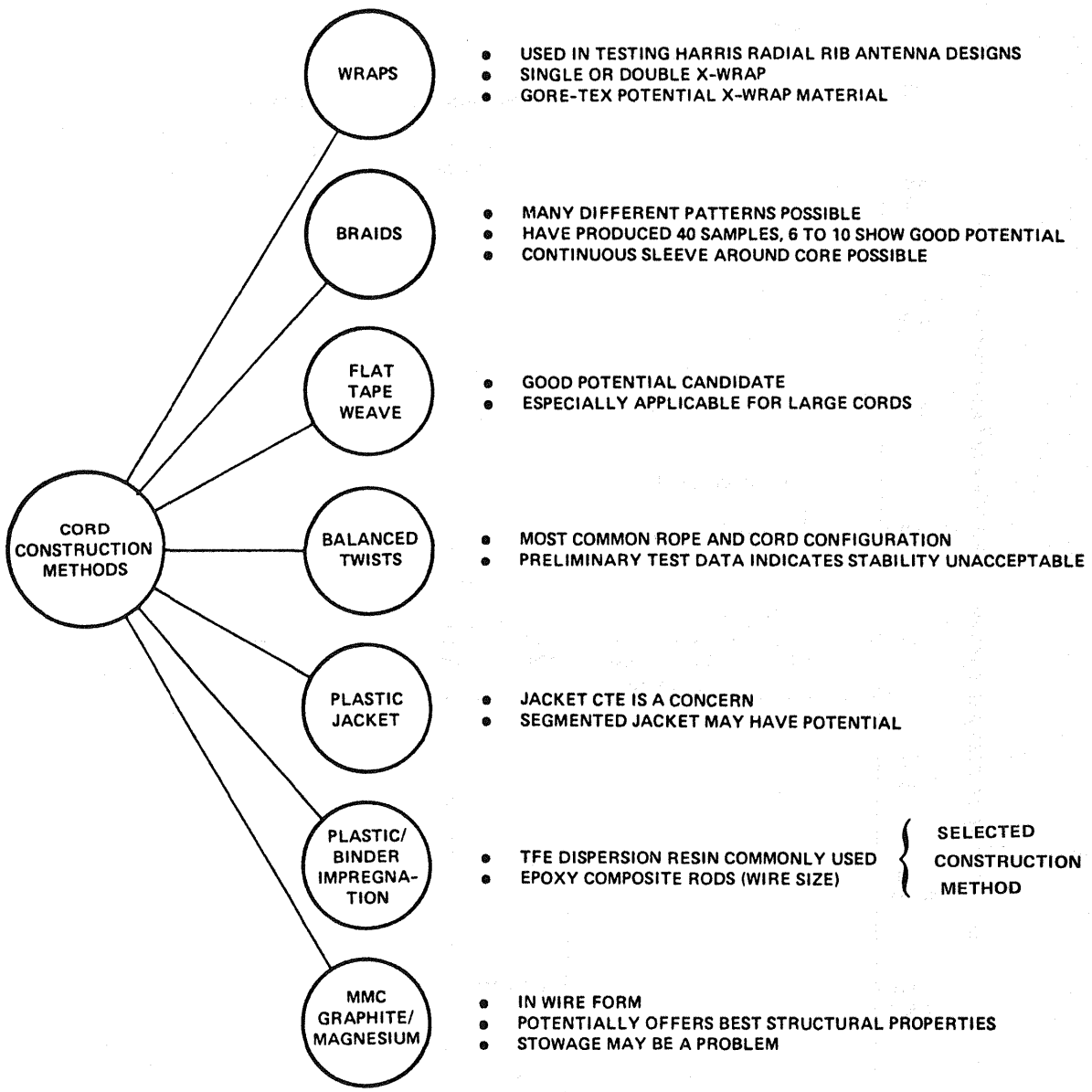

[4]Teflon: Registered trademark of E.I. du Pont de Nemour & Co., Inc.

CABLES JOINT MANUFACTURING

The unique configurations of cable junctions presented problems in joining techniques. After various trade studies were completed, the following joint concept was selected as being the most readily implementable and providing uniform structural properties. To meet the primary goal of build to dimension for the point design, an assembly method was devised which would yield the lowest manufacturing tolerances. The method selected involves maintaining control of both geometry and preload during the manufacturing process. Individual cords are loaded and positioned over accurately placed tooling pegs at each cable junction. The appropriate regions of Teflon coating on the cords are stripped-off and adhesive applied. A graphite epoxy board fitting is placed over the tool pegs and bonded to the cords. The result is a very high strength joint for transitioning load around angles in the cables while still maintaining full cable properties. The various joints and cord quantities per panel are shown in the following three figures.

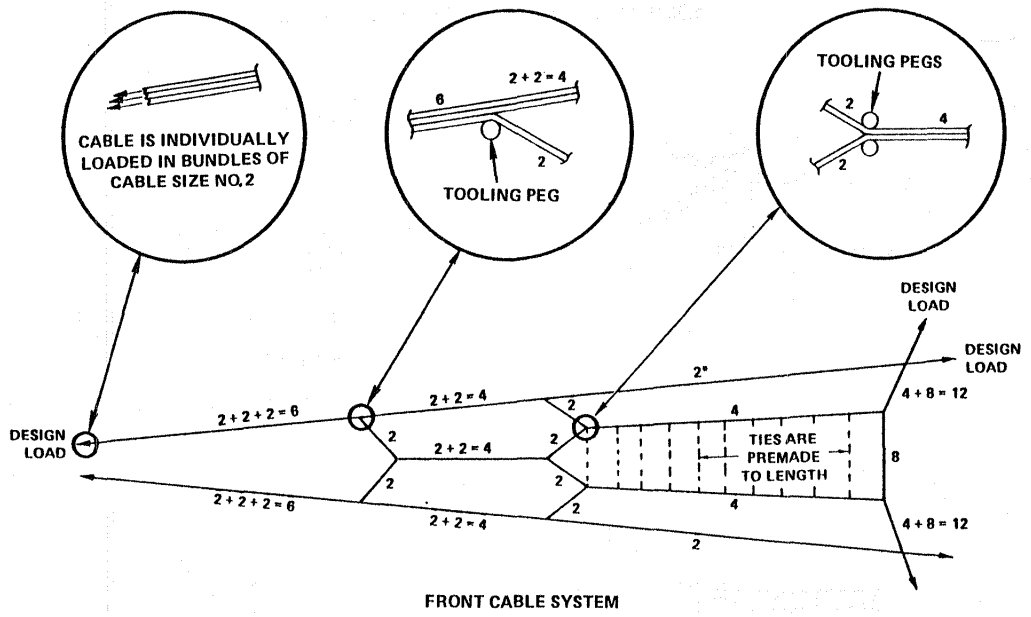

FRONT CABLE SYSTEM

*NUMBERS INDICATE CABLE SIZE

(see continuation on next page)

CABLE JOINT MANUFACTURING (CONTINUED)

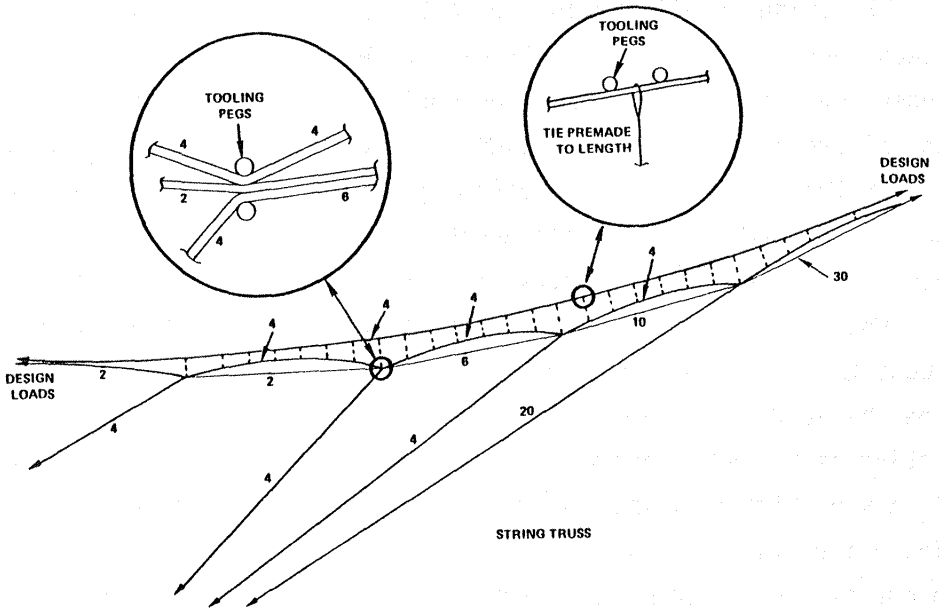

CABLE JOINT MANUFACTURING PROCESS

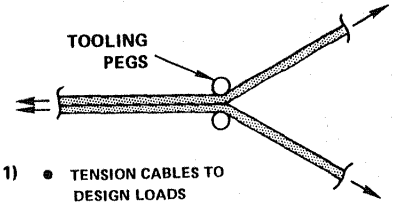

1) • TENSION CABLES TO DESIGN LOADS

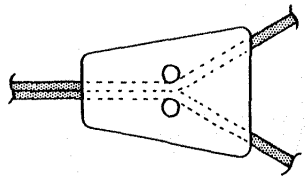

3) • TO APPLY EPOXY ADHESIVE TO GRAPHITE/EPOXY FITTING

• PLACE FITTING OVER TOOLING PEGS WITH ADHESIVE IN CONTACT WITH CORDS

• ALLOW 24 HOURS FOR ADHESIVE CURE

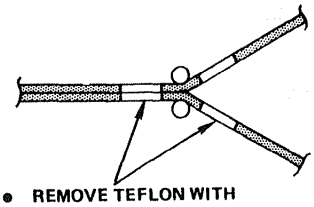

2) • REMOVE TEFLON WITH MINIATURE BUTANE TORCH

• APPLY EPOXY ADHESIVE TO CABLE AREAS

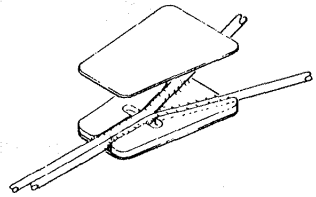

4) • REMOVE FITTING AND CABLES FROM TOOLING PEGS AND BOND LAMINATE CAP TO EXPOSED CABLE SIDE OF FITTING

GRAPHITE CABLE COEFFICIENT OF THERMAL EXPANSION

The coefficient of thermal expansion is determined by means of a deflection test setup using a long cord specimen which is heated and cooled over the appropriate temperature range. Deflection is measured at various temperature increments. It can be seen by the curve below that good repeatability of strain versus temperature occurs and the resulting CTE is very low (Approximately -0.4 x 10^{-6} cm/cm/^{o}C).

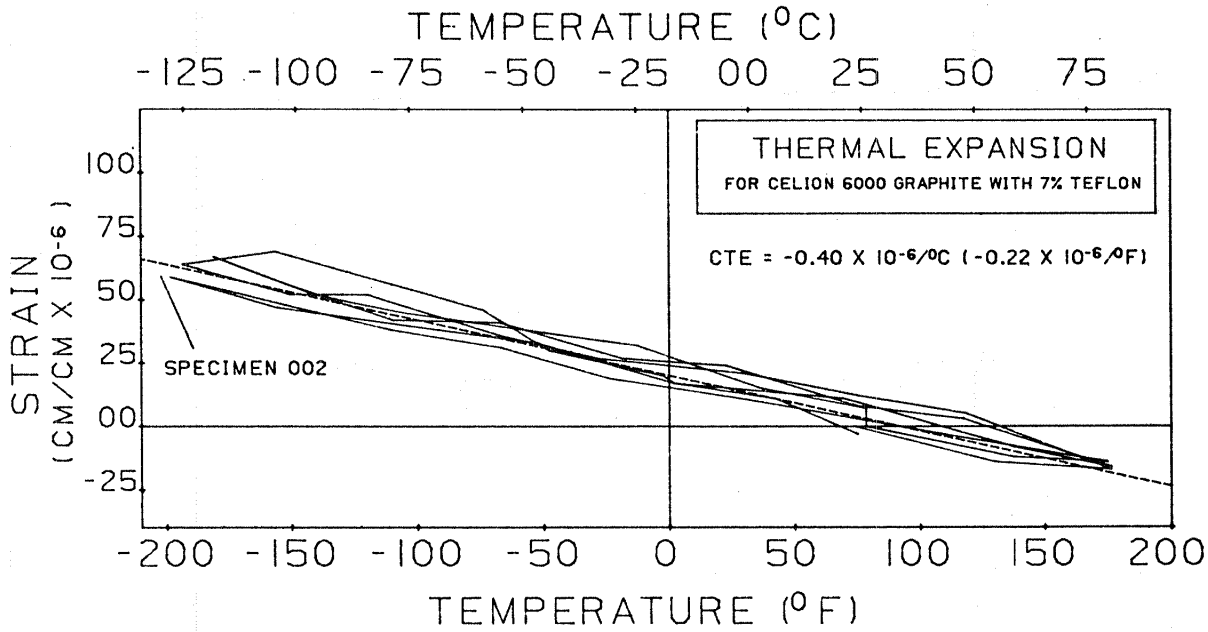

GRAPHITE CABLE STIFFNESS

The figure below shows the results of load/strain tests for a number two cord (CELION 6000 graphite fiber) with a 7% Teflon coating. The curve shows the relatively linear characteristics of the graphite material over the load range indicated. The cable has an EA (Modulus of Elasticity X Area) of approximately 40,000 N (9000 pounds) over the load range of interest.

LOAD VS. STRAIN FOR CELION 6000 GRAPHITE WITH 7 % TEFLON (NO. 2 CORD)

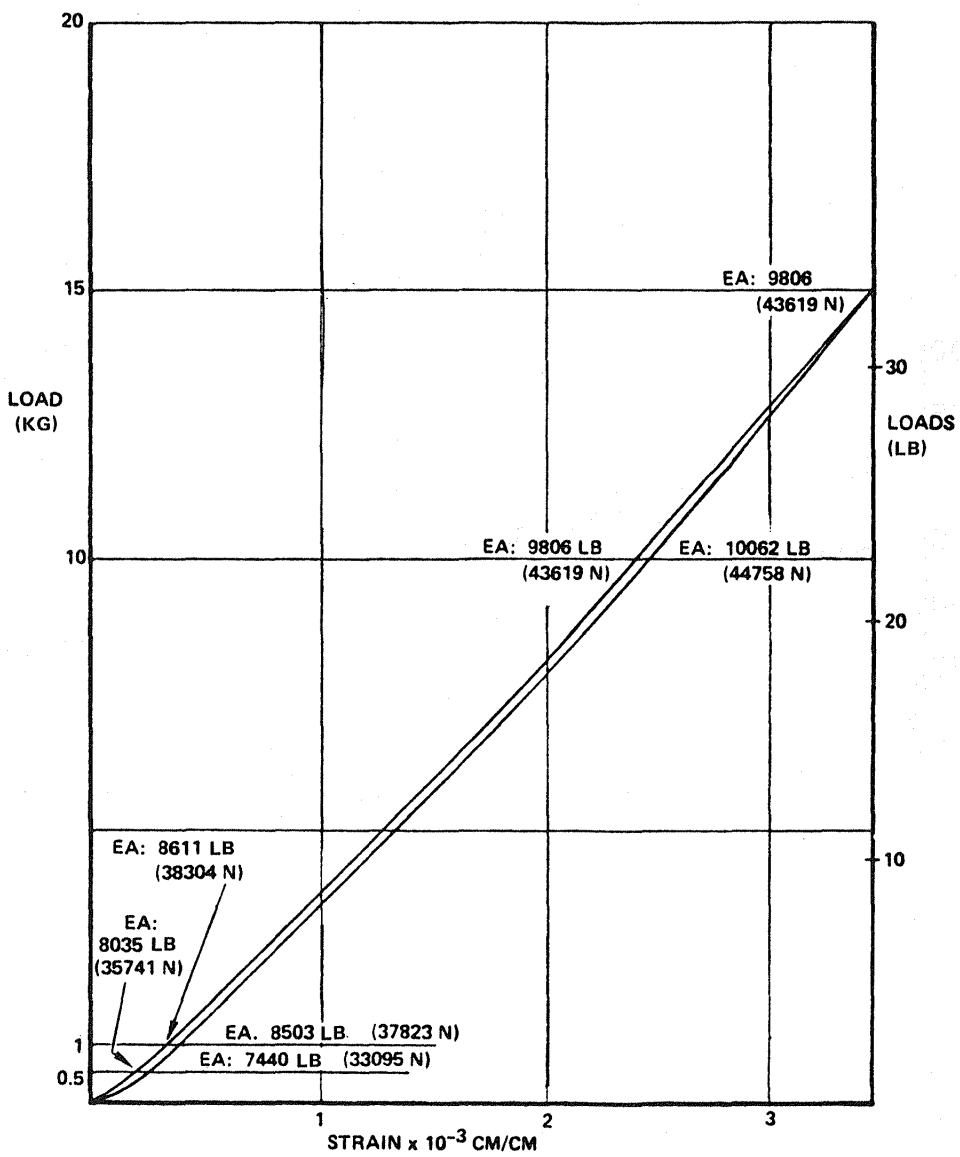

CABLE DEVELOPMENT RESULT SUMMARY

The chart below highlights some of the results of the cable development task. Results for the Teflon coated graphite cords were very encouraging from a structural, thermal-elastic, residual strain and manufacturing sense. Further work is required to develop statistical basis allowables for cable properties.

- **THE SELECTED TEFLON COATED GRAPHITE CORD MATERIAL OFFERS THE FOLLOWING ADVANTAGES COMPARED TO QUARTZ:**
  - **THREE TIMES HIGHER MODULUS (E)**
  - **TWICE THE STRENGTH**
  - **EXHIBITS NO RESIDUAL STRAIN (AVERAGE OF FOUR SAMPLES)**
  - **MEASURED CTE OF -0.41/^{o}C (-0.23/^{o}F) AND OTHER FIBERS FROM MANUFACTURERS WITH PREDICTED ZERO CTE**
  - **30% LOWER WEIGHT**
  - **GOOD HANDLING TOUGHNESS**
- **CABLES ARE ADAPTABLE TO SPACE ENVIRONMENT**
- **TEFLON COATING ON CORDS FACILITATED THE DEVELOPMENT OF IMPROVED JOINT DESIGNS**
- **DEVELOPED LSST CORD MANUFACTURING PHILOSOPHY**
- **DEVELOPED TEST PROCEDURES AND EQUIPMENT**

DEMONSTRATION MODELS AND FULL SCALE ELEMENTS

Demonstration and element verification models were fabricated to support the Hoop/Column antenna design. Designs were generated for a half-scale surface adjustment breadboard and a 1/6-scale deployable model of the complete reflector. These model designs will be fabricated in Phase II of the program. Program model objectives are specified below:

OBJECTIVES

- PROVIDE HOOP/COLUMN DISPLAY MODELS WHICH SATISFY FOCUS MISSION CONFIGURATION REQUIREMENTS
- IDENTIFY CRITICAL COMPONENTS AND FABRICATE FULL OR PARTIAL SCALE VERIFICATION MODELS
- BUILD ACTIVE SURFACE CONTROL BREADBOARD MODEL CAPABLE OF INCORPORATING S.A.M.S.
- BUILD ENGINEERING BREADBOARD MODELS REQUIRED TO SUPPORT DESIGN TRADE-OFFS

HOOP HINGE JOINT MODEL

One critical element of the design is the hoop and its deployment method. A model of three full-scale hinge joints with truncated hoop segments was fabricated to evaluate the hoop's deployment, synchronization, and repeatability. A single drive unit deploys the model with synchronization being accomplished by means of synchronizing strips connecting adjacent hinge platforms and drive motion accomplished by means of a pushrod link.

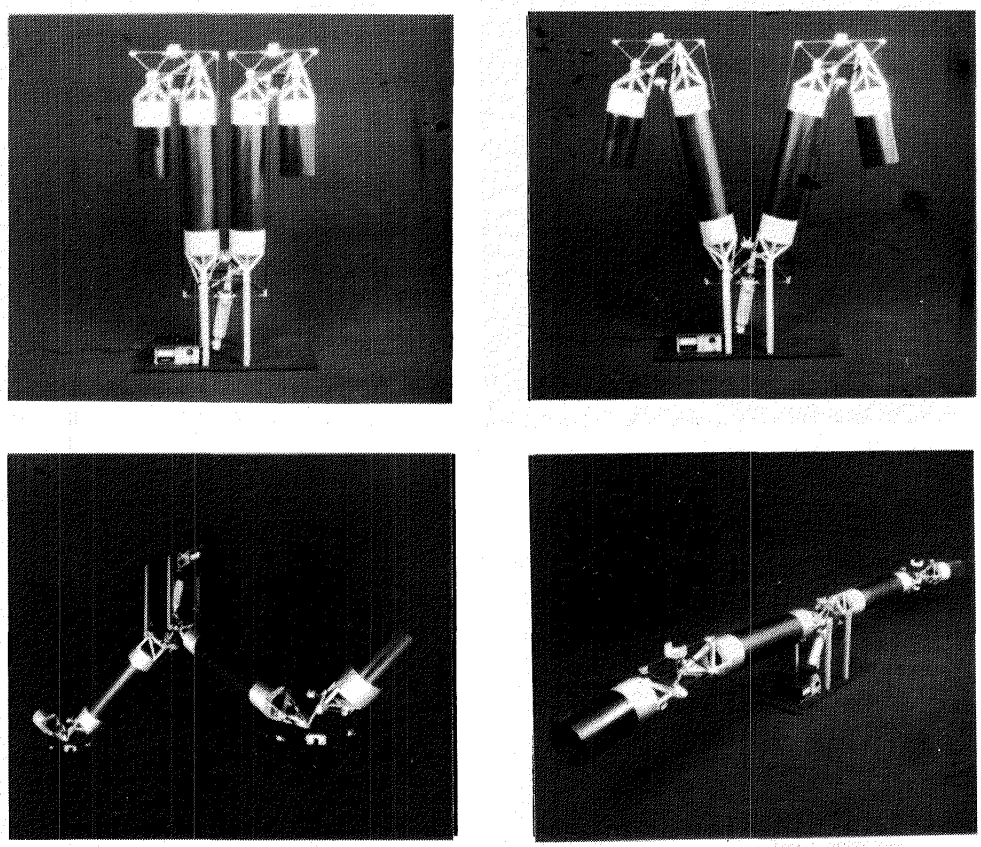

THE HOOP HINGE JOINT MODEL HAS VERIFIED THE HOOP DEPLOYMENT MECHANISM DESIGN

DEPLOYABLE MAST MODEL

Design verification of the mast was accomplished by means of a deployment model. This model represents an approximate 1/5-scale of the point design.

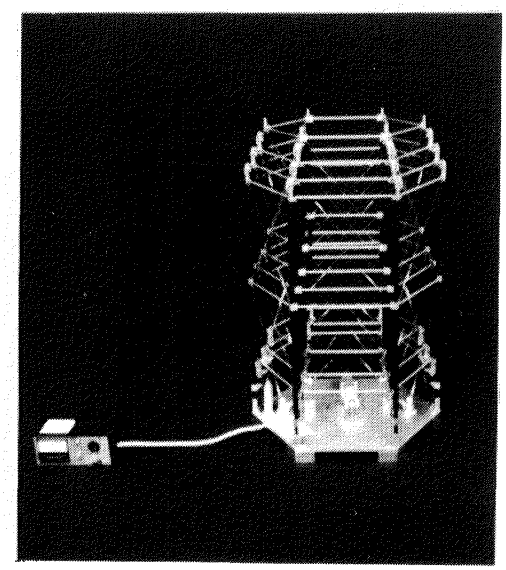

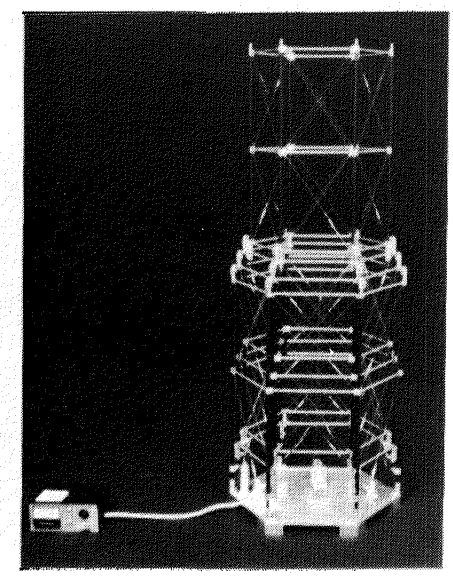

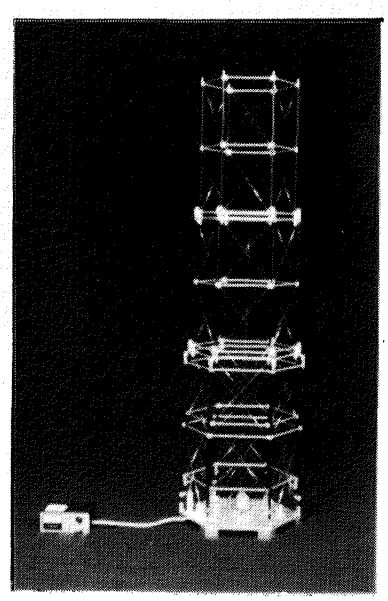

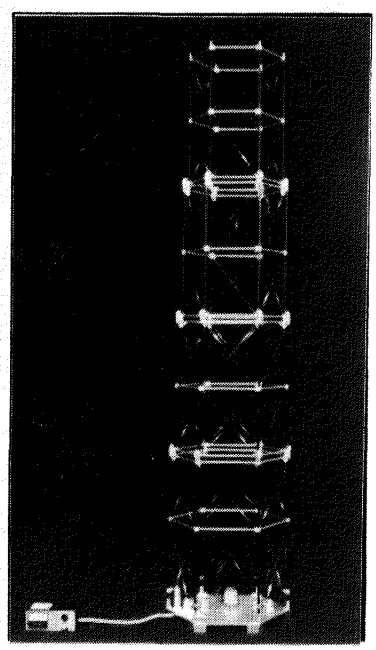

THE MAST MODEL HAS VERIFIED MAST DEPLOYMENT

50-Meter SURFACE MODEL

A half-scale (or 50-meter diameter) size surface adjustment breadboard model was selected to provide a realistic assessment of the manufacturing techniques, analytical models and the ability to adjust the contour. The present phase of the program has completed the design and analysis efforts associated with the configuration. The procurement, fabrication, assembly, and test operations will be accomplished during the second phase of the program in FY 81 and FY 82. Upon completion of the fabrication and assembly operations, the model will incorporate an engineering model of the Surface Accuracy Measurement System (SAMS) to evaluate the integrated performance. The breadboard objectives are given below:

OBJECTIVES

- DEMONSTRATE SURFACE ADJUSTMENT CAPABILITY
- VERIFY ANALYTICAL MODELS
- EVALUATE FABRICATION AND ASSEMBLY TECHNIQUES
- PROVIDE TEST-BED FOR OPERATIONAL DEMONSTRATION OF SAMS
- PROVIDE DATA AS INPUT TO SCALING LAWS

SURFACE MODEL CONFIGURATION

This artist depiction of the 50-Meter Surface Model shows the four gores which comprise the test article along with the boundary tooling required to support it. The boundary tooling is designed to provide high stiffness and, therefore, predictable boundary conditions.

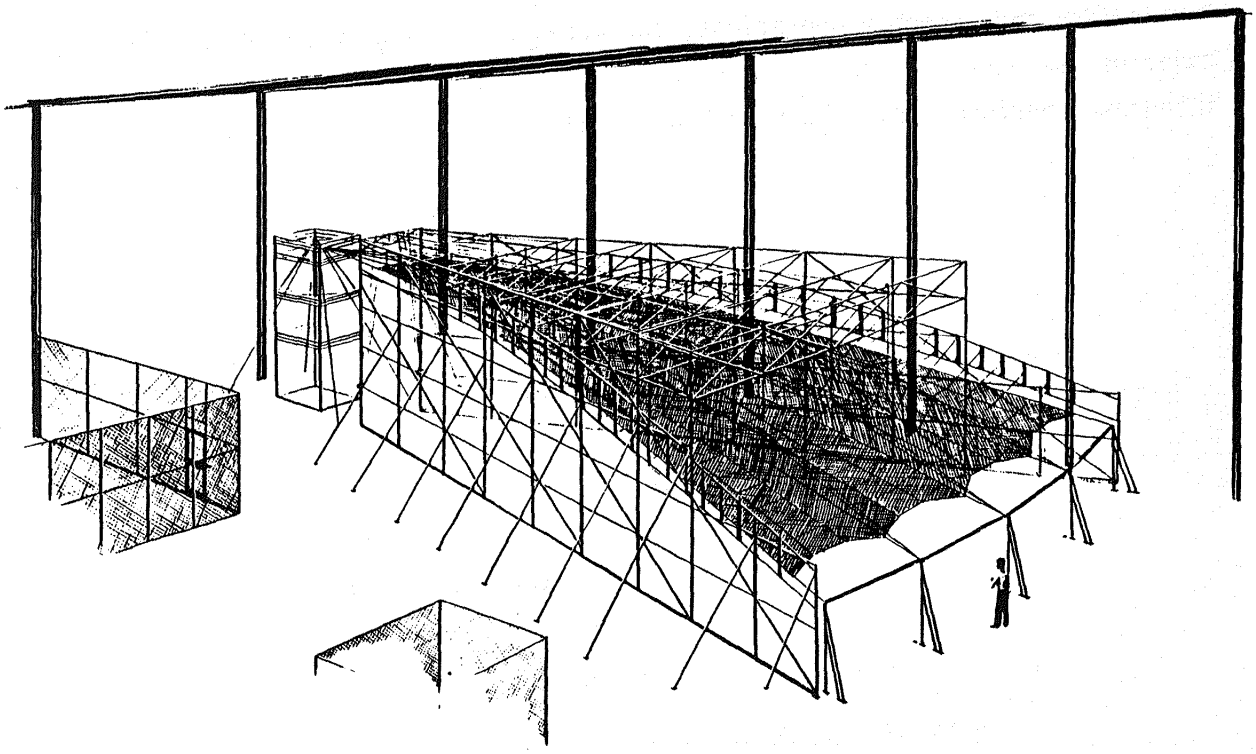

SURFACE MODEL FINITE ELEMENT MODEL

Detailed analytical models were made to assess the performance of the 50-Meter Surface Model. The figure below is a graphic representation of the four-gore finite element model used in the analysis. Artificial displacements were induced in each control cord to determine the resulting surface perturbation. These data then permitted an evaluation of the overall adjustment capability of the entire model. The next figure displays the results of this analysis.

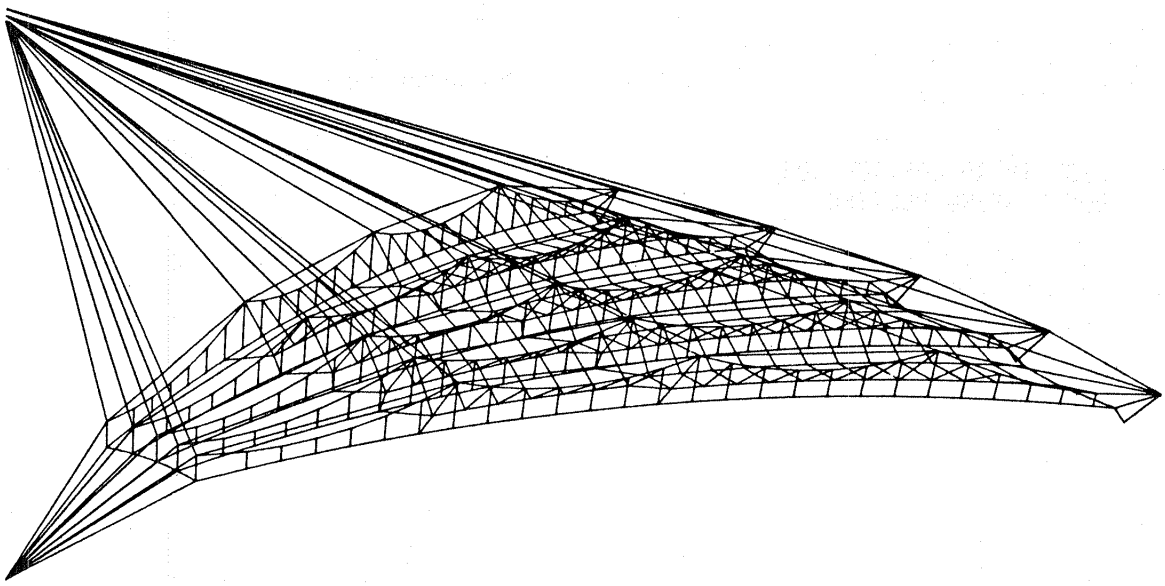

SURFACE EFFECTS OF CONTROL CORD DISPLACEMENT

The figure below shows the surface effects of a 2.5-mm (0.10 in.) displacement along the number three control cord. The displacements of surface node points are indicated by the numbers on the figure which represent normal surface displacements in 0.025 mm (0.001 in.).

Iterative measurements and adjustments of either the model or analytical software will be performed during model testing. The influence coefficients of each adjustment will be determined analytically and correlated by test. This method will result in a full interaction model capable of predicting cable displacements required to enhance the surface in orbit.

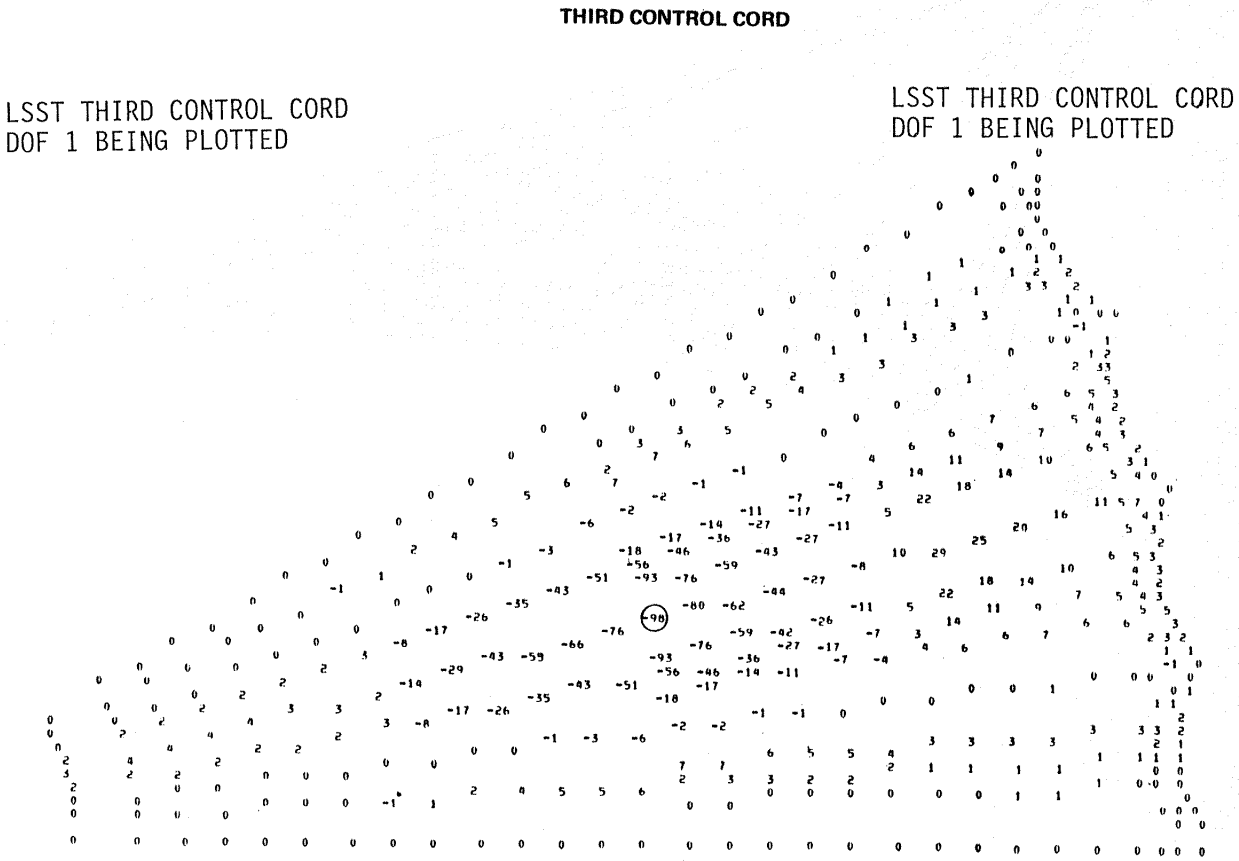

15-METER MODEL

A 15-meter diameter model will be fabricated in Phase II of the program to evaluate system level performance. The objectives of the task are stated below:

OBJECTIVES

VERIFY THE 100 METER POINT DESIGN IN TERMS OF:

- **DEPLOYMENT KINEMATICS**
  - **HOOP**
  - **MAST**
- **DEPLOYMENT RELIABILITY AND REPEATABILITY**
- **FAILURE MODES INVESTIGATION**
- **SURFACE INTERACTION**
- **MANUFACTURING TECHNIQUES**
- **SCALING**

15-METER MODEL CONFIGURATION

The artist's rendering below shows the configuration of the 15-meter model. The model will be capable of deployment and stow cycles, repeatability measurements, cup-up/cup-down contour measurements and a series of deployment and failure modes testing.

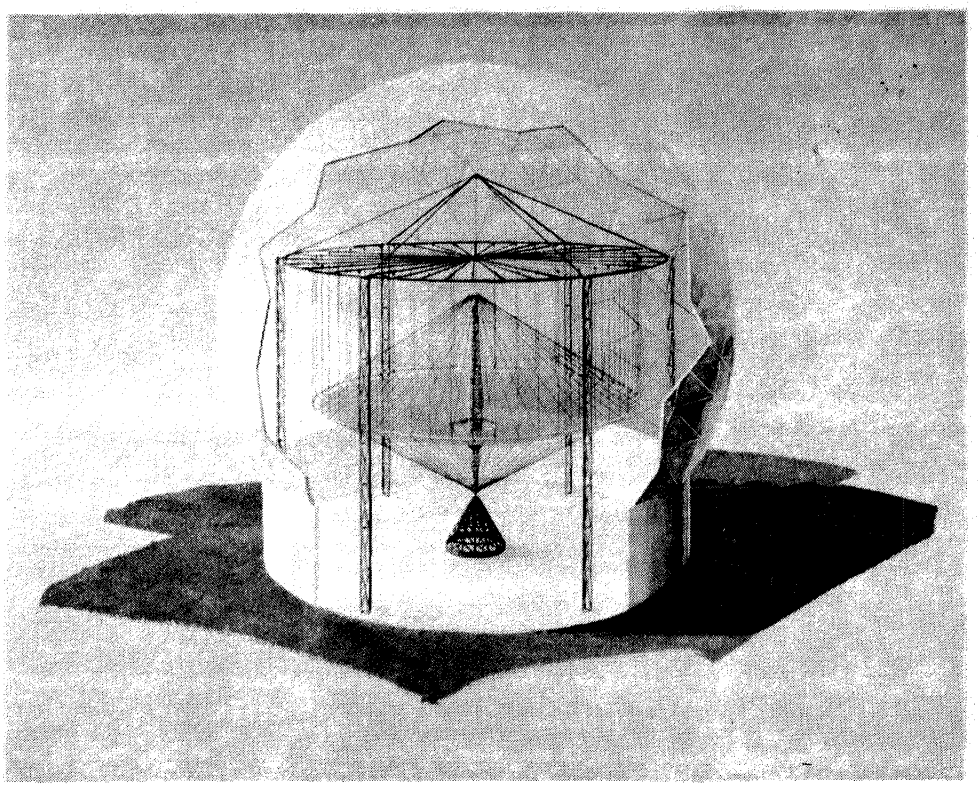

PHASE I RESULTS SUMMARY

- MET ALL TECHNICAL OBJECTIVES WITHIN COST AND SCHEDULE
- HOOP-COLUMN DESIGN FEASIBILITY IS VERIFIED
- HOOP-COLUMN SHOWN TO HAVE BROAD APPLICABILITY
- ADVANCED GRAPHITE CABLE STATE-OF-THE-ART

PHASE II PLANS

The program is accomplished in two phases. Phase I is completed and the activities are reported in this document. Phase II is initiated in FY 81 and completed in FY 84. The activities that are accomplished under each phase are summarized below:

TASK	PHASE I (COMPLETED)	PHASE II (PLANNED)
1. ANTENNA DESIGN AND PERFORMANCE	• COMPLETED PRELIMINARY DESIGN AND ANALYSES OF 100 m POINT DESIGN.	• UPDATE AS REQUIRED BY VERIFICATION MODEL TESTING. • ANALYZE THE STRUCTURAL EFFECTS OF REPLACING THE FRONT GRAPHITE HOOP CONTROL CABLES WITH DIELECTRIC (QUARTZ) CABLES.
2. MATERIAL DEVELOPMENT	• SELECTED CABLE MATERIAL AND CONSTRUCTION.	• DEVELOP DIELECTRIC FRONT HOOP CONTROL CABLES. • DEVELOP STATISTICAL BASIS ALLOWABLES FOR CABLE PROPERTIES.
3. ADVANCED CONCEPTS	• COMPLETED.	• NO ACTIVITY PLANNED.
4. ECONOMIC ASSESSMENT	• COMPLETED.	• UPDATE MODELS AND RESULTS TO REFLECT COST DATA FROM VERIFICATION MODELS.
5. DEMONSTRATION MODELS	• BUILT DESK TOP MODEL OF QUADAPERATURE POINT DESIGN. • BUILT FULL SCALE HOOP JOINT ELEMENT MODEL. • BUILT 1/6 SCALE DEPLOYABLE MAST MODEL. • DESIGNED 50 METER SURFACE BREADBOARD MODEL. • DEVELOPED CONCEPT FOR RF VERIFICATION MODEL.	• BUILD AND TEST 50 METER SURFACE BREADBOARD MODEL. • BUILD AND TEST RF VERIFICATION MODEL.
6. 15 m ENGINEERING MODEL	• DEVELOPED CONCEPTUAL DESIGN.	• DESIGN, BUILD, AND TEST 15 METER DIAMETER ENGINEERING MODEL.

3.0 SYSTEMS REQUIREMENTS

The LSST program identified specific spaceborne focus missions which require state-of-the-art large antenna structural developments for successful implementation. Specifically, these missions include the soil moisture radiometer, very long baseline interferometry (VLBI), and communications. The focus mission descriptive data is listed in Figure 3.0-1. During the formative stages of the LSST program, the missions data were interpreted in terms of the required aperture sizes, shapes, and performance. Since aperture performance is defined by a number of mission dependent factors, specific reflector parameters (F/D, RMS roughness, etc.) become mission dependent. A description of how the reflector characteristics have been systematically derived from the LSST focus mission requirements is defined in Paragraph 3.1. Applicability of the Hoop/Column antenna for designs other than those defined in the focus missions is discussed in Paragraph 3.2.

3.1 Development of Antenna Requirements and the Point Design Philosophy

Specific focus missions for communications, microwave radiometry, and radio astronomy were provided by NASA along with specific antenna/spacecraft configurations which served as a first step in defining the systems associated with these missions. Harris then developed a more detailed antenna parameter list which was used to fully characterize these antenna systems. This list was used as a basis for evaluations to identify the critical technologies associated with each antenna system. These critical technologies have been termed technology drivers. The technology drivers from the three missions have been traded to define a mission configuration which would be best suited for the point design. Specifically, the radiometer (HRSMR) mission design, Figure 3.1-1, requires a significant advancement of the state-of-the-art in large deployable spherical reflectors of approximately 660 meters. Extremely long booms of 573 meters and circular arrays of 177 meters also needed development. These and other significant technology drivers placed this mission application of large space structures in the far term category.

LSST MISSION SCENARIO SUMMARY

MISSION / PARAMETER	COMMUNICATIONS				MICROWAVE RADIOMETER SYSTEM	RADIO ASTRONOMY (VLBI)
	ADVANCED		PSS			
FREQUENCY (GHz)	4-6	11-14	0.87	2.0	1.4	1.4-22
POINTING ACCURACY (DEGREES)	0.035	0.035	0.035	0.035	0.1	0.01
BEAM NUMBER	219	219	TBD	219	200-300	1
BEAM ANGLE (DEGREES)	0.256	0.256	TBD	0.256	0.06	FREQUENCY DEPENDENT
BEAM ISOLATION (dB)	-30	-30	-30	-30	N/A	N/A
ORBIT ALTITUDE	GEO	GEO	GEO	GEO	LEO	LEO
RESOLUTION (km)	N/A	N/A	N/A	N/A	1	10^{-5}/SEC* / 10^{-3}/SEC**
REVIST COVERAGE (DAYS)	N/A	N/A	N/A	N/A	3	N/A
SWATH ANGLE (DEGREES)	N/A	N/A	N/A	N/A	$\pm$30	N/A
LIFE TIME (YEARS)	>20	>20	>20	>20	>20	>20

*TARGET
**GOAL

Figure 3.0-1. Focus Mission Data for Communications, Radiometry and Radio Astronomy

RADIOMETER TECHNOLOGY DRIVERS

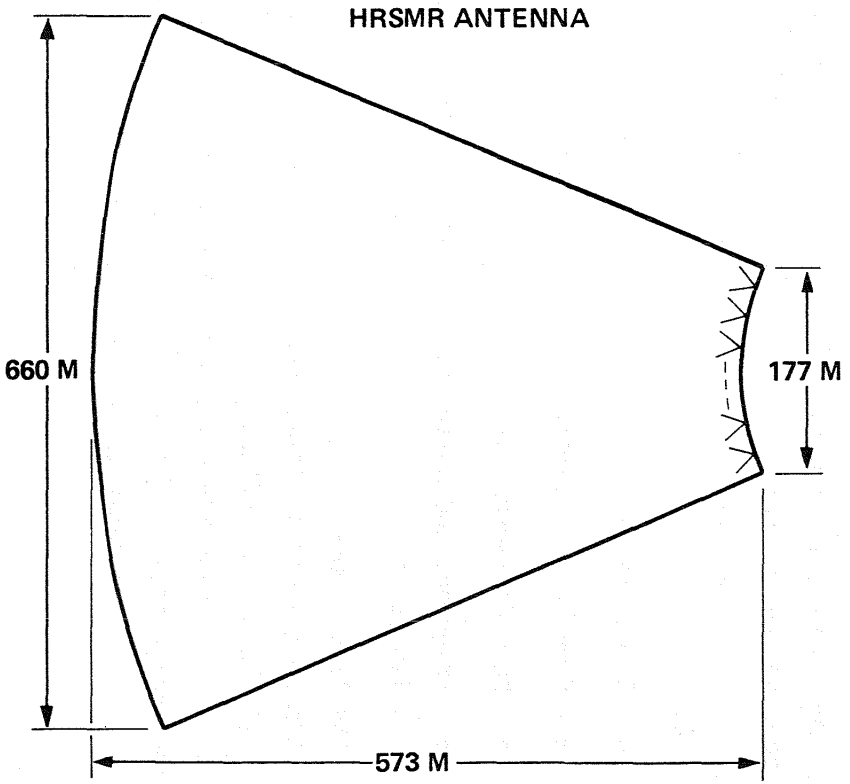

HRSMR ANTENNA REQUIREMENTS

- 660 METER SPHERICAL REFLECTOR
- 177 METER CIRCULAR FEED ARRAY
- 573 METER BOOMS
- 200 FEEDS/FEED ARRAY
- OPERATING FREQUENCY: 1.4 GHz
- BEAM EFFICIENCY OF 94%
  - λ /50 SURFACE ROUGHNESS
  - EXTREMELY LONG FEEDS OR SOPHISTICATED MATCHING TECHNOLOGY
- ORBITING ALTITUDE: 650 km

Figure 3.1-1. Radiometer Technology Drivers

Further trade-offs were performed on the Communications and Radio Astronomy missions and it was concluded that the Advanced Communications mission possessed the largest number of technology drivers which were realizable in near term, i.e., in the 1990's.

The Advanced Communications system requires operation in the 4-6 GHz and 11-14 GHz bands simultaneously. It was decided early in the evaluation of this mission that enough difficulty in the area of new technology would be experienced for a single frequency band. Hence, the 11-14 GHz requirement was dropped until the design matured significantly. Referring again to the Advanced Communications mission requirements (Figure 3.0-1), it can be seen that 219 very closely spaced beams covering the Continental United States (CONUS) is required. This system must be centrally located over the U.S. in geosynchronous (GEO) orbit, meaning that the coverage comprises a solid angle of $\pm 3^{o}$ E-W by $\pm 1.5^{o}$ N-S about the antenna centered boresight. Utilizing this information and working backing through the design process places rather difficult feed design constraints on this system. It was understood that the antenna system for this application would possess the following characteristics:

- Offset reflector to eliminate blockage
- High F/D to minimize coma distortions
- Beam Crossovers at the -3 dB power points
- Frequency and polarization diversity to maximize beam-to-beam isolation

The large number of beams, the relatively high beam crossover level, and the beam isolation requirements revealed that an antenna design utilizing a single offset reflector would not simultaneously meet those system goals. Initially, a high F/D = 1.5 was chosen to minimize coma distortions and low cross polarization. The feed illumination function was chosen to have a -15 dB reflector edge taper to maintain low secondary near-in and far-out side lobes (established by the beam isolation requirements). With these design criteria it was found that the secondary beam crossovers would occur at

the -9 dB levels, which does not meet the crossover requirements (see Figure 3.1-2). Four offset apertures must be used with secondary beam interleaving to accomplish the beam plan design goal. Harris chose to utilize a single parent reflector system with four offset apertures (Figure 3.1-3). This antenna configuration is termed the Quad Aperture. Each offset aperture has an individual boresight. The boresights of all apertures (A, B, C, and D) are not coincident but are parallel which implies that the reflector surfaces form cusps rather than a continuous surface. Each offset aperture is fed by an individual feed array containing one-fourth of the total number required to create 219 secondary beams.

The baseline design description and characteristics are detailed in the Antenna Specification and Requirements Document (ASRD) prepared in this program. Final disposition of this document is under joint control of NASA and Harris. Updates to this document will be made at TBD intervals to ensure that the system baseline is maintained. A description of the contents of the ASRD is contained in Figure 3.1-4.

The Advanced Communications technology drivers would significantly advance the antenna state-of-the-art. However, the point design selected on this program must result in a system configuration which meets the Advanced Communication mission in addition to being applicable to other applications which required a high level of technology readiness. This resulted in enlarging the Quad Aperture design for the 4-6 GHz band to a parent reflector diameter of 100 meters. The resultant individual aperture size (D/λ) was then appropriate to an operating band of 1.6-2.4 GHz (40.6 meters in diameter).

3.2 Hoop-Column Applicability

Since the Quad Aperture point design has been increased in size to advance technologies other than just those required for the Advanced Communications antenna system, a large deployable antenna technology base is available for applications to other missions. In particular, the missions associated with the Scenario Summary of Figure 3.0-1 would benefit from the point design technology developments. Additionally, missions not included in Figure 3.0-1 which have direct need of the available technologies from the point design are shown in Figures 3.2-1 through 3.2-4.

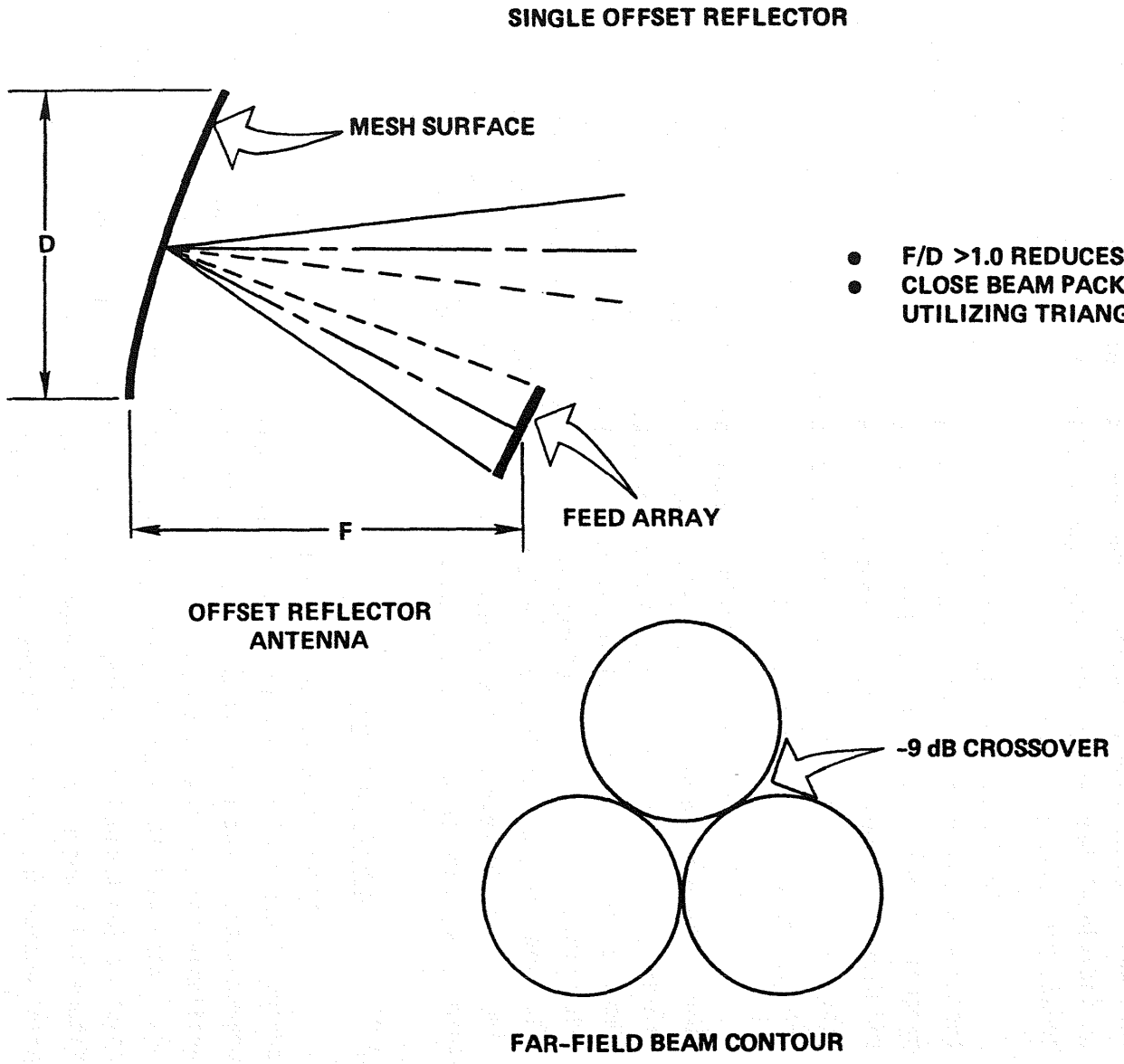

- F/D >1.0 REDUCES COMA
- CLOSE BEAM PACKING ACHIEVED BY UTILIZING TRIANGULAR LATTICE

Figure 3.1-2. Single Offset Reflector

QUAD APERTURE ANTENNA

FOUR OFFSET REFLECTORS

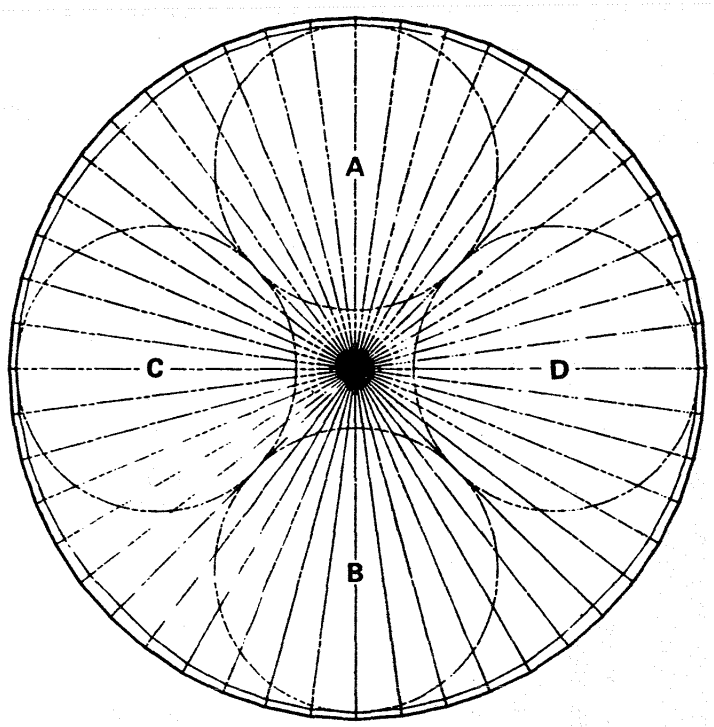

A) QUAD APERATURE REFLECTORS

FOUR REFLECTOR BEAM INTERLEAVING

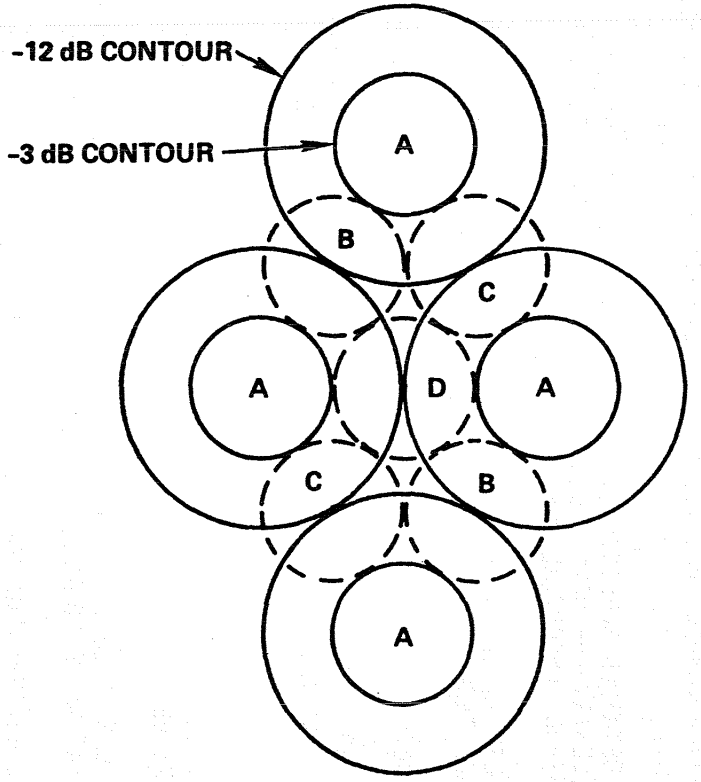

B) SECONDARY PATTERN CHARACTERISTICS

- -12 dB BEAMWIDTH 0.52°
- -3 dB BEAMWIDTH 0.26°
- 3° N-S BY 6° E-W CONTIGUOUS COVERAGE BY 219 BEAMS

Figure 3.1-3. Quad Aperture Antenna

- SCOPE

  - ESTABLISHES REQUIREMENTS FOR PERFORMANCE, DESIGN, FABRICATION, TEST, AND QUALITY ASSURANCE PROVISIONS OF 100-METER POINT DESIGN HOOP/COLUMN ANTENNA

  - CONTAINS DETAILED SPECIFICATIONS WHICH ENCOMPASS A COMPLETE ANTENNA PROGRAM (DESIGN → DEVELOPMENT → TEST → FLIGHT); BROADER IN SCOPE THAN EXISTING CONCEPTUAL DESIGN PROGRAM PHASE.

    - DETAILED ANALYSIS/TEST TASKS IN DOCUMENT DO NOT SUPERCEDE OR REPLACE TASKS ASSOCIATED WITH CURRENT DESIGN EFFORTS

    - DOCUMENT NOT INTENDED AS SOW FOR CONCEPTUAL DESIGN PHASE

    DOCUMENT PROVIDES PROGRAM FRAMEWORK AND BREADTH OF TASKS REQUIRED FOR EVENTUAL EVOLVEMENT INTO A FLIGHT HARDWARE PROGRAM PHASE

- FUNCTIONAL

  - SPECIFICATIONS ARE FOR A POINT DESIGN THAT IS NOT NECESSARILY MISSION-UNIQUE

    - WORST-CASE DESIGN PARAMETERS AND TECHNOLOGY DRIVERS FROM A COMBINATION OF COMMUNICATIONS, RADIOMETRY, AND ASTRONOMY MISSIONS

  - REPRESENTS ANTENNA PROGRAM WITH COMPOSITE COMPLEXITY $\geq$ COMPLEXITY OF ANY OF INDIVIDUAL MISSIONS

- REQUIREMENTS COVER: CONFIGURATION, PERFORMANCE (MECHANICAL AND RF), OPERABILITY (INCLUDING PRE-FLIGHT, FLIGHT, ORBITAL, AND OTHER ENVIRONMENTS), DESIGN AND CONSTRUCTION, INTERFACES, AND QUALITY ASSURANCE (INCLUDING DEVELOPMENT, ACCEPTANCE, AND QUALIFICATION TESTING)

- DOCUMENT IS "PRELIMINARY;" WILL BE UPGRADED, REVISED, REWRITTEN AS PROGRAM/DESIGN MATURES AND AS SHUTTLE DATA BECOMES AVAILABLE

  - NASA INPUTS NOT ONLY DESIRABLE BUT REQUIRED FOR MEANINGFUL DOCUMENT

Figure 3.1-4. Antenna Specification and Requirements Document Summary (Sheet 1 of 2)

- SUPPLEMENTARY APPENDICES
  - "A": STRUCTURAL ANALYSIS CRITERIA (JOHN SHIPLEY)
    - A CONCISE STRUCTURAL ANALYSIS APPROACH FOR THE FLIGHT PROGRAM
    - CONTAINS DEFINITION OF KEY TERMS, DETAILED STRESS PROCEDURES, DOCUMENTATION AND MODELING INFORMATION, REQUIREMENTS, ENVIORNMENTS, AND OTHER DETAILED STRESS-RELATED ITEMS
  - "B": THERMAL ANALYSIS CRITERIA (ERIK GRANHOLM)
    - A CONCISE THERMAL ANALYSIS APPROACH FOR THE FLIGHT PROGRAM
    - CONTAINS DEFINITION OF TERMS, DETAILED REQUIREMENTS LIST, DETAILED ENVIRONMENT DESCRIPTIONS, THERMAL ANALYSIS PROCEDURES AND APPROACH, DOCUMENTATION PLANS, AND MATERIAL PROPERTIES COMPILATION
  - "C": MANUFACTURING AND ASSEMBLY PLAN (TBD)

Figure 3.1-4. Antenna Specification and Requirements Document Summary (Sheet 2 of 2)

MOBILE COMMUNICATIONS SATELLITE

OPERATIONAL SYSTEM

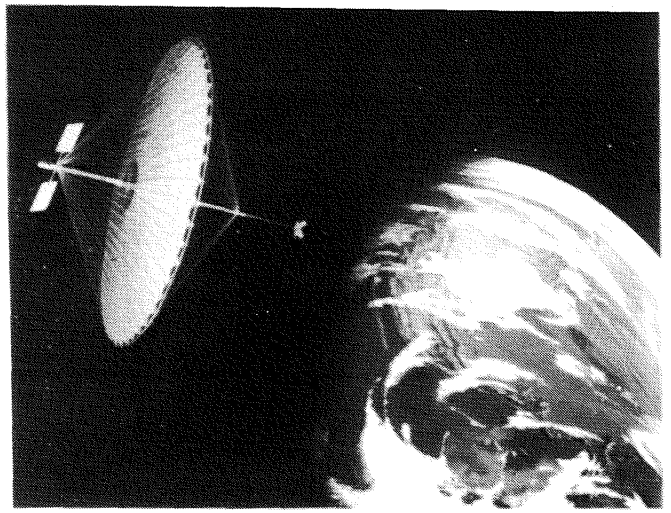

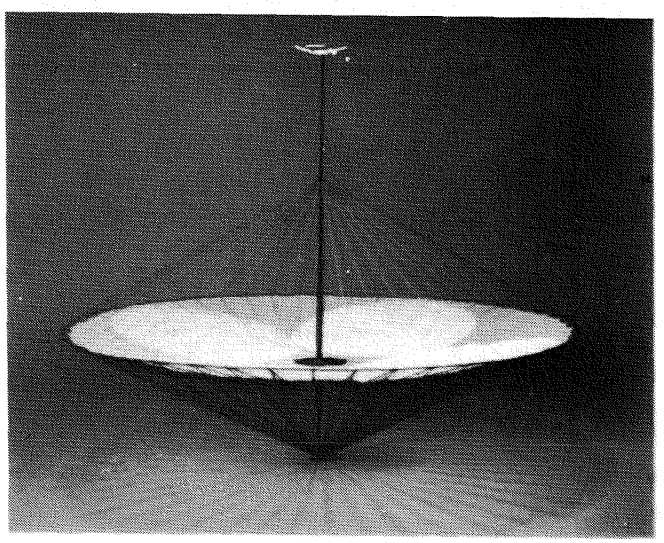

- U.S. DOMESTIC COVERAGE
- OPERATING BAND: 806–890 MHz
- FOUR SUB-BAND DIVISION
- SYSTEM OFFSET REFLECTOR SIZE INCLUDES:
  - 32 METERS (39 BEAMS)
  - 49 METERS (70 BEAMS)
  - 61 METERS (110 BEAMS)
- MULTIPLE REFLECTORS PROVIDE ADVANTAGES IN:
  - BEAM ISOLATION
  - FEED ARRAY AVAILABLE AREA
- HOOP/COLUMN QUAD APERTURE ALLOWS MULTIPLE REFLECTORS WHILE:
  - MINIMIZING DEPLOYMENT MECHANISM (ENHANCES RELIABILITY)
  - PROVIDING EFFICIENT STOWED VOLUME VERSUS EVEN TWO INDEPENDENT REFLECTORS
  - MINIMIZING WEIGHT

Figure 3.2-1. Mobile Communications Satellite

INTELSAT VI COMMUNICATIONS SATELLITE

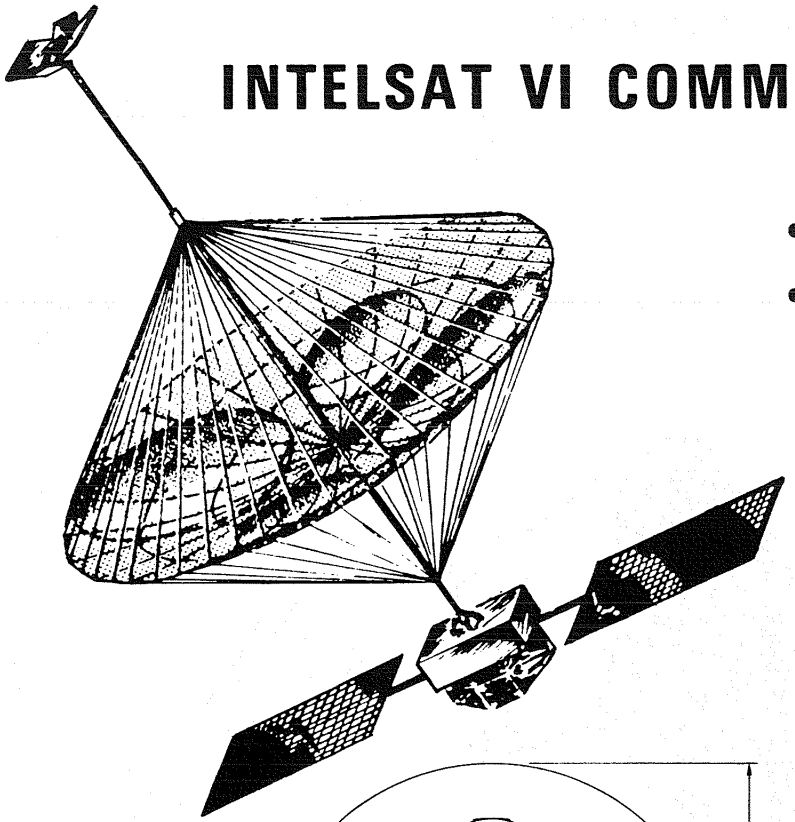

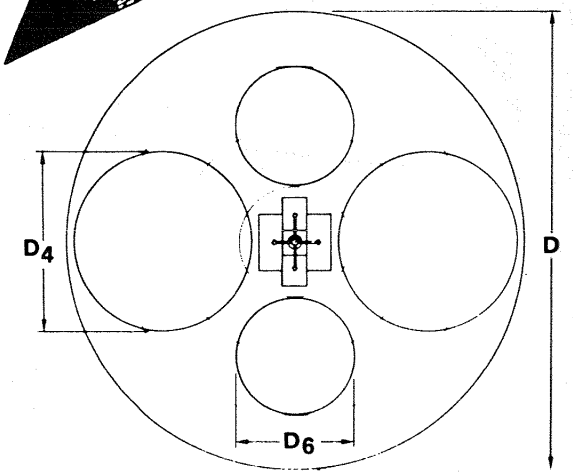

- SPECTRUM REUSE EXPANSION OF THE 4–6 GHz BAND
- ANTENNA SYSTEM REQUIREMENTS
  - DOWNLINK (3.7–4.2 GHz)
    - SPOT BEAM DIAMETER = 1.3°
    - 2 APERTURES
    - REFLECTOR DIAMETER (D_4) = 4.08M (13.4 FT)
  - UPLINK (5.925–6.425 GHz)
    - SPOT BEAM DIAMETER = 1.3°
    - 2 APERTURES
    - REFLECTOR DIAMETER (D_6) = 2.70M (8.8 FT)

QUAD-APERTURE HOOP/COLUMN PROVIDES EFFICIENT 4 REFLECTOR APPROACH:

- 11 METER DIAMETER
- EFFICIENT STOWED PACKAGE
  - 1 METER LENGTH
  - 0.5 METER DIAMETER
  - COMPATIBLE WITH ARIANE LAUNCH VEHICLE
- LOW WEIGHT: 150 POUNDS MAXIMUM

Figure 3.2-2. INTELSAT VI Communications Satellite

ORBITING VLBI RADIO ASTRONOMY

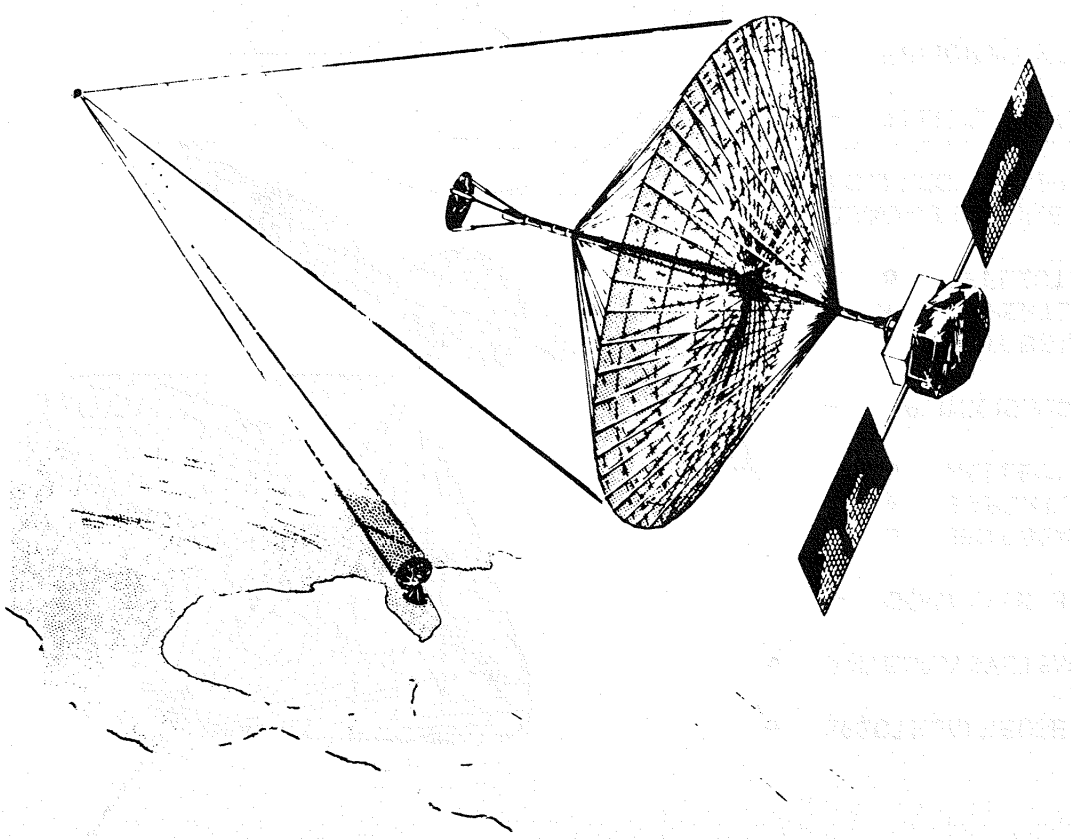

- NEAR TERM EXPLORER CLASS MISSION REQUIRES DEFINITION OF LARGE DEPLOYABLE ANTENNA CONCEPTS
- TWO ANTENNA SIZES (FREQUENCIES) EXAMINED:
  - 15 METERS (8.4 GHz)
  - 55 METERS (2.3 GHz)
- ANTENNA DIRECTIVITY/BEAMWIDTH IDENTICAL FOR BOTH ANTENNAS
- ANTENNA IS A DEPLOYABLE HOOP/ COLUMN CASSEGRAIN WITH F/D = 0.7
- FEED IS A HIGH EFFICIENCY MULTIMODE CORREGATED HORN
  - PROVIDES SYMMETRICAL BEAM IN ALL PLANES
  - HIGH FEED BEAM EFFICIENCY
- HOOP-COLUMN MEETS ALL ANTENNA REQUIREMENTS

Figure 3.2-3. Orbiting VLBI Radio Astronomy

FUTURE RADIOMETER MISSIONS

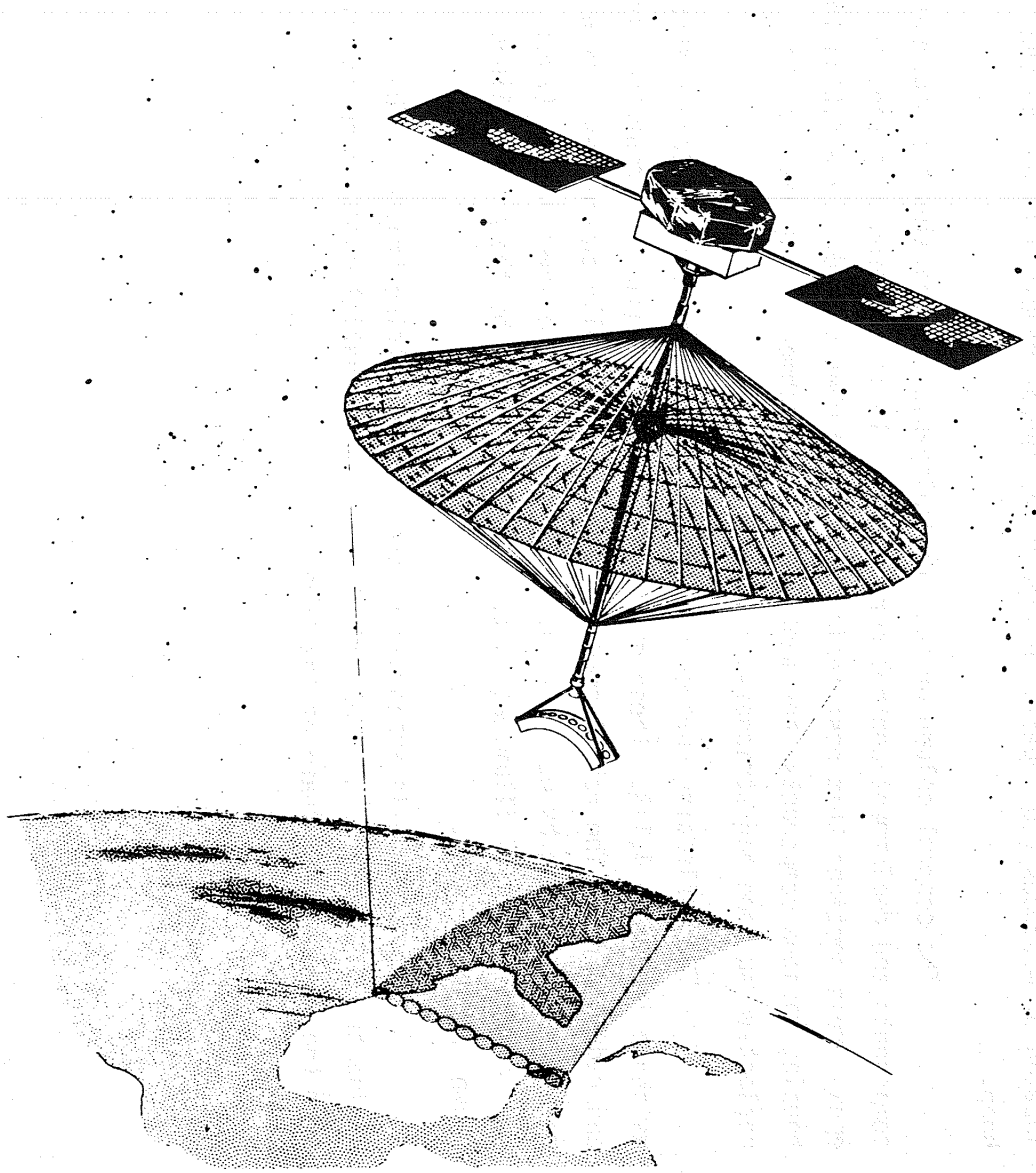

- REFLECTOR SIZES 30 AND 100 METERS
- OPERATING FREQUENCY: 1.4 AND 10 GHz
- RADIOMETERS REQUIRE ANTENNA (BEAM) EFFICIENCIES $\geq 90\%$
- FACTOR INFLUENCING ANTENNA EFFICIENCY INCLUDE:
  - ILLUMINATION EFFICIENCY
  - SPILLOVER EFFICIENCY
  - BLOCKAGE EFFICIENCY
  - FEED PHASE EFFICIENCY
  - SURFACE ROUGHNESS
- $\lambda/50$ ROUGHNESS RESULTS IN 98% EFFICIENCY
  - $\lambda/30$ SURFACE ROUGHNESS PROVIDES 94% EFFICIENCY
- HOOP/COLUMN MEETS RADIOMETER REQUIREMENTS

Figure 3.2-4. Future Radiometer Missions

4.0 POINT DESIGN DESCRIPTION

4.1 Introduction

The major elements of the Hoop/Column point design are delineated by Figure 4.1-1. The fundamental elements of the structure include the hoop, the upper and lower hoop support cables, the hub, and the upper and lower mast. This structure supports a RF reflective surface consisting of the mesh, shaping ties, secondary drawing surface, and the surface control stringers.

The hoop's function is to provide a rigid, accurately located structure to which the reflective surface attaches. It is comprised of 48 rigid segments which are hinged together to allow them to be compactly folded in the stowed configuration (see Figure 4.1-2). These segments are 6-inch diameter thin wall tubes constructed of graphite/epoxy laminate. Motors are located at 4 places (90^{o} apart) to supply the energy required to deploy the hoop.

The central column or mast is deployable and contains the microwave components and deployment control cord spools. It is composed of graphite/epoxy truss sections that nest inside each other when stowed. In addition to housing various components, the mast provides attachment locations for the reflective surface and stringers.

The reflective surface consists of four separate paraboloid dishes as shown in Figure 4.1-3. These dishes are shaped by means of circumferential and radial cords. The radial cord members are essentially catenaries, which maintain their shape by means of ties extending from the lower string truss cord members. The RF illumination area is represented by the phantom lines shown in Figure 4.1-3.

The surface is supported by the hoop and string trusses. The string trusses are a network of radial and circumferential cords which emanate from the mast and terminate at the hoop.

LSST POINT DESIGN – DEPLOYED

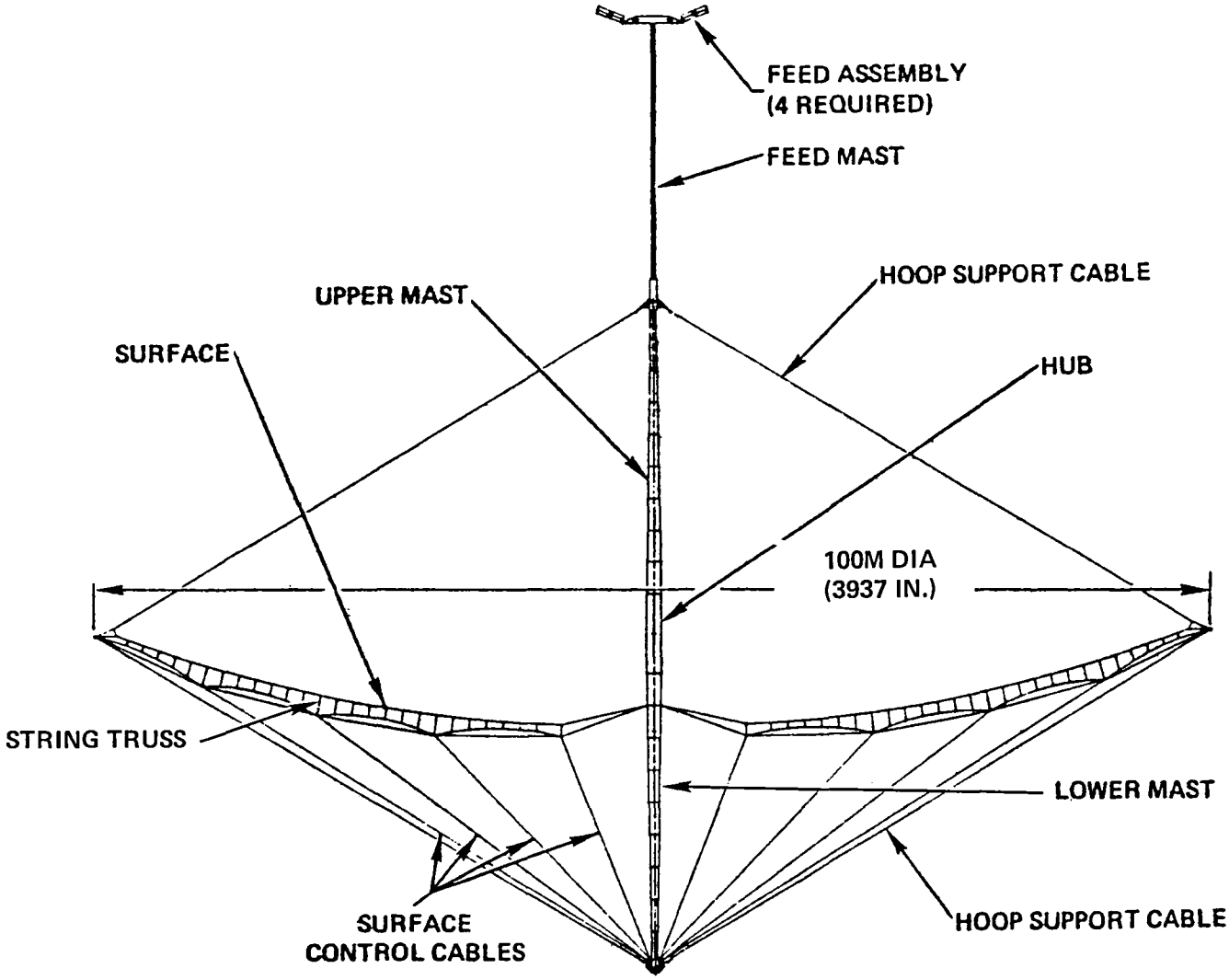

Figure 4.1-1. LSST Point Design - Deployed

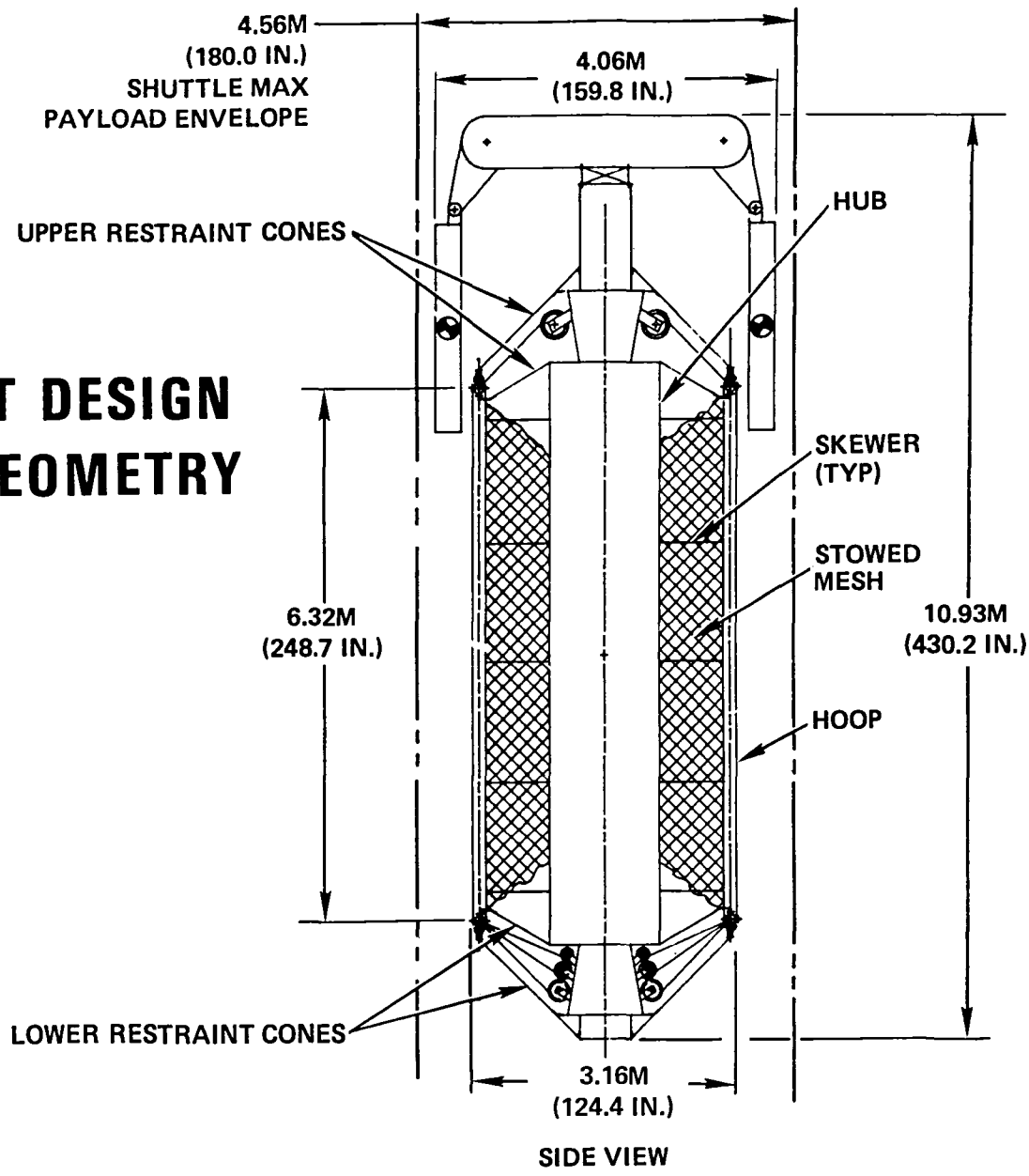

Figure 4.1-2. LSST Point Design - Stowed Geometry

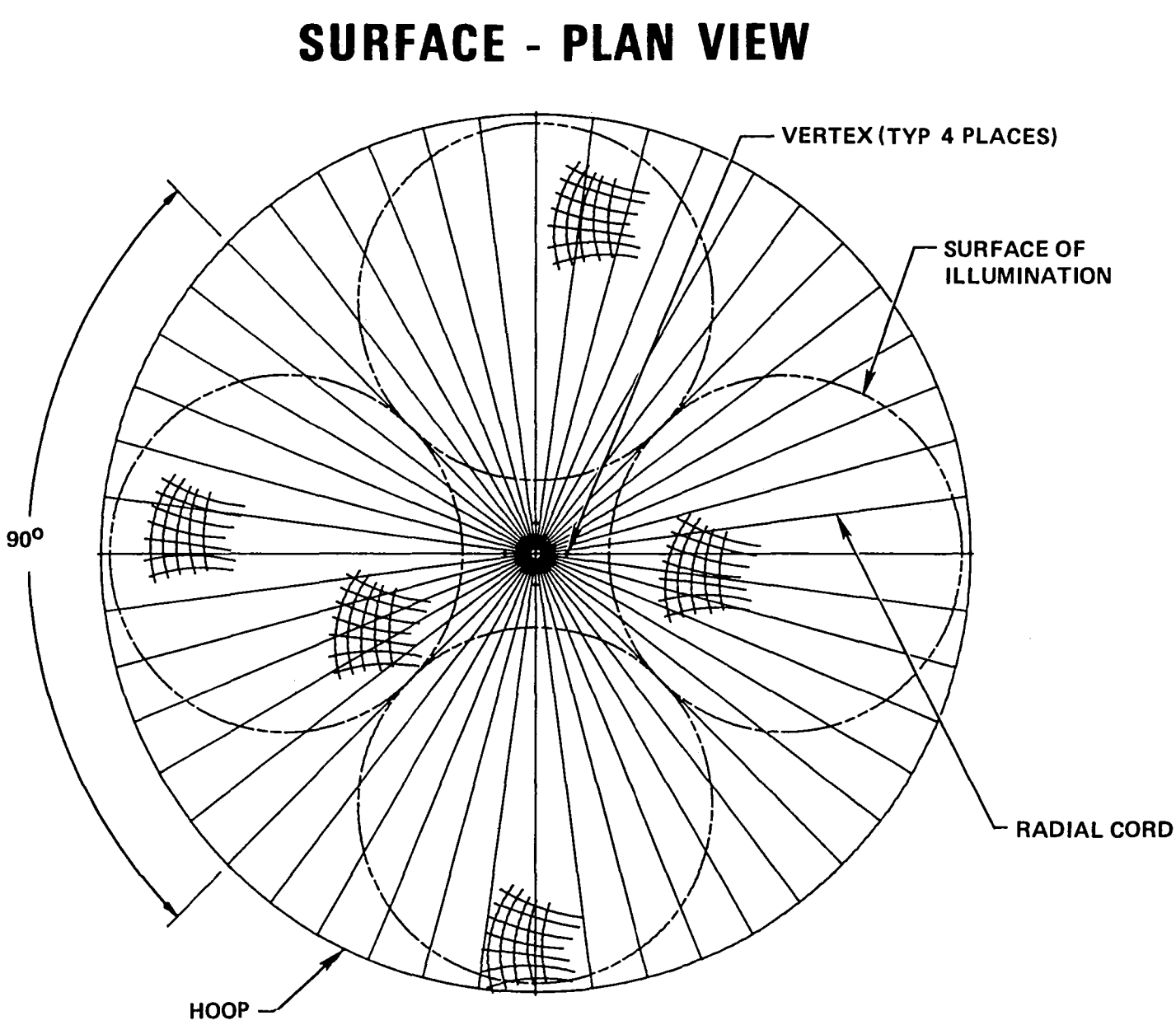

Figure 4.1-3. Surface - Plan View

The focal length of the surface is 62.12 meters and the diameter of each of the illumination surfaces is 40.6 meters, which corresponds to an F/D of 1.53 for each surface.

The deployment of the antenna is illustrated in Figure 4.1-4. It is initiated by the deployment of the cable driven mast. The hoop is then free to deploy. The hoop motors are activated and the hoop begins its synchronized deployment. The hoop is controlled with respect to the mast by means of the 96 hoop support cables, which emanate from the upper and lower extremities of the mast. After the hoop completes its deployment, the mast preload segment is deployed. This segment, by means of linear actuators, extends the mast through the last portion of its deployment and preloads the entire system.

The Antenna Restraint System consists of cone interfaces between the stowed hoop and column which react the axial, transverse and torsional loads created during the stowed environment.

The hoop support cables and the surface control cables are housed on reels which are energized by negator springs. These springs provide restowability of the cables and control of the hoop during deployment. In addition, they do not allow any slackage in the cables and are therefore snag preventives.

A mesh restowable cable system has also been integrated into the mesh management scheme. This cable is used primarily for management of the mesh during the antenna's restow cycle.

All of the above elements will be discussed in more detail in the following point design description.

4.2 Hoop Design

The hoop has a deployed diameter of 100 meters. When stowed, it nestles within the confines of the shuttle bay and has an outside diameter of 3.16 meters (see Figure 4.1-2). By virtue of its four motors it has sufficient power to deploy itself against:

LSST DEPLOYMENT SEQUENCE

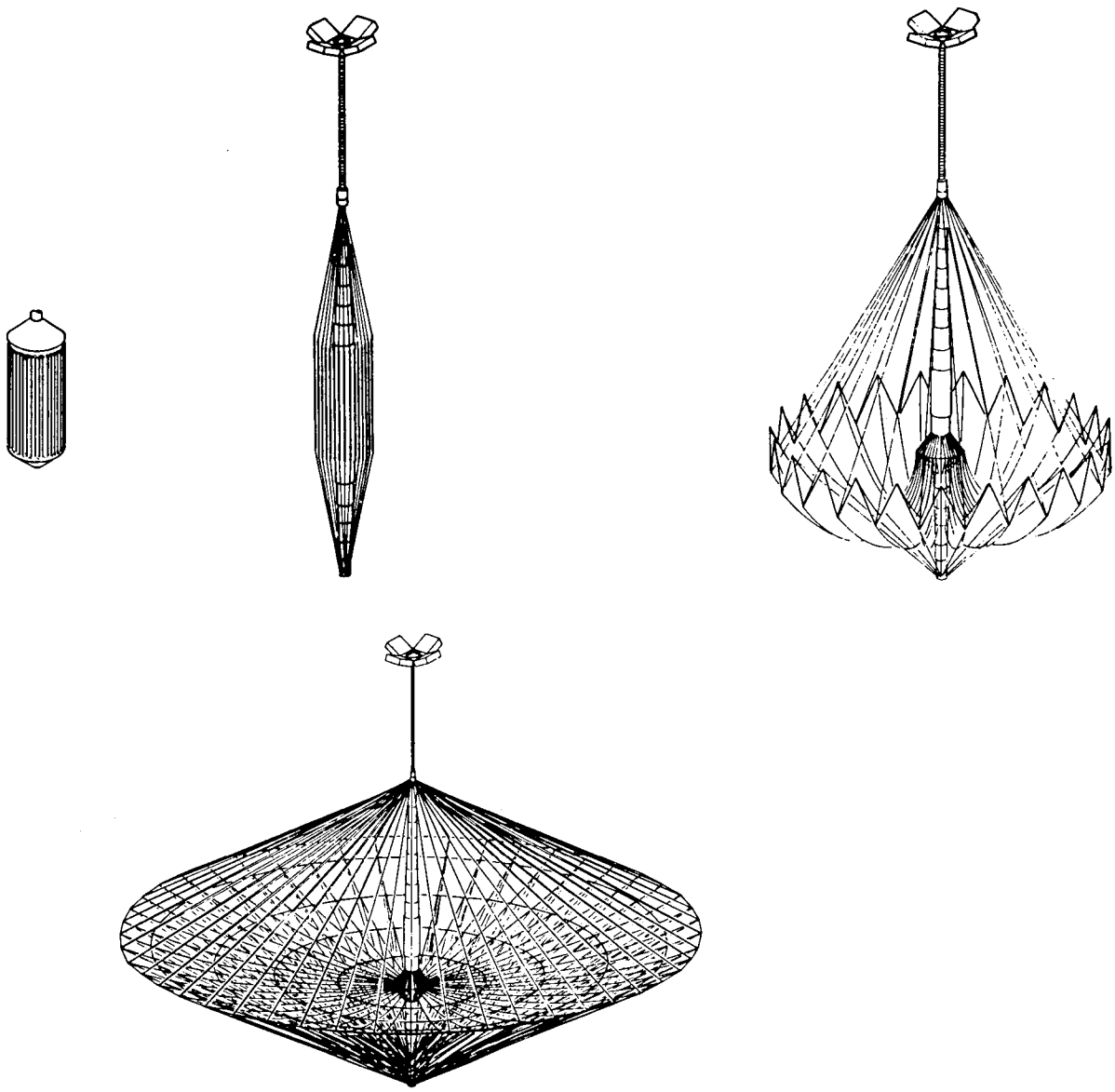

Figure 4.1-4. LSST Deployment Sequence

- The surface releasing from constraining skewers
- The forces developed by the hoop support and surface control cables as they unwind from their respective spools
- The hoop's own internal friction

In order to ensure a smooth and organized deployment, the joints are kinematically linked to one another. From a reliability view point this is highly desirable because of the hoop's ability to transmit the energy of the motors to any joint which is under stress due to either a linkage malfunction or a random snag.

The hoop has a double hinge at each joint as shown in Figure 4.2-1, which permits rotation from its vertical stowed position to its horizontal deployed position. The joints of the hoop describe a right circular cylinder at all stages during its deployment as shown in Figure 4.2-2. The individual hoop segments simply rotate from a vertical to horizontal attitude about an axis through the center of each member. These axes are radial lines forming a plane normal to the axis of the mast.

The hoop is energized by the four motors which are located 90^{o} apart. Graphite strips run from platform to platform to maintain the hinge platforms parallel to themselves during deployment. These strips, in conjunction with spherical ended push rods, kinematically link the hoop segments to one another providing the control necessary for synchronization of the hoop.

4.3 Mast Design

The mast, as shown in Figure 4.3-1, has a stowed height of 6.9 meters and a deployed height of 57.73 meters. When stowed, the mast preloads itself by means of a restraint cable. This preload allows the stowed mast to resist the inertial loads experienced during the preoperational environment. The mast deploys in a telescopic manner. It must deploy against the force of its restraint cable, the forces generated by the hoop support and surface control cables as they unwind from their spools, and the mast's own internal frictional forces.

SINGLE STAGE HOOP – SIDE VIEW

DEPLOYED POSITION

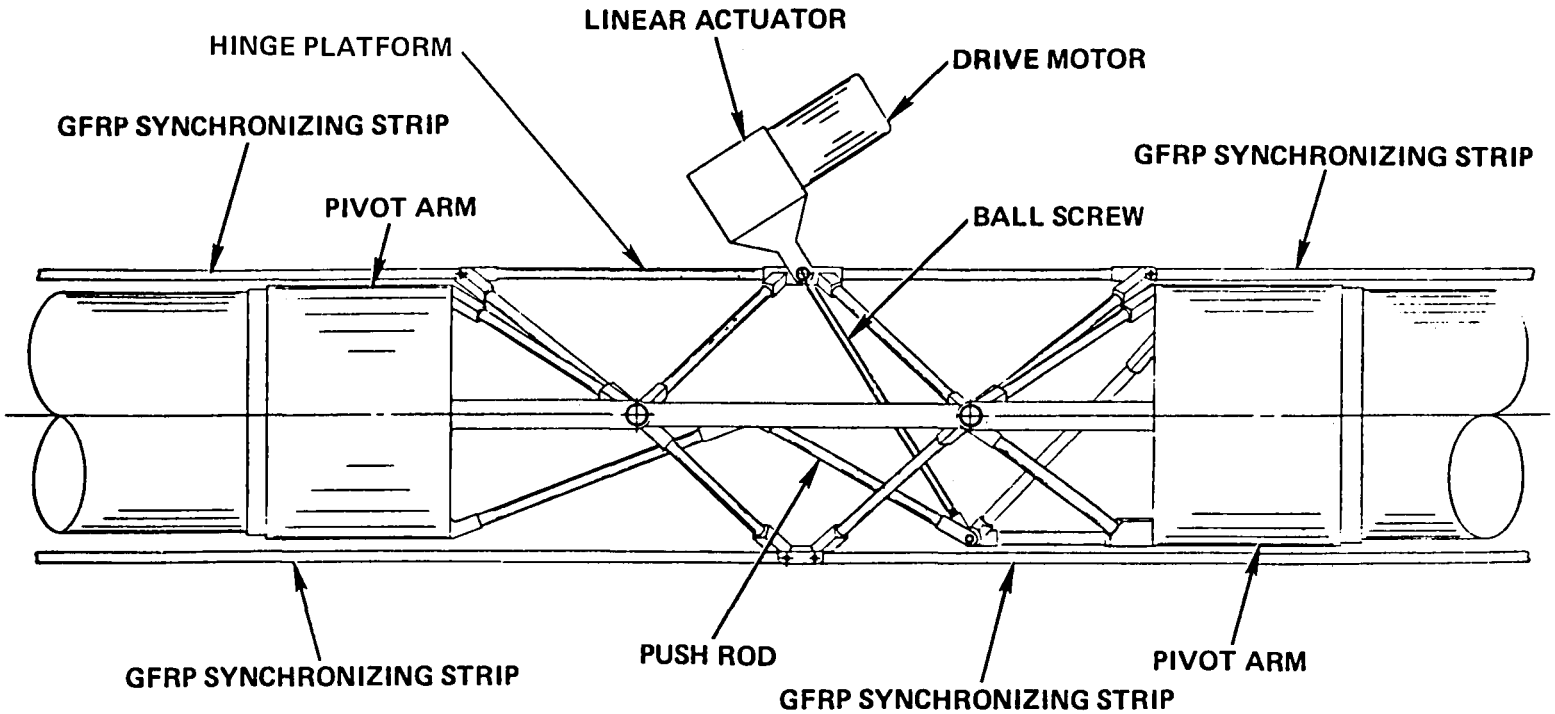

Figure 4.2-1. Single Stage Hoop - Side View

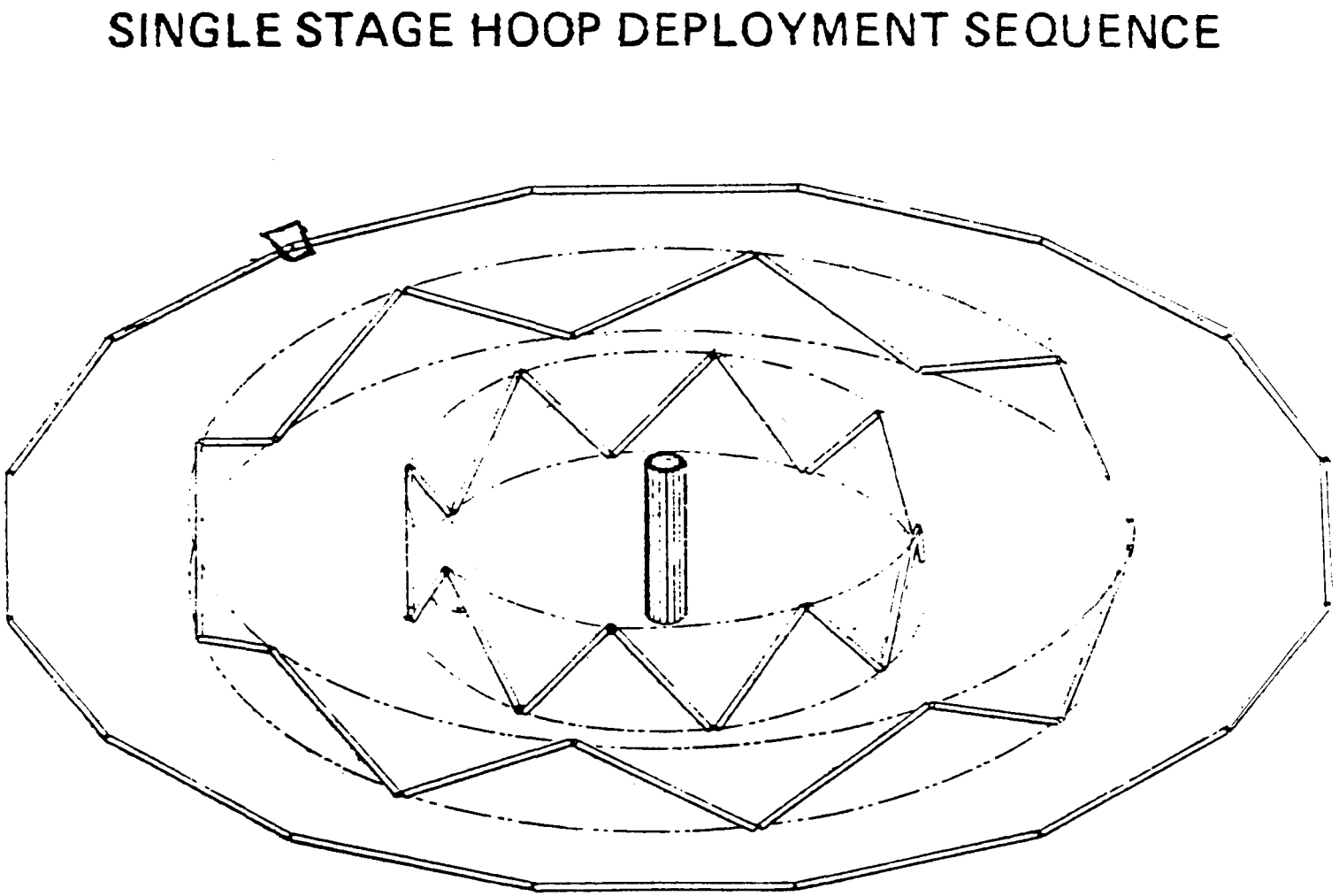

Figure 4.2-2. Single Stage Hoop Deployment Sequence

CABLE DRIVEN MAST

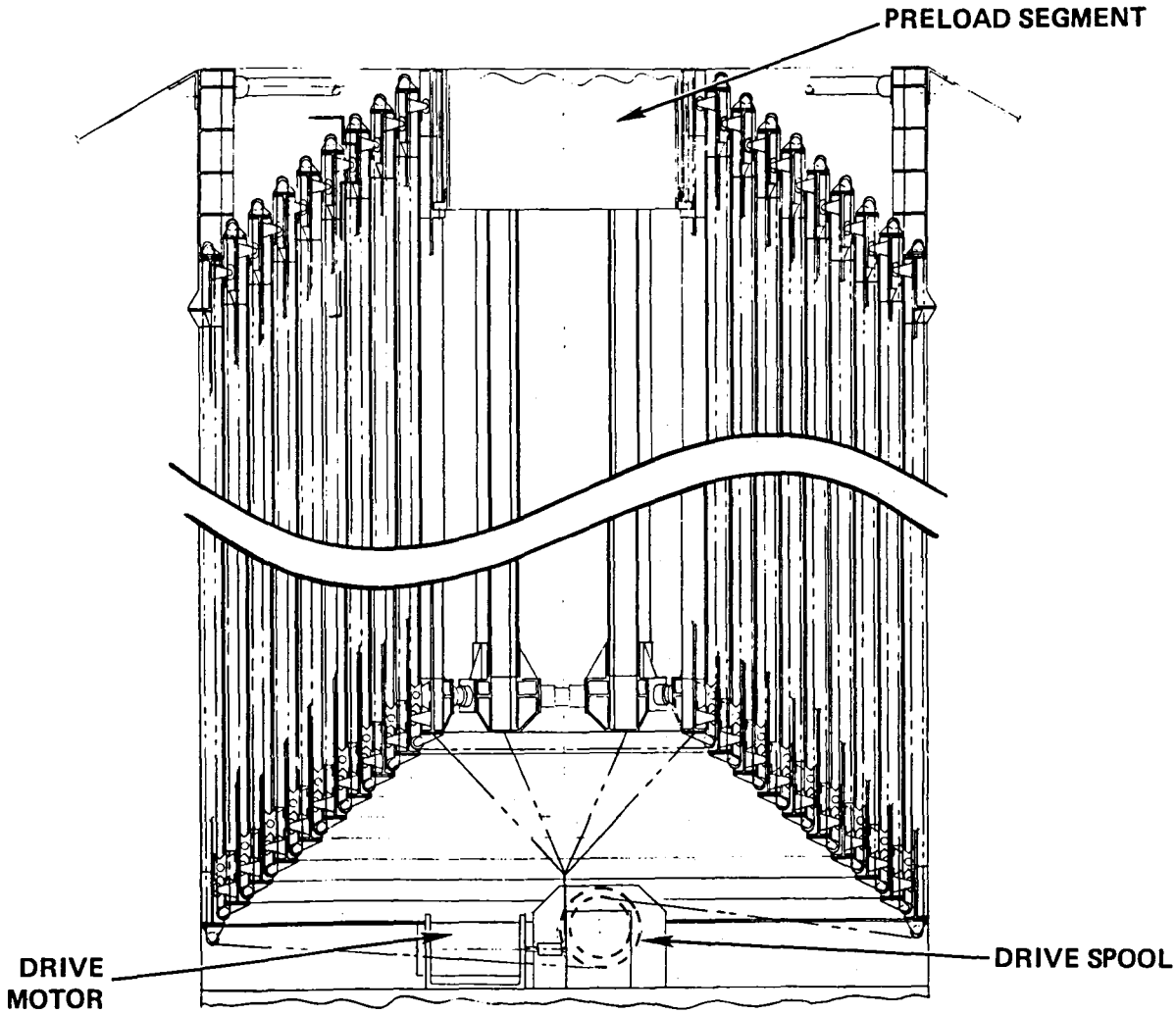

Figure 4.3-1. Cable Driven Mast

The mast is comprised of a lattice type structure and has a hexagonal cross section as shown in Figure 4.3-2. At each point of the hexagon a vertical tube section is located. These six members are the major load carriers of the mast. Each mast section is subdivided by circumferential rings, which have the effect of maintaining the $\frac{L}{\rho}$ of the tubes sections to 120 or less. The bays of each section are diagonally braced by graphite tension cables for shear stiffness.

The tubular sections also serve as tracks for the sections to translate with respect to one another. Each mast section has rollers located at its extremities on the upper and lower circumferential fittings. In addition, the latches which interface the sections to each other at deployment are housed within the lower circumferental fittings. The latches and rollers are depicted in Figure 4.3-3.

The deployment cable is routed through the outermost segment (hub) and over pulleys on the upper and lower flanges of adjacent sections. The cable is routed through a level wind device and terminated on a spool. In addition to the deployment cable, the restraint cable is also wound on this spool. This cable, which attaches to the innermost mast section, is used to restow the mast and also to restrain the mast during its deployment to prevent the mast from overrunning. The mast's deployment is initiated by retrieval of the cable upon the spool. The mast segments are then deployed in a proportional type manner until all segments are latched.

The innermost segment of this mast is screw driven as shown in Figure 4.3-4. It is comprised of three motors coupled to two actuator screws by worm gears. The purpose of this mast segment is to preload the entire antenna subsequent to the cable driven mast deployment.

The mast hub structure, shown in Figure 4.3-5, is identical to that described for the mast. It is the outermost segment of the entire mast and consequently the primary structural element of the mast. The hub's circumferential rings serve a dual function of dividing up the bays as well as providing slip joint interfaces for the mesh management skewers which extend radially from the hoop segments when stowed.

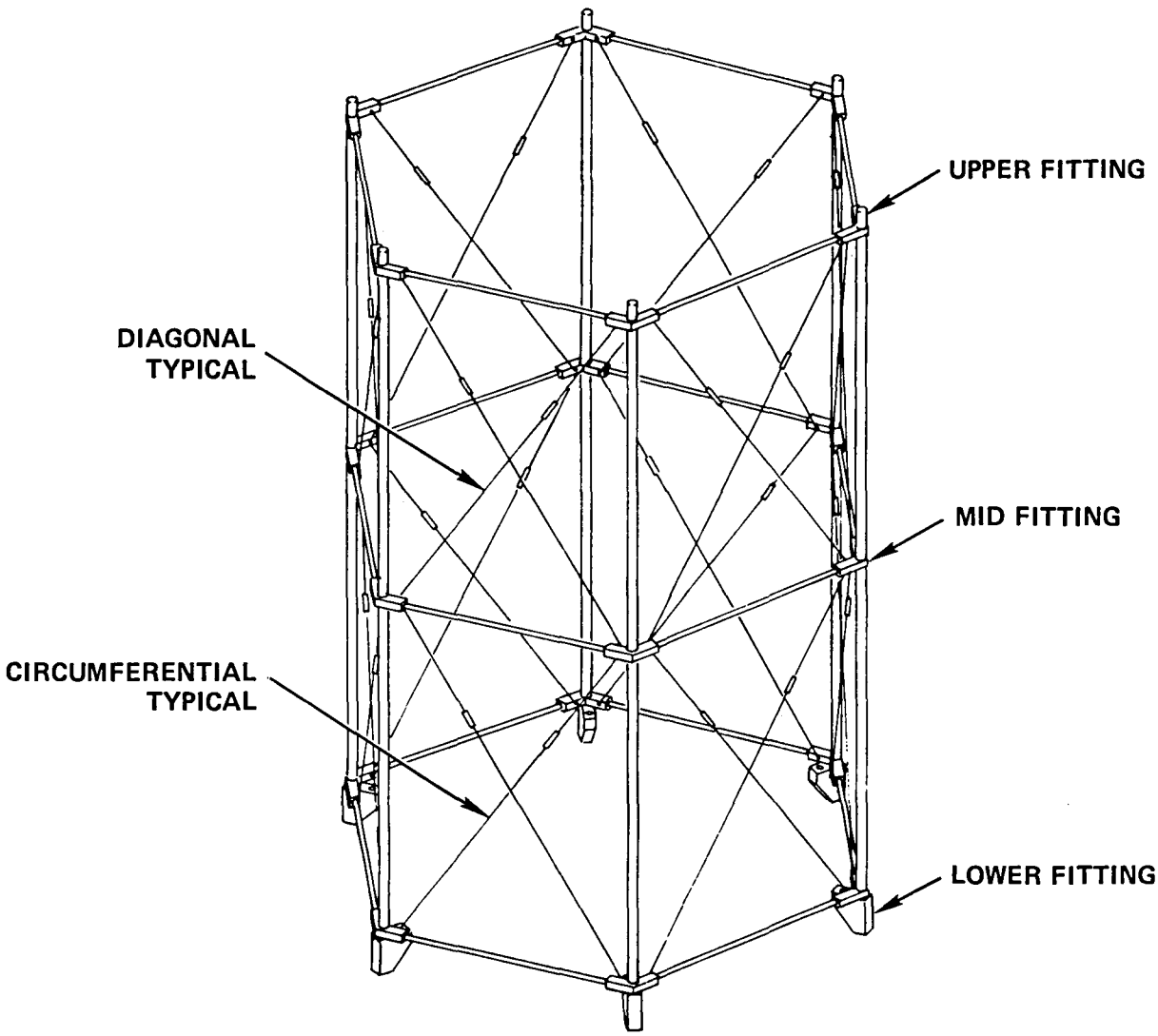

Figure 4.3-2. Typical Mast Segment

LATCH, PULLEY, ROLLER

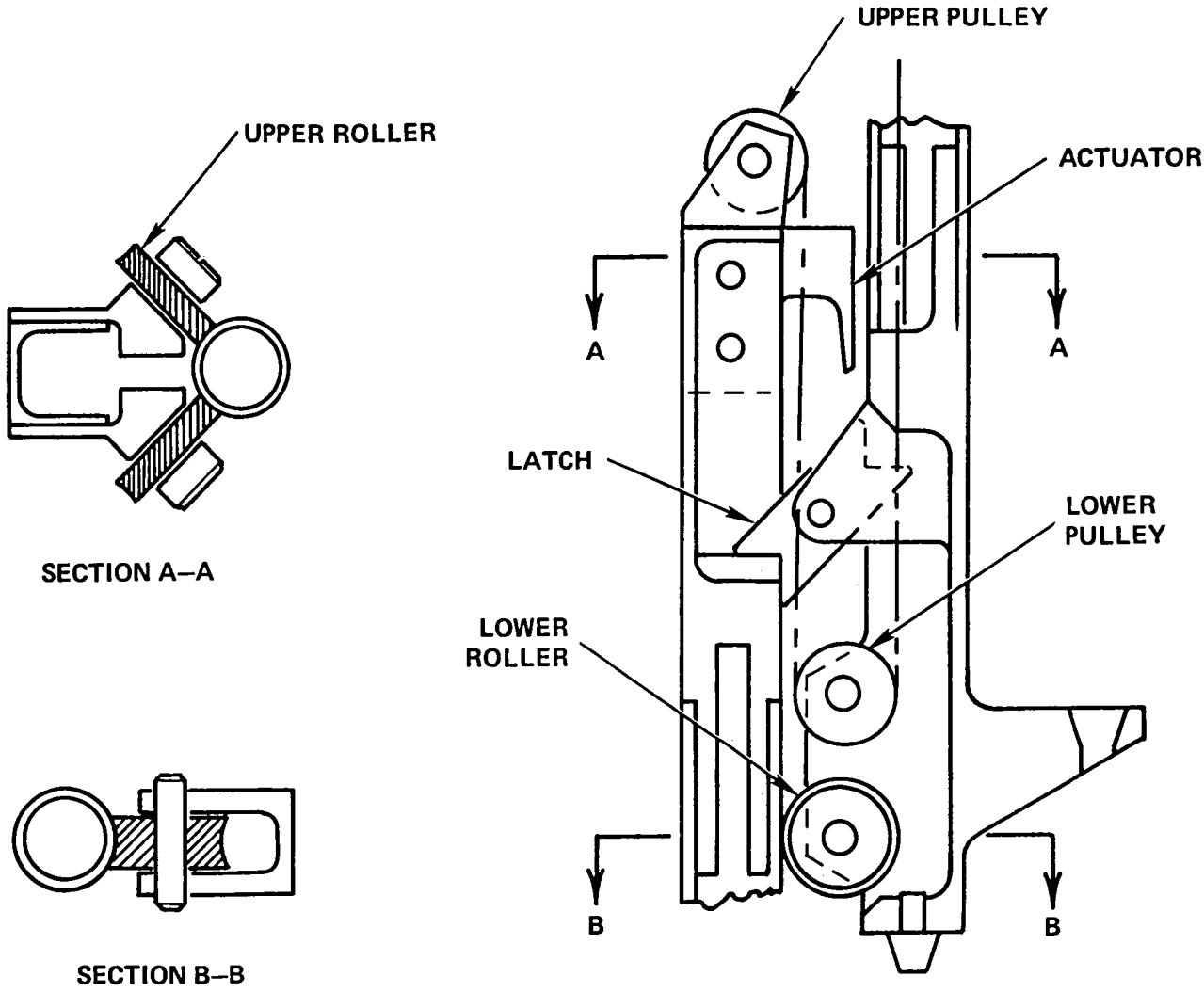

Figure 4.3-3. Latch, Pulley, Roller

PRELOAD MAST SEGMENT

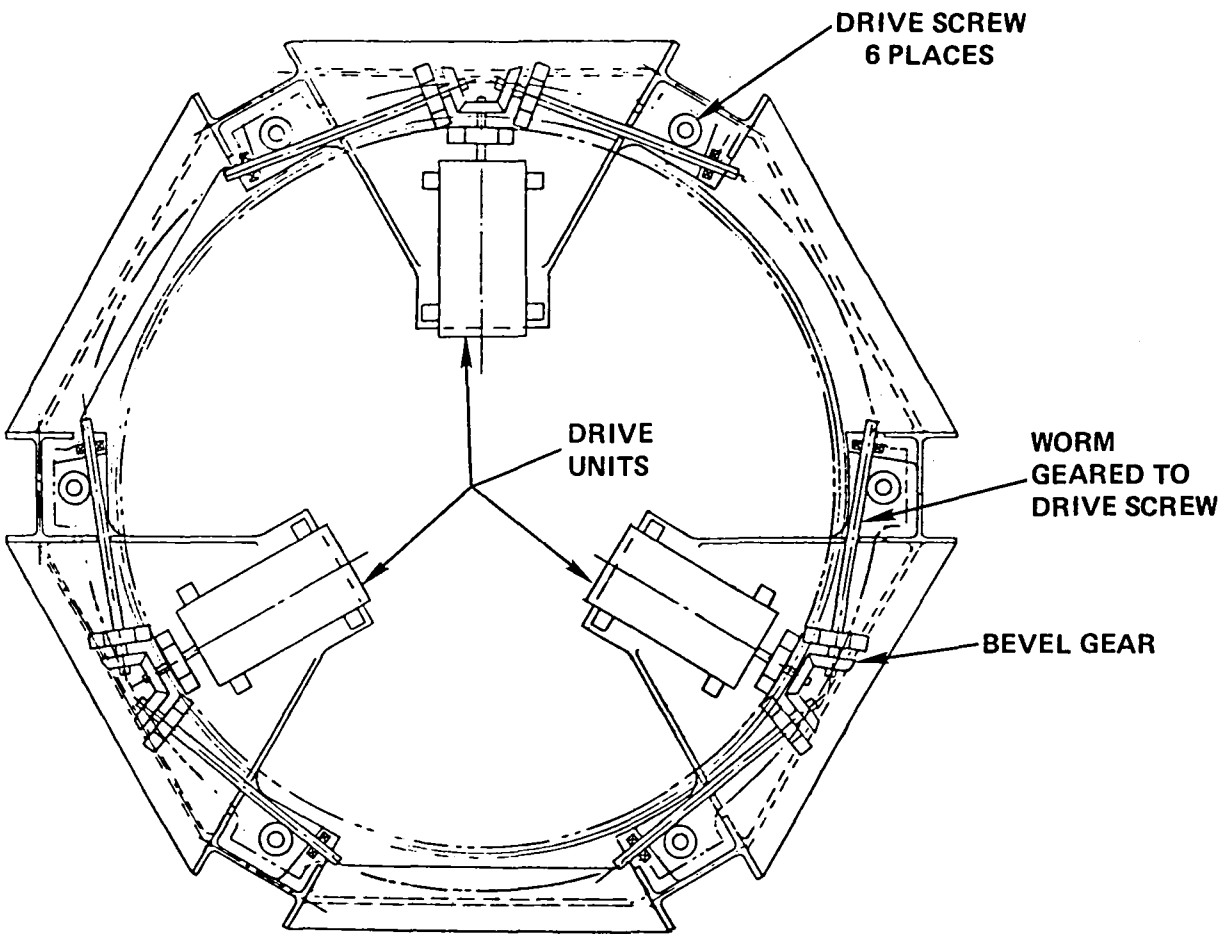

Figure 4.3-4. Preload Mast Segment

HUB

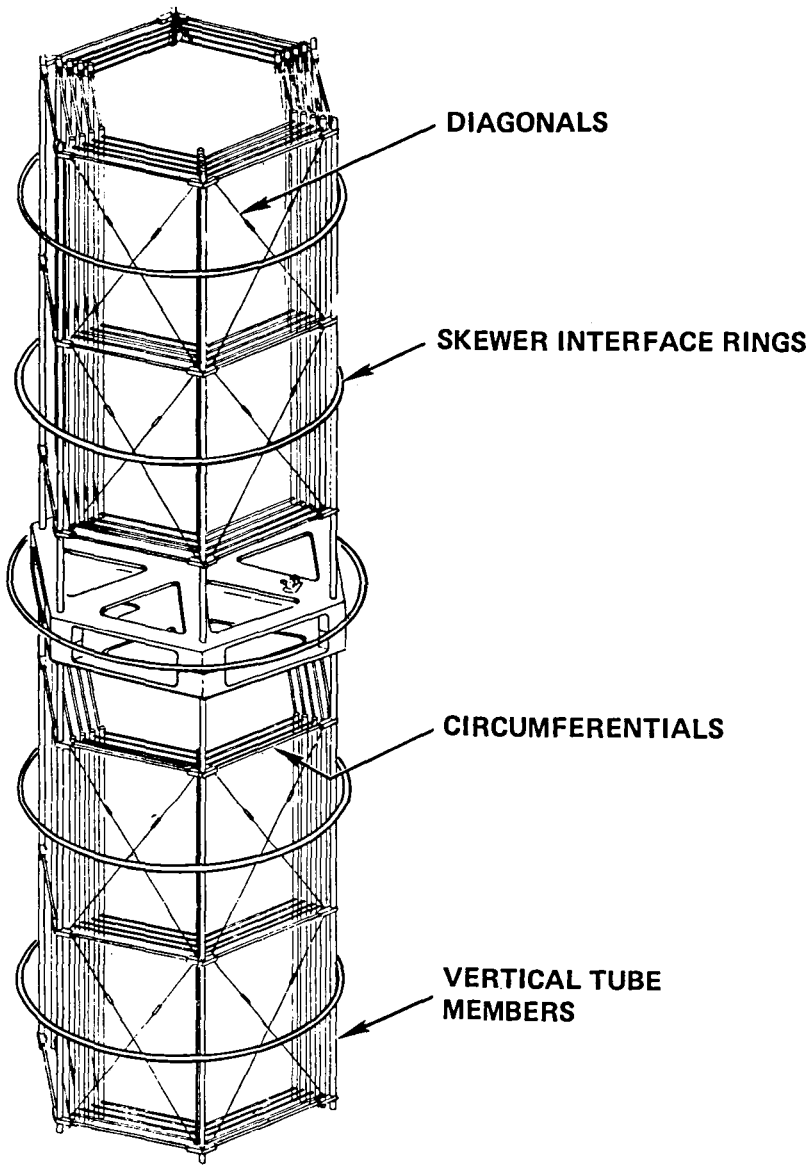

Figure 4.3-5. Hub

4.4 Surface Design

The basic geometry of the surface is dictated by the RF requirements. The point design antenna operates at a frequency of 2.0 GHz and has a beam to beam isolation of 30 dB down from peak power. To efficiently perform within this range, each of the four apertures must have a surface roughness RMS of no greater than 0.3 inch with a maximum defocus of 10 inches. A top view of the surface is shown in Figure 4.1-3. Each of the apertures are parabolic and have a diameter of 40.6 meters and F/D of 1.53. The overall surface of the antenna is comprised of 48 mesh gore segments.

The mesh is knit from 0.0012 inches diameter molybdenum wire and is gold plated to enhance its RF reflectivity. It is knit in tricot knit with 0.25-inch openings.

The parabolic shape of the mesh is maintained by means of graphite surface shaping ties which are located along the edge of each gore. These ties, shown in Figure 4.4-1, are connected to the gore edge cords which weave through the mesh to provide a load path. To minimize pillow effects, surface cords and ties are routed through the mesh in the pattern shown in Figure 4.4-2. The tie loads derived from the surface are reacted into the rear cantenaries. These cantenaries are supported at hard points which interface with the surface control cables. The surface control cables emanate from spools which mount on the base of the mast and are utilized in final adjustment of the surface subsequent to deployment.

Outboard and inboard intercostals react the radial tension field of the mesh and cords. The intercostals are graphite cords which are laced to the mesh. The intercostals also form the common interface between the surface and the hoop and hub.

The junctions of the cords and the intercostal end fittings are fabricated of low thermal expansion graphite/epoxy and invar. A detailed description of these junctions is provided in Paragraph 6.4.3.

RADIAL CORD

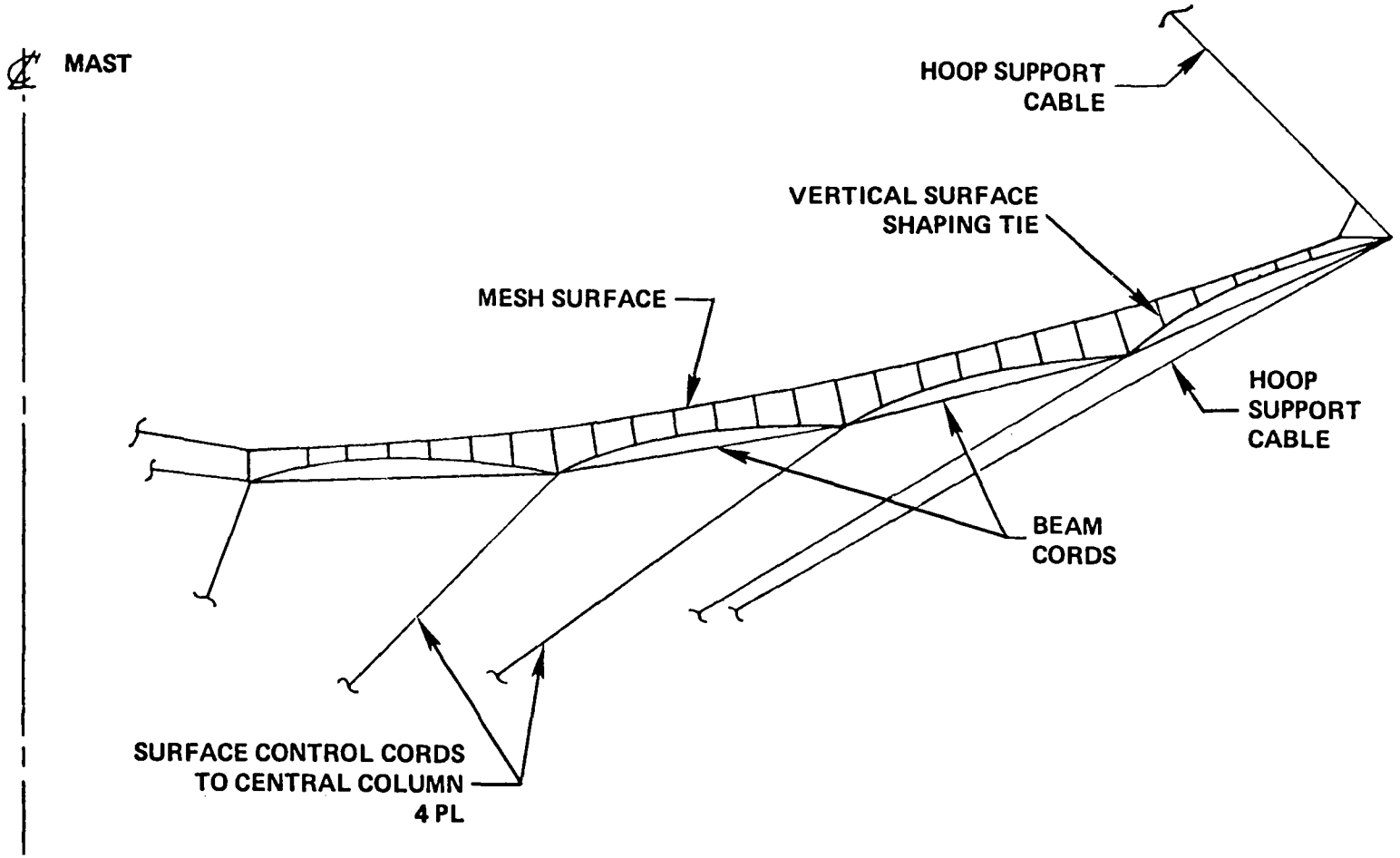

Figure 4.4-1. Radial Cord

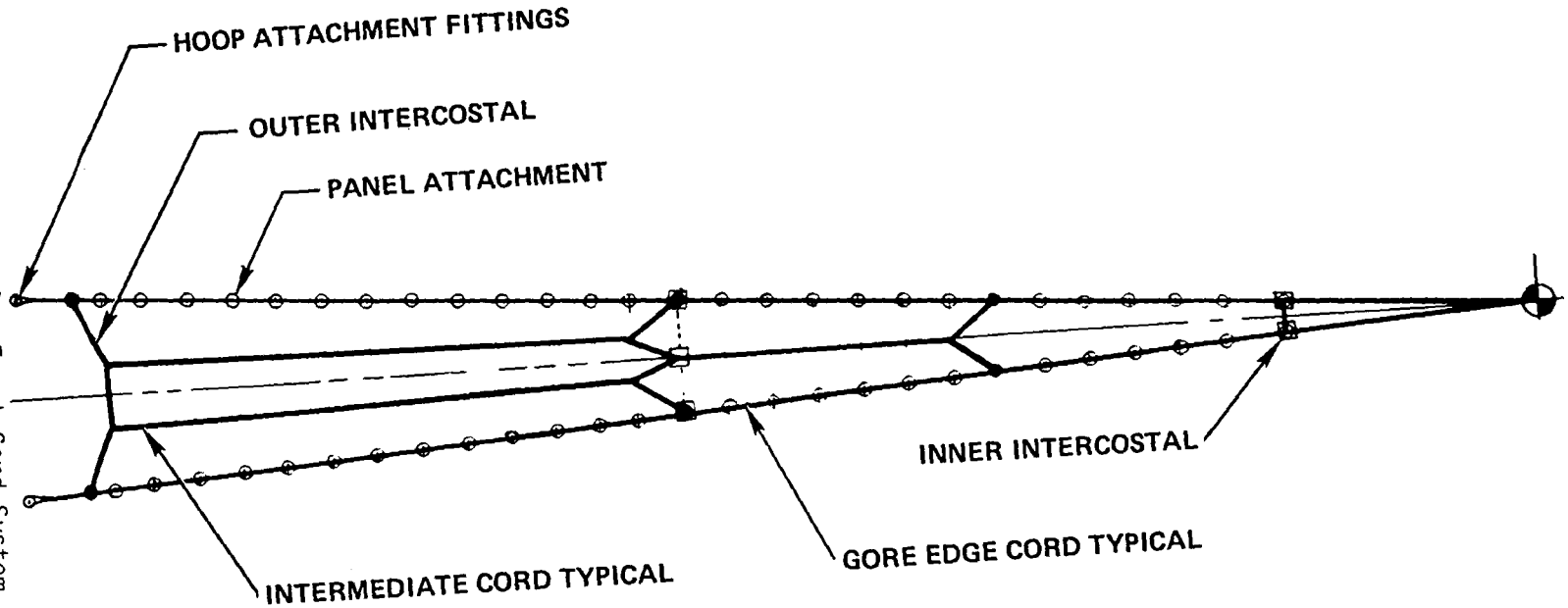

Figure 4.4-2. Front Cord System

4.5 Antenna Restraint System

The Antenna Restraint System is shown in Figures 4.5-1 and 4.5-2. The purpose of this system is to support the major components to withstand the stowed preoperational environments. The restraint system is comprised of upper and lower restraint cones which are attached to the upper and lower extremities of the mast. The cone interfaces six places with the hoop segments. These interfaces are cone and socket type joints and primarily react axial loads.

The upper and lower lateral restraint cones are attached to the upper and lower extremities of the hub. These cones interface with each of the 48 hoop segments in a "cradle" type manner and react torsional as well as lateral loadings. Upon deployment of the mast, the upper and lower restraint cones are decoupled from the hoop and is free to deploy radially from the cradle interfaces of the lateral restraint cones.

This restraint system lends itself well to restowability. Subsequent to the hoop's restorage into the cradles of the lateral restraint cones, the mast is stowed and reseated into the segments.

4.6 Hoop/Cable Management System (Figure 4.6-1)

The hoop is synchronized with respect to itself, however, there is a need for the hoop to be controlled with respect to the hub. It is desirable that the hoop deploy somewhat symmetrically with respect to the hub in elevation as well as radial. The hoop is controlled in this manner by means of the 96-hoop support cable spools. These spools are back driven against the deployment of the four hoop deployment motors. The back drive energy of these spools is provided by negator springs which are located internally to each spool as shown in Figure 4.6-2. During the hoop's deployment, these springs are reverse wound upon the two internal output spools. Upon restowage, the springs are rewound upon their respective storage spools. Each spool exerts approximately 1/2 pound tension in the cable, and the spools act independently. As the hoop deploys, it is kept in a symmetrical position with respect to the mast by virtue of the symmetrical load pattern from the control cables. In the

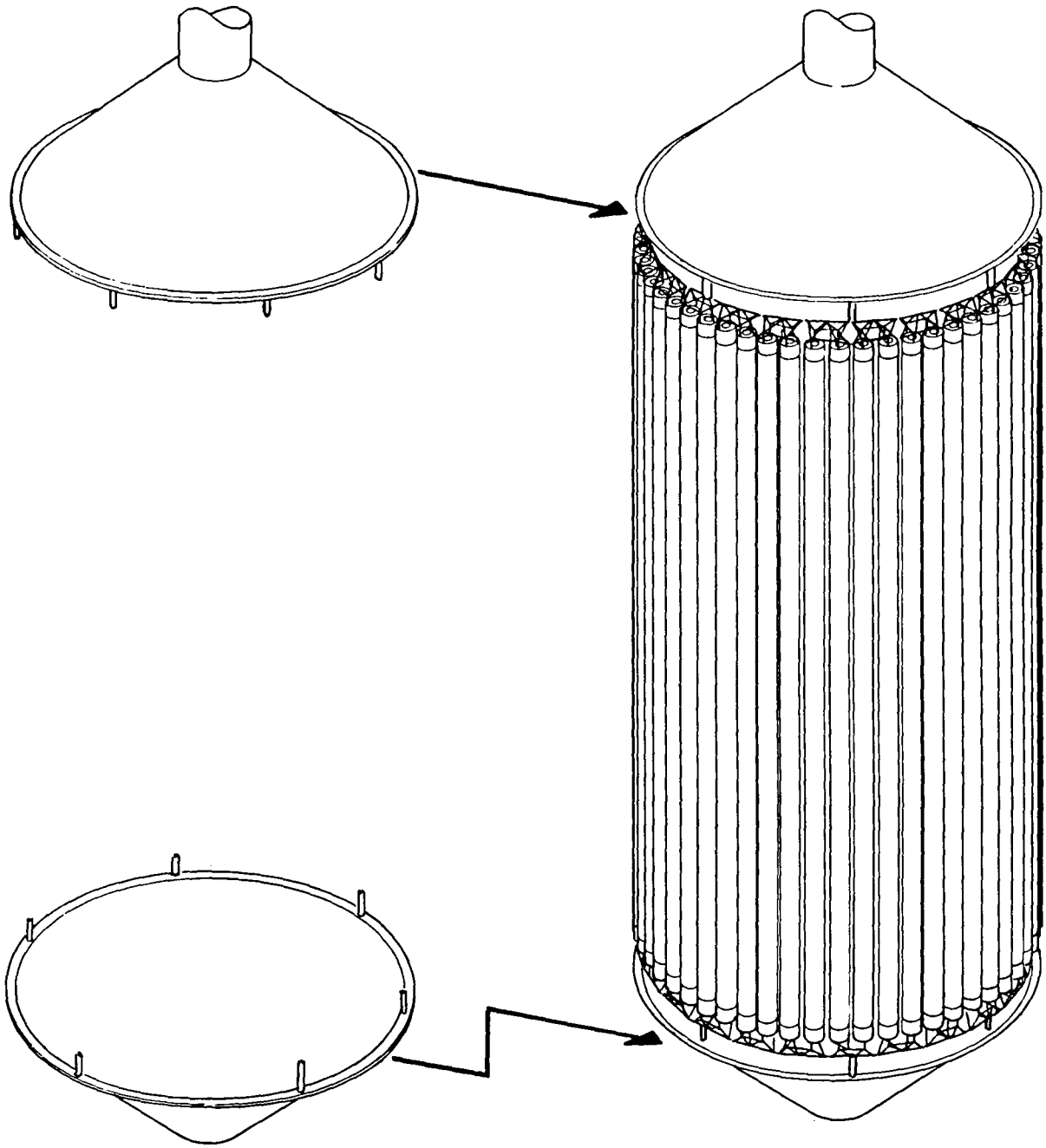

Figure 4.5-1. Stowed Reflector Final Assembly

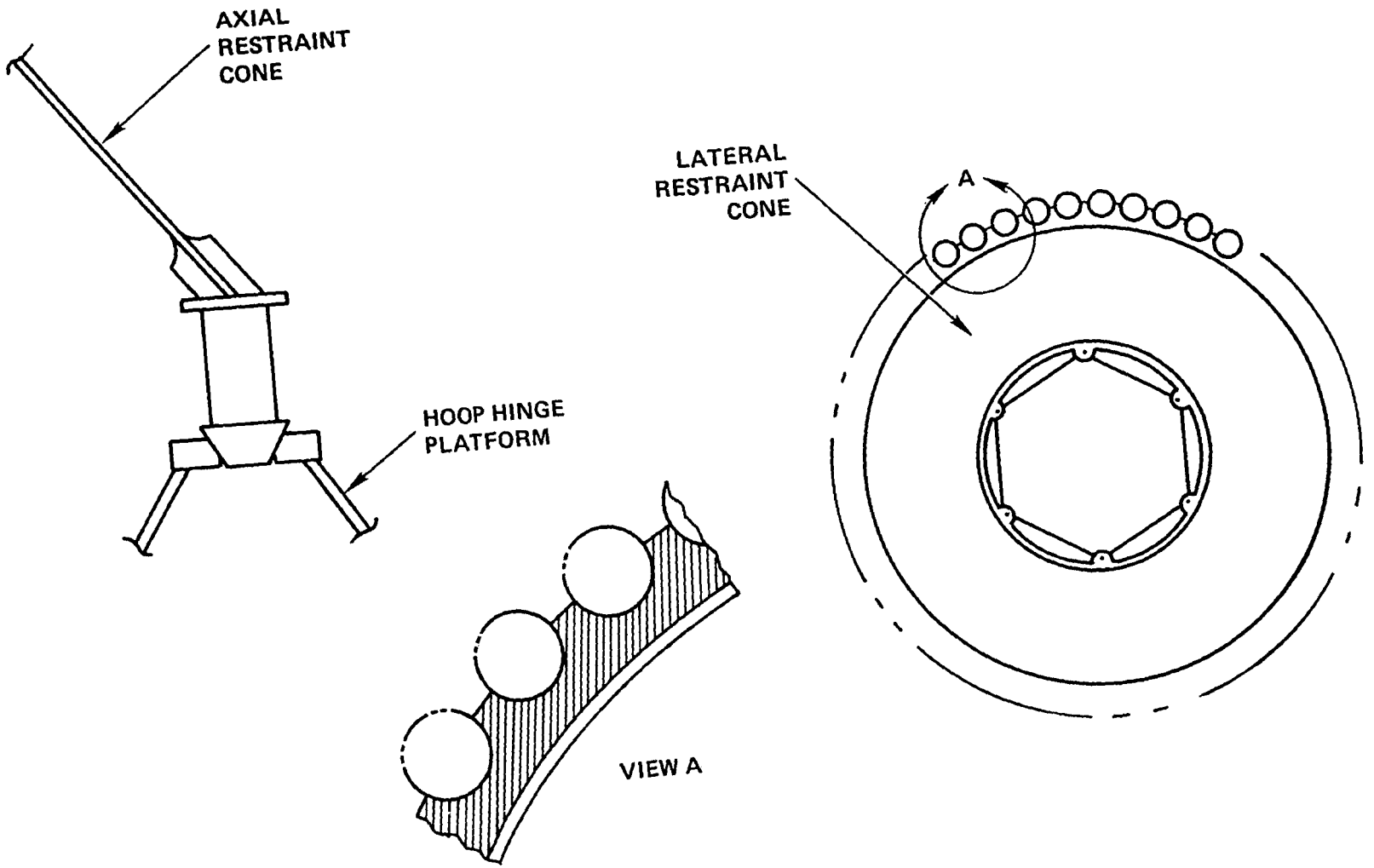

Figure 4.5-2. Restraint Cone Interfaces

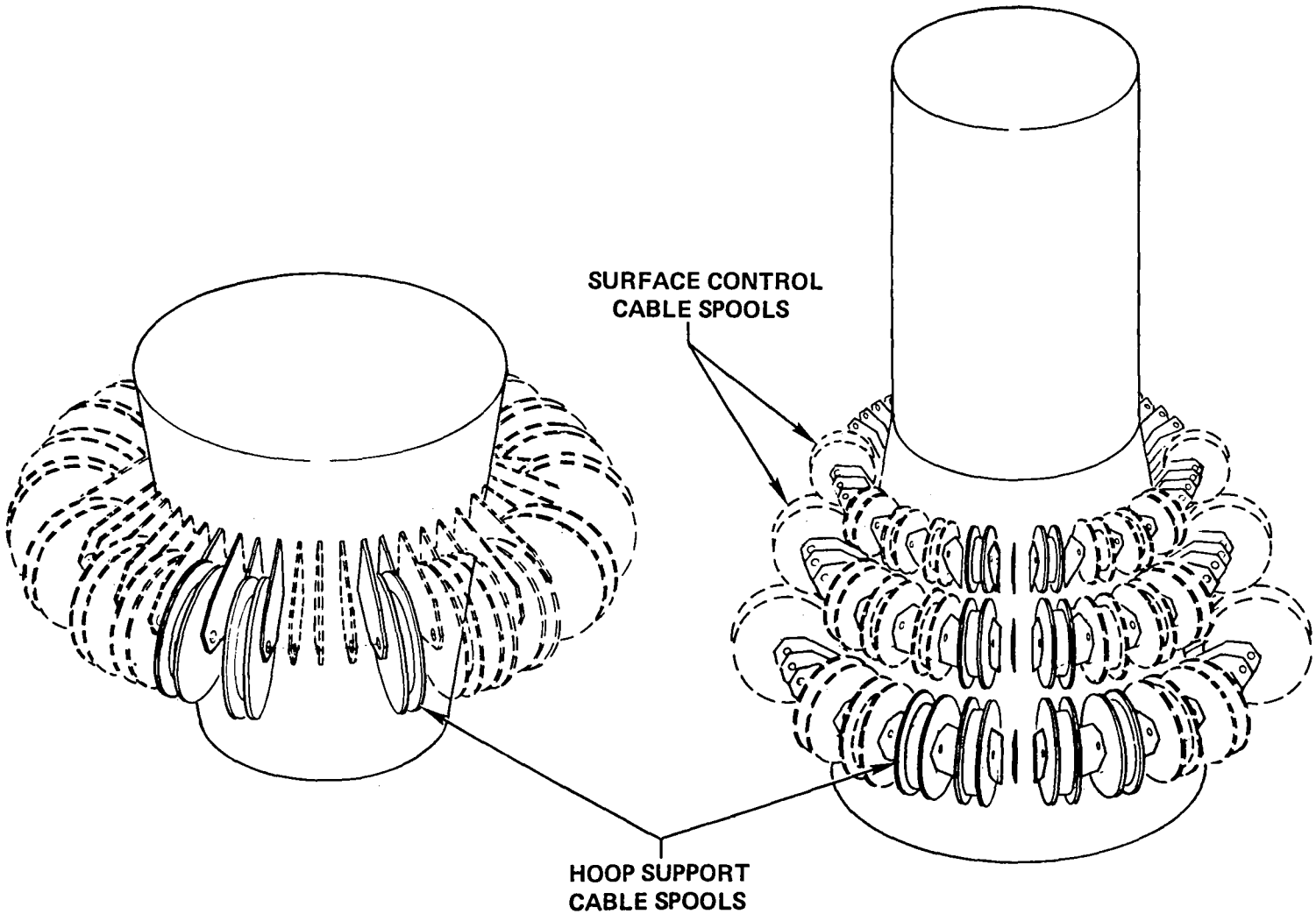

Figure 4.6-1. Cable Management - Upper and Lower Mast Segments

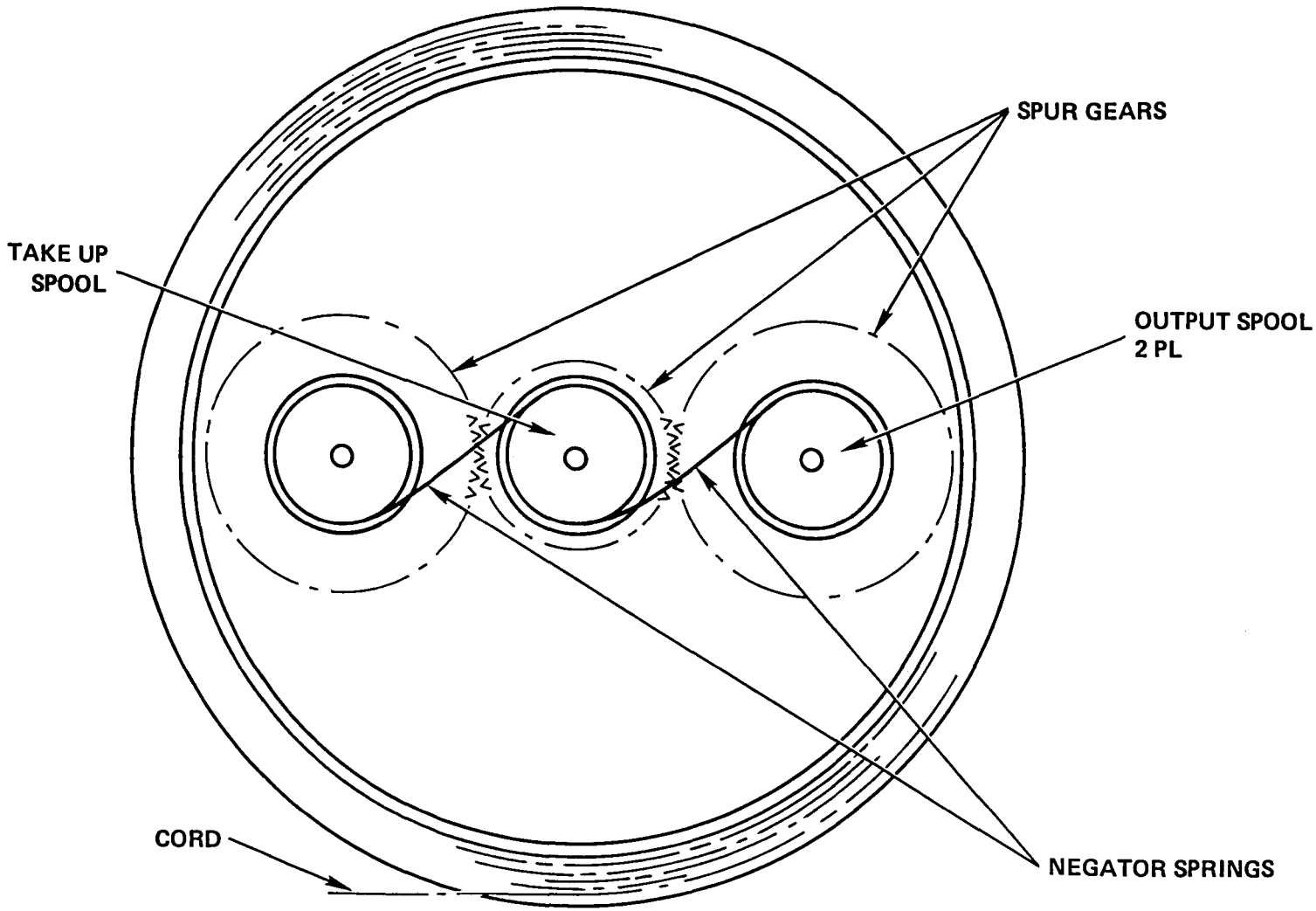

Figure 4.6-2. Takeup Spool - Cutaway

event of a snag, this pattern is perturbated and there is a change in the angular attitude of the cables with respect to the hoop. This angle change in conjunction with the constant force in the cables provide the energy to restore the hoop to its symmetrical mode.

4.7 Mesh Management

In order to ensure a smooth deployment, a minimum snag environment must be created in regard to the mesh and associated structure. The design must also provide for positive mesh capture during the dynamics of the launch environment. Figure 4.7-1 depicts the mesh stowage scheme. The mesh is packaged within the annular cavity between the hoop and the hub, and is folded in an accordian type manner. The mesh is supported by skewers, as shown in Figure 4.7-2, which extend radially from the hoop. There are four skewers and one restow cable per hoop segment. The skewers and cable penetrate the mesh and are interfaced to the hub by means of a slip joint. As the hoop deploys, the mesh is paid off of the skewers and restow cable in an orderly fashion. By virtue of the attachment of the skewers to the hoop, the inboard mesh is paid out initially, with succeeding layers being paid out as the hoop deploys radially outward. Upon full deployment of the mesh from the skewers, the skewers are rotated by means of torsional springs to a position adjacent to the segments. This prevents their interference with the mesh during restowing of the antenna.

The mesh is restowed by means of the restow cables as shown in Figure 4.7-3. These cables are looped through the mesh approximately every meter along the center of each gore. As the hoop restows itself, the restow cable spool rewinds the cable. The mesh, because of the method by which the cable is routed through it, folds itself in an accordian manner, adjacent to the hub. As this occurs, the surface control cables and the hoop support cables are rewound upon their respective spools. This process continues until the hoop segments are fully stowed and in the cradle interfaces of the upper and lower restraint cones.

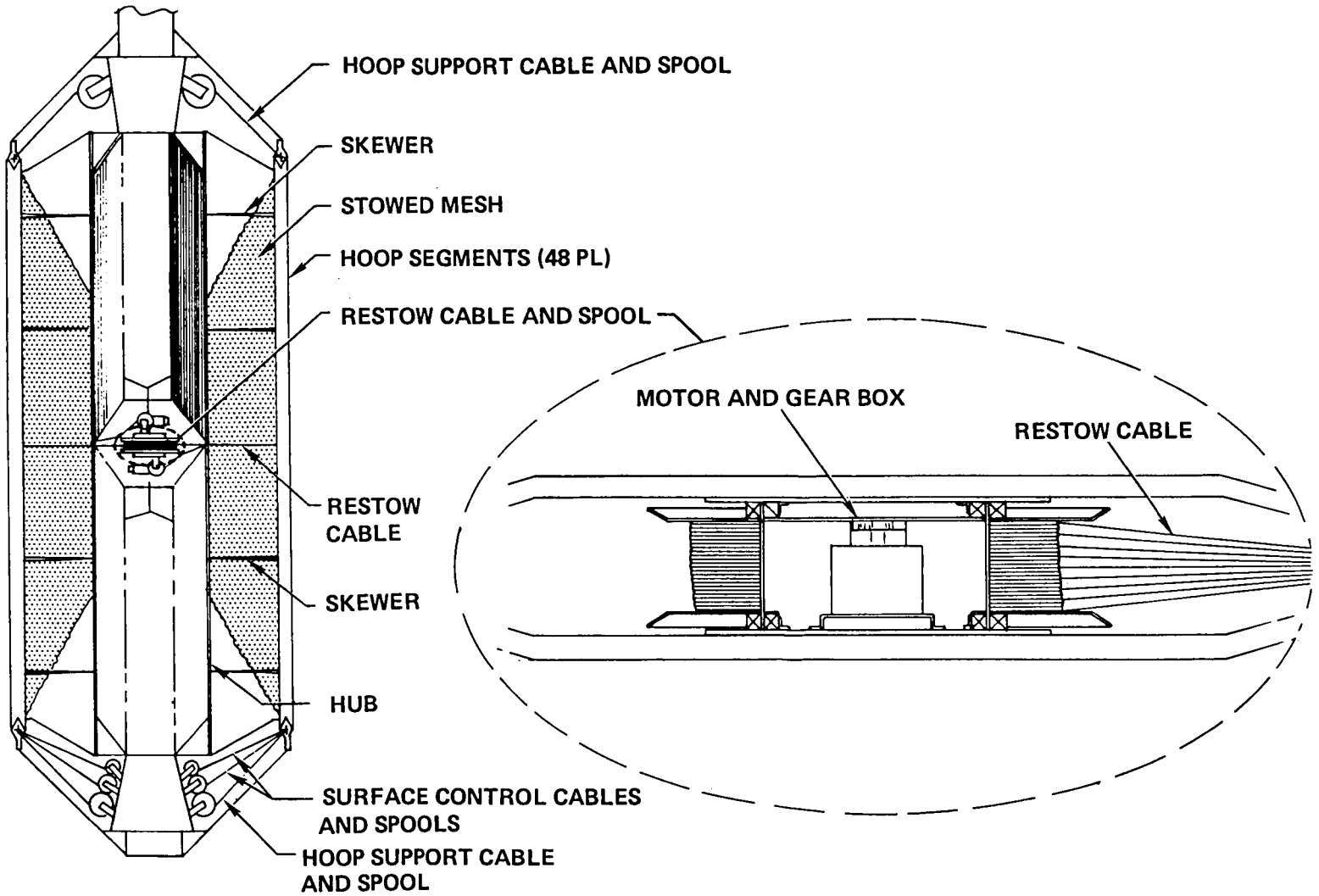

Figure 4.7-1. Restow Cable

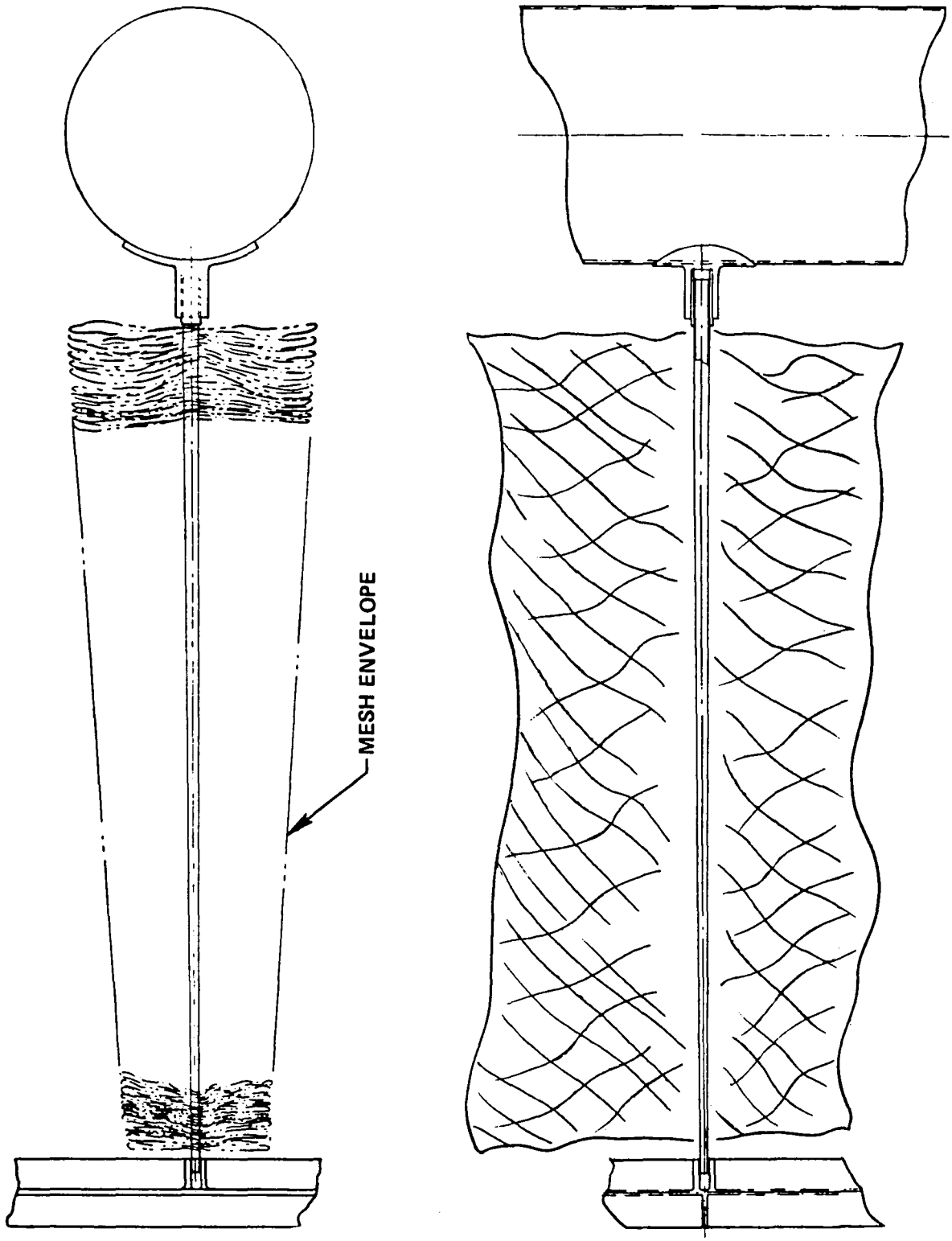

Figure 4.7-2. Skewer/Mesh Plan View

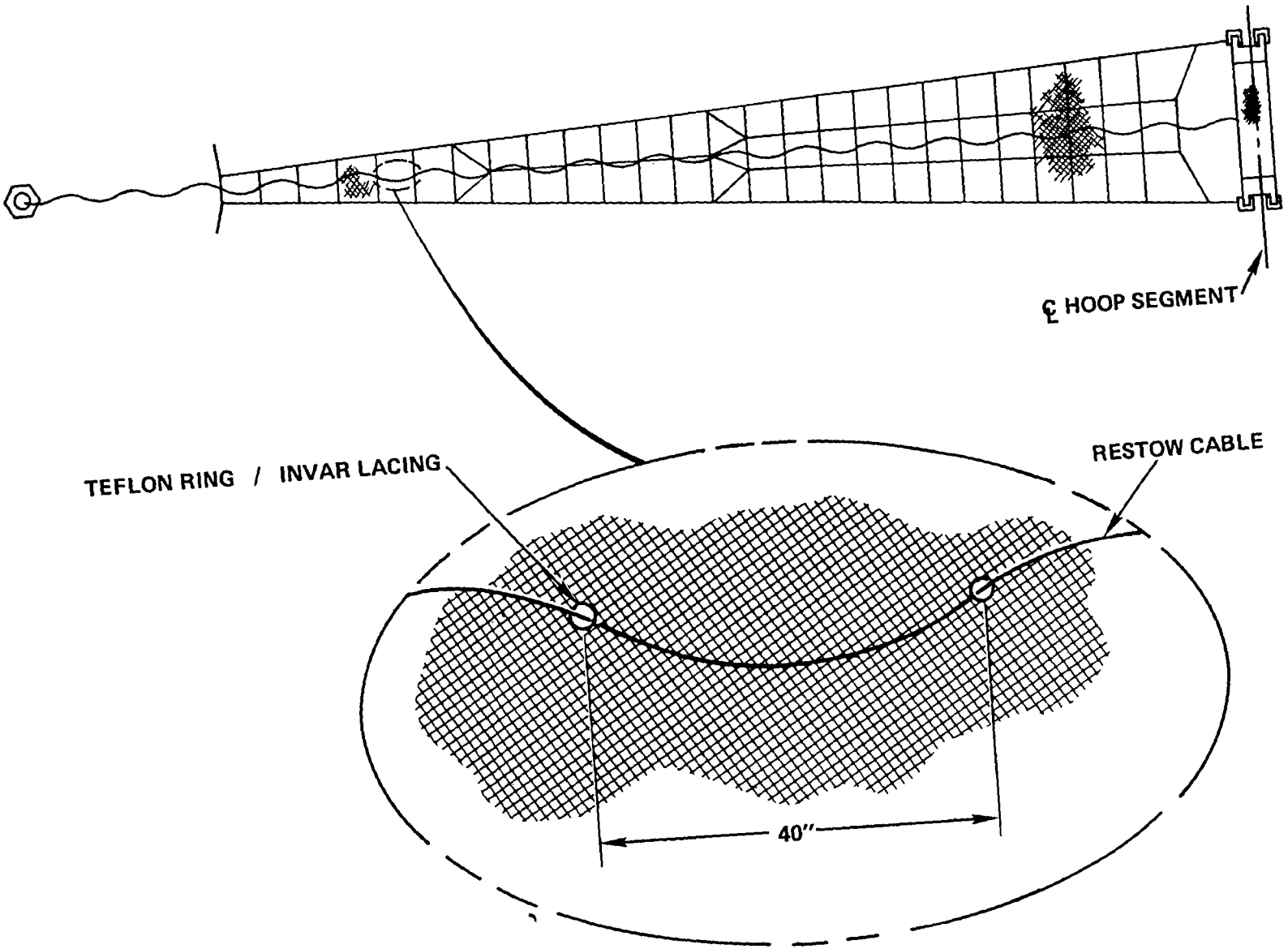

Figure 4.7-3. Restow Cable Route

4.8 Feed Mast

Figure 4.8-1 depicts a conception of the feed mast. The feed mast sits atop the main structural mast of the reflector. It has two primary requirements: 1) it must have a high deployed height to stowed height ratio and, 2) it must be stiff enough to ensure there is no detrimental dynamic coupling with the adjacent structure during antenna control. The feed mast has three continuous longerons. These longerons are made of graphite/epoxy and have a solid rod cross section. The mast is latticed with cross diagonals to reduce the $\frac{L}{\rho}$ of the longerons. The three longeron members are stowed in a cannister by means of a helical type winding into a volume efficient housing.

4.9 Thermal Control Design

The objective of the thermal analysis is to achieve temperature control for the various antenna components during the intended mission profile. Antenna RF performance is directly related to thermal design adequacy through thermoelastic effects. Therefore, the antenna will be thermally designed to operate within temperature limits consistent with material allowables and acceptable RF performance.

The LSST Antenna was examined to determine thermally critical components that require temperature control to minimize antenna mispointing and defocus. Various thermal control materials representing a wide range of thermal properties were selected for analysis. Orbital temperature extremes of a 6-inch diameter GFRP tube, the component selected for the parametric studies, were then calculated.

4.9.1 Analysis

The tube modeled was 24 inches long with a 0.026-inch wall thickness. As shown in Figure 4.9.1-1, the tube was divided into eight circumferential nodes and internal radiation was included. The models were developed and solved using MITAS II (Martin Marietta Interactive Thermal Analysis System). Figure 4.9.1-2 shows the thermal concepts that were investigated. Temperature levels and responses were obtained for full sun steady state conditions followed by a 1.5-hour eclipse.

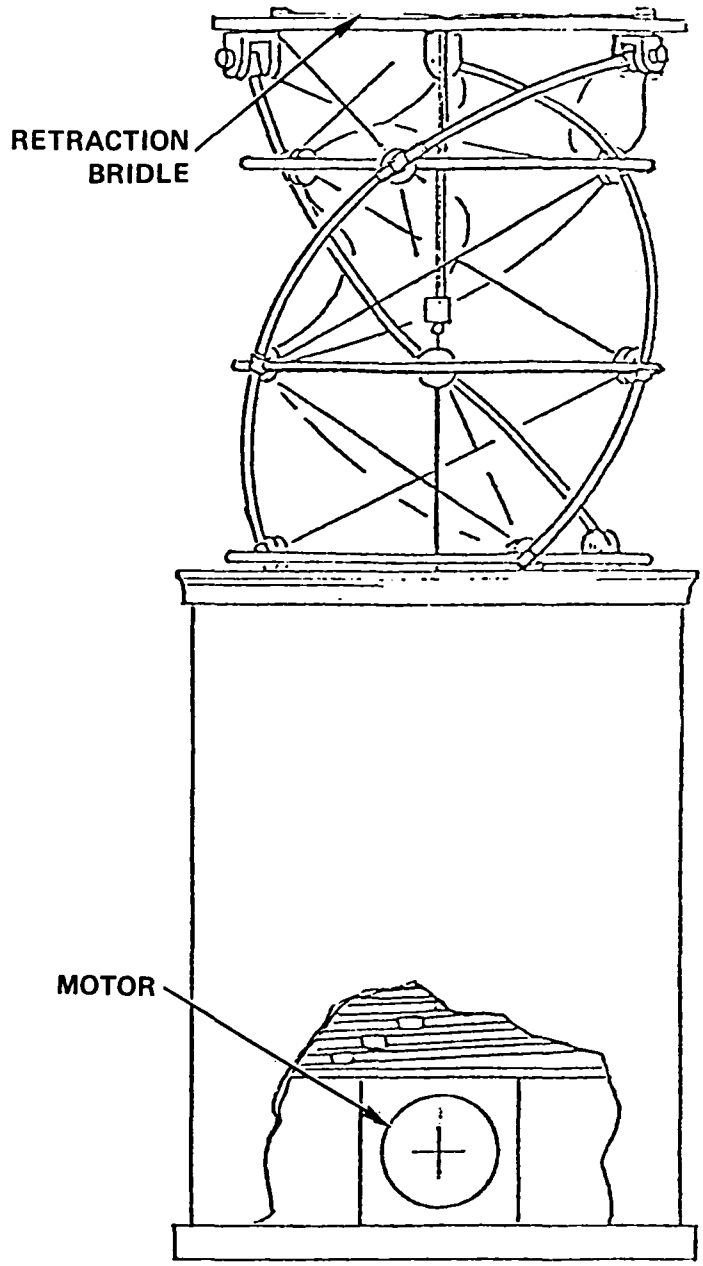

Figure 4.8-1. Continuous Longeron

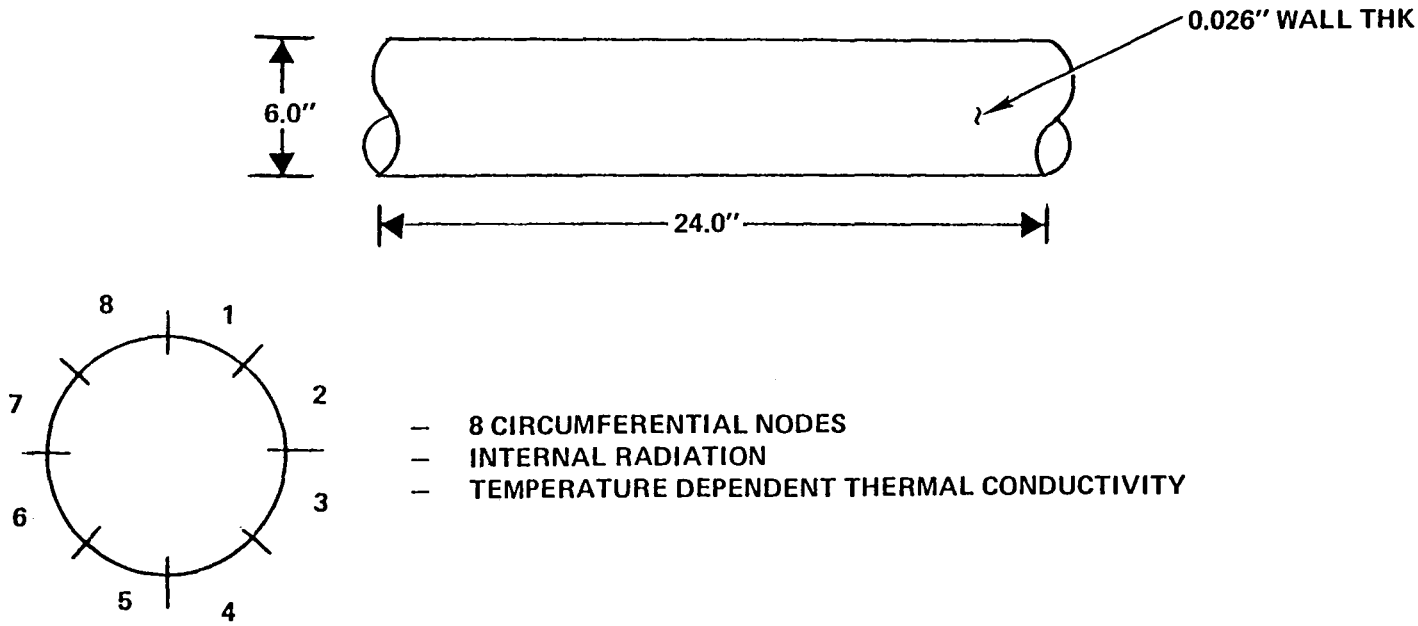

Figure 4.9.1-1. LSST Hoop/Column Antenna Graphite Structural Thermal Model

LSST HOOP/COLUMN ANTENNA
THERMAL CONCEPTS INVESTIGATED

CONCEPT	α / ϵ	SURFACE TYPE
S13G-LO	0.2/0.9 = 0.22	SOLAR REFLECTOR
MLI	0.025/0.05 = 0.50*	TOTAL REFLECTOR
ALUM PIGMENTED COATING	0.25/0.25 = 1.0	MEDIUM SURFACE
BARE GRAPHITE	0.92/0.81 = 1.14	TOTAL ABSORBER
VDA	0.15/0.05 = 3.0	TOTAL REFLECTOR

*EQUIVALENT PROPERTIES

α = SOLAR ABSORBITIVITY

ϵ = EMISSIVITY

Figure 4.9.1-2. LSST/Column Antenna Thermal Concepts Investigated

4.9.2 Results

Maximum steady state temperatures (T_{max}), minimum eclipse temperatures (T_{min}), the differences between the minimum and the maximum temperatures (T_{Fluct}), and the gradients in the tube (ΔT_{max}) are shown in Figure 4.9.2-1. The maximum allowable temperature of GFRP was assumed to be 175° F. Depending on the amount of structural loading, GFRP temperatures in excess of 175° may cause high temperature creep. The minimum allowable temperature was assumed to be -200 °F which is the qualification temperature for the bond between the GFRP and the aluminum fitting.

Plots of the GFRP orbital temperature extremes are shown in the top portion of Figure 4.9.2-2. The cross-hatched area in the plot represents the previously discussed allowable temperature extremes. The bottom plot of Figure 4.9.2-2 shows the temperatuare gradients around the tube.

The ideal thermal control material performs three functions: 1) maintains components with allowable temperature extremes, 2) minimizes orbital temperature fluctuations, and 3) minimizes temperatuare gradients within the component. As can be seen from Figure 4.9.2-2, MLI represents the most effective means of thermal control. Not only does MLI leave over a 100° F margin from both minimum and maximum temperature extremes, but it also induces the smallest GFRP temperature gradient. Aluminum paint appears to be the second best candidate with only the lower end of the allowable temperature extreme being slightly violated. It is felt that with the addition of aluminum fittings into a thermal model, the higher thermal capacitance of the aluminum fittings would keep the region of the GFRP - aluminum bond greater than -200° F. The other cases examined violate the allowable temperatures by at least 50° F.

PRELIMINARY ANALYSIS RESULTS

CONCEPT	T_{MAX} (^{o} F)	T_{MIN} (^{o} F)	T_{FLUCT} (^{o} F)	T_{MAX} (^{o} F)
S13G-LO	-62	-303	241	56
MLI	-7	-76	69	5
AL PAINT	103	-221	324	48
BARE	164	-295	459	130
VDA	256	-65	321	19

Figure 4.9.2-1. Preliminary Analysis Results

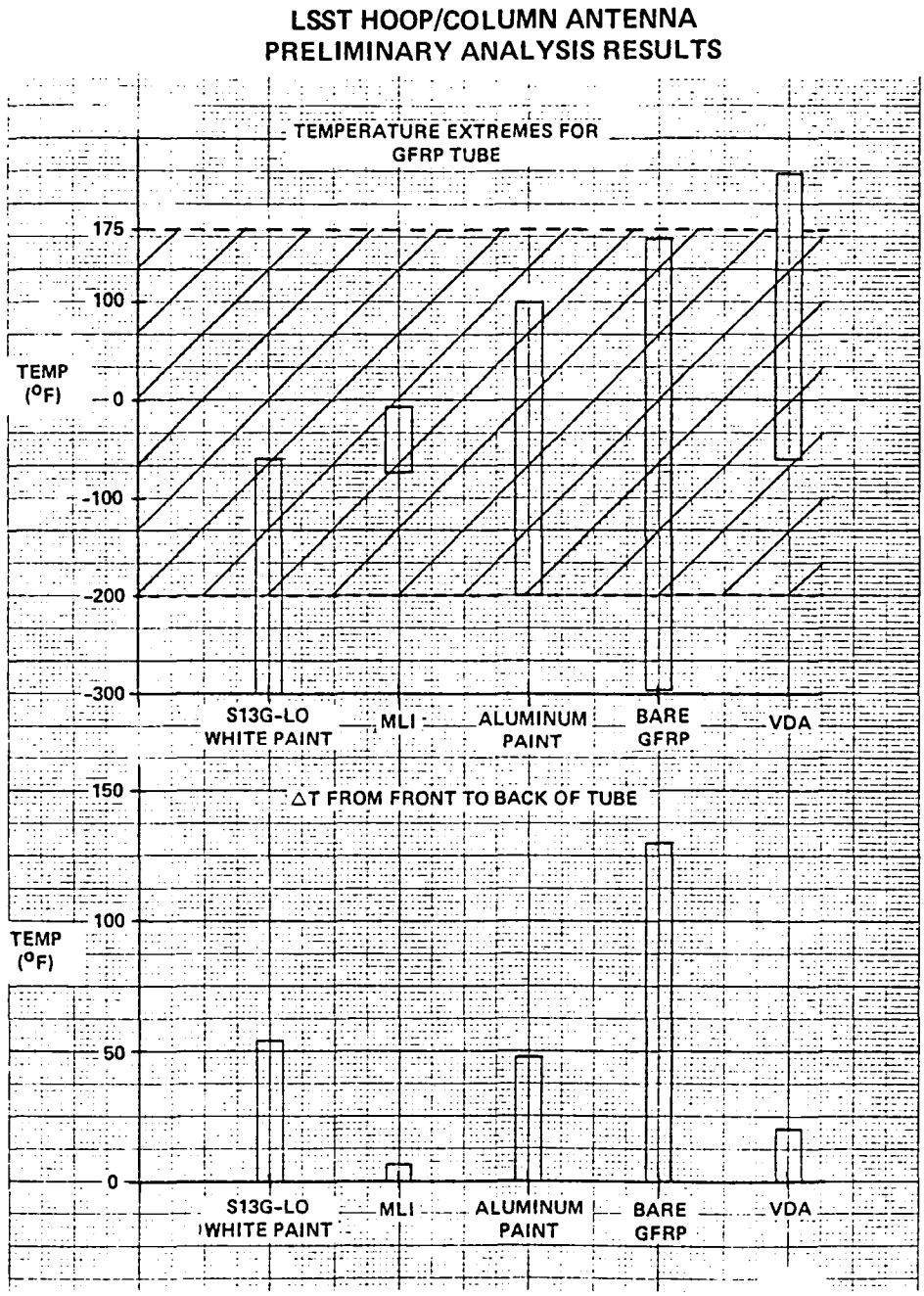

Figure 4.9.2-2. LSST Hoop/Column Antenna
Preliminary Analysis Results

4.9.3 Conclusions and Recommendations

As previously stated, MLI represents the most effective means of thermal control. Where possible in the thermal control system MLI was used, but because of the complex stowage and deployment kinematics, MLI cannot be used in certain areas. The motivation behind this study was the examination of thermal control material alternatives to MLI. Preliminary results show that thermal control materials other than MLI could be utilized in the design. For the hoop GFRP where MLI could be used without a snagging problem, it was incorported in the thermal control design. For the mast GFRP MLI could not be used, and aluminum pigmented paint was selected as the thermal control material. The α/ε of 1, along with the relatively low ε for a reduced cool down rate, made the paint the best alternative to MLI. The aluminum fittings on both the mast and the hoop were the last components examined. Because of the high α/ε of the bare fittings, about 6, a control material is necessary. Again, a low ε surface is desirable to retard the cool down rate. The thermal control material which best fit the criteria for optical properties and application was as first-surface-mirror tape. A summary of the thermal control subsystem is shown in Figures 4.9.3-1 and 4.9.3-2.

4.10 Mass Properties

4.10.1 Introduction

The objective of this section is to supply a present and projected mass properties for a LSST flight design. The best possible estimate of weight and center of gravity for the 100-meter point design deployable antenna will be given. Included is a detailed weight breakdown giving the total projected weight and subtotals of each major subassembly as described in the LSST drawing package.

4.10.2 Reported Weight Versus Specified Weight

The total weight of 100-meter point design in a flight configuration is: 3941.887 pounds projected and 4475.753 pounds contingency. There is presently no weight requirement for this program, however, an objective of less than 4000 pounds was established.

LSST HOOP/COLUMN ANTENNA
THERMAL CONTROL SUBSYSTEM

ELEMENT	THERMAL DESIGN DESCRIPTION
HOOP GFRP	INTERIOR–THREE (3) LAYERS OF 1/3 MIL EMBOSSED, DOUBLE ALUMINIZED KAPTON
	FACE SHEET–1.0 MIL ALUMINIZED KAPTON,[5] KAPTON SIDE OUT
MAST GFRP	ALUMINUM PIGMENTED SILICONE PAINT
FITTINGS	AS REQUIRED:
	FIRST SURFACE MIRROR (VACUUM DEPOSITED ALUMINUM) TAPE
	VACUUM DEPOSITED ALUMINUM
	POLISHED BARE METAL

Figure 4.9.3-1. LSST Hoop/Column Antenna
Thermal Control Subsystem

[5]Kapton: Registered trademark of E.I. du Pont de Nemours & Co., Inc.

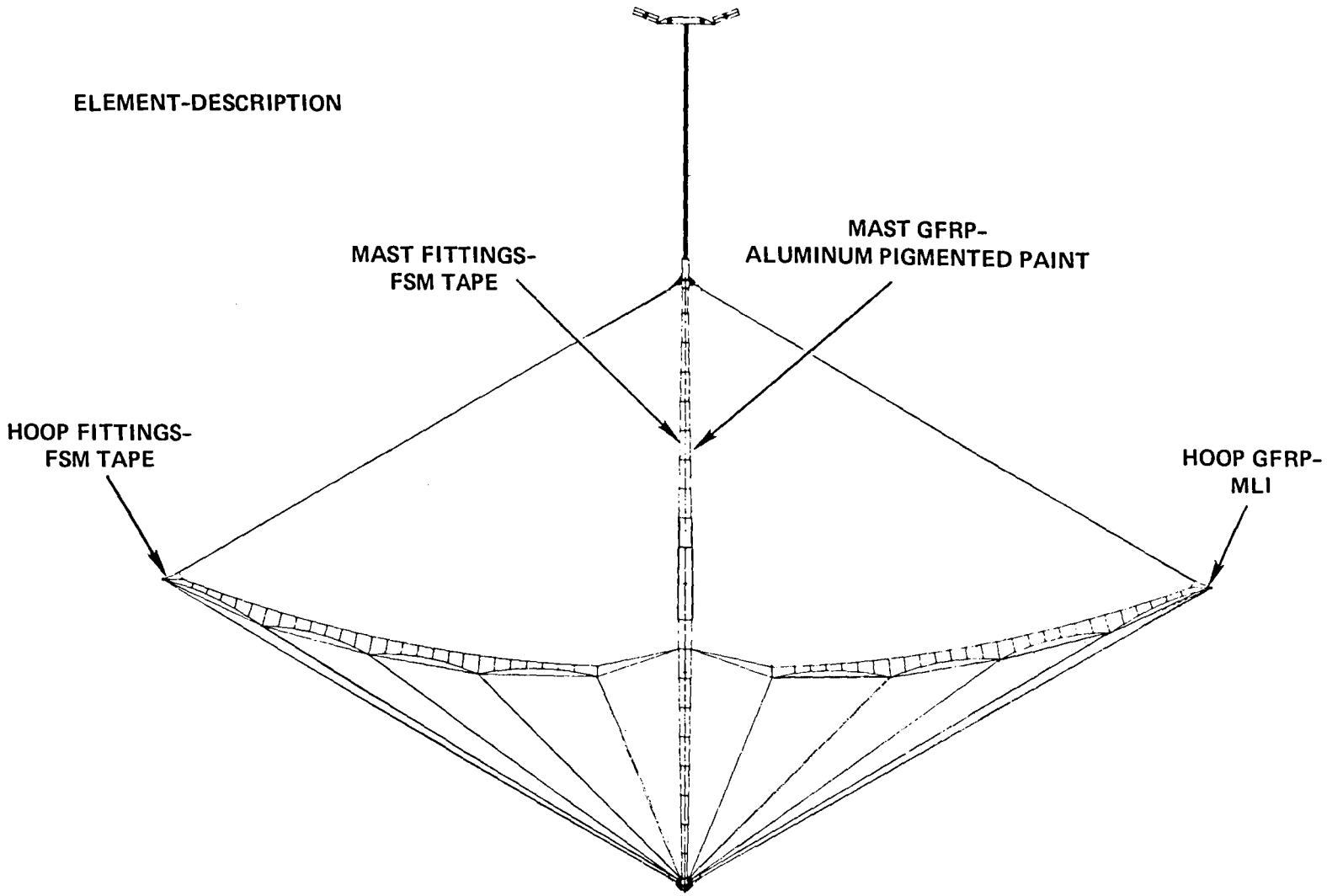

Figure 4.9.3-2. LSST Hoop/Column Antenna Thermal Control Subsystem

4.10.3 Current Mass Properties Summary Report

From the mass properties data file, Figure 4.10.3-1 provides the current weight and its contingency for major assembly line items. In Figure 4.10.3-2 a typical example of the breakdown by subassembly and piece part levels is given. On each line of the listing is the following data (if applicable) for each item:

- Drawing number
- Description
- Quantity required per unit
- Current weight
- Change in weight from previous report
- Weight with contingency
- Contingency code (see Paragraph 4.10.4)

4.10.4 Weight Contingency Chart

Figure 4.10.4-1 shows the weight per contingency breakdown. Figure 4.10.4-2 gives an explanation of how the contingency rating (E, CL, PR, CR, PA, and A) is assigned to each item.

4.10.5 Mass Properties Analysis for LSST

This analysis results in the mass properties (center of gravity and moments of inertia) of the 100-meter point design antenna. The moment of inertia (MOI) program is utilized to solve for the mass properties from a model of the antenna containing finite nodes distributed throughout the structure. Assignments of the weights of all equipment considered to be flight configuration is made to the nodes in the model. Figure 4.10.5-1 shows results of the nodal model analysis.

CURRENT WEIGHT OF MAJOR ASSEMBLIES

ITEM NO.	GROUP DESCRIPTION	CURRENT WEIGHT POUNDS	CONTINGENCY WEIGHT POUNDS
001	HOOP ASSEMBLY	643.430	722.461
051	HUB ASSEMBLY	144.600	162.574
101	MAST ASSEMBLY	1180.491	1341.378
201	FEED SUPPORT ASSEMBLY	300.000	335.993
276	LONG RESTRAINT ASSEMBLY	155.550	174.896
301	TRANSVERSE RESTRAINT ASSEMBLY	118.040	132.202
326	SURFACE TARGET ASSEMBLY	2.000	2.358
401	FEED ASSEMBLY	600.000	677.997
501	MESH STOWAGE ASSEMBLY	21.350	25.185
551	THERMAL CONTROL ASSEMBLY	201.596	237.879
601	WIRING CABLING ASSEMBLY	248.810	293.587
701	INSTRUMENTATION ASSEMBLY	17.000	20.055
751	OPTICAL ALIGNMENT	20.000	23.599
801	REFLECTOR SURFACE ASSEMBLY	289.020	325.585
	TOTAL	3941.887	4475.753

Figure 4.10.3-1. Current Weight of Major Assemblies

ITEM NMBR	DRAWING NMBR	ITEM DESCRIPTION	QTY	CURRENT WEIGHT	CHANGE	CONTING WEIGHT	DESG CODE	NOTE
110		UPPER MAST ASSEMBLY	(1)	91.784		103.358		
110		MAST TYPE I - UPPER	1	0.000		0.000		
111		TUBE	96	22.110		24.763	CL01	
112		LWR FTG	48	12.000		13.439	CL01	
113		UPPER FTG	48	12.000		13.439	CL01	
114		MID FTG	48	12.000		13.439	CL01	
115		DIAGONAL ASSY	192					
115A		CABLE	AR	6.972		8.226	E 01	
115B		TURNBUCKLE	192	3.840		4.300	CL01	
115C		EYE FTG	384	1.920		2.150	CL01	
		SUB TOTAL =		12.732 *		14.676 *		
116		ROLLER ASSY	96					
116A		ROLLER	96	4.800		5.375	CL01	
116B		PIN	96	.096		.107	CL01	
116C		RETAINING RING	192	.384		.430	CL01	
		SUB TOTAL =		5.280 *		5.912 *		
117		LATCH ASSY	48					
117A		LATCH	48	1.910		2.139	CL01	
117B		PIN	48	.254		.284	CL01	
117C		RETAINING RING	96	.288		.322	CL01	
		SUB TOTAL =		2.452 *		2.745 *		
118		CIRCUMFERENTIAL	144	10.656		11.934	CL01	
119		EPOXY, MAST JOINTS						
120A		VERT TUBES	384	.691		.815	E 01	
120B		CIRC. TUBES	576	.461		.543	E 01	
		SUB TOTAL =		1.152 *		1.358 *		
125		FIBERGLASS, MAST JNTS						
126A		VERT. TUBES	384	.826		.974	E 01	
126B		CIRC. TUBES	576	.576		.679	E 01	
		SUB TOTAL =		1.402 *		1.653 *		

Figure 4.10.3-2. Typical Weight Breakdown

GROUP	DESCRIPTION	WEIGHT BY DESIGNATOR CODE E	CL	PR	CR	PA	A
001	HOOP ASSEMBLY	30.850	612.580	0.000	0.000	0.000	0.000
051	HUB ASSEMBLY	10.700	133.900	0.000	0.000	0.000	0.000
101	MAST ASSEMBLY	321.732	858.759	0.000	0.000	0.000	0.000
201	FEED SUPPORT ASSEMBLY	0.000	300.000	0.000	0.000	0.000	0.000
276	LONG. RESTRAINT ASSY	11.500	144.050	0.000	0.000	0.000	0.000
301	TRANSVERSE RSTRNT ASSY	0.000	118.040	0.000	0.000	0.000	0.000
326	SURFACE ASSEMBLY	2.000	0.000	0.000	0.000	0.000	0.000
401	FEED ASSEMBLY	100.000	500.000	0.000	0.000	0.000	0.000
501	MESH STOWAGE ASSEMBLY	21.350	0.000	0.000	0.000	0.000	0.000
551	MLI ASSEMBLY	201.596	0.000	0.000	0.000	0.000	0.000
601	WIRING/CABLING ASSY	248.810	0.000	0.000	0.000	0.000	0.000
701	INSTRUMENTATION	17.000	0.000	0.000	0.000	0.000	0.000
751	OPTICAL ALIGNMENT	20.000	0.000	0.000	0.000	0.000	0.000
801	REFLECTOR ASSEMBLY	31.680	257.340	0.000	0.000	0.000	0.000
	TOTAL	1017.218	2924.669	0.000	0.000	0.000	0.000

::::

Figure 4.10.4-1. Weight Contingency Breakdown

Function/Usage of Part		PERCENT CONTINGENCY						
		E	CL	PR	CR	PA	A	Code
Source of Weight Input & Design Definition		Weight Based on Estimate	Calculated From Detailed Layout Drawing	Calculated From Pre-Released Drawing	Calculated From Released Drawing	Actual Weight, Preliminary Hardware	Actual Weight, Flight Hardware	
Structural and Thermal Control		18	12	8	4	2	0	01
Electrical and Electronic Components and Assemblies	0 to 1.0 pound items	30	25	20	10	5	0	02
	1.0 to 3.0 pound items	20	20	15	5	3	0	03
	3.0 pound & up items	15	15	10	5	3	0	04
Batteries		20	15	10	5	3	0	05
Wiring/Cabling		50	35	25	5	3	0	06
Pyro Devices		25	15	10	5	3	0	07
Instrumentation		100	50	25	5	3	0	08

Figure 4.10.4-2. Weight Contingency Values

WEIGHT (FLIGHT CONFIGURATION) 3941.887 lb

CENTER OF GRAVITY LOCATION FROM CENTER OF HUB (INCHES)

DEPLOYED:	$\bar{x}$ = 0.0000	STOWED: $\bar{x}$ = 0.0000
	$\bar{y}$ = 0.0000	$\bar{y}$ = 0.0000
	$\bar{z}$ = 368.9739	$\bar{z}$ = 41.2431

MOMENTS/PRODUCTS OF INERTIA ABOUT ANTENNA ORIGIN LOCATED AT INTERFACE PLANE (SLUG-FT^2)

DEPLOYED:	Ixx = 1518797.5625	STOWED: Ixx = 20278.1038
	Iyy = 1518797.5625	Iyy = 20278.1038
	Izz = 729246.8281	Izz = 1257.9675

Figure 4.10.5-1. Center of Gravity and Moments of Inertia

4.11 Surface Accuracy Measurement System

The Surface Accuracy Measurement System of the antenna consists of 48 receivers located at the lower periphery of the hub as shown in Figures 4.11-1 and 4.11-2. Three gore line targets and one rigid hoop target are located at each of the 48 gores.

The envelope which was chosen for each receiver is 4 inches in diameter by 20 inches in length. Each receiver provides coverage of the three active LED targets located at the appropriate mesh shaping tie points as well as the active LED targets on the hoop. One receiver per gore was chosen to minimize scanning requirements. The included angle of view for each receiver is approximately 16^{o}. The targets are narrow beam emitting diodes.

4.12 Point Design Description Summary

A description summary of the Maypole (Hoop/Column) antenna is provided in Figure 4.12-1.

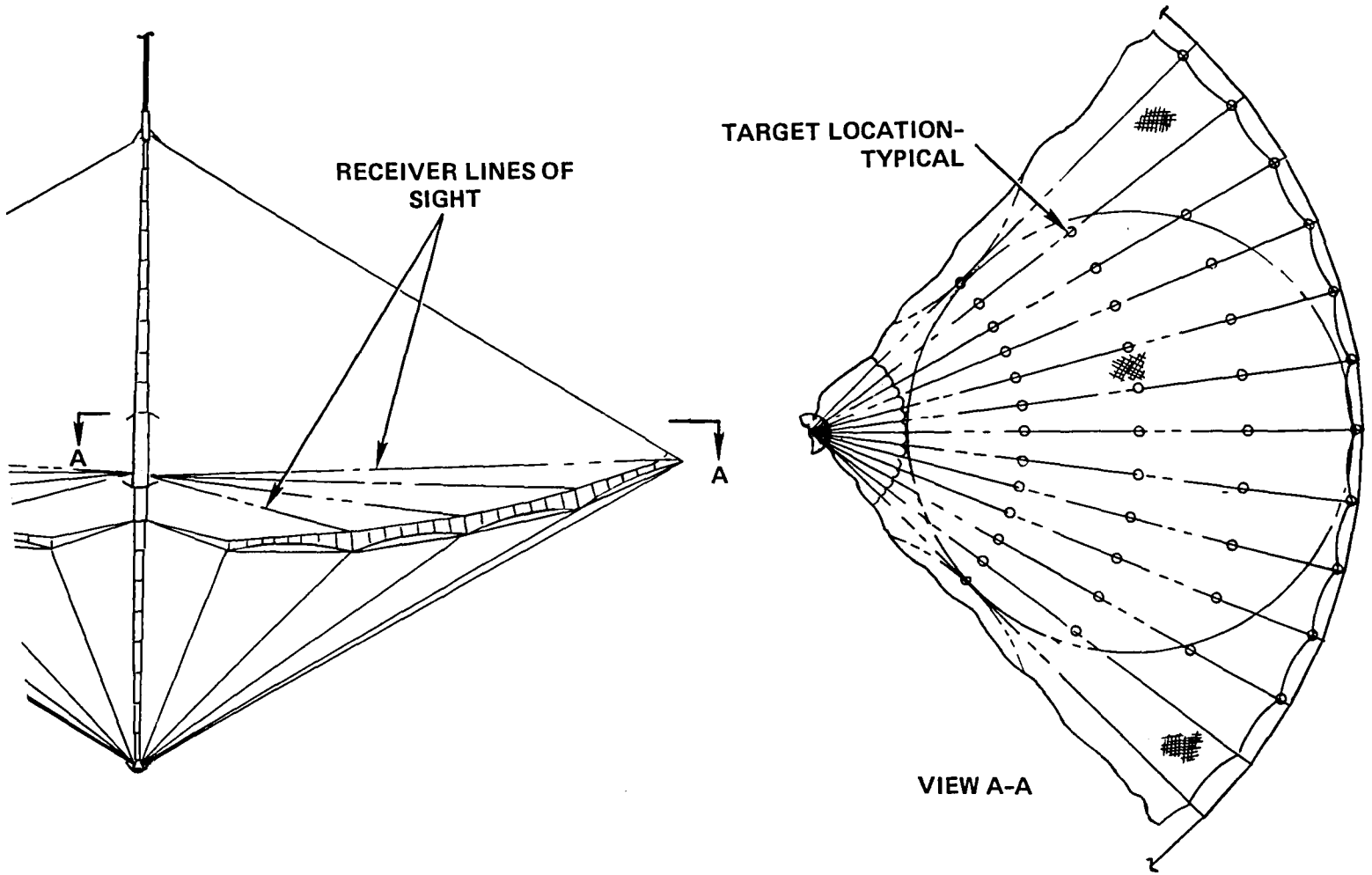

Figure 4.11-1. SAMS Integration

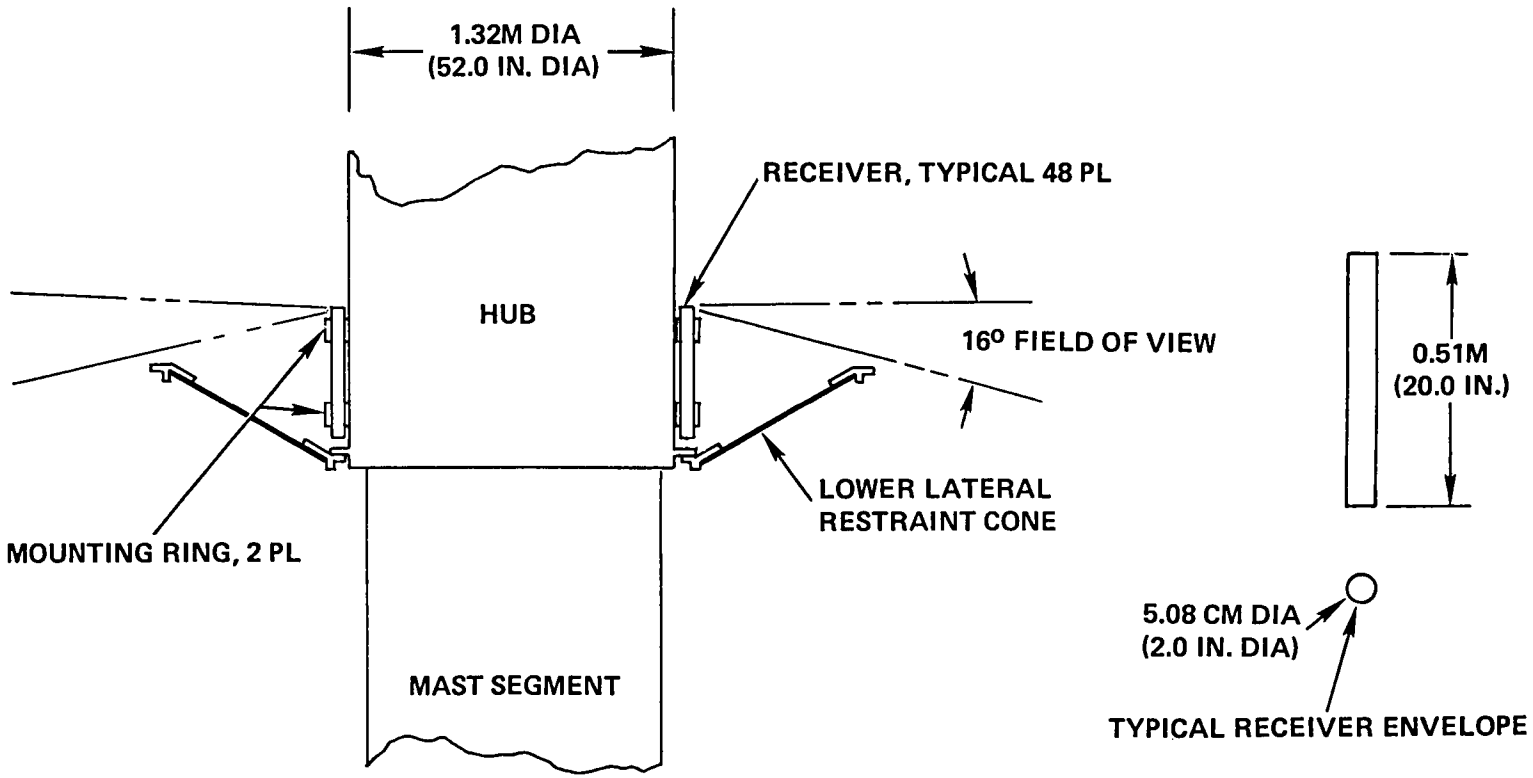

Figure 4.11-2. SAMS Integration

- Basic Antenna Parameters
  - Aperture Size, Reflector (40 meters) 4 places
  - Focal Length (62.12 meters)
  - Feed System
  - Effective f/D = 1.53
  - Beam to Beam Isolation (-30 dB)
  - Center Frequency (2.0 GHz)
  - Number of Beams (219)
  - Half-Power Beam Width (0.26°)
- Deployed Geometry
  - Overall Diameter (100 meters)
  - Overall Length (83.02 meters)

    (From the theoretical intersection of the lower hoop support cords to the centerline of the deployed feed array)
  - Reflector Mast Length (57.74 meters)

    (From the theoretical intersection of lower hoop support cords to the theoretical intersection of the upper hoop support cords)
- Stowed Geometry
  - Diameter of Stowed Hoop (3.01 meters)

    (Centerline to Centerline)
  - Overall Length of the Antenna (10.926 meters)

    (From the feed support frame to the preload section)
  - Overall Width (4.059 meters)

    (Stowed feed to stowed feed)
  - Max Girth of Antenna (4.46 meters)

Figure 4.12-1. Point Design Description (Sheet 1 of 4)

Element	Design Parameters
Hub	• Description: Hexagonal Cross Section latticed structure, comprised of verticals, mid and end fittings diagonals, and circumferentials
	- Verticals
	• Graphite tubes • Diameter, 1.00 inch • Wall thickness, 0.042 inch • Layup (0°, $+45^\circ$, 0°, -45°, 0°) • HMS 3501-6 Graphite
	- Diagonals
	• 0.063 inch diameter cable, Graphite Teflon coated
	- Circumferentials
	• Graphite tubes • Diameter, 0.50 inch • Wall thickness, 0.021 inch • Layup (90°, $+45^\circ$, -45°, 0°) • HMS 3501-6 Graphite
	- Upper, Lower and Mid Fittings
	• Material, Aluminum 7075-T7351
	• Overall Length, 57.73 meters
	• Outside Diameter, 1.32 meters
Mast	• Description: Same shape, same structure as hub Upper and lower mast telescope out of the hub 9 telescoping sections (18 total)
	- Typical section length, 2.78 meters

Figure 4.12-1. Point Design Description (Sheet 2 of 4)

Element	Design Parameters
Hoop	• Description: Circular structure consisting of 48 segments which are graphite tubular members; segments kinematically linked by means of push rods, hinge platforms, and strips
	- Segments
	• Graphite tubes • Diameter, 6 inches (0.152 meters) • Wall thickness, 0.021 inch (0.53 mm) • Layup (90^0, 0^0, $+45^0$, -45^0) • HMS 3501-6 Graphite
	- Hinge Platforms (Tubular framework with nodal fittings)
	• Tubes
	- Material, Aluminum, 6061-T - Diameter, 0.038 inch (9.65 mm) - Wall thickness, 0.028 inch (0.51 mm)
	• Nodal Fittings
	- Material, Aluminum 7075, T7351
	- Push Rod
	• Aluminum Tube • Diameter, 0.5 inch (12.7 mm) • Wall thickness, 0.04 inch (1.016 mm)
Surface	• Description: Quad Aperture 12 gores per aperture, surface comprised of front cords, rear cords, intercostals, end fittings, and mesh
	- Mesh
	• 1.2 mil diameter wire (monofilament) molybdenum, gold plated, tricot knot
	- Front and rear cords, intercostals, Graphite, ranging from 4 to 30 strand; respective E's of 18,000 pounds to 135,000 pounds
	- Aperture diameter, 1598.42 inches (40 meters)
	• End fittings, 0.030 inch thick, invar

Figure 4.12-1. Point Design Description (Sheet 3 of 4)

Element	Design Parameters
Surface Control Cords	• Description: Graphite cords, 4 cords per gore edge (numbered from inboard to outboard direction) - Cord No. 1: 4 strand, AE = 18,000 pounds - Cord No. 2: 4 strand, AE = 18,000 pounds - Cord No. 3: 4 strand, AE = 18,000 pounds - Cord No. 4: 20 strand, AE = 90,000 pounds
Hoop Support Cables	• Description: Graphite, - Upper cable 4 strand, AE = 18,000 pounds - Lower cable 4 strand, AE = 18,000 pounds
Hoop Drive Units	• Description: - DC permanent magnet, 4 motors located 90^{o} apart (each motor is redundant) - Output shaft torque, 250 in-lb
Mast Drive Units	• Description: - DC permanent magnet, 2 motors - Output shaft torque, 35 in-lb
Preload Segment Drive Unit	• Description: - DC permanent magnet, 3 motors - Output shaft torque, 20 in-lb - Aluminum Pigmented Silicone
Hub/Mast Thermal Protection	• Paint on verticals and circumferentials First surface mirror (vacuum deposited aluminum) • Tape on upper, lower and mid fittings, 0.5 mil
Hoop Thermal Protection	• Segments - Interior, three layers of 1/3 mil embossed, double aluminized Kapton; Exterior, 1 mil aluminized Kapton (Kapton side out) • Joints, First surface mirror tape (vacuum deposited aluminum)

Figure 4.12-1. Point Design Description (Sheet 4 of 4)

5.0 ANTENNA PERFORMANCE

This section describes the performance analyses and results for the Hoop/Column antenna design. Included are:

5.1 Dynamics/Structural Performance

5.2 Thermal Performance

5.3 Contour Analysis

5.4 RF Performance

5.5 Antenna Size Versus Stowed Envelope

5.1 Dynamics/Structural Performance

Introduction

The purpose of the structural analysis of the point design is to assess feasibility of the concept, identify structural characteristics and determine requirements for sizing of major structural members.

There are three configurations which require structural analysis (see Figure 5.1-1). They are: 1) Deployed configuration where the mast is erect, and the hoop is fully open and the control cables and the surface are tensioned; 2) the stowed configuration where the mast is collapsed and the hoop is reduced to minimum radius for transportation and launch; and 3) deploying which consists of two phases, mast erection and hoop deployment. For structural analysis these configurations must be considered as a satellite system which consists of the elements in Figure 5.1-2. At present the reflector components are well defined but detailed designs of the feed, feed mast, spacecraft, solar arrays and IUS do not exist as they are beyond the scope of this task. The weights are estimated for these components so that initial effects may be considered in the analytical models. Also, feed mast stiffness estimates are based on an ASTRO MAST type design. It is believed that the values used in this analysis can be obtained for a mast of approximately 76.2 cm (30 inches) diameter.

Disturbances affecting the structural performance of the Hoop/Column antenna satellite system derive from various external and internal sources. The external sources of disturbance consist of solar and terrestrial related effects and the interaction of exogenous systems, e.g., in ground transportation or launch. The internal sources include torques and forces induced by the drive mechanism, the attitude control torques and thermally induced internal loading. These disturbances are categorized by frequency content in Figure 5.1-3. Disturbances which have frequency content that is less than 1/5 the lowest natural frequency are considered static and greater than 1/5 the lowest natural frequency are considered dynamic (lower modes of the antenna are in the 0.1 to 0.3 Hz range).

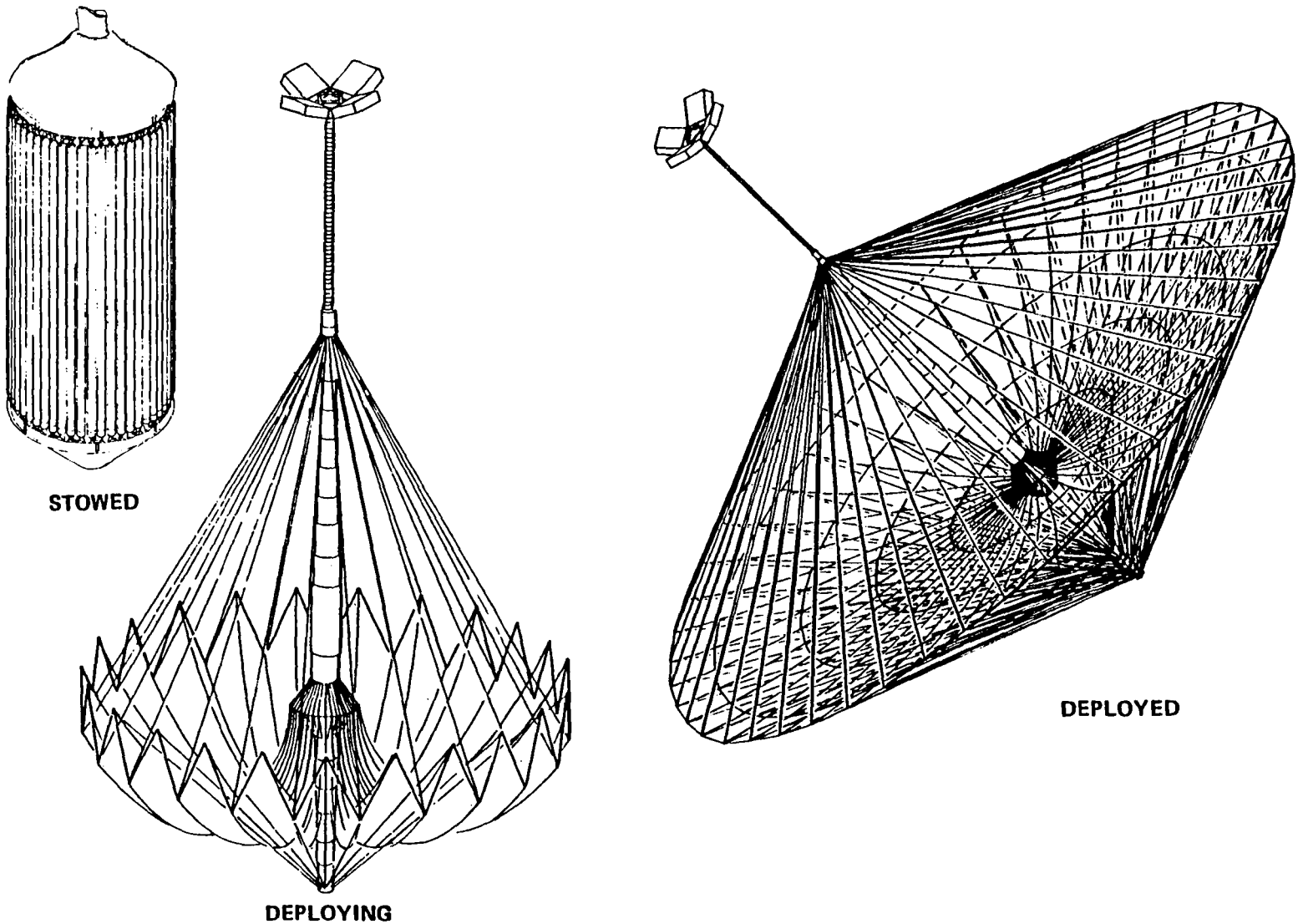

Figure 5.1-1. System Configuration

POINT DESIGN COMPONENTS

- ANTENNA MAST (SEGMENTS, FITTINGS AND MOTORS)
- MESH SURFACE PARTS
- SURFACE CONTROL CORDS
- HOOP (TUBES, MLI, END FITTINGS AND MOTORS)
- HOOP CONTROL CABLES
- FEEDS AND FEED SUPPORTS
- FEED MAST
- SOLAR ARRAYS WITH SUPPORT BOOMS
- SPACECRAFT
- IUS

Figure 5.1-2. Point Design Components

ENVIRONMENTS EFFECTING STRUCTURAL PERFORMANCE

- QUASI-STATIC
  - THERMAL LOADING (INCLUDING THERMAL SHOCK FROM ECLIPSING)
  - SOLAR AND EARTH RADIATION
  - GRAVITY GRADIENT
  - SOLAR PANEL MOTION REACTION TORQUES
  - PRETENSION LOADING
- TRANSIENT
  - LAUNCH VIBRATION
  - THRUST TRANSIENTS FOR ATTITUDE CONTROL AND STATION-KEEPING
  - BEARING AND DRIVE TRANSIENTS FOR SOLAR PANELS, INERTIA WHEELS AND OTHER MECHANISMS
  - RELEASE SHOCKS

Figure 5.1-3. Environments Effecting Structural Performance

Of the environments mentioned in Figure 5.1-3, pretension forces have the most effect on structural performance. The following are all effected by pretension:

1. System Stability (Buckling)
2. Torsional Frequencies of the System
3. Mast Stability and Frequency
4. Thermal Elastic Performance

In order to accomplish the analysis objectives the following items are being addressed in this evaluation:

1. System Stability
2. Deployed Dynamics
3. Deployment Kinematics
4. Stowed Dynamics
5. Major Element Stress Analysis

5.1.1 System Stability

Both the overall antenna system buckling and detailed element stability of a hoop segment, and the mast and the effect of four bar linkage hoop joint are presented in the paragraphs that follow. In addition, the effect of antenna radius, cord angle, and number of segments is discussed.

5.1.1.1 Overall Buckling of the Antenna

Preliminary assessment of critical buckling load and mode shape for the antenna was made using the NASTRAN computer program. A finite element model of the antenna consisting of the hoop, mast, upper hoop support cables and lower hoop support cables was developed. A computer plot of the model is shown in Figure 5.1.1.1-1. A description of the finite element model is given in the structural analysis appendix.

NASTRAN FINITE ELEMENT STABILITY MODEL OF 100 METER DIAMETER
HOOP–COLUMN ANTENNA

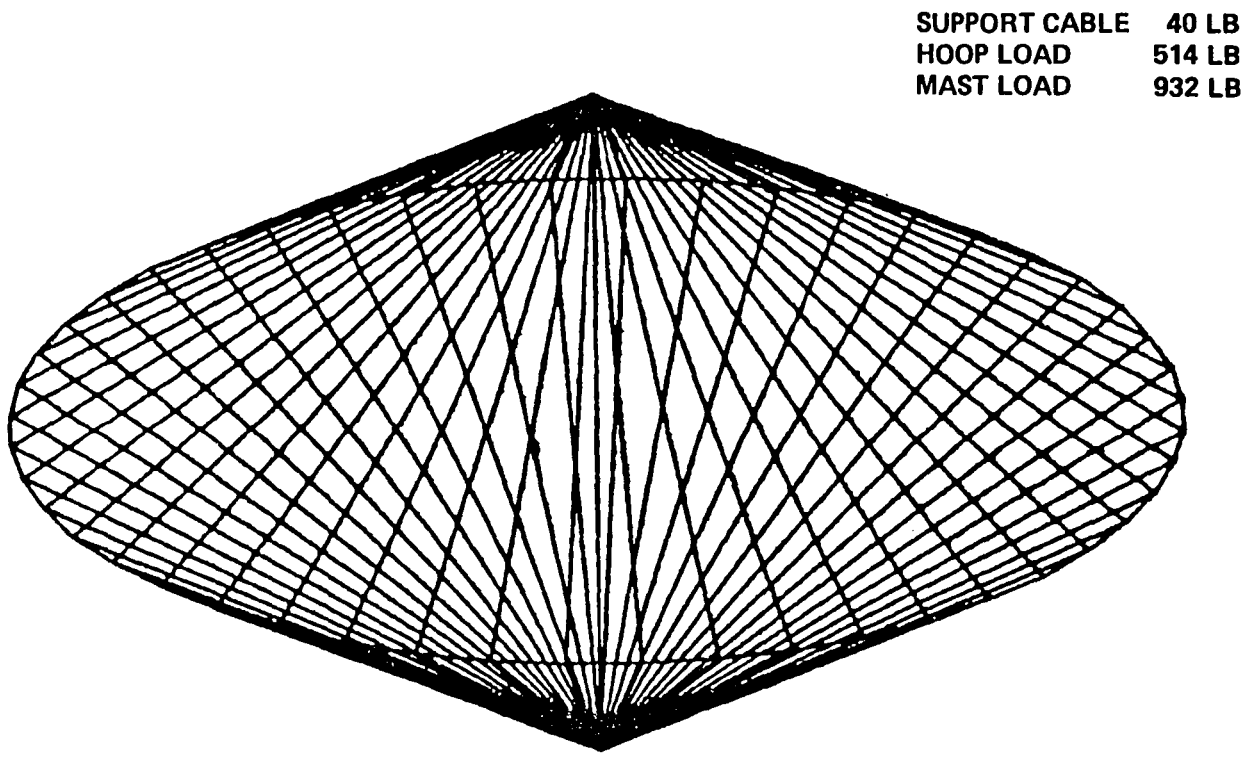

Figure 5.1.1.1-1. NASTRAN Finite Element Stability Model of 100-Meter Diameter Hoop-Column Antenna

The buckling analysis was performed by solving the eigenvalue problem.

$$[K + \lambda K_g] \{\Delta\} = 0$$

where K is the stiffness matrix, K_g is the geometric stiffness, the solutions λ_i are the eigenvalues and the corresponding vectors are $\{\Delta_i\}$. The matrix K_g is dependent on geometry and loading conditions, thus control cable pretension. A pretension of 40 pounds was generated in the model by an artificial temperature change. The critical buckling load is then obtained from

$$T_c = \lambda_i T$$

where T is the pretension used to generate K_g. The resulting hoop load is 514 pounds and the mast load is 912 pounds.

The antenna stability is a function of hoop and support cable stiffnesses. To evaluate one parameter at a time, the hoop stiffness was held constant and the support cable stiffness was varied.

A plot of support cable load at buckling versus support cable stiffness is shown in Figure 5.1.1.1-2. Two cases were run to generate the curve. The relationship between the cable load at buckling and cable AE is linear. Based on test data of graphite cords, an AE = 180,000 pounds is achievable for a preload of 40 pounds.

The lowest buckled mode shape is shown in Figures 5.1.1.1-3 and 5.1.1.1-4. These NASTRAN computer plots show the buckled mode shape plotted on top of the undeformed shape for the entire model, Figure 5.1.1.1-3, and for clarity the hoop is shown in Figure 5.1.1.1-4. It can be seen that the hoop is moving out-of-plane (Z direction) with alternating plus and minus displacements at each hinge joint.

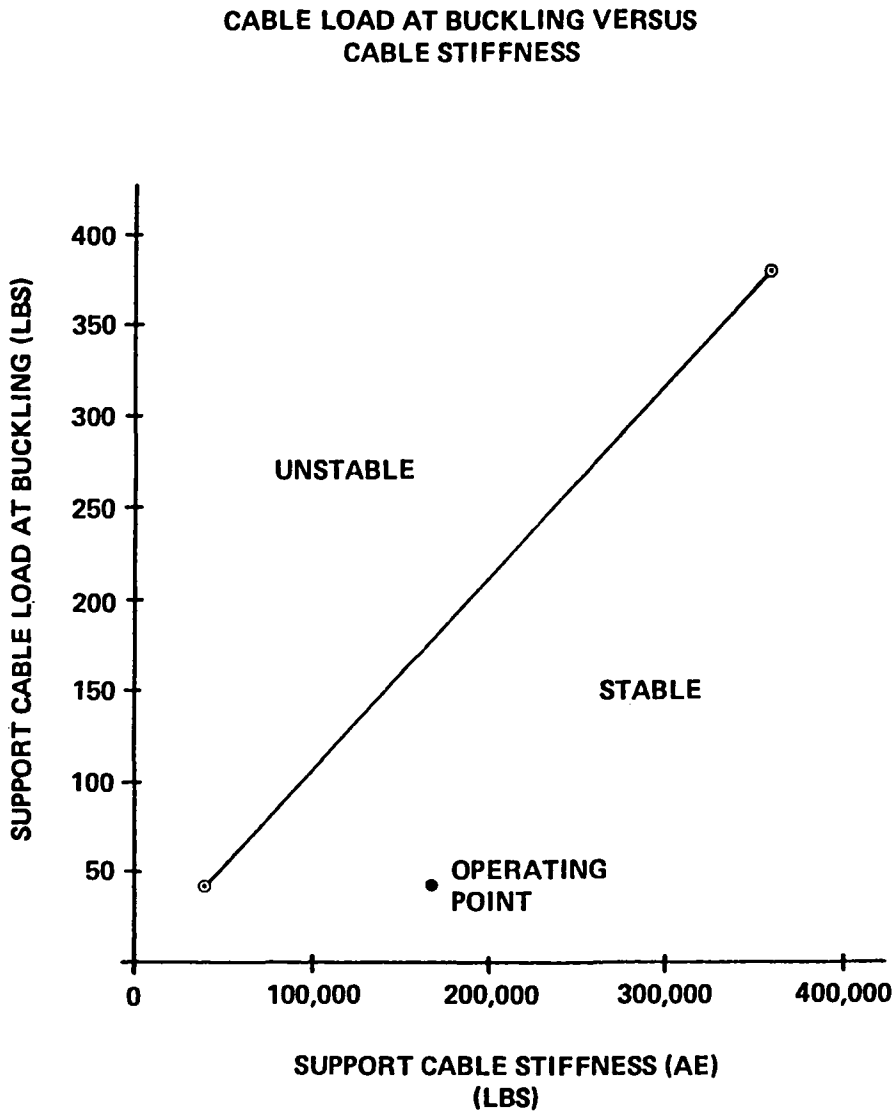

Figure 5.1.1.1-2. Cable Load at Buckling Versus Cable Stiffness

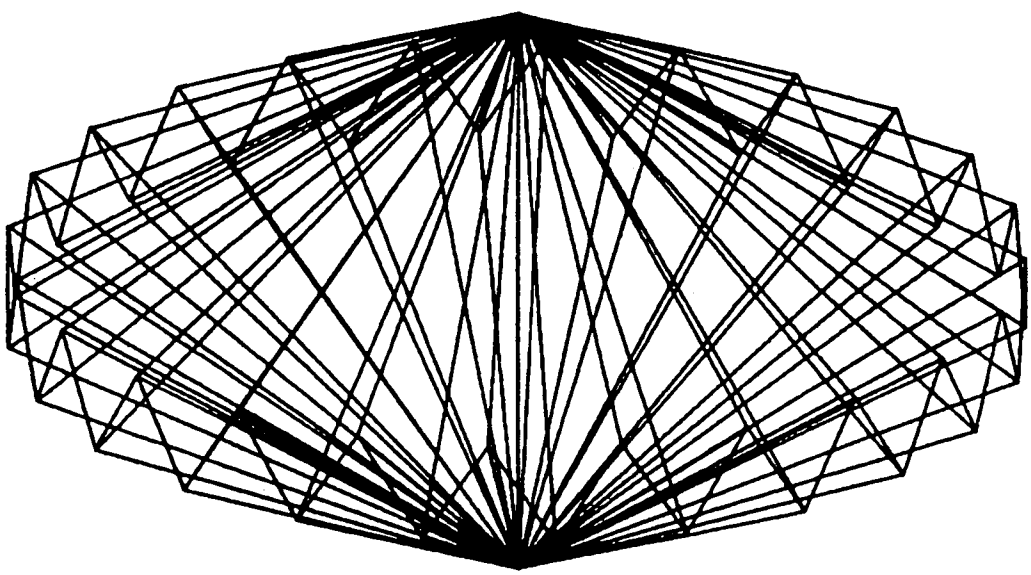

Figure 5.1.1.1-3. Buckled Mode Shape Entire Model

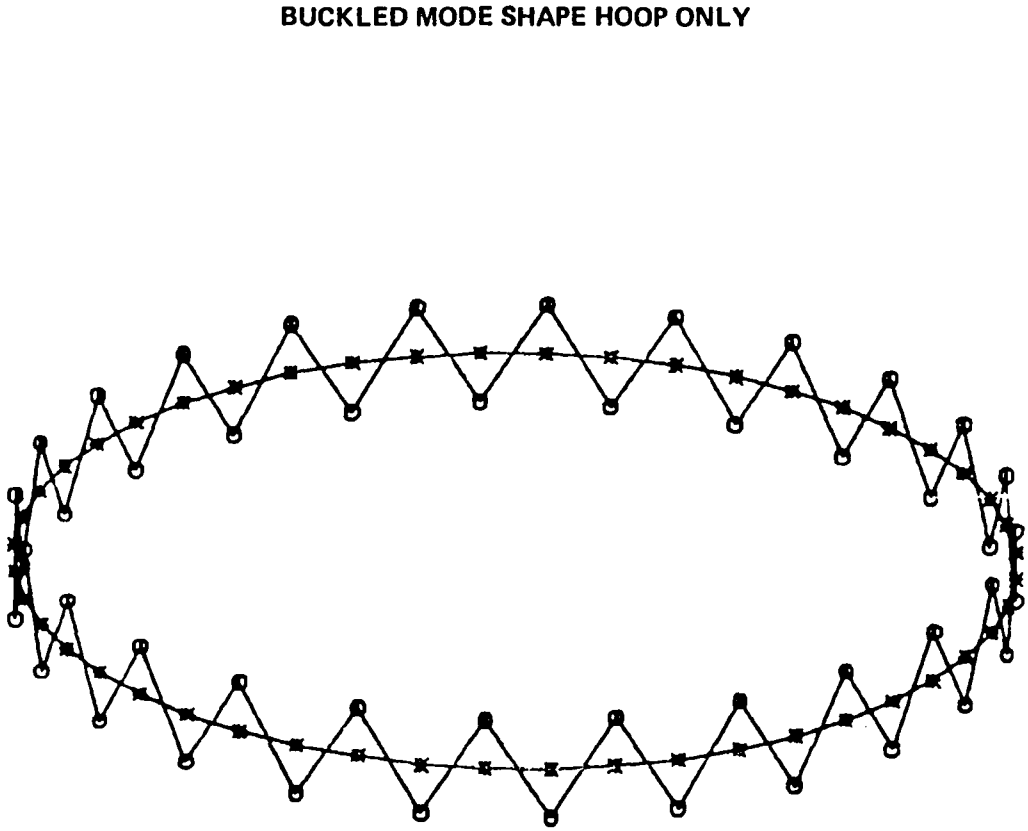

Figure 5.1.1.1-4. Buckled Mode Shape Hoop Only

Knowing the model shape, a greatly simplified model can be used to extract information about hoop/column stability. The model is presented in Figure 5.1.1.1-5 and its geometric relationship with the hoop/column is shown in Figure 5.1.1.1-6. Note that the check falls on the NASTRAN curve in Figure 5.1.1.1-2. The effect of changing radius, number of hoop segments and cable inclination can easily be predicted. Critical Tension T is independent of antenna radius (right hoop). The effect of changing number of segments is shown in Figure 5.1.1.1-7 and Figure 5.1.1.1-8 shows the effect of variation of angle. The actual antenna preload distribution is shown in Figure 5.1.1.1-9. The surface tension has the effect of reducing the angle between hoop control cable loadings from what would correspond to two cable system. The resulting reduction in stability is computed in this figure.

In the global stability model the joints were modeled as simple hinges. Concern over the effect of the more complex four bar linkage joint (shown in Figure 5.1.1.1-10) on stability needs to be addressed. To do this a detailed NASTRAN model of the joint was developed (see Figure 5.1.1.1-11), and was placed at the center of four segments in the model shown in Figure 5.1.1.1-12. Figure 5.1.1.1-13 computed the stability of this system with a system of all simple joints and the stability of the global model.

5.1.1.2 Buckling of the Mast Assembly

The critical buckling load for the Mast Assembly was determined using NASTRAN. A sketch of the finite element model used for this analysis is shown in Figure 5.1.1.2-1. One beam element was used to represent each of the extendable portions of the mast. Section properties and dimensions used in this analysis are shown in the structural analysis appendix.

Results of this analysis show that the critical buckling load is, P_{cr} = 7439 pounds. The compressive load in the mast at overall buckling of the antenna is 2309 pounds. Therefore, buckling of the antenna will occur before buckling of the mast.

The buckled mode shape is shown in Figure 5.1.1.2-2. This is a NASTRAN plot of the buckled mode shape plotted on top of the undeformed shape. Also, it is an isometric view, not a view in the plane of buckling.

SIMPLIFIED HOOP/COLUMN STABILITY

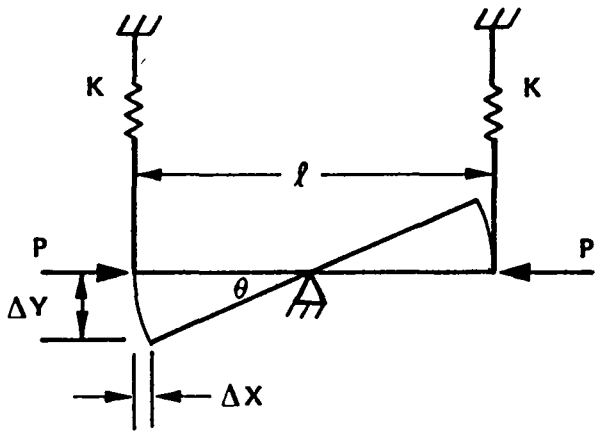

WORK OF FORCE P: $W_P = 2P\ \Delta X$

STRAIN ENERGY: $U = (2)\left(\frac{1}{2}\right) K(\Delta Y)^2$

$$\Delta X = \frac{\ell}{2}(1 - \cos\theta)$$

$$\Delta Y = \frac{\ell}{2}\sin\theta$$

INSTABILITY: $U - W < 0$

$$U - W = K\left(\frac{\ell}{2}\right)^2 \sin^2\theta - 2P\left(\frac{\ell}{2}\right)(1 - \cos\theta)$$

$$= \frac{K\ell^2}{4}\sin^2\theta - 2P\frac{\ell}{2}\frac{1}{1+\cos\theta}\sin^2\theta$$

NEUTRAL STABILITY: $P_c = \underline{\frac{K\ell}{2}}$

Figure 5.1.1.1-5. Simplified Hoop/Column Stability

SIMPLIFIED HOOP/COLUMN STABILITY

HOOP COLUMN GEOMETRIC CONFIGURATION

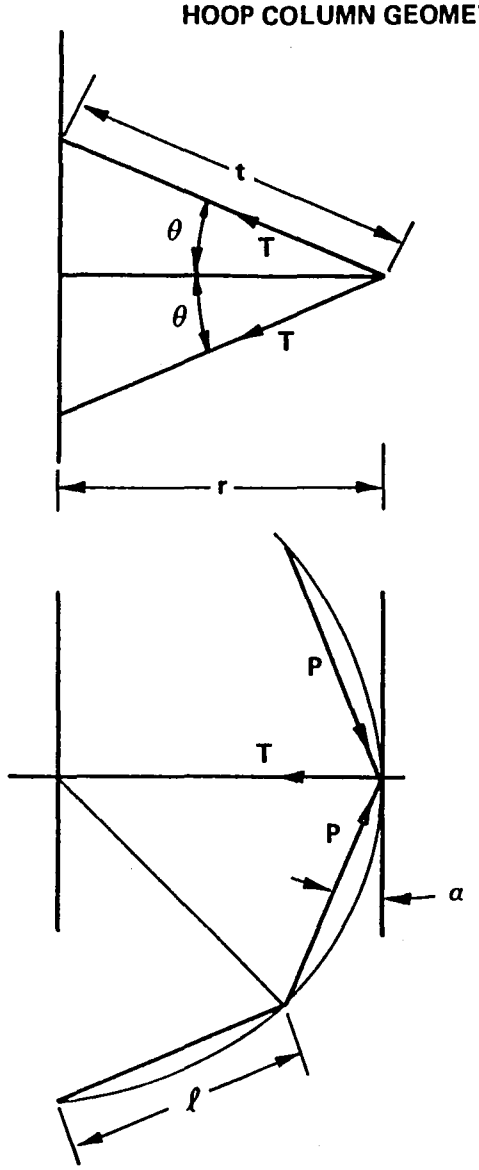

$\ell = 2r \sin \alpha$

$r = t \cos \theta$

$2T_c \cos \theta = 2P_c \sin \alpha$

STIFFNESS: $K_v = \left(\frac{1}{2}\right)(2)\frac{AE}{t} \sin^2 \theta$

$K_v = \frac{AE}{r} \cos \theta \sin^2 \theta$

NEUTRAL STABILITY:

$T_c = \frac{K_v \ell}{2} \frac{\sin \alpha}{\cos \theta} = \frac{K_v}{2} 2r \sin \alpha \frac{\sin \alpha}{\cos \alpha}$

$\underline{\underline{T_c = AE \sin^2 \theta \sin^2 \alpha}}$

CHECK CALCULATION

AE = 1.0 E5
$\theta = 30^o$
α = 3.75 (48 HOOP SEGMENTS)

T_c = (1.0 E5) (0.25) (0.04277)
= 107.0

Figure 5.1.1.1-6. Simplified Hoop/Column Stability Hoop/Column Geometric Configuration

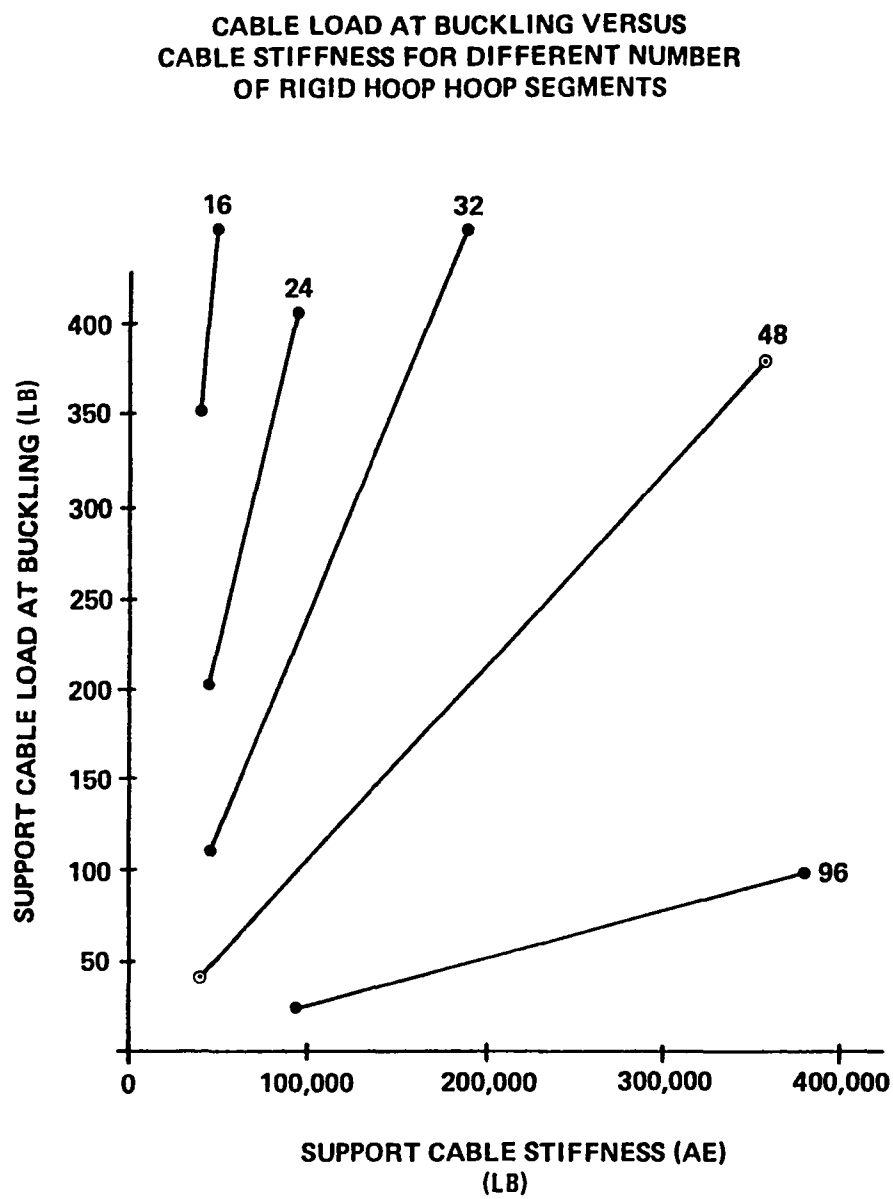

Figure 5.1.1.1-7. Cable Load at Buckling Versus Cable Stiffness for Different Number of Rigid Hoop Hoop Segments

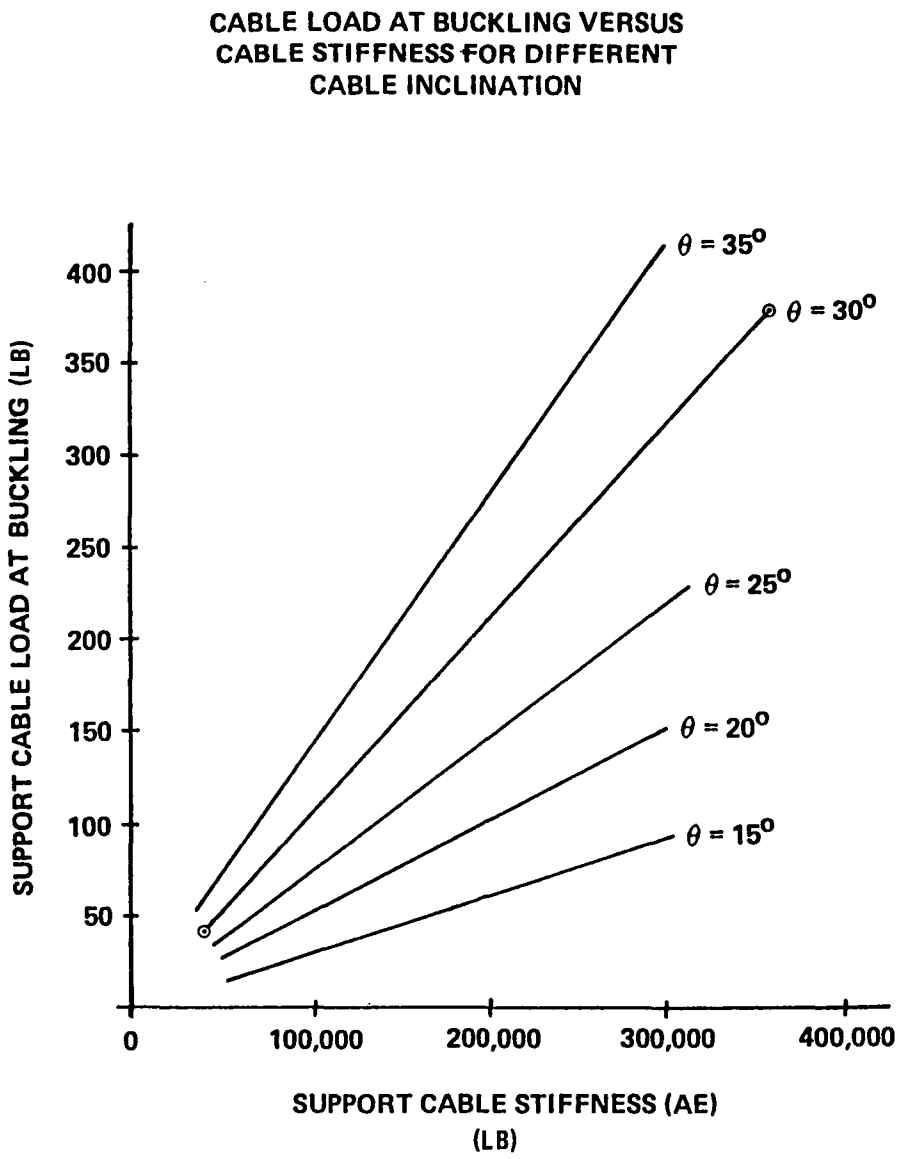

Figure 5.1.1.1-8. Cable Load at Buckling Versus Cable Stiffness for Different Cable Inclination

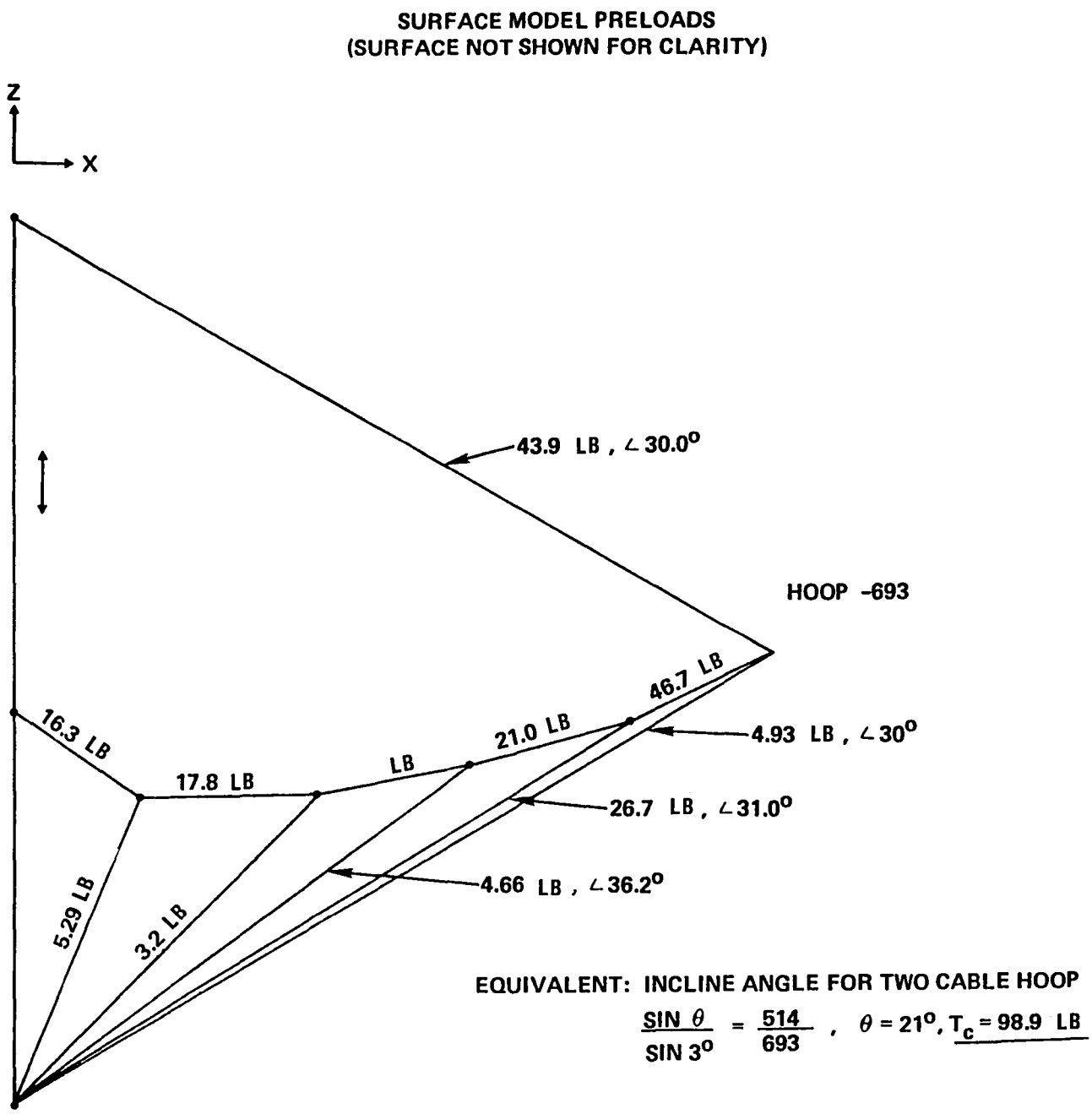

Figure 5.1.1.1-9. Surface Model Preloads
(Surface not Shown for Clarity)

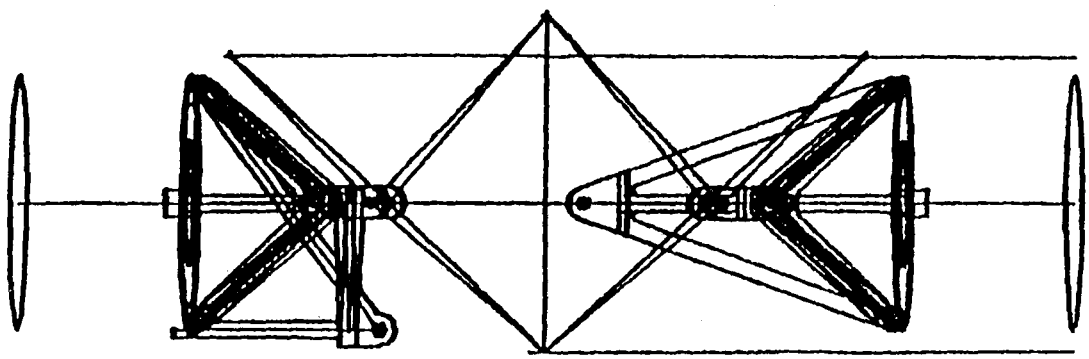

Figure 5.1.1.1-10. Four Bar Linkage Hoop Joint

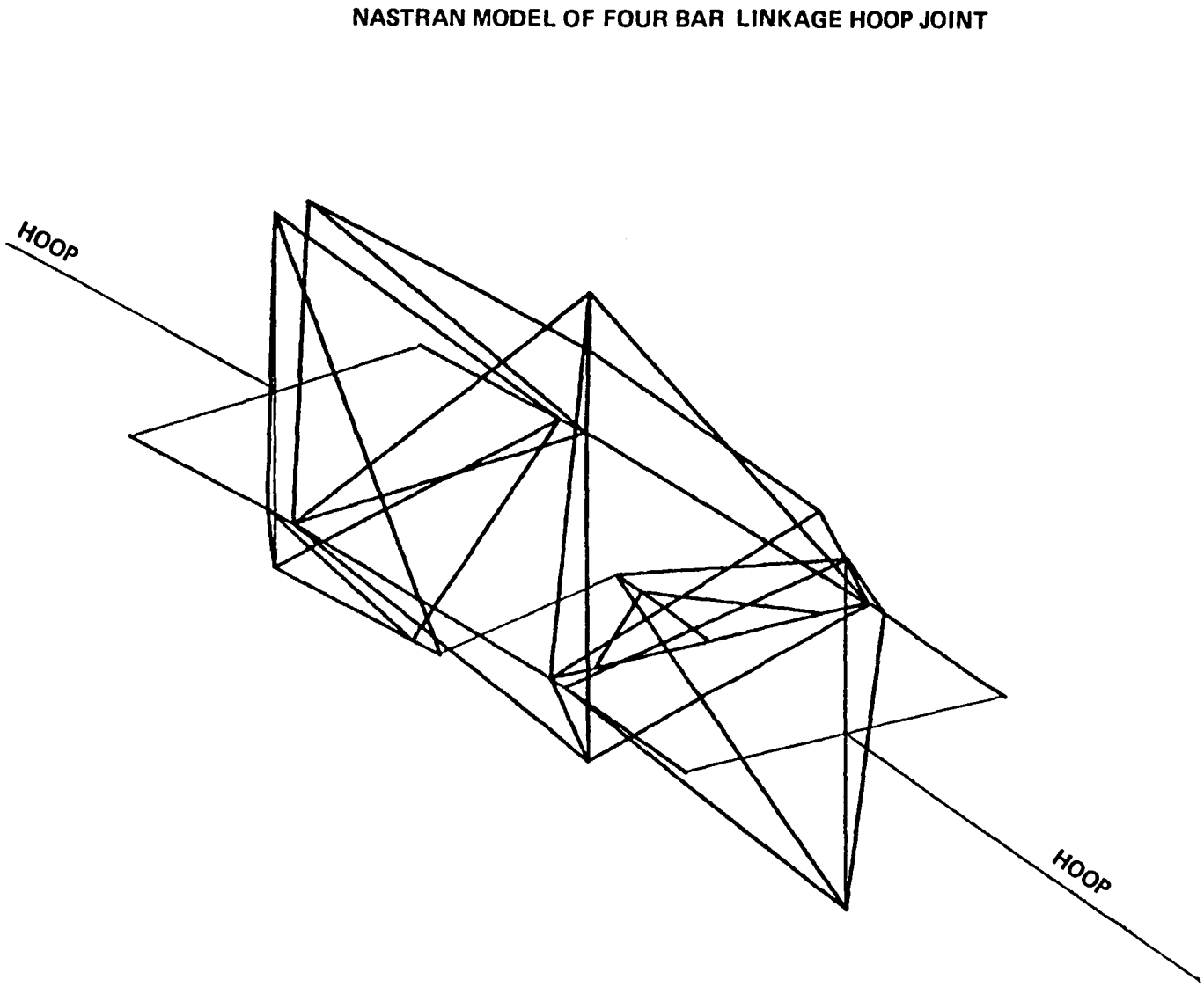

Figure 5.1.1.1-11. NASTRAN Model of Four Bar Linkage Hoop Joint

FOUR SEGMENT MODEL FOR EVALUATION OF FOUR BAR HOOP JOINT

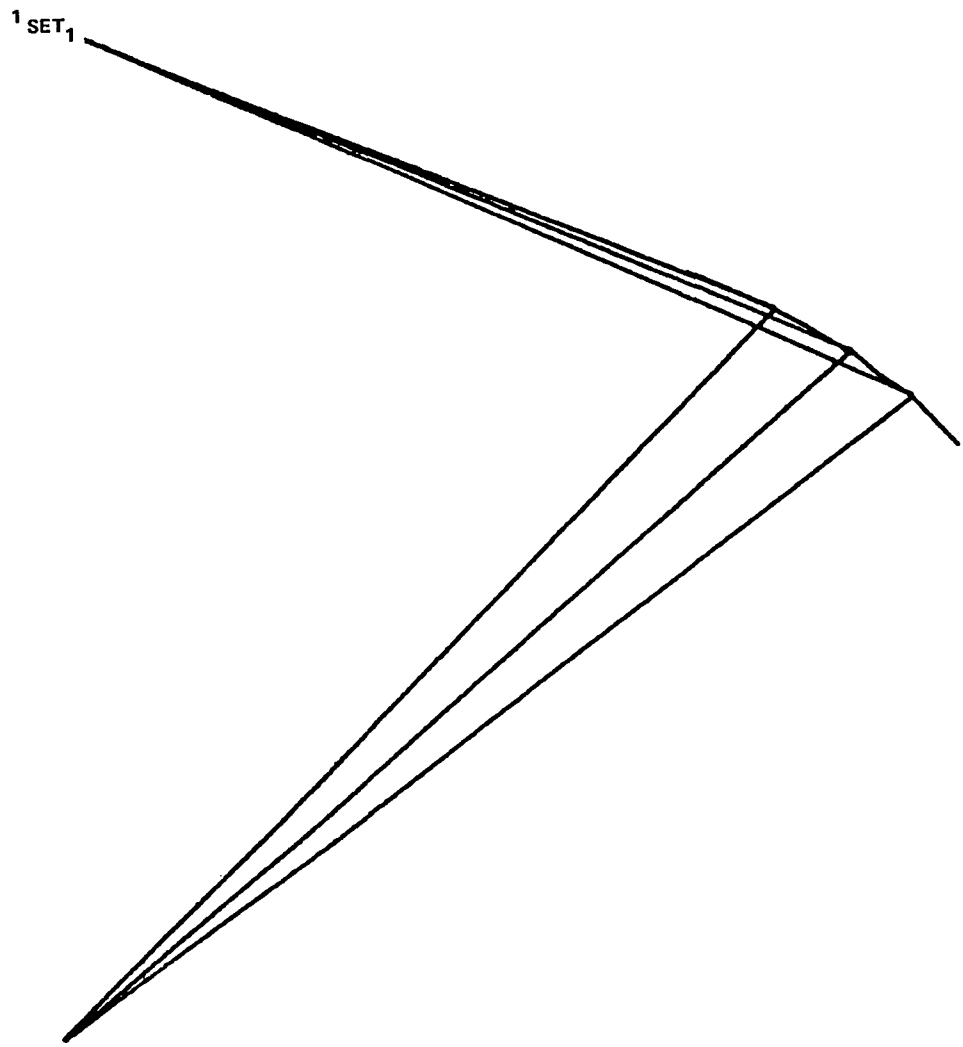

Figure 5.1.1.1-12. Four Segment Model for Evaluation of Four Bar Hoop Joint

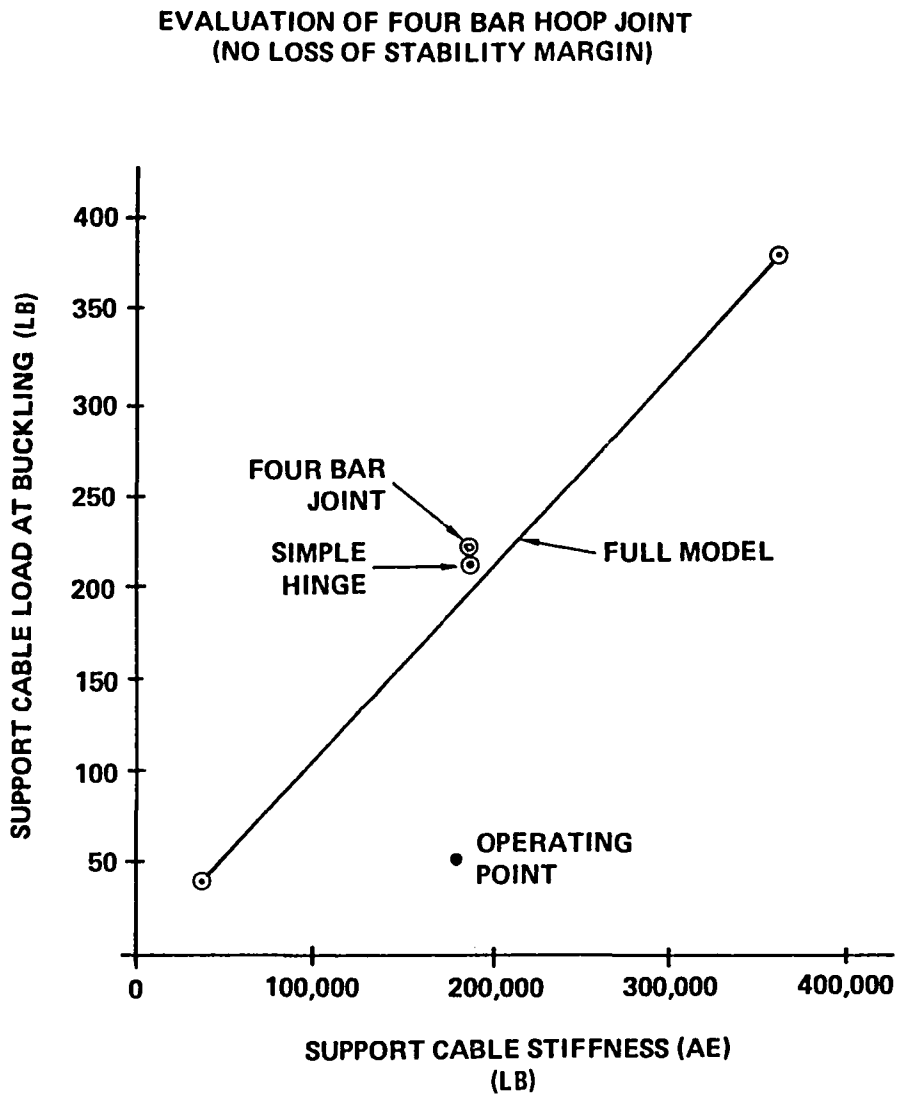

Figure 5.1.1.1-13. Evaluation of Four Bar Hoop Joint (No Loss of Stability Margin)

NASTRAN MAST STABILITY MODEL

L = 109" – EACH SEGMENT

SEGMENT	A (IN^2)	J (IN^4)	$I_2 = I_3$ (IN^4)
1,20	0.758	17.2	51.1
2,19	0.758	33.0	66.1
3,18	0.758	49.0	83.1
4,17	0.758	64.8	102.0
5,16	0.758	80.6	122.9
6,15	0.758	96.6	145.7
7,14	0.758	112.4	170.4
8,13	0.758	128.2	197.1
9,12	0.758	144.2	225.7
10,11	0.758	159.9	256.4

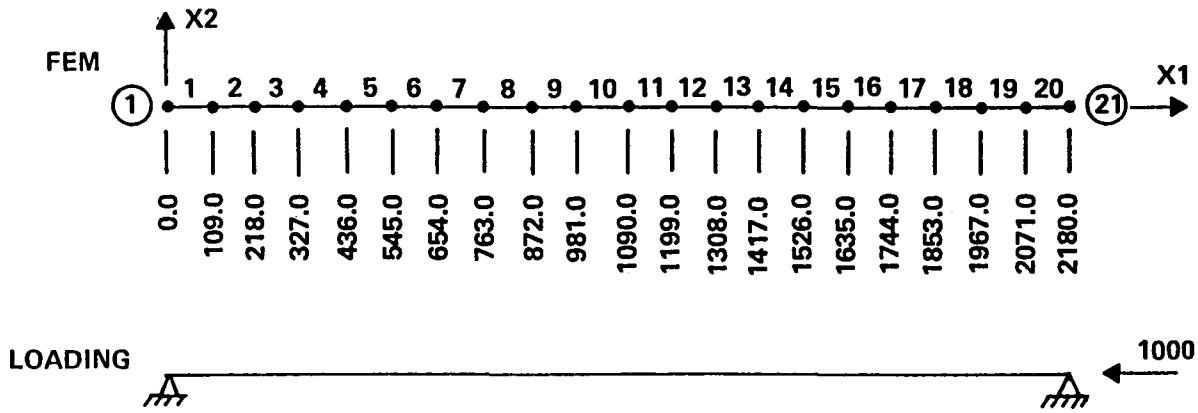

Figure 5.1.1.2-1. NASTRAN Mast Stability Model

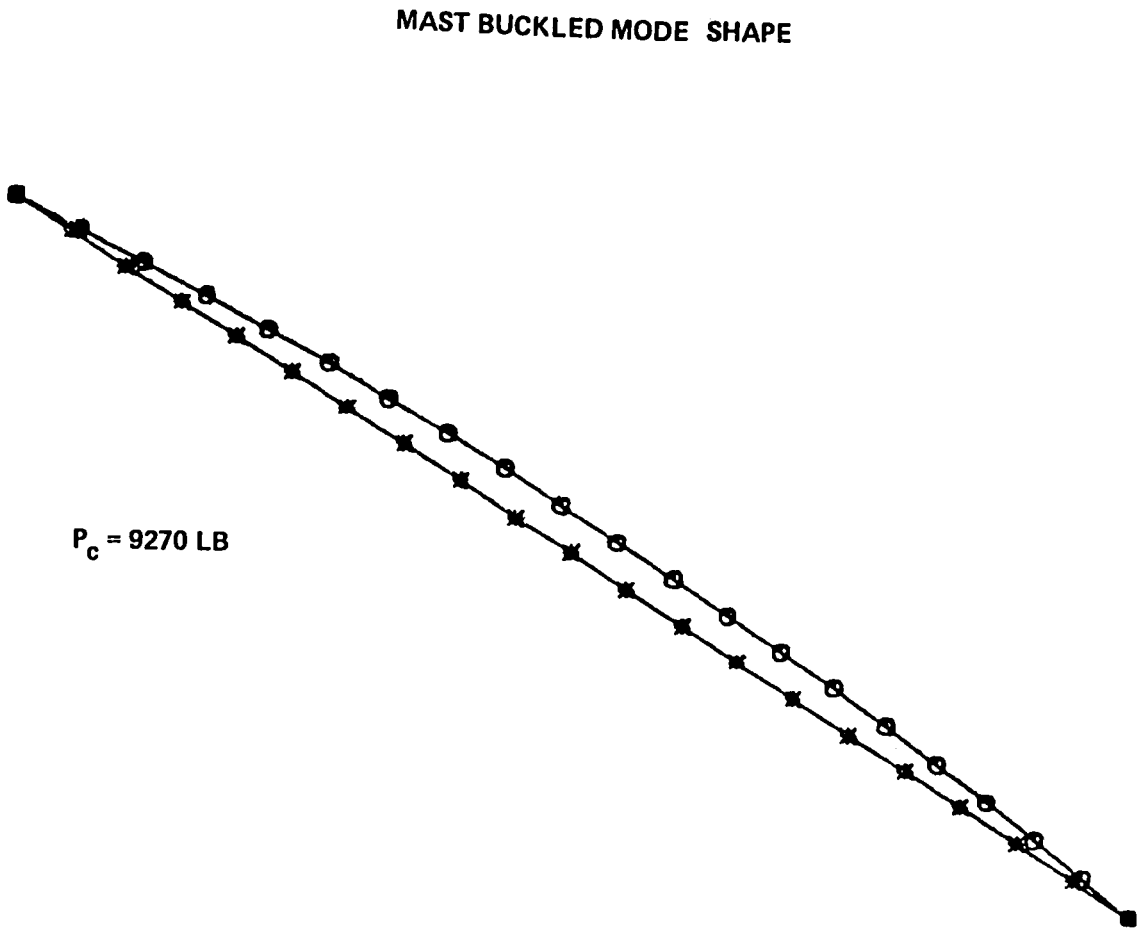

Figure 5.1.1.2-2. Mast Buckled Mode Shape

5.1.1.3 Local Buckling of the Mast

Local buckling of the mast was assessed by calculating the critical buckling load of a detailed model of a single segment at the end of the Mast Assembly. The model is shown in Figure 5.1.1.3-1. It was assumed that the boundary condition is cantilevered from one end and that the load contained a torsional (artificial) component of 10 percent. Refer to the structural analysis appendix for dimensions and section properties. The critical buckling load is 36,700 pounds. This result shows that local buckling of the mast will occur after overall mast buckling, and that overall antenna buckling is the critical mode.

5.1.1.4 Hoop Critical Buckling Load

The critical buckling load for the hoop can be computed with the equation:

$$P_{cr} = \frac{\pi^2 EI}{\ell^2}$$

which defines the critical buckling load for a pinned-pinned beam. In the deployed configuration ℓ = 257.49 inches. Thus,

$$P_{cr} = \frac{\pi^2 (10.6E6) (2.17)}{(257.49)^2} = 3424 \text{ pounds}$$

In the stowed configuration ℓ = 128.74. Thus,

$$P_{cr} = \frac{\pi^2 (10.6E6) (2.17)}{(128.74)^2} = 12{,}922 \text{ pounds}$$

The stability of the point design under pretension loading is best summarized by the margins shown in Figure 5.1.1.4-1.

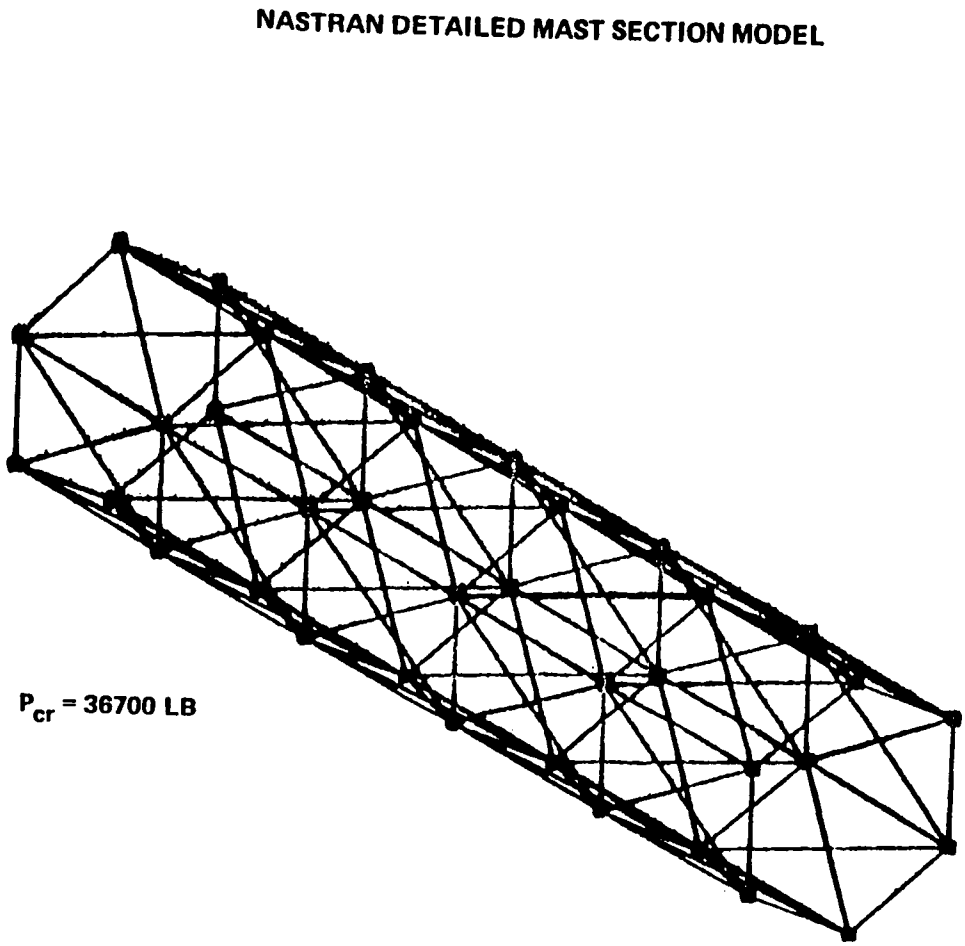

Figure 5.1.1.3-1. NASTRAN Detailed Mast Section Model

HOOP/COLUMN MARGINS OF SAFETY FOR PRETENSION LOADS

ITEM	LOADING	FAILURE	ALLOWABLE STRESS OR LOAD	MARGIN OF SAFETY
SYSTEM	DESIGN PRE-TENSION 43.9 LB	STABILITY	98.9 LB	+0.80
	FULL SUN PRE-TENSION 48.9 LB	STABILITY	98.9 LB	+0.67
UPPER HOOP	FULL SUN PRE-TENSION 48.9 LB	TENSION ULT	$(40_{st} \times 5.75 \frac{LB}{st})$ = 230 LB	+2.76
TOTAL MAST	FULL SUN 1370 LB COMP	STABILITY	9270 LB	+4.4
VERTICAL MAST MEMBER	FULL SUN 1370/6 LB COMP	COMP ULT	14700 PSI	+5.80
HOOP	FULL SUN 772 LB COMP	STABILITY	3422 LB	+2.54
	FULL SUN 772 LB COMP	COMP ULT	14700 PSI	+6.43

MARGINS INCLUDE 1.25 FACTOR

Figure 5.1.1.4-1. Hoop/Column Margins of Safety for Pretension Loads

5.1.2 Deployed Dynamics

The objective of the deployed dynamic analysis is to predict the dynamic characteristics of the hoop/column antenna. Both a detailed finite element model of the point design and simplified antenna dynamic models are presented in what follows. The simplified models yield a check on the detailed model and also provides analytical information on the Hoop/Column antenna design.

A finite element model of the point design was developed using NASTRAN. Figure 5.1.2-1 shows a view of the entire model and Figure 5.1.2-2 shows the same view with the control cables removed. The model is a two-for-one 24-gore model with cables of double stiffness. Experience at Harris has shown excellent correlation of two-for-one models with test results. Also, the surface does not have the detail of the half-gore model used in the surface design definition. However, the degree of lumping evidenced here is not unusual in dynamic analysis modeling. Figure 5.1.2-3 gives the components of the model and Figure 5.1.2-4 gives the system mass properties. Detailed information about the model structural description is available in the structural analysis appendix.

Two NASTRAN runs were required to obtain dynamic information. In the first, an artificial temperature distribution was defined to generate the antenna pretension field and compute geometric stiffness. The second run was a conventional normal miles run but with the geometric stiffness added to the standard stiffness matrix. Figure 5.1.2-5 gives the frequencies of the lower 12 modes. Plots of some of these modes are presented in Figures 5.1.2-6a through 5.1.2-6h.

In addition to the finite element analysis, simple computation of model frequencies were computed by assuming that the antenna responds as decoupled two degree-of-freedom systems. These computations are shown in Figures 5.1.2-7 through 5.1.2-9. The frequency expressions presented in these figures can be used to estimate the performance of a variety of Hoop/Column configrations. Results of varying the radius and assuming the mass grows linearly with radius are shown in Figure 5.1.2-10. It should be pointed out that mast and feed mast bending modes will interact with the surface modes studied here.

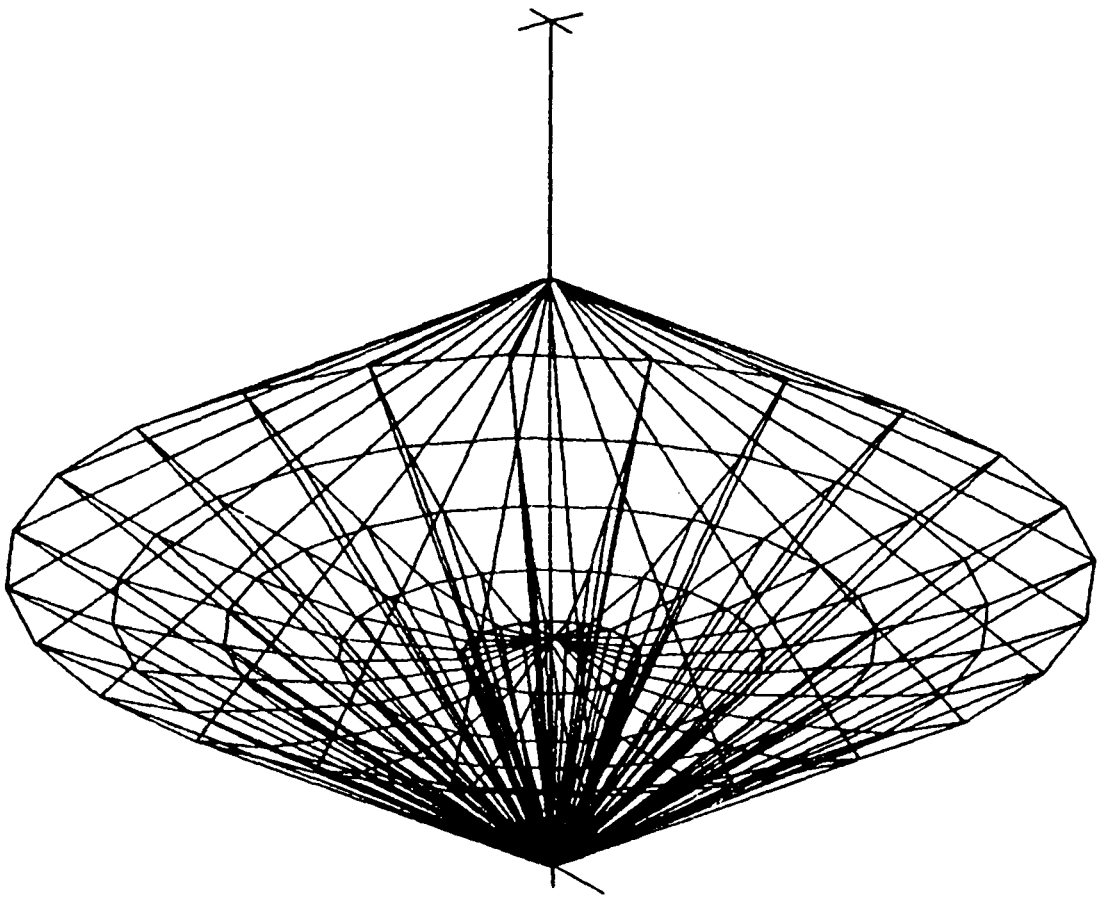

Figure 5.1.2-1. NASTRAN 100-Meter Deployed Dynamics Model

NASTRAN 100 METER DEPLOYED DYNAMICS MODEL WITH CONTROL CORDS REMOVED

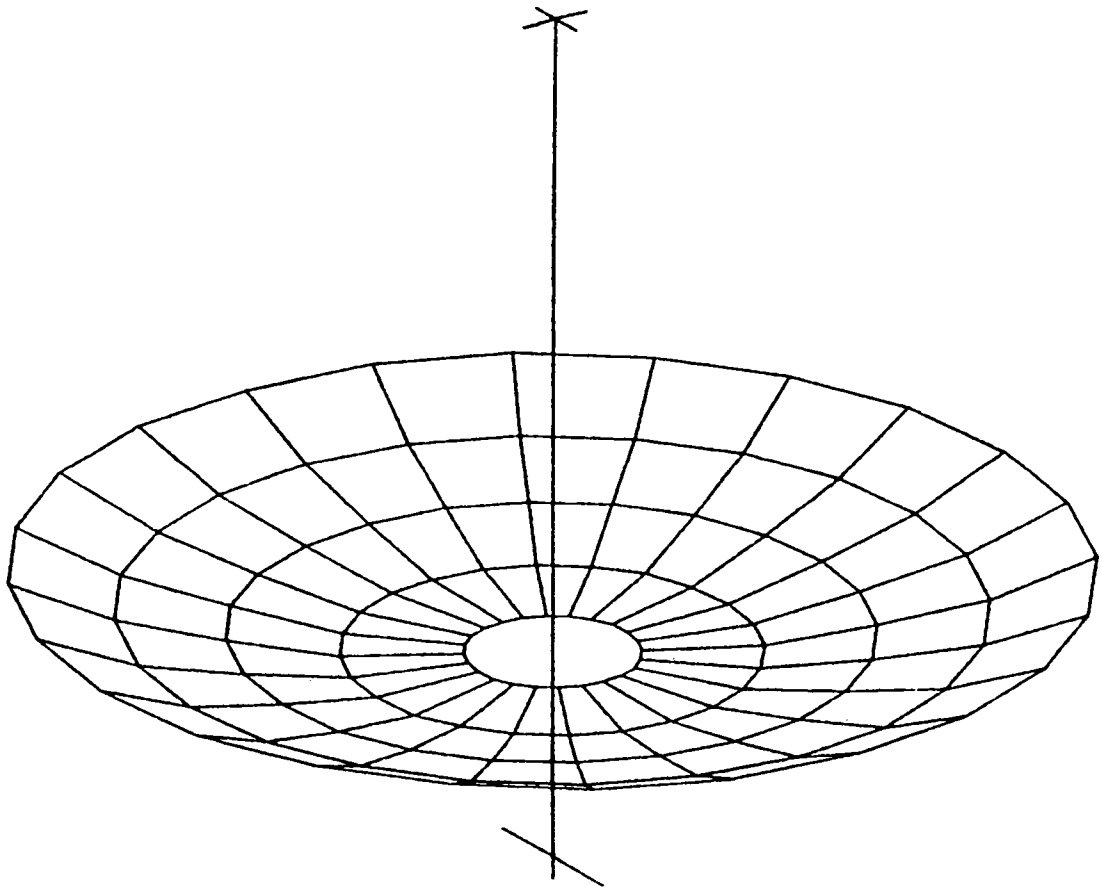

Figure 5.1.2-2. NASTRAN 100-Meter Deployed Dynamics Model With Control Cords Removed

POINT DESIGN COMPONENTS

COMPONENT	WEIGHT LB	WEIGHT KG
ANTENNA MAST (SEGMENTS, FITTINGS AND MOTORS)	1427	649
REFLECTOR ASSEMBLY	284	135
SURFACE CONTROL CORDS	83	30
HOOP (TUBES, MLI, END FITTINGS AND MOTORS)	755	343
HOOP CONTROL CABLES	57	26
FEEDS AND FEED SUPPORTS	900	409
FEED MAST (ASTRO MAST)	388	177
SOLAR ARRAYS WITH SUPPORT BOOMS	120	55
SPACECRAFT	1300	591
IUS	10000	4545

Figure 5.1.2-3. Point Design Components

NASTRAN MODEL MASS PROPERTIES

WEIGHT (LB) : 15423

C. G. (X, Y, Z) (IN.): (0.0, 0.0, -696.4)

INERTIA MATRIX ($LB\text{-}IN^2$)

I_{xx} = 1.626 E10

I_{yy} = 1.627 E10

I_{zz} = 3.5 E9

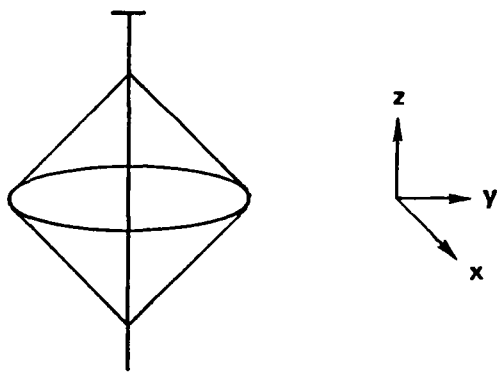

Figure 5.1.2-4. NASTRAN Model Mass Properties

100M POINT DESIGN
DEPLOYED DYNAMICS MODEL NORMAL MODES

MODE NO.	GENERALIZED MASS (Kg)	FREQUENCY Hz	DESCRIPTION
1 – 6	–	0.0	RIDIG BODY
7	79.1	0.15	ANTENNA TORSION
8	2.7	0.19	MAST BENDING, SURFACE PITCH
9	2.7	0.19	MAST BENDING, SURFACE YAW
10	60.6	0.31	MAST TORSION, SURFACE SHEAR
11	15.5	0.67	MAST 2ND TORSION, SURFACE SHEAR
12	0.71	0.88	MAST 2ND BENDING, SURFACE PITCH
13	0.62	0.91	MAST 2ND BENDING, SURFACE PITCH
14	0.78	1.6	MAST 3RD BENDING, SURFACE PITCH

Figure 5.1.2-5. 100-Meter Point Design
Deployed Dynamics Model Normal Modes

DEPLOYED DYNAMIC MODEL MODE 7

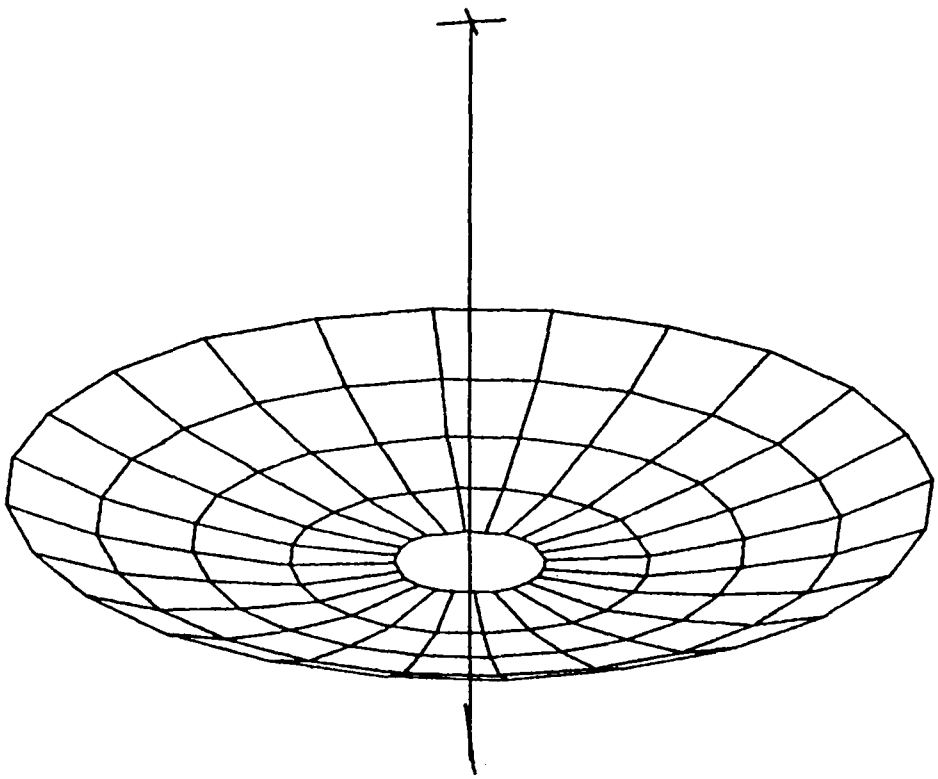

Figure 5.1.2-6a. Deployed Dynamic Model Mode 7

DEPLOYED DYNAMIC MODEL MODE 8

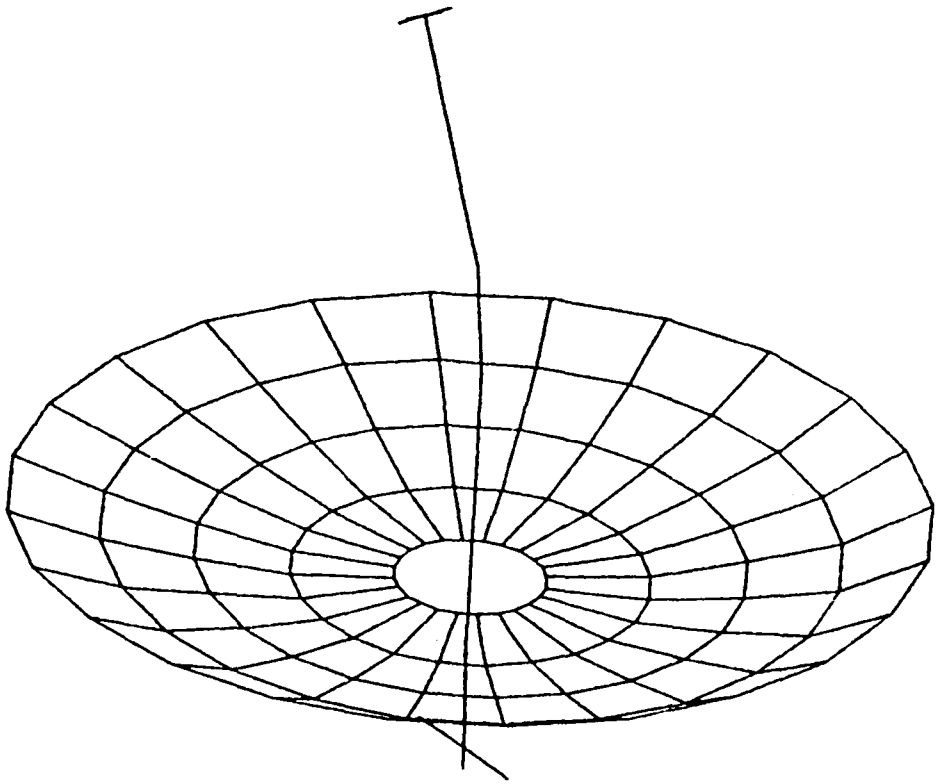

Figure 5.1.2-6b. Deployed Dynamic Model Mode 8

DEPLOYED DYNAMIC MODEL MODE 9

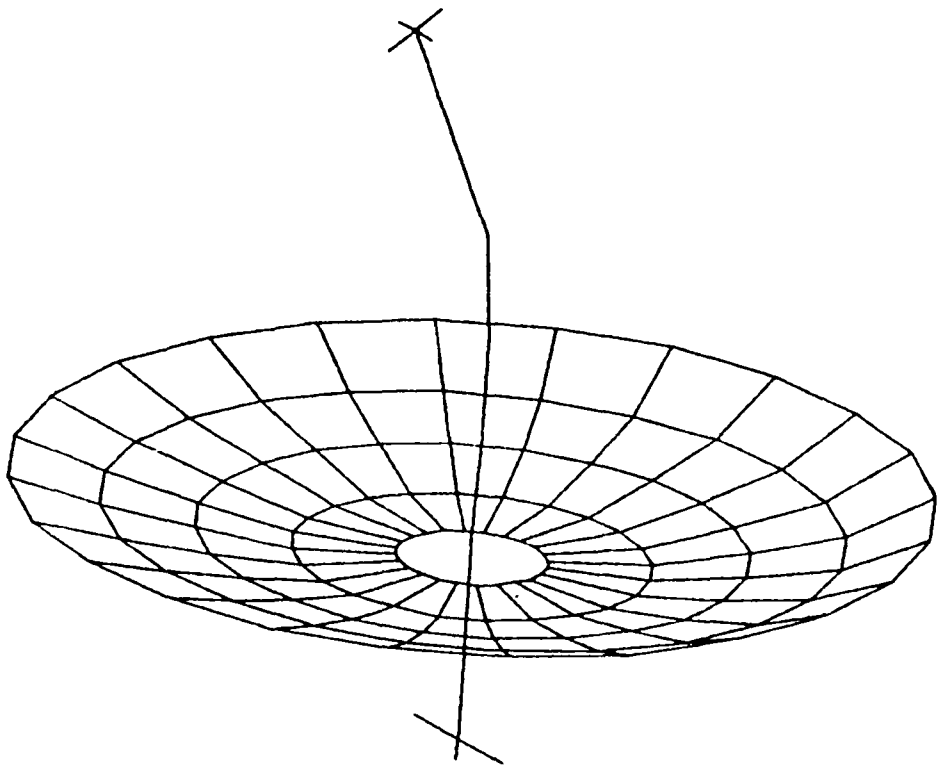

Figure 5.1.2-6c. Deployed Dynamic Model Mode 9

DEPLOYED DYNAMIC MODEL MODE 10

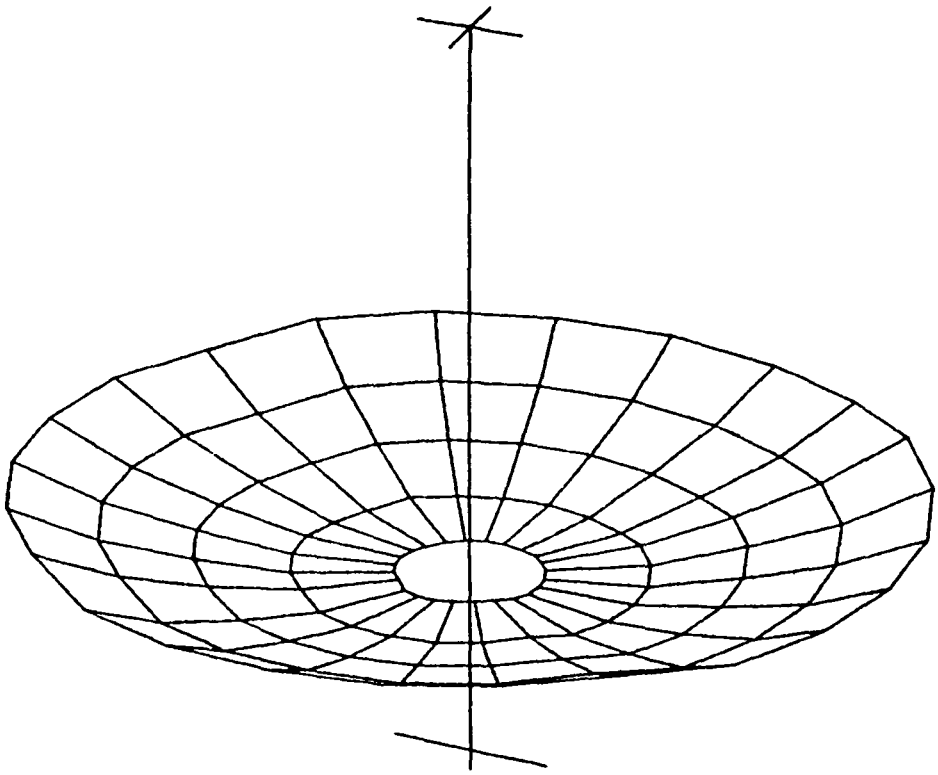

Figure 5.1.2-6d. Deployed Dynamic Model Mode 10

DEPLOYED DYNAMIC MODEL MODE 11

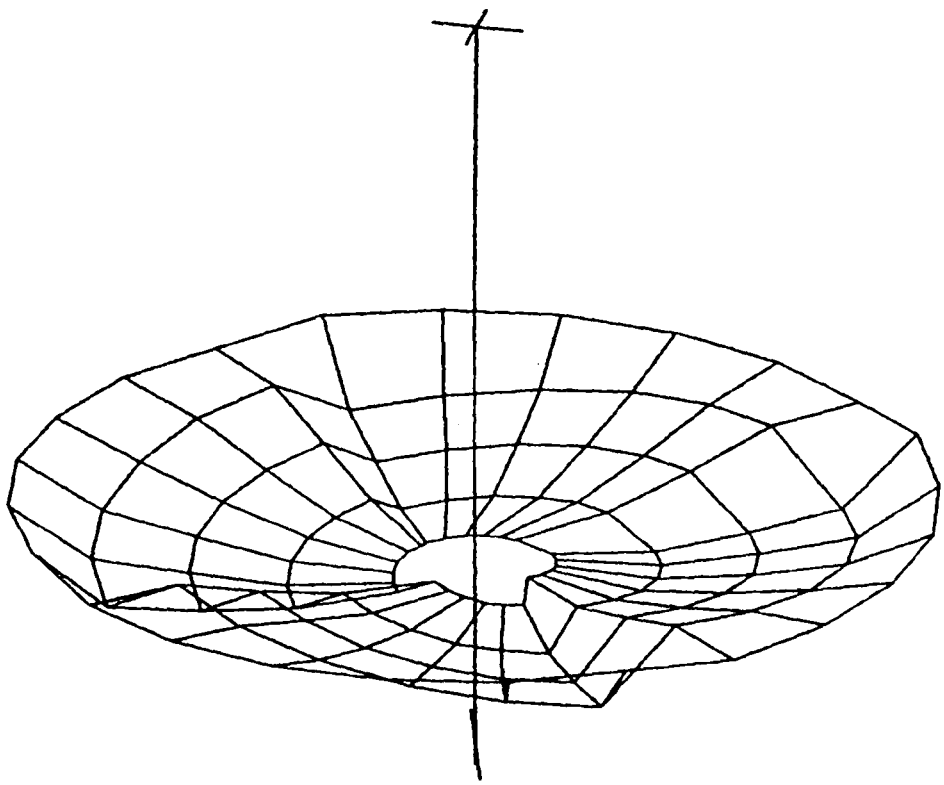

Figure 5.1.2-6e. Deployed Dynamic Model Mode 11

DEPLOYED DYNAMIC MODEL MODE 12

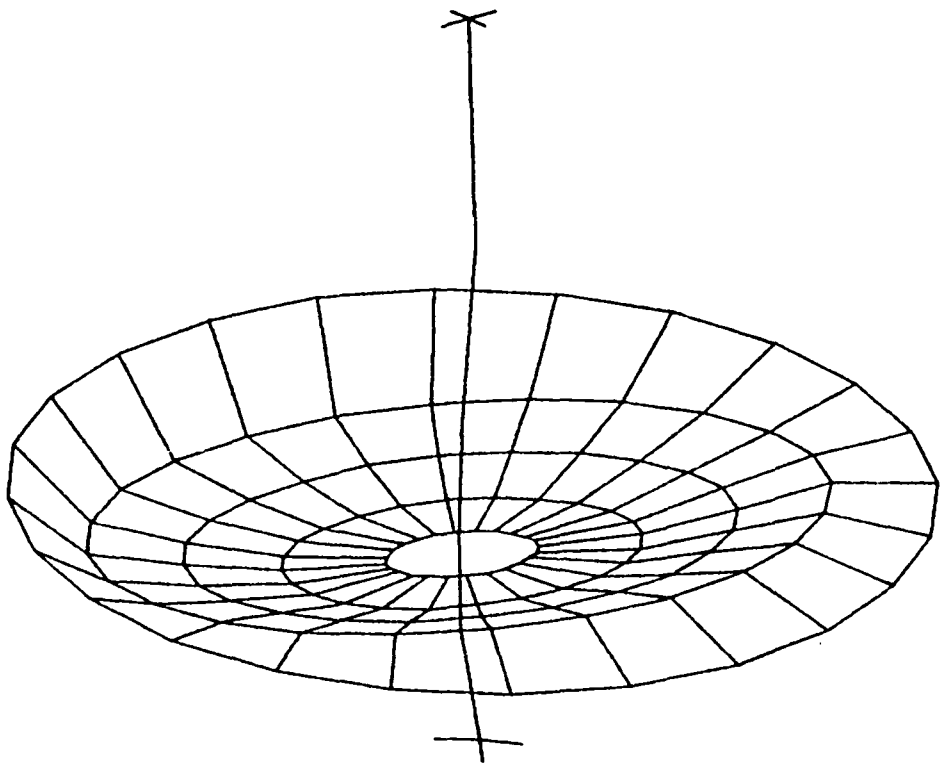

Figure 5.1.2-6f. Deployed Dynamic Model Mode 12

DEPLOYED DYNAMIC MODEL MODE 13

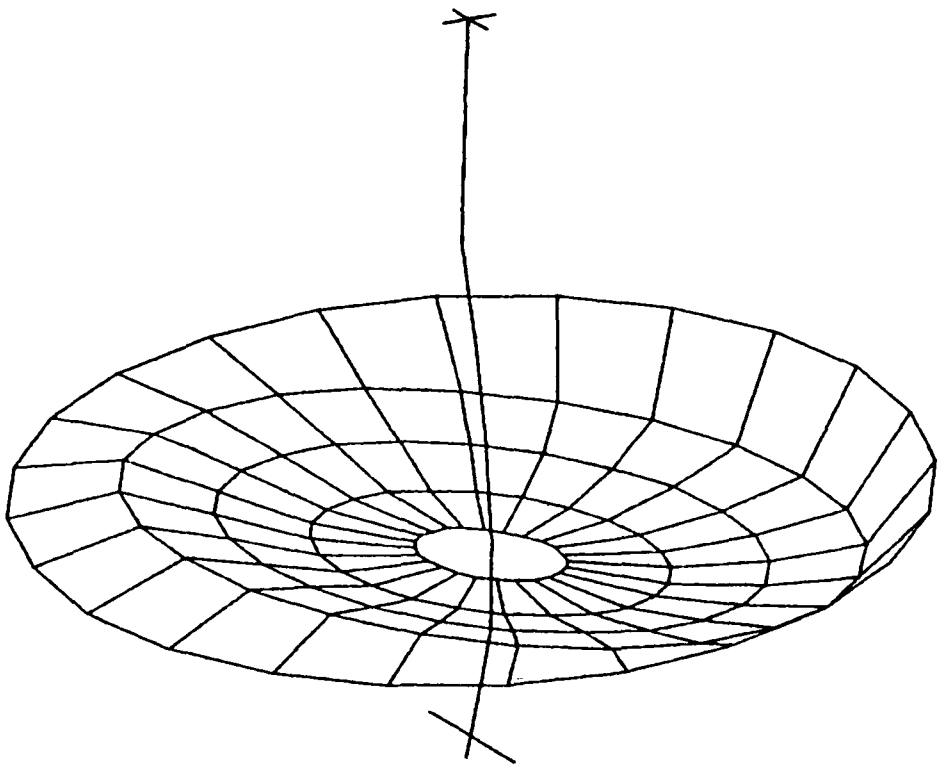

Figure 5.1.2-6g. Deployed Dynamic Model Mode 13

DEPLOYED DYNAMIC MODEL MODE 14

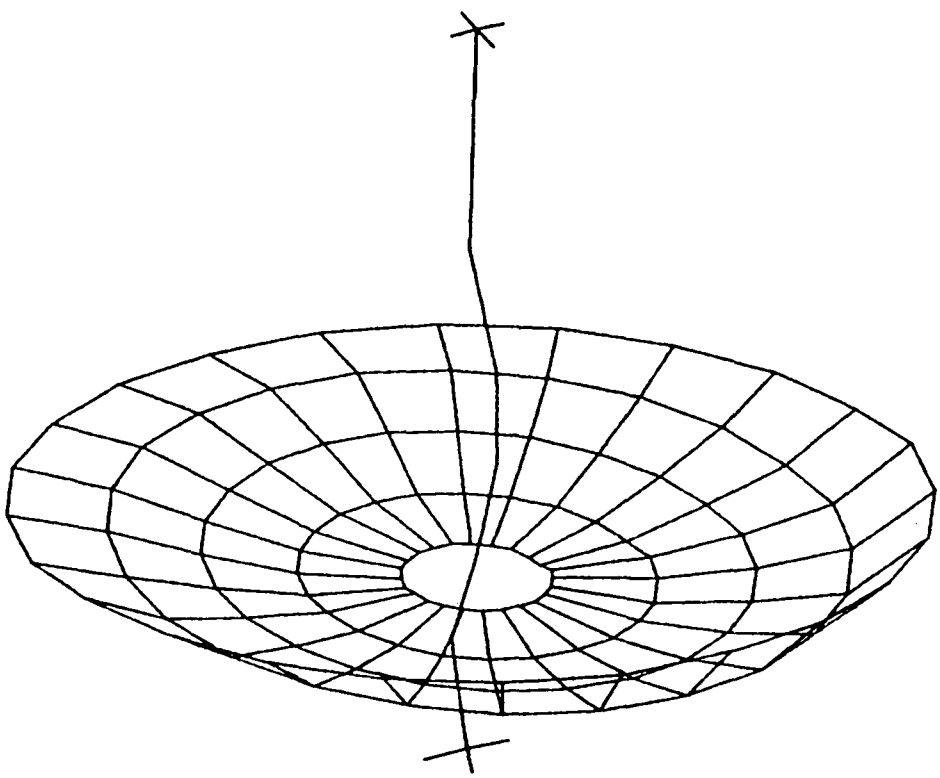

Figure 5.1.2-6h. Deployed Dynamic Model Mode 14

SIMPLE TORSION MODE COMPUTATION (RIGID HOOP AND MAST)

- F ~ COMPRESSION IN HOOP
  θ ~ RELATIVE ROTATION
  β ~ 360/2N
  r ~ HOOP RADIUS
  r_m ~ MAST RADIUS
  t ~ RESULTANT TENSION
  g ~ GRAVITATIONAL CONSTANT, 386 IN/SEC^2

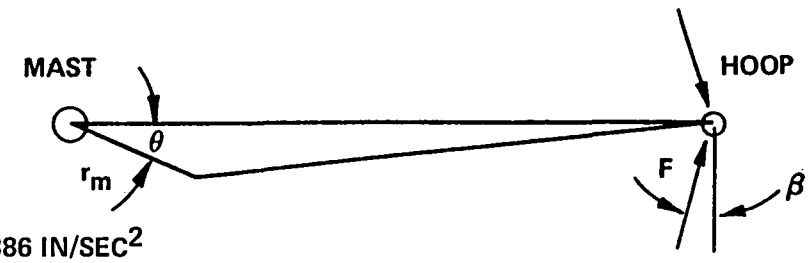

- $\text{TORQUE}_M = t\, r_m \sin\theta \Rightarrow K_\theta = N t r_m,\ t = 2F \sin(\beta)$
- EQ OF MOTION

$$\frac{1}{g}\begin{bmatrix} J_M & \\ & J_H \end{bmatrix}\begin{Bmatrix} \ddot{\theta}_1 \\ \ddot{\theta}_2 \end{Bmatrix} + \begin{bmatrix} K_\theta & -K_\theta \\ -K_\theta & K_\theta \end{bmatrix}\begin{Bmatrix} \theta_1 \\ \theta_2 \end{Bmatrix} = \begin{Bmatrix} 0 \\ \end{Bmatrix}$$

- FREQUENCY EQUATION:

$$f = \frac{1}{2\pi}\left(\frac{K_\theta (J_M + J_H)}{g\ J_M J_H}\right)^{1/2}$$

- POINT DESIGN: $J_M = 4.84\ E7$ LB-IN^2, $J_H = 3.48\ E8$ LB-IN^2, $F = 693$ LB, $r_m = 23$ IN.

$f = 0.149$ Hz

Figure 5.1.2-7. Simple Torsion Mode Computation (Rigid Hoop and Mast)

SIMPLE VERTICAL MODE COMPUTATION (RIGID HOOP MAST)

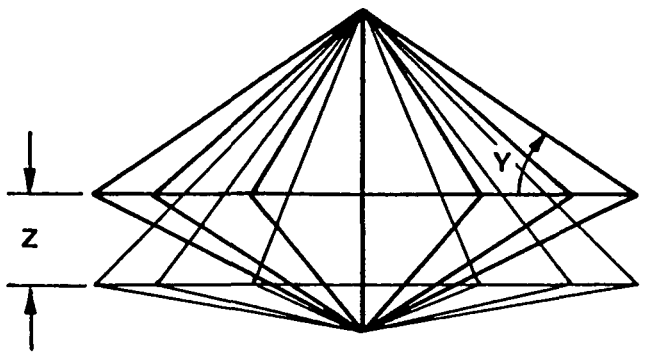

- AE ~ CABLE UNIT STIFFNESS, t ~ CABLE TENSION
  Y ~ CABLE INCLINATION ANGLE
  Z ~ RELATIVE VERTICAL DISPLACEMENT
  r ~ RADIUS
- VERTICAL STIFFNESS PER CABLE:

$$K_Z = \frac{\cos Y}{r} \left(AE \sin^2 Y + t \cos^2 Y\right)$$

- TOTAL VERTICAL STIFFNESS: $K = 2N K_Z$
- EQUATION OF MOTION:

$$\frac{1}{g}\begin{bmatrix} M_H & \\ & M_M \end{bmatrix} \begin{Bmatrix} \ddot{Z}_1 \\ \ddot{Z}_2 \end{Bmatrix} + \begin{bmatrix} K & -K \\ -K & K \end{bmatrix} \begin{Bmatrix} Z_1 \\ Z_2 \end{Bmatrix} = \begin{Bmatrix} 0 \end{Bmatrix}, \quad f = \frac{1}{2\pi}\left(\frac{K(M_H + M_M)}{g M_H M_M}\right)^{1/2}$$

- POINT DESIGN: $M_M = 14316$ LB, $M_H = 1105.9$, $K_Z = 19.8$ LB/IN

  $f = 4.2$ Hz

Figure 5.1.2-8. Simple Vertical Mode Computation (Rigid Hoop and Mast)

SIMPLE PITCH MODE COMPUTATION (RIGID HOOP AND MAST)

AE ~ CABLE UNIT STIFFNESS, t ~ CABLE TENSION
Y ~ CABLE INCLINATION
θ ~ RELATIVE ROTATION
β ~ CABLE AZIMUTH
r ~ RADIUS

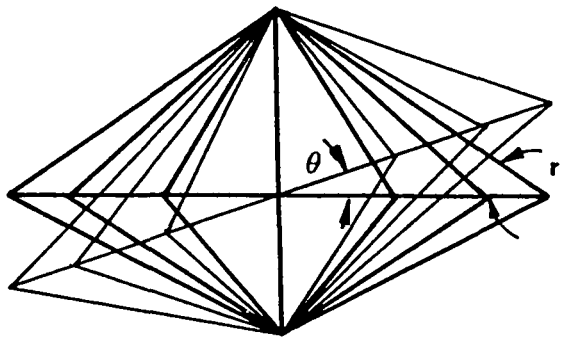

- VERTICAL STIFFNESS PER CABLE:

$$K_Z = \frac{COSY}{r} (AE \, SIN^2 Y + t \, COS^2 Y)$$

- PITCH ROTATION STIFFNESS:

$$K_P = 2 K_Z r^2 \sum_{i=1}^{N} COS^2 \left(\frac{360}{N} i\right) = K_Z r^2 N, \; N/4 \sim INTEGER$$

- EQUATION OF MOTION:

$$\frac{1}{g}\begin{bmatrix} I_H & \\ & I_M \end{bmatrix}\begin{Bmatrix} \ddot{\theta}_1 \\ \ddot{\theta}_2 \end{Bmatrix} + \begin{bmatrix} K_P & -K_P \\ -K_P & K_P \end{bmatrix}\begin{Bmatrix} \theta_1 \\ \theta_2 \end{Bmatrix} = \begin{Bmatrix} 0 \end{Bmatrix}$$

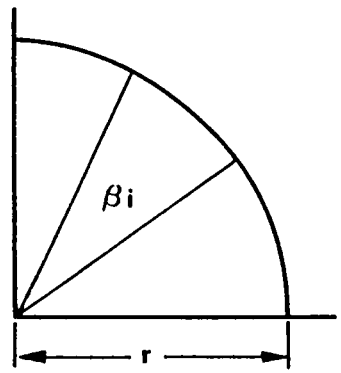

- FREQUENCY EQUATION:

$$I_H I_M W^4 + (I_M + I_H) K_P W^2 = 0,$$

$$f = \frac{1}{2\pi} \left(\frac{K_P (I_M + I_H)}{g \, I_M \, I_H}\right)^{1/2}$$

- POINT DESIGN: AE = 1.8 E5 LB, t = 40 LB, Y = 30°, r = 1968.5 IN., N = 48, I_H = 4.3 E9 LB-IN^2, I_M = 11.9 E9 LB-IN^2

  K_Z = 19.8 LB/IN., K_P = 3.68 E9, f = 3.34 Hz

Figure 5.1.2-9. Simple Pitch Mode Computation (Rigid Hoop and Mast)

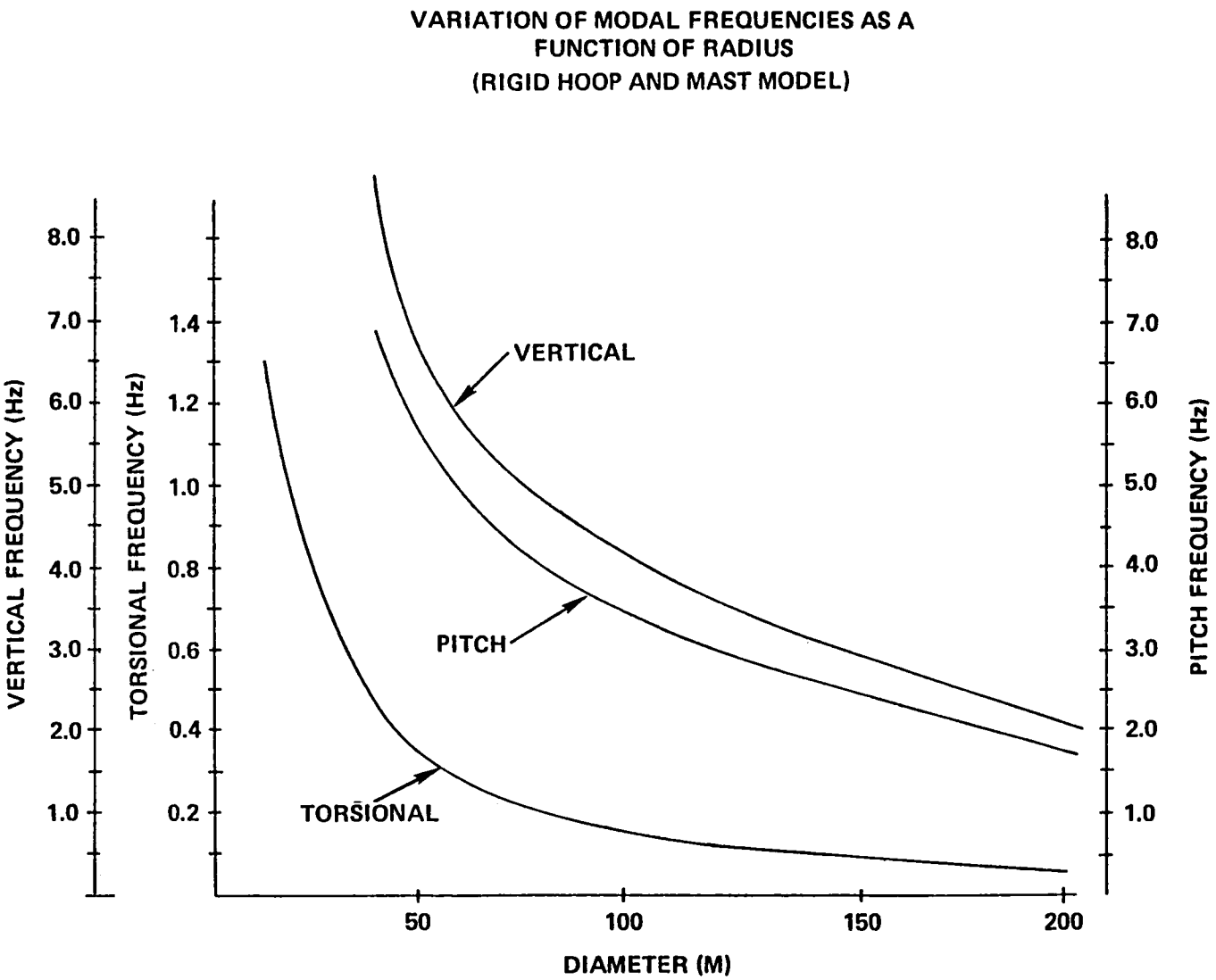

Figure 5.1.2-10. Variation of Modal Frequencies as a Function of Radius (Rigid Hoop and Mast Model)

5.1.3 Deployment Kinematics

An analysis of the Hoop/Column antenna hoop deployment is depicted in Figure 5.1.3-1. The hoop deploys in a quasi-static manner and the analysis presents the equilibrium forces as a function of hoop angle of deployment. Tabular results are given in Figure 5.1.3-2 and these results are plotted in Figure 5.1.3-3.

Two possible complications which will result in a nonuniform deployment must be considered. The first is uneven deployment caused by a potential snag. Figure 5.1.3-4 gives a simplified analysis of a snag condition. Figure 5.1.3-5 shows the effect of snag loading on the change in cable inclintion angle for various angles of deployment. It can be concluded that even though deployment is sensitive to snag conditions, successful deployment will not be hampered by snags of several pounds. The second complication is deployment in a rotating reference frame where the change in hoop inertia during deployment will cause an angular difference between the mast and hoop. Figure 5.1.3-6 gives an analysis of this condition. From the equation developed there, the angular difference will be no greater than one degree for an initial angular velocity of the system of 0.1 deg/sec. This velocity should not be difficult to obtain and the resulting angle will be compatible with cord design considerations.

5.1.4 Stowed Dynamic Analysis

Depending on the mounting configuration, the STS launch, land, and transportation loads can have a significant effect on spacecraft design. The objective of this section is to make a preliminary assessment of stowed configuration loading conditions on the point design Hoop/Column antenna satellite system.

Detailed designs for many of the antenna satellite system components does not exist nor does the definition of the interface between the spacecraft and the STS. Thus, the present effort is limited in scope to the model shown in Figure 5.1.4-1 which includes the hoop, hoop restraint system, mast, feed support, and feeds. The remaining components are attached to the end opposite the feed and are supported by the boundary mode.

IDEAL DEPLOYMENT

- t ~ CABLE TENSION
  F ~ HOOP COMPRESSION LOADING
  Y ~ CABLE INCLINATION ANGLE
  β ~ (360/2N)
  ℓ ~ LENGTH OF HOOP SEGMENT
  α ~ ANGLE OF DEPLOYMENT
  Q ~ JOINT TORQUE Δ
  L ~ 1/2 MAST HEIGHT

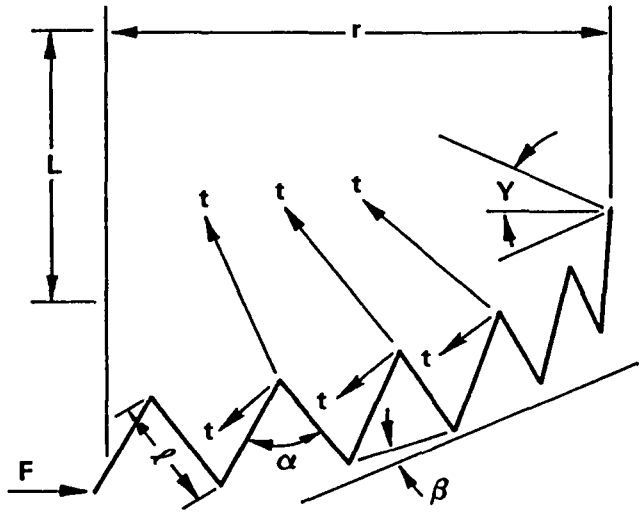

- COMPRESSIVE FORCE: $F = \frac{t \cos Y}{\sin \beta}$
- JOINT TORQUE Δ : $Q = \ell \cos\left(\frac{\alpha}{2}\right) F$
- RADIUS: $r = L \cot Y = \frac{N\ell}{2\pi} \sin\left(\frac{\alpha}{2}\right)$
- TORSIONAL FREQUENCY: $f \approx \frac{1}{2\pi} \left(\frac{Nt\, r_m\, (J_M + J_H)}{J_M\, J_H}\right)^{1/2}$

J_M ~ MAST POLAR INERTIA

J_H ~ HOOP POLAR INERTIA

$J_H = M_H \cdot r^2$

- POINT DESIGN: L = 1123 IN., t = 0.5 LB AT Y = 0, 1.0 LB AT Y = 90, ℓ = 257.49
  J_M = 4.84 E7 LB-IN^2, M_H = 755 LBS, r_m = 23 IN.

Figure 5.1.3-1. Ideal Deployment

POINT DESIGN DEPLOYMENT KINEMATICS

IDEAL DEPLOYMENT

α (DEG)	r (IN)	V (DEG)	F (LB)	Q (IN-LB)	f (Hz)	t (LB)
30	509.1	65.6	3.56	885.4	0.0168	0.565
60	984.5	48.8	6.29	1402.6	0.0168	0.625
90	1390.9	38.9	8.04	1463.9	0.0168	0.676
120	1703.5	33.4	9.19	1183.1	0.0168	0.72
150	1900.0	30.6	9.74	649.1	0.0168	0.74
180	1968.5	29.9	9.96	0	0.0183	0.75

Figure 5.1.3-2. Point Design Deployment Kinematics - Ideal Deployment

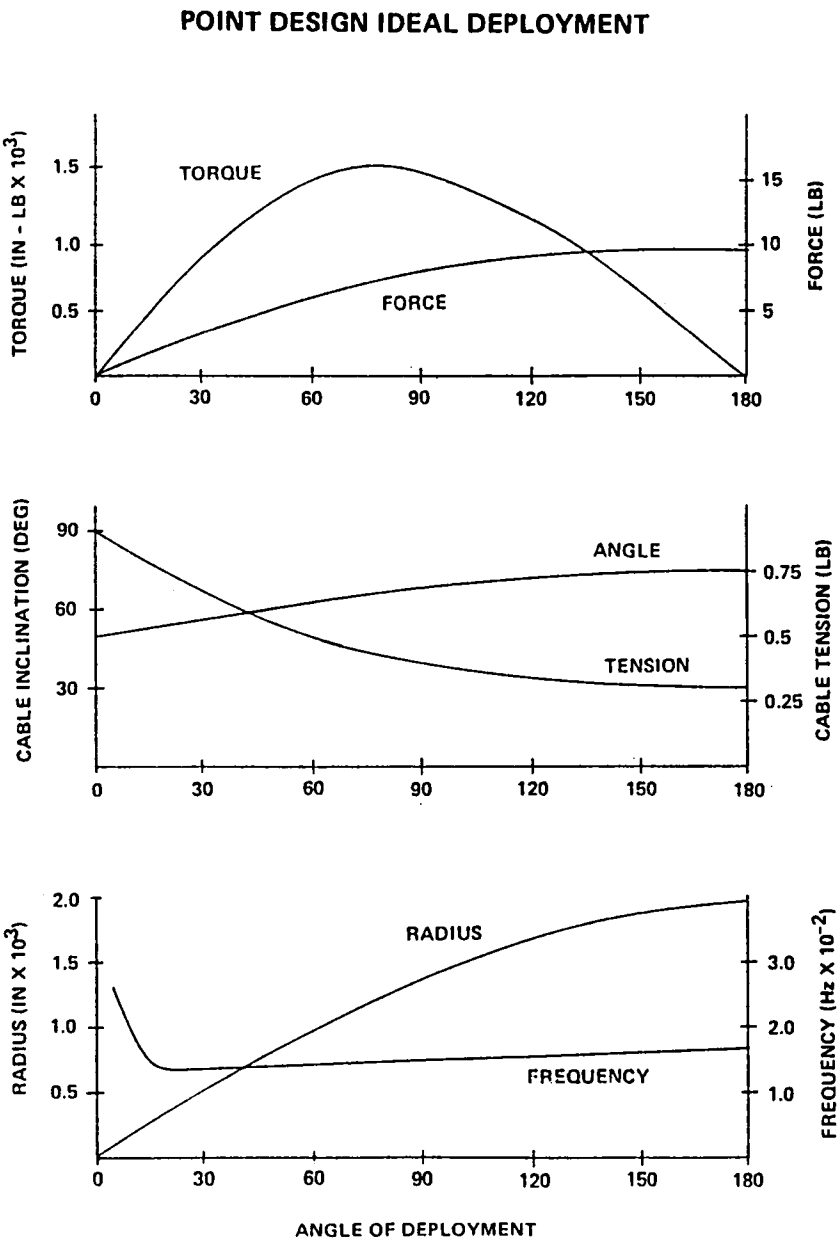

Figure 5.1.3-3. Point Design Ideal Deployment

SIMPLE SNAG ANALYSIS (RIGID HOOP)

- **DEFINITIONS**

  N ~ NUMBER OF CORDS
  t ~ CORD TENSION
  P ~ SNAG FORCE
  Y ~ CORD INCLINATION, Y_1, Y_2, Y_i DEFL
  CORD LOCATION

- **ASSUMPTIONS:**

  a) HOOP IS RIGID
  b) CORDS DO NOT REACH LIMITS

- **EQUILIBRIUM X DIRECTION**

$$\sum_{i=1}^{N} 2t \sin \beta_i \cos Y_i + P = 0$$

- **APPROXIMATIONS:**

  a) IGNORE β DEFLECTION AND LET Y_i's BE EITHER Y_1 OR Y_2
  b) LET $Y_1 = Y + \zeta$, $Y_2 = Y - \delta$

- **EQUILIBRIUM EQ SIMPLIFIED**

$$\frac{2Nt}{\pi} (\cos Y_1 - \cos Y_2) - P = 0 \qquad \frac{4Nt}{\pi} \sin Y \sin \zeta = P$$

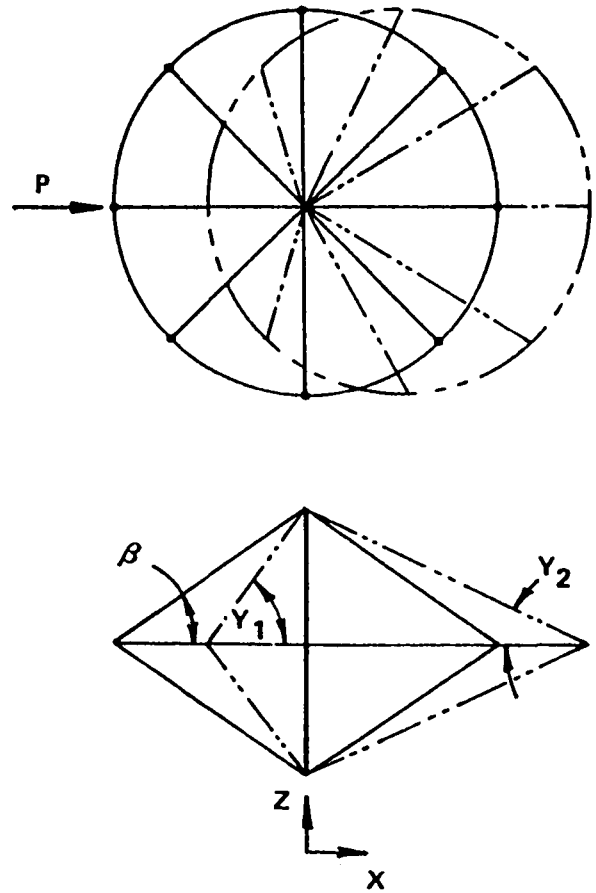

Figure 5.1.3-4. Simple Snag Analysis (Rigid Hoop)

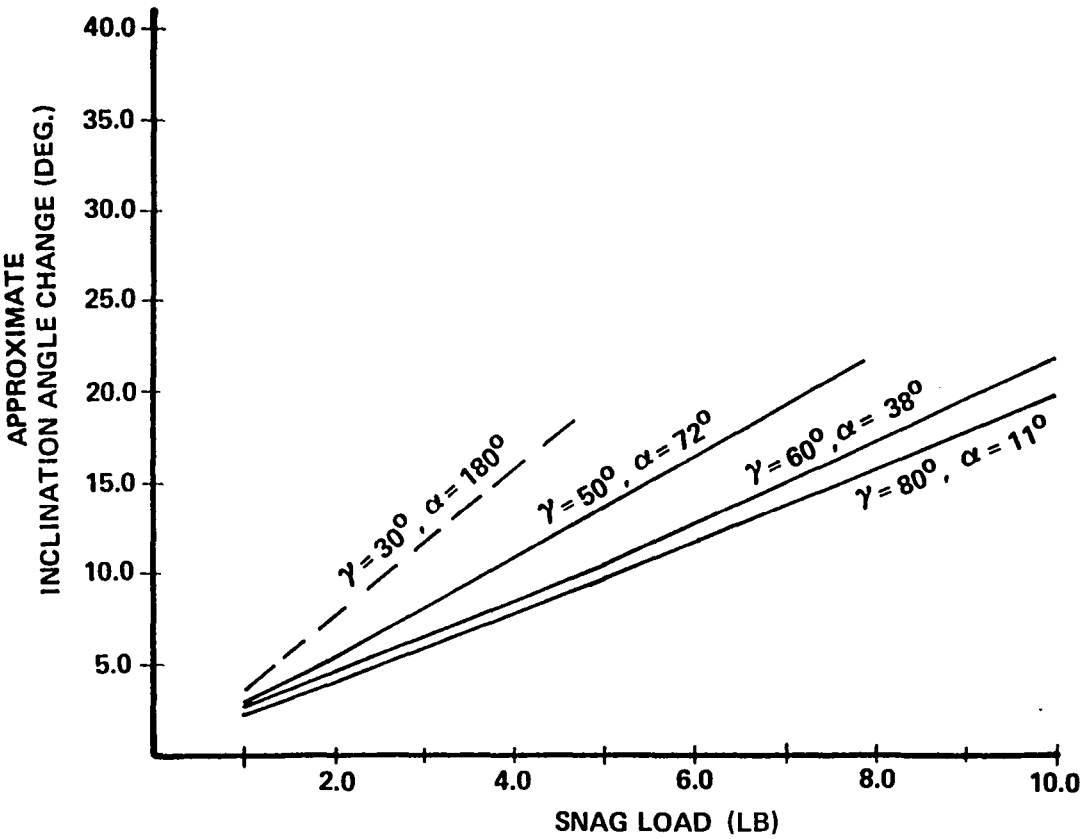

INCLINATION ANGLE CHANGE VERSUS SNAG LOAD FOR VARIOUS DEPLOYMENT ANGLES/NOMINAL INCLINATION ANGLES 48 CORDS, t = 0.5 LB/CORD

Figure 5.1.3-5. Inclination Angle Change Versus Snag Load for Various Deployment Angles/Nominal Inclination Angles 48 Cords, t = 0.5 Lb/Cord

SIMPLIFIED ANALYSIS OF DEPLOYMENT IN A ROTATING REFERENCE FRAME

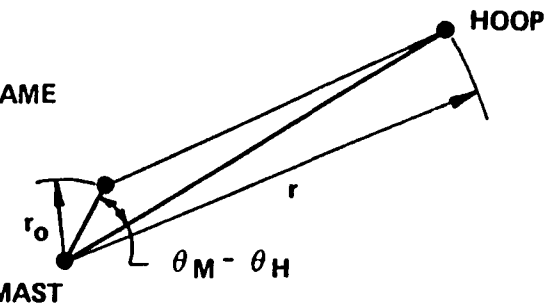

- MAST AND HOOP ROTATING ANGULAR VELOCITY Ω_o
- HOOP DECOUPLED FROM MAST FOR FINITE DEPLOYMENT. THEN RECOUPLED ANGULAR VELOCITY: MAST Ω_o, HOOP $\Omega_o \left(\frac{r_o}{r}\right)^2$
- USE THE ABOVE VELOCITIES FOR INITIAL CONDITIONS FOR THE FREE TORISONAL MODE (MIN FREQ f = 0.0154 Hz, MAX RADIUS DIFFERENCE (30 IN. TO 2000 IN.)

$$|\theta_M - \theta_H| = \frac{1}{2\pi f}\left(1 - \left(\frac{r_o}{r}\right)^2\right)\Omega_o = \frac{1}{2\pi(0.0154)}\left(1 - \left(\frac{30}{2000}\right)^2\right)\Omega_o$$

$$= 10.33\ \Omega_o$$

Figure 5.1.3-6. Simplified Analysis of Deployment in a Rotating Reference Frame

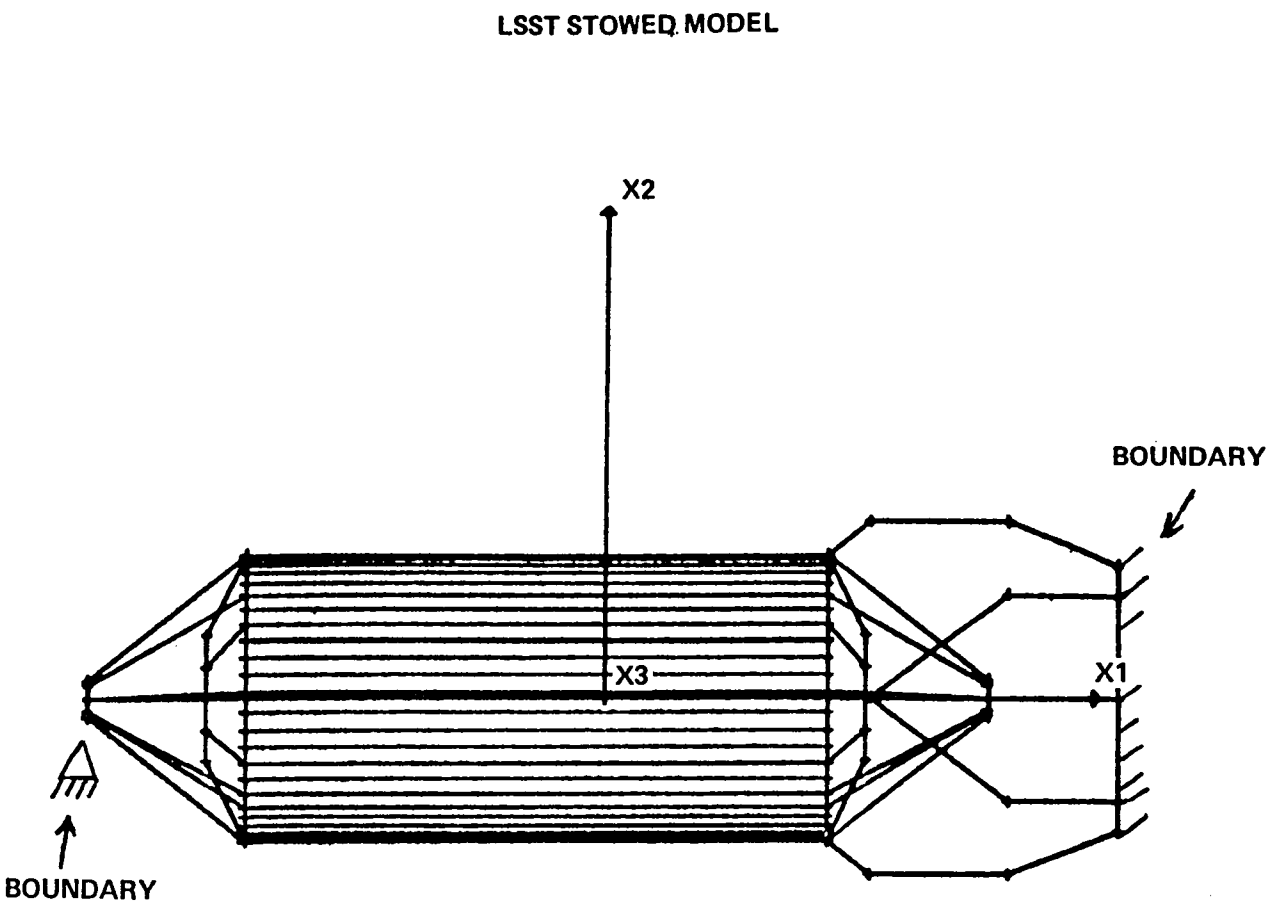

Figure 5.1.4-1. LSST Stowed Model

STS environmental predictions were used to generate a simple set of static equivalent loading conditions. These loads were applied to the model defined above*. In addition, normal modes analysis was performed for the model. Results of these analyses are given in Figures 5.1.4-2 through 5.1.4-5.

The results presented represent a first step in stowed dynamic analysis. The next step would be to include more definite modeling of the STS interface and other satellite system components. When this is done, some refinements would be possible. For example, it would be desireable to raise the lower modes of the model by stiffening the support cones. This could be done with a minimum weight impact. It does appear, however, that from data available now that the Hoop/Column design is acceptable for shuttle loads and transportation.

*Details of this model are discussed in the structural analysis appendix.

STOWED MODES DESCRIPTION (100M)

MODE	FREQUENCY	DESCRIPTION
1	3.80	
2	6.84	
3	6.92	MODES 1-8 ARE CHARACTERIZED BY A TRANS-
4	7.62	LATIONAL MOTION OF THE HOOP SEGMENT/
5	9.32	RESTRAINT CONE INTERFACE ABOUT THE
6	9.34	LONGITUDINAL AXIS OF THE STRUCTURE
7	9.36	(i.e., IN THE X2-X3 PLANE)
8	9.43	
9	9.54	MODES 9 AND 10 ARE TRANSLATIONAL MOTION OF
10	9.56	THE FEED CG'S TANGENTIAL TO THE CIRCLE THEY FORM
11	9.75	MODE 11: FEED CG'S TRANSLATE RADIALLY
12	9.81	MODE 12: SEE MODES 9 AND 10
13	10.07	
14	10.439	MODES 13-15: SAME AS 1-8
15	10.444	

Figure 5.1.4-2. Stowed Modes Description (100-Meter)

100M STOWED DYNAMIC ANALYSIS

MARGINS OF SAFETY

ITEM	LOADING	FAILURE MODE	ALLOWABLE STRESS OR LOAD	MARGIN OF SAFETY
RESTRAINT CONE	5G AXIAL 6.25G TRANS	STABILITY	P_{cr} = 49695 LB M_{cr} = 187857 IN-LB	+3.4
	5G AXIAL 6.25G TRANS	COMPRESSION	14700 PSI	HIGH
INDEX CONE	5G AXIAL 6.25G TRANS	STABILITY	P_{cr} = 16331 LB M_{cr} = 212900 IN-LB	+7.5
MAST VERT ELEMENT	5G AXIAL 6.25G TRANS	STABILITY (LOCAL)	P_{cr} = 6973	+6.3
	5G AXIAL 6.25G TRANS	COMPRESSION	14700 PSI	+0.95
HOOP	5G AXIAL 6.25G TRANS	BENDING	16600 PSI	+4.4
	5G AXIAL 6.25G TRANS	STABILITY	13688 LB	+7.07

Figure 5.1.4-3. 100-Meter Dynamic Analysis - Margins of Safety

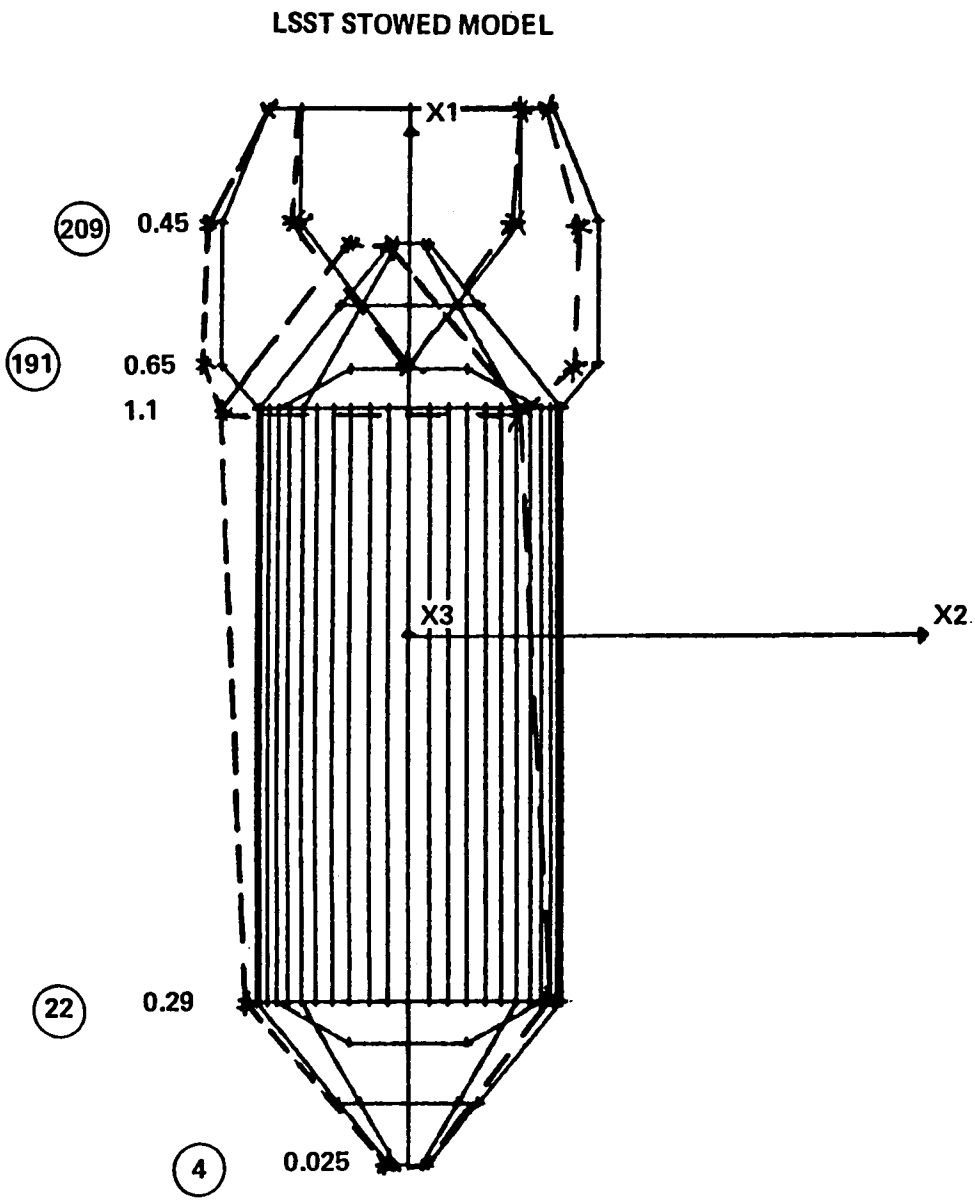

Figure 5.1.4-4. LSST Stowed Model

MOUNTING REACTIONS

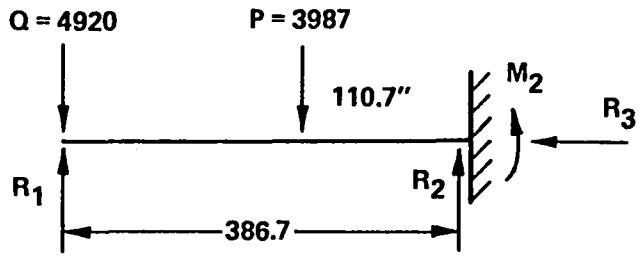

R_1 = 33500 LB

R_2 = 22200 LB

M_2 = 1.53 E6 IN-LB

R_3 = 55700 LB

Figure 5.1.4-5. Mounting Reactions

5.2 Thermal Performance

This section describes thermal models, results of the analysis, and thermal design conclusions and recommendations.

5.2.1 Description of Hoop and Mast Models

Transient thermal models were developed for segments of the hoop and mast to determine their orbital thermal response. The environmental assumptions and boundary conditions which were used in the model are shown in Figure 5.2.1-1. Because of orbit and structural symmetry, 1/4 of the hoop and 1/4 of a representative segment of the mast were utilized in the model (see Figure 5.2.1-5). Figures 5.2.1-2 through 5.2.1-4 contain description of the nodal locations for the model. Heating rates on portions of the mast section were assumed to include worst case shading from opposite members of the mast sections not included in the model. Therefore, these mast sections receive solar flux for approximately 1/2 of the orbit and are shaded in the remaining part of the orbit.

A more detailed segment of the hoop was modeled to verify the relatively coarse granularity in the larger model. Results from the detailed model are plotted in Figure 5.2.1-6 along with results from the larger model for the case of a steady state full Sun. Figure 5.2.1-6 shows that the 4 node model predicts approximately the same hoop temperatures as the 16 node model. Therefore the 4 node model is sufficient, and can be used with confidence.

Both models were developed using the KITAS II computer code discussed in Section 4.10. Listings of both programs are contained in Appendix A.

5.2.2 Hoop and Mast Thermal Analysis Results

Initial temperatures were estimated and the model was run until orbital quase-steady state conditions were reached. The initial temperatures were those for steady state full Sun conditions at the sub-solar point, and after 3 orbits stabilization was reached.

Hoop fitting and GFRP thermal performance are shown shown in Figures 5.2.2-1 through 5.2.2-4. Figure 5.2.2-1 shows the circumferential

LSST HOOP/COLUMN ANTENNA ORBITAL CONSIDERATIONS

- ORBIT CHARACTERISTICS
  - GEOSYNCHRONOUS
  - CIRCULAR
  - EQUATORIAL
  - EARTH ORIENTED
- SOLAR FLUX = 430 BTU/HR-FT^2 (AVERAGE)
- EARTH IR = 3 BTU/HR-FT^2
- ALBEDO = 0
- 1.5 HOUR EARTH ECLIPSE

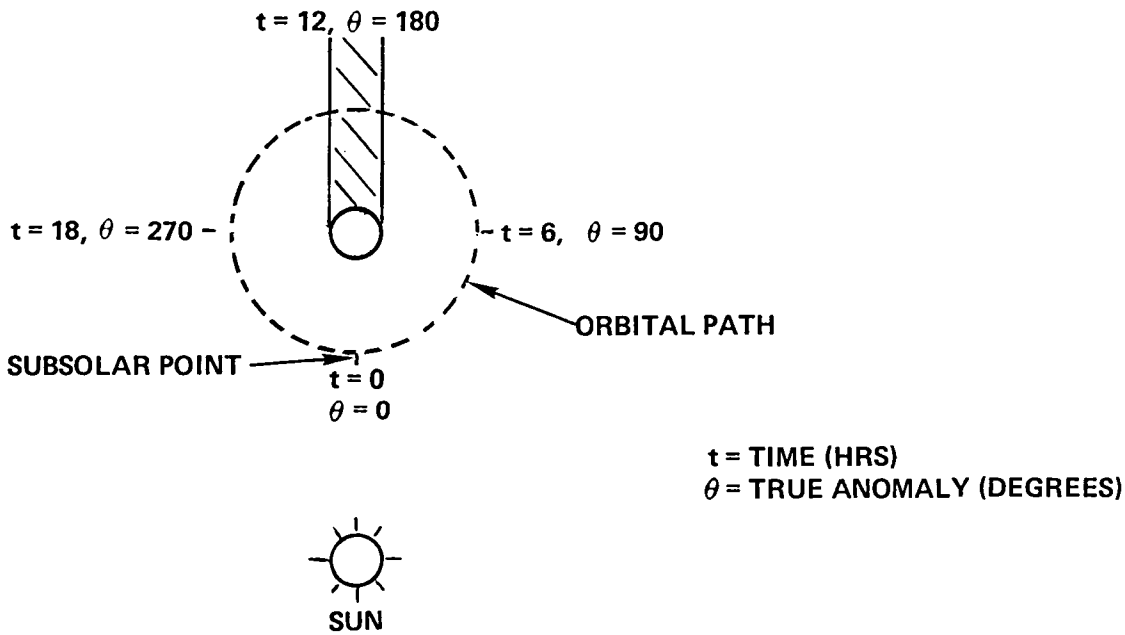

Figure 5.2.1-1. LSST Hoop/Column Antenna Orbital Considerations

LSST HOOP/COLUMN ANTENNA
THERMAL MODEL
NODE NUMBERING SCHEME

NODE ID NUMBERS	LOCATION	NUMBER OF NODES
11, 21, 31, ... 121	HOOP–TYPE I ALUMINUM FITTING	12
12, 22, 32, ... 122	HOOP–TYPE II ALUMINUM FITTINGS	12
15, 25, 35, ... 125	HOOP–GFRP–TYPE I SIDE	12
16, 26, 36, ... 126	HOOP–MLI–TYPE I SIDE	12
17, 27, 37, ... 127	HOOP–GFRP–TYPE II SIDE	12
18, 28, 38, ... 128	HOOP–MLI–TYPE II SIDE	12
501, 502, ... 506	MAST–GRAPHITE CABLES	6
511, 521, 531	MAST–ALUMINUM FITTINGS	3
512, 522, 532	MAST–GFRP–0.5 INCH O.D.	3
515, 535	MAST–GFRP–1.0 INCH O.D.	2
99	SPACE RADIATION SINK	1
	TOTAL NUMBER OF NODES	87

Figure 5.2.1-2. LSST Hoop/Column Antenna Thermal Model Node Numbering Scheme

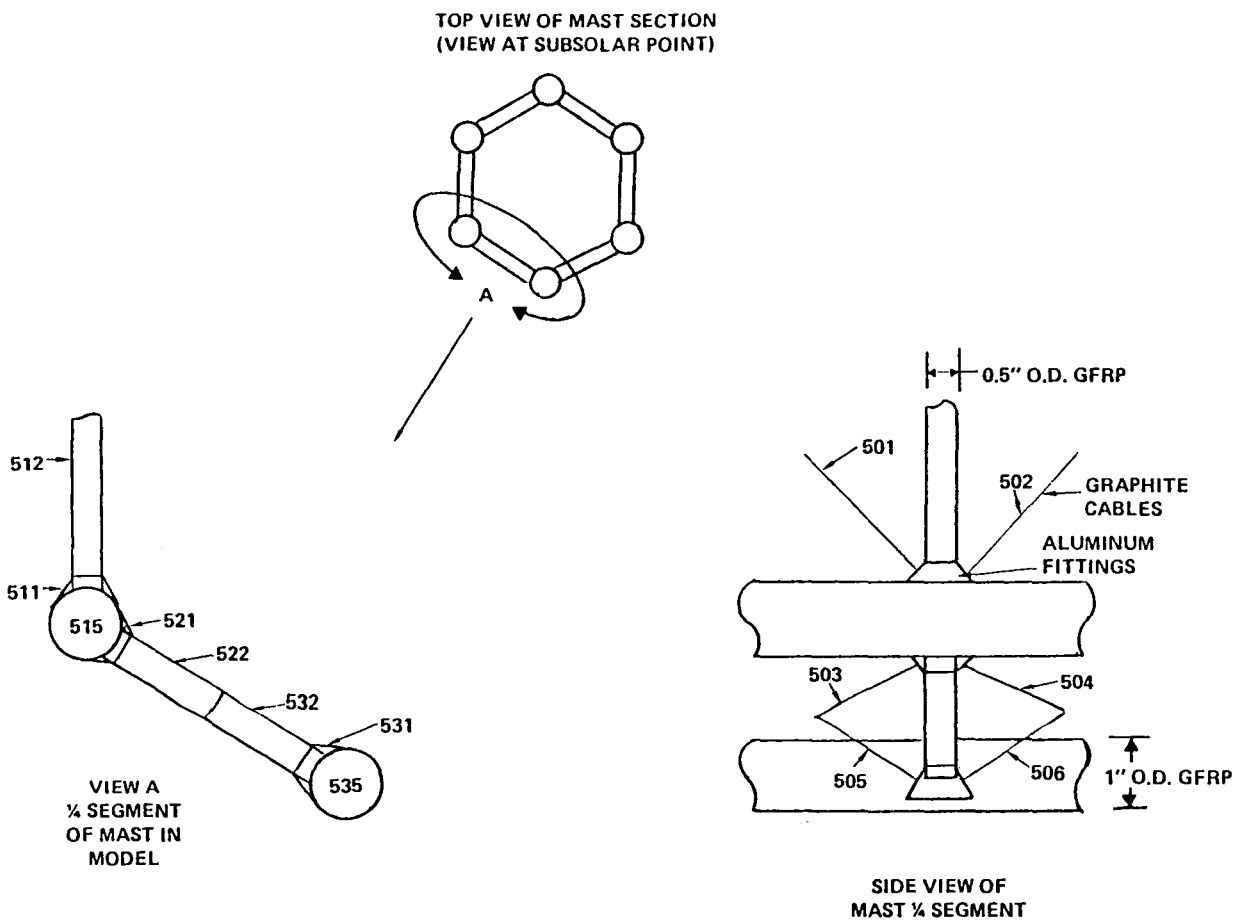

Figure 5.2.1-3. Nodal Locations for Mast Model

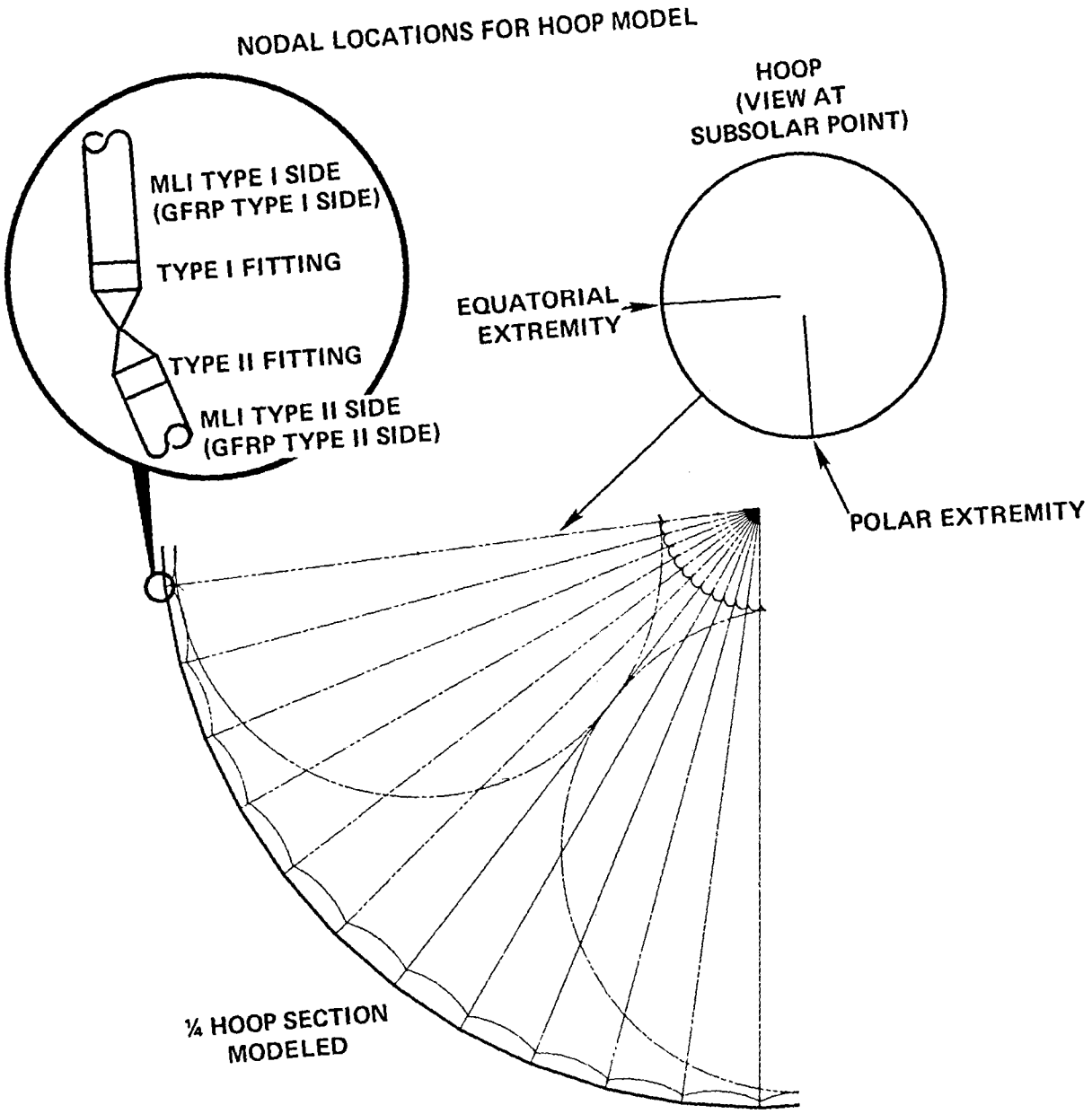

Figure 5.2.1-4. Nodal Locations for Hoop Model

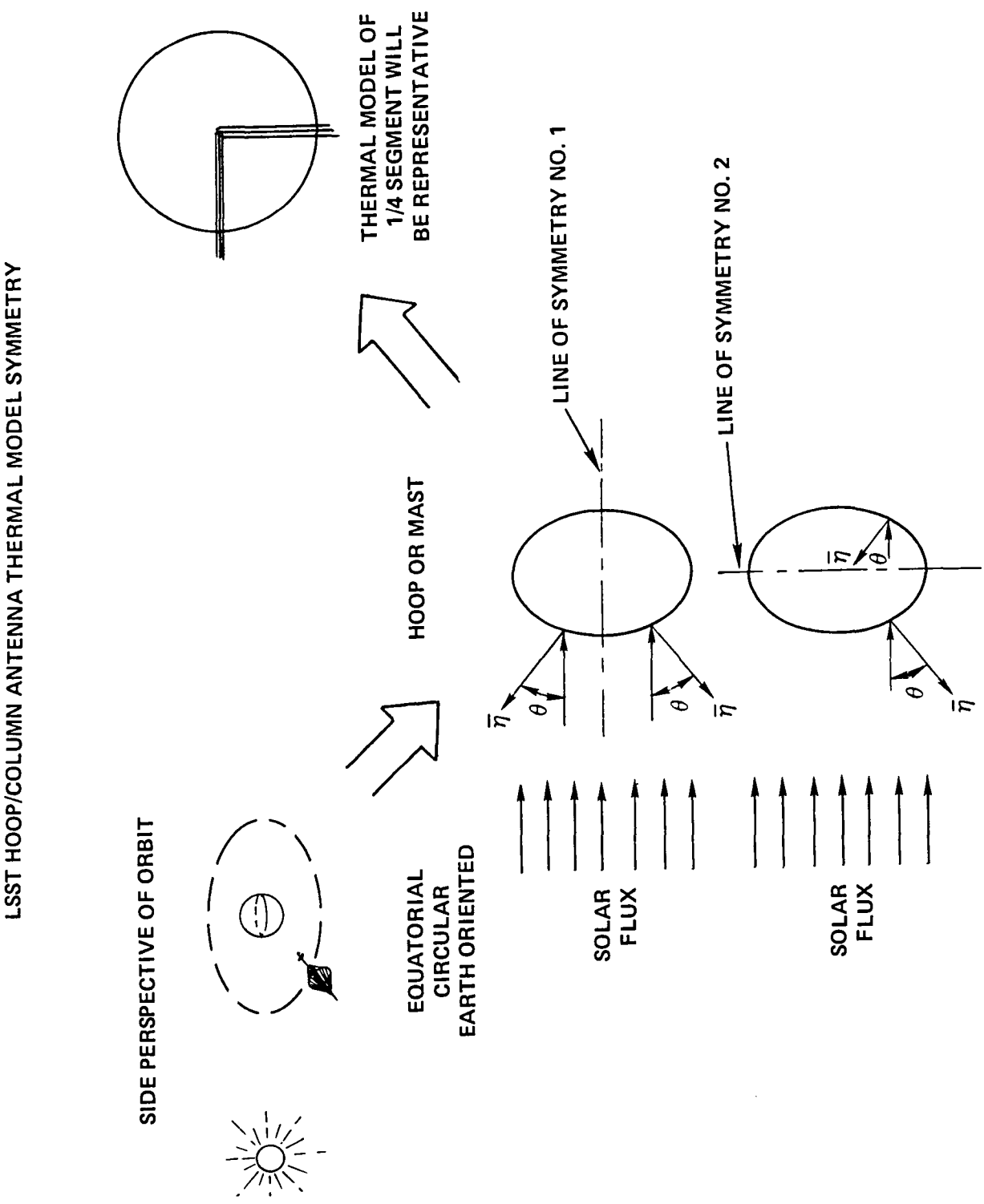

Figure 5.2.1-5. LSST Hoop/Column Antenna Thermal Model Symmetry

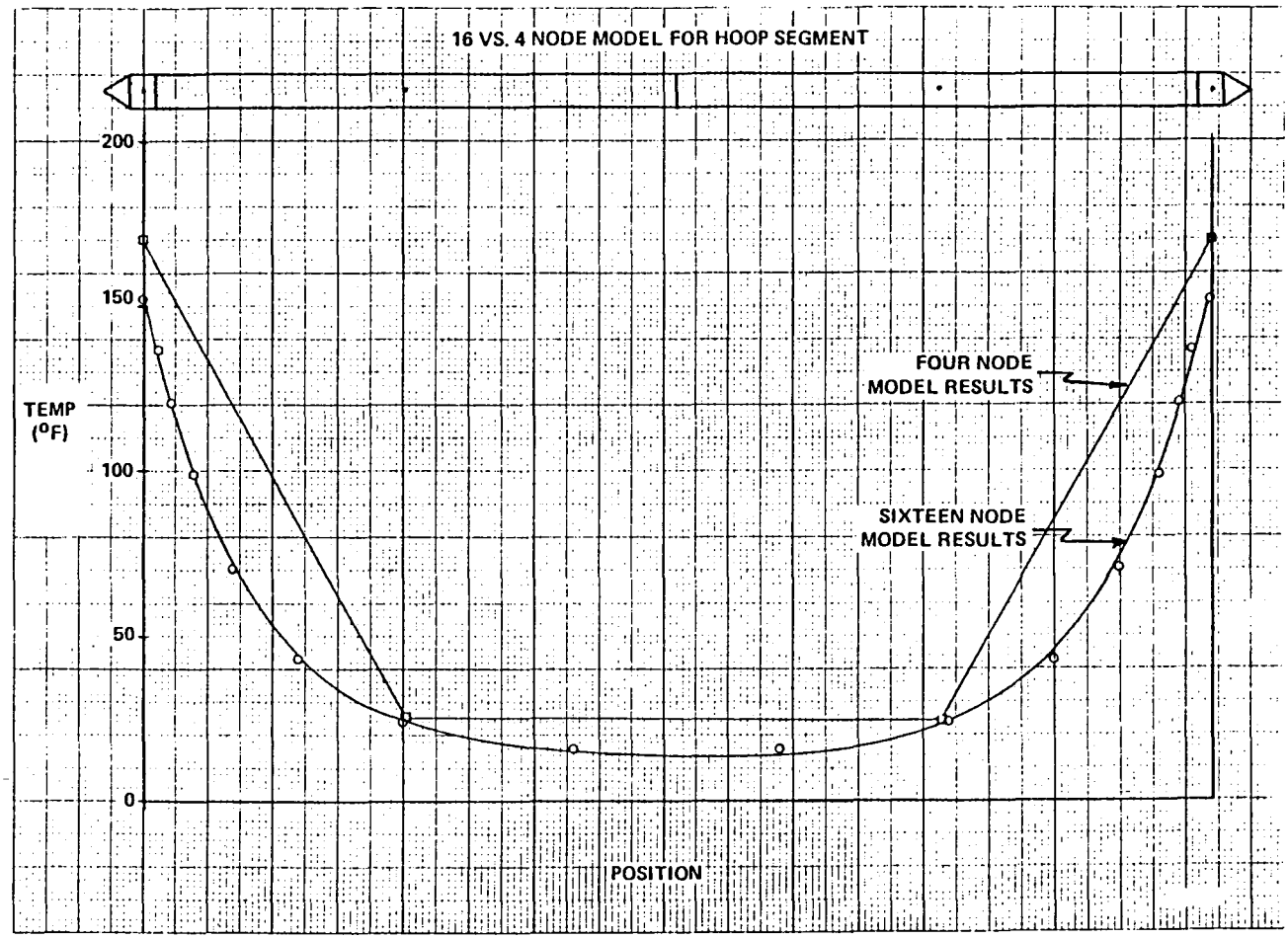

Figure 5.2.1-6. LSST Hoop/Column Antenna
16 vs. 4 Node Model for Hoop Segment

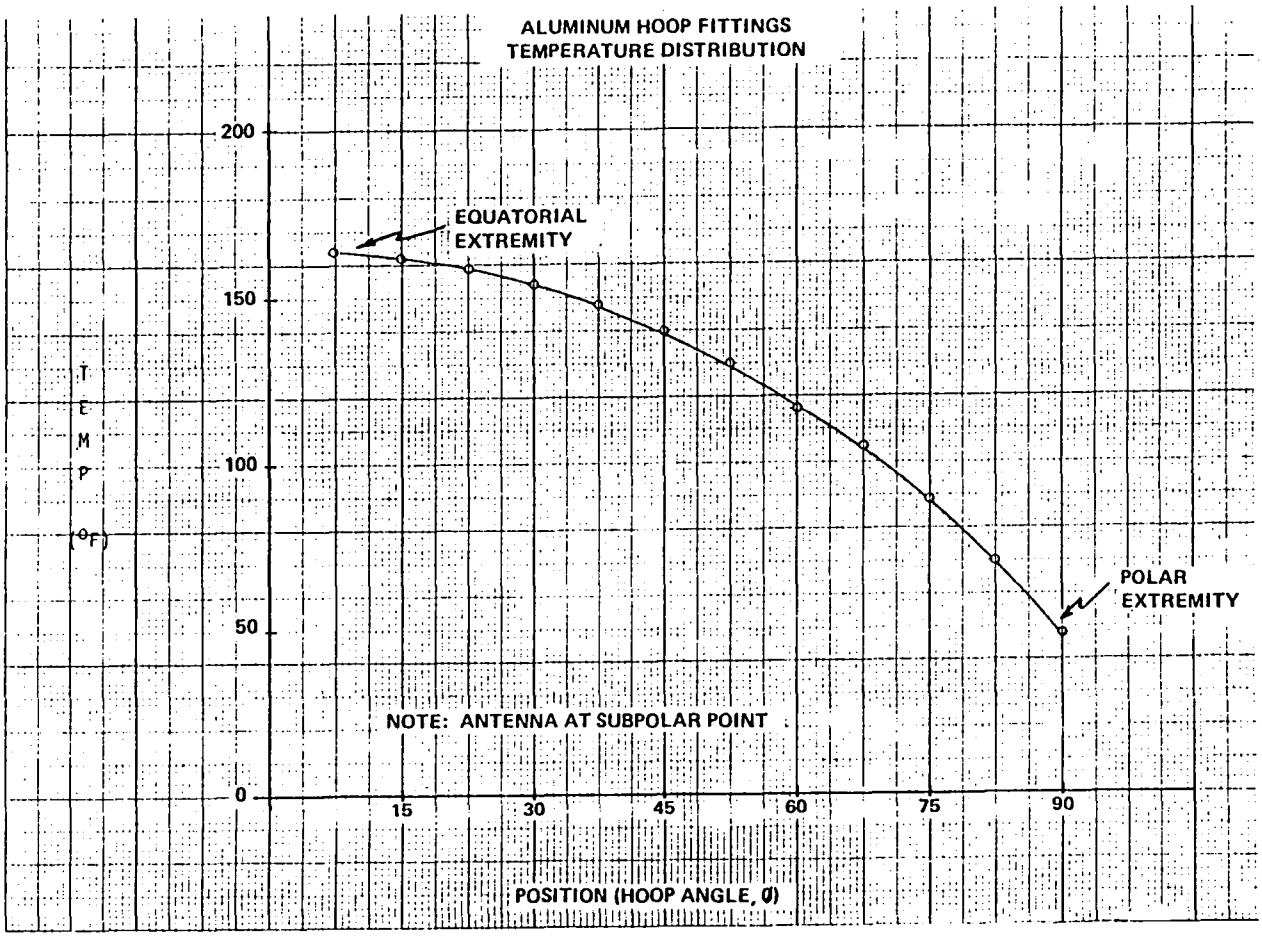

Figure 5.2.2-1. LSST Hoop/Column Antenna
Aluminum Hoop Fittings Temperature Distribution

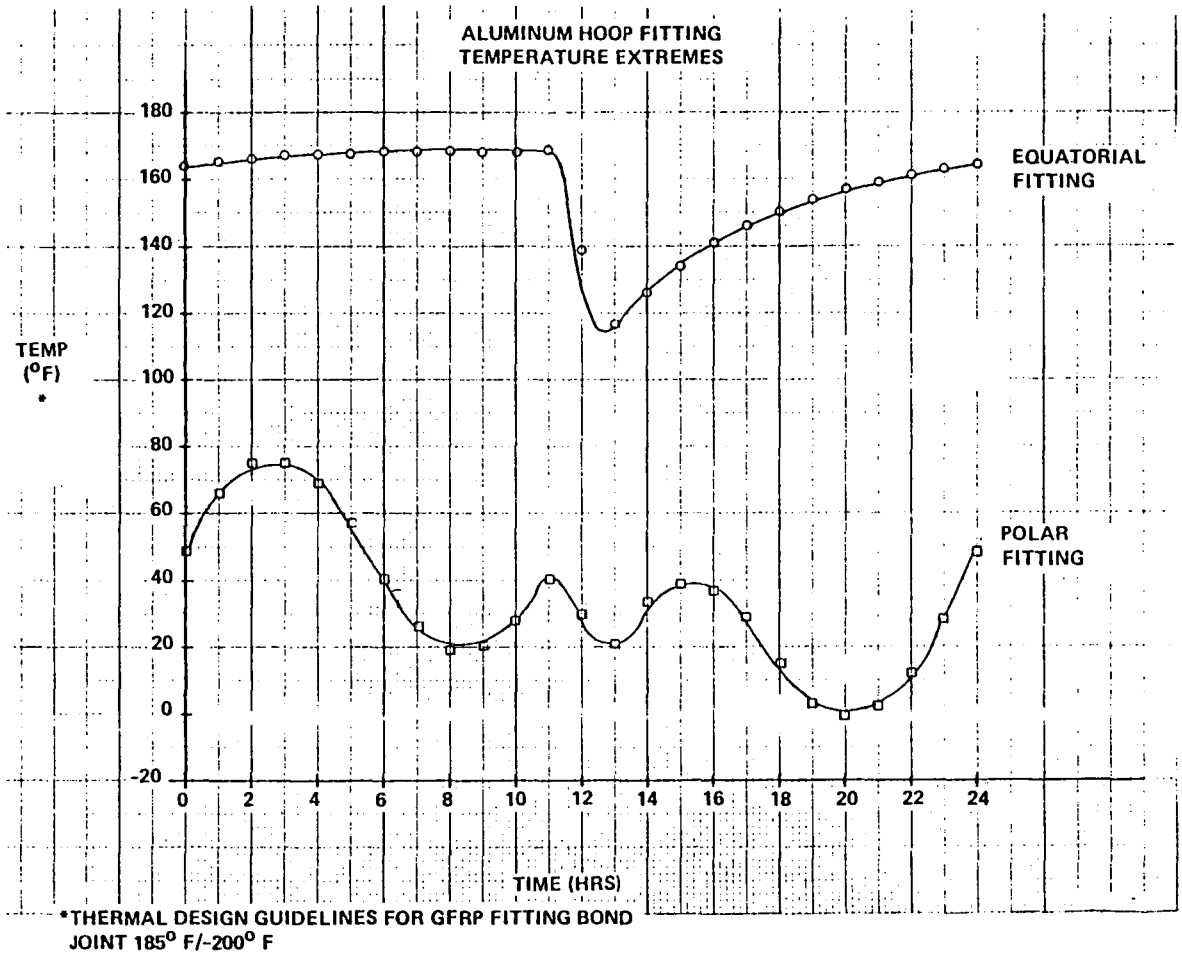

Figure 5.2.2-2. LSST Hoop/Column Antenna Aluminum Hoop Fitting Temperature Extremes

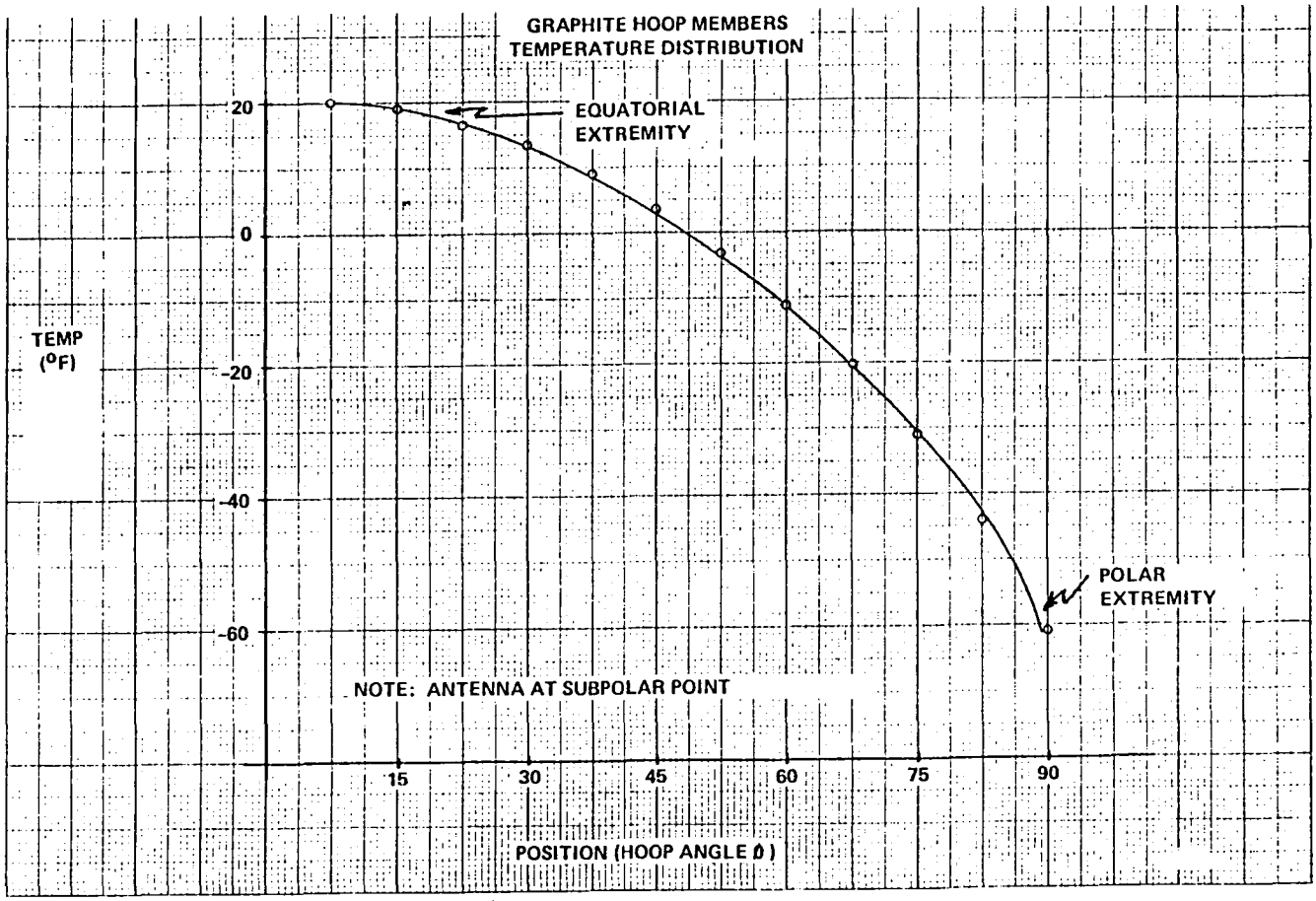

Figure 5.2.2-3. LSST Hoop/Column Antenna
Graphite Hoop Members Temperature Distribution

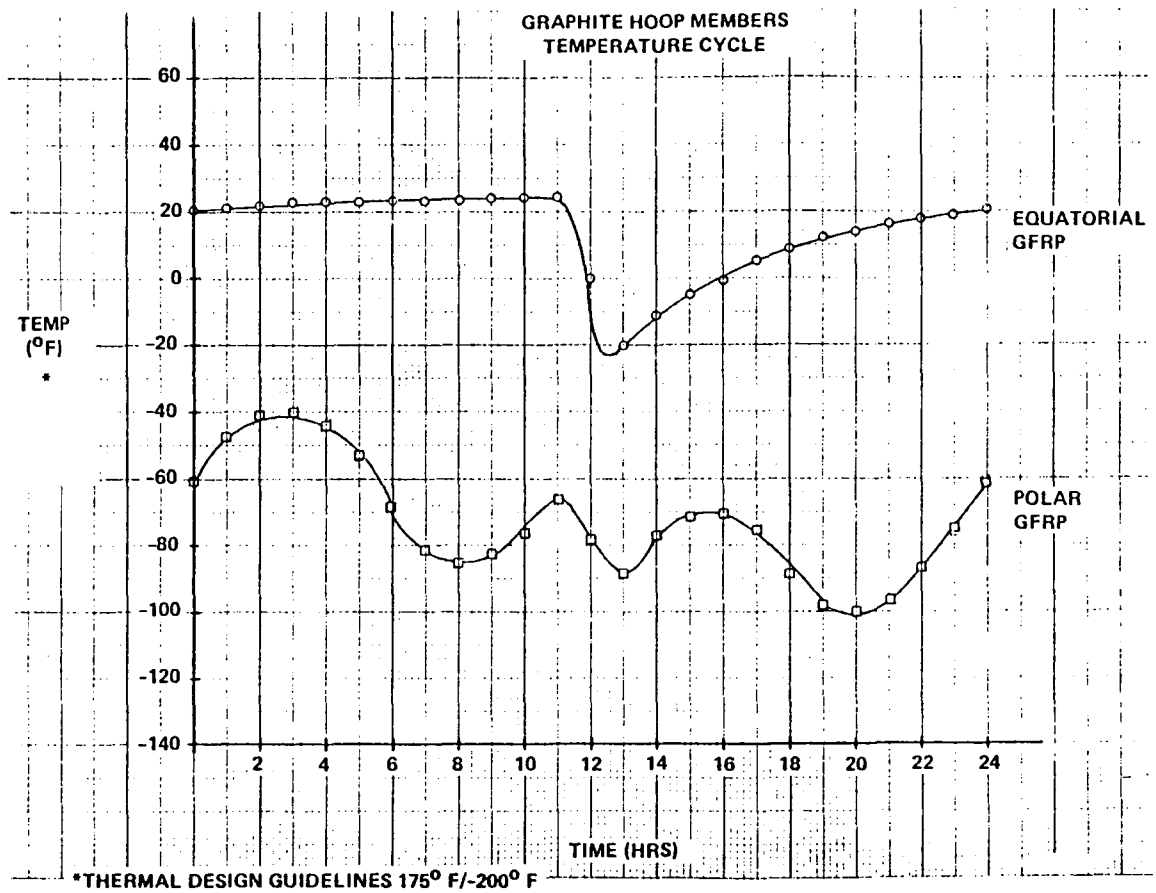

Figure 5.2.2-4. LSST Hoop/Column Antenna
Graphite Hoop Members Temperature Cycle

temperatures in the hoop aluminum fittings at the sub-solar point. As expected the temperature distribution closely resembles a cosine curve. Figure 5.2.2-2 shows temperature histories for fittings on the 90^{o} hoop segment extremeties. The top curve shows the equatorial (always oriented perpendicular to the Sun), while the bottom curve shows the polar fitting (varies from perpendicular to parallel to the Sun). Figures 5.2.2-3 and 5.2.2-4 show the corresponding curves for the hoop GFRP members. However, the hoop GFRP experiences both lower temperature gradients and lower orbital temperature fluctuations than hoop fittings due to the superior hoop MLI effectiveness over fitting FSM tape.

Mast thermal performance is described in Figure 5.2.2-5 and 5.2.2-6. The temperature response of the 1.0-inch O.D GFRP mast members is shown in Figure 5.2.2-5 for the worst case shading condition as previously discussed. The two curves are slightly different because of the orientation of the aluminum fittings on the sections with respect to the solar flux. This worst case shading is evident from the plots; however, the time when the actual cool-down begins is at t = 8 hours when the members are becoming more parallel to the solar flux. Figure 5.2.2-6 shows the orbital temperature response of the 0.5-inch O.D. GFRP mast members. The 0.5-inch members experience greater eclipse cool-down rates than the 1.0-inch members due to their reduced thermal capacitance.

The results from the hoop and mast thermal models are summarized in Figure 5.2.2-7 along with the qualification temperature limit for corresponding antenna components. Results of the thermal analysis indicate that in no instance are qualification temperature limits exceeded. The thermal design recommendations for the LSST Hoop and Mast structural members are presented in Figure 5.2.2-8.

5.2.3 Cable Temperature Program

A program to calculate graphite surface control cable temperatures was developed. A flowchart of the program is shown in Figure 5.2.3-1. Given a nodal coordinate file and a stringer connectivity file, the program calculates the stringer temperatures for the orbital orientation of interest,

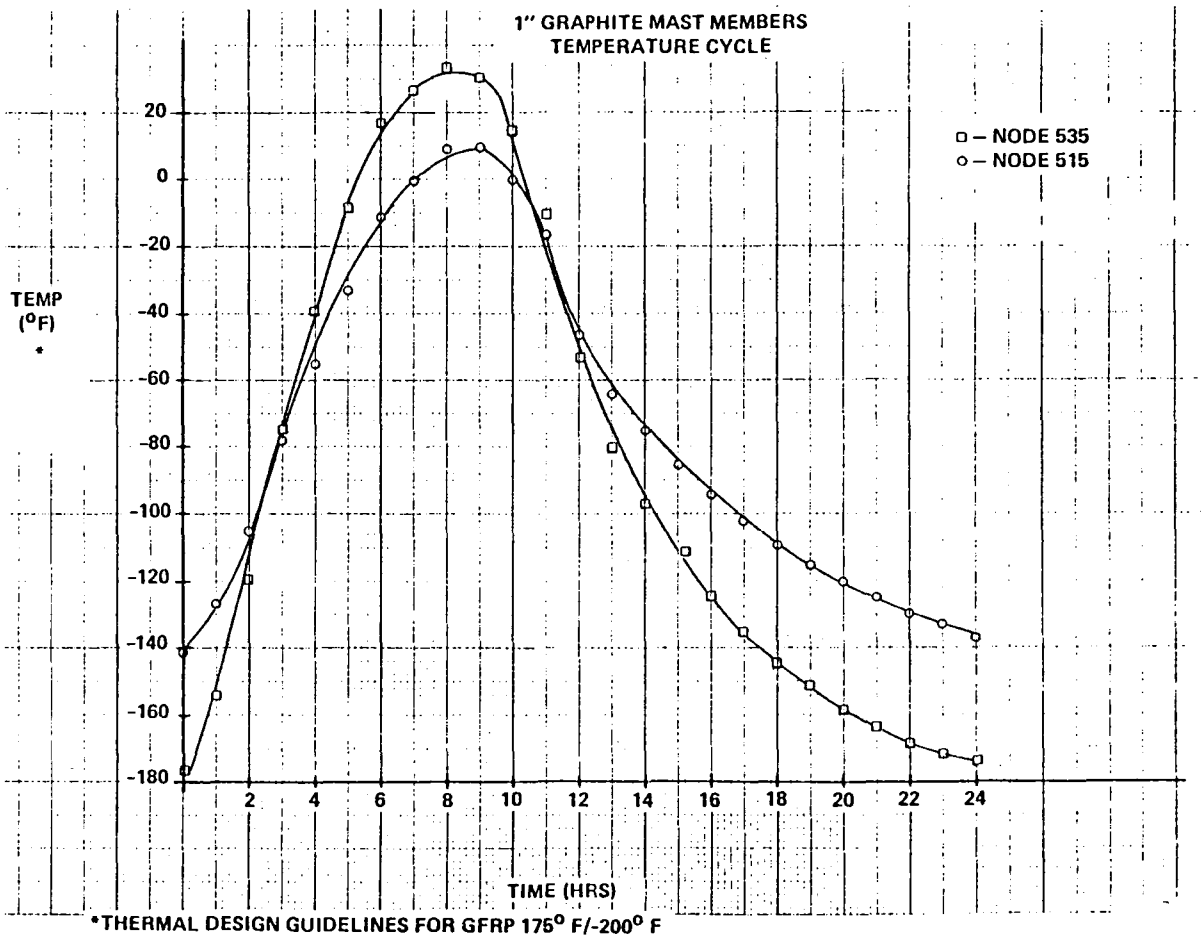

Figure 5.2.2-5. LSST Hoop/Column Antenna 1" Graphite Mast Members Temperature Cycle

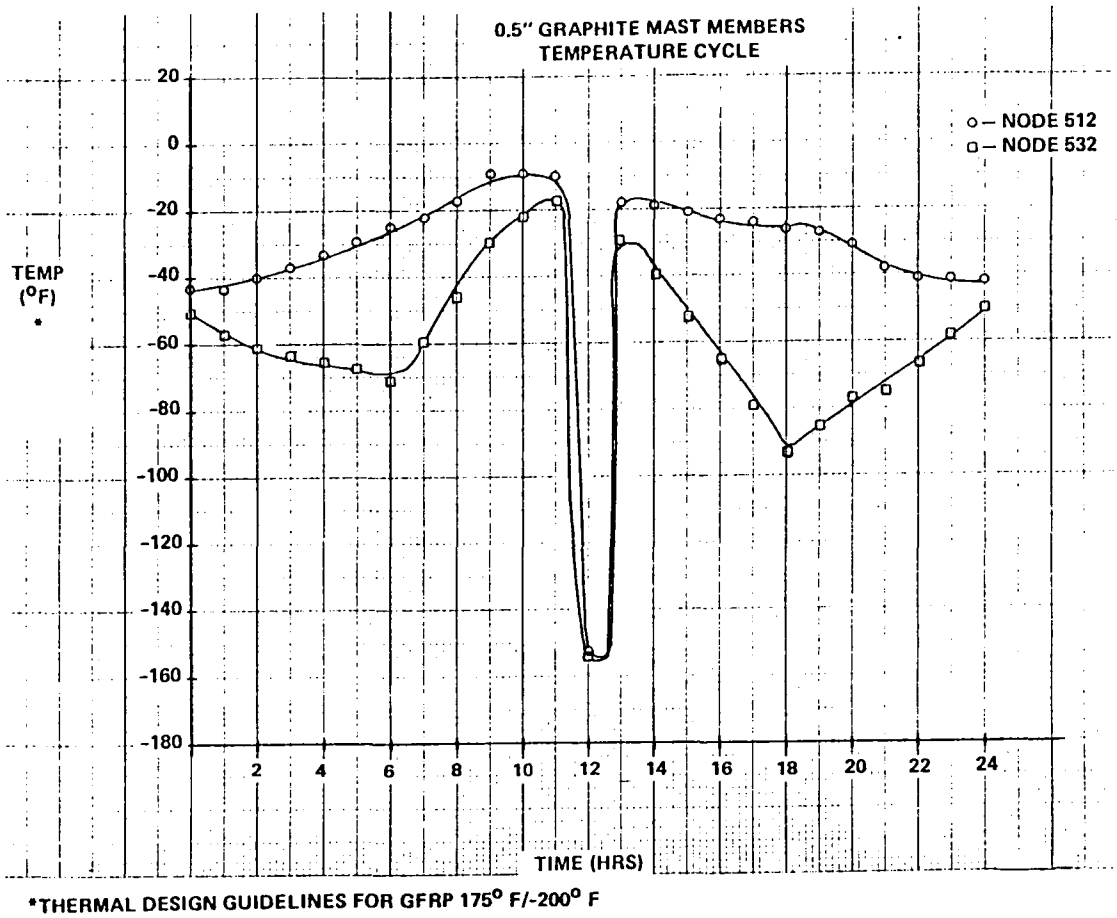

Figure 5.2.2-6. LSST Hoop/Column Antenna 0.5" Graphite Mast Members Temperature Cycle

Component	Tmax(°F @ t(Hrs)	Tmin(°F) @ t(Hrs)	ΔT(°F)	Allowable Temps Max/Min °F
Hoop GFRP	25 @ 11	-100 @ 20	125	235/-260
Hoop Aluminum Fittings	171 @ 11	-1 @ 20	172	185/-230*
Mast 1" OD GFRP	35 @ 8	-154 @ 0	188	235/-260
Mast 0.5" OD GFRP	-9 @ 10	-154 @ 12	163	235/-260
Mast Aluminum Fittings	32 @ 9	-191 @ 0	203	185/-230*

*Bond Joint Allowable Temps

Figure 5.2.2-7. Orbital Temperature Excursions for LSST Antenna Structural Components

LSST HOOP/COLUMN ANTENNA
THERMAL ANALYSIS CONCLUSIONS

ANTENNA CAN BE THERMALLY
CONTROLLED THROUGH IMPLEMENTATION
OF PROPOSED THERMAL DESIGN

ELEMENT	THERMAL DESIGN RECOMMENDATIONS
HOOP GFRP	INTERIOR–THREE (3) LAYERS OF 1/3 MIL EMBOSSED, COUBLE ALUMINIZED KAPTON
	FACE SHEET–1.0 MIL ALUMINIZED KAPTON, KAPTON SIDE OUT
MAST GFRP	ALUMINUM PIGMENTED SILICONE PAINT
FITTINGS	AS REQUIRED:
	FIRST SURFACE MIRROR (VACUUM DEPOSITED ALUMINUM) TAPE
	VACUUM DEPOSITED ALUMINUM
	POLISHED BARE METAL

Figure 5.2.2-8. LSST Hoop/Column Antenna Thermal Analysis Conclusions

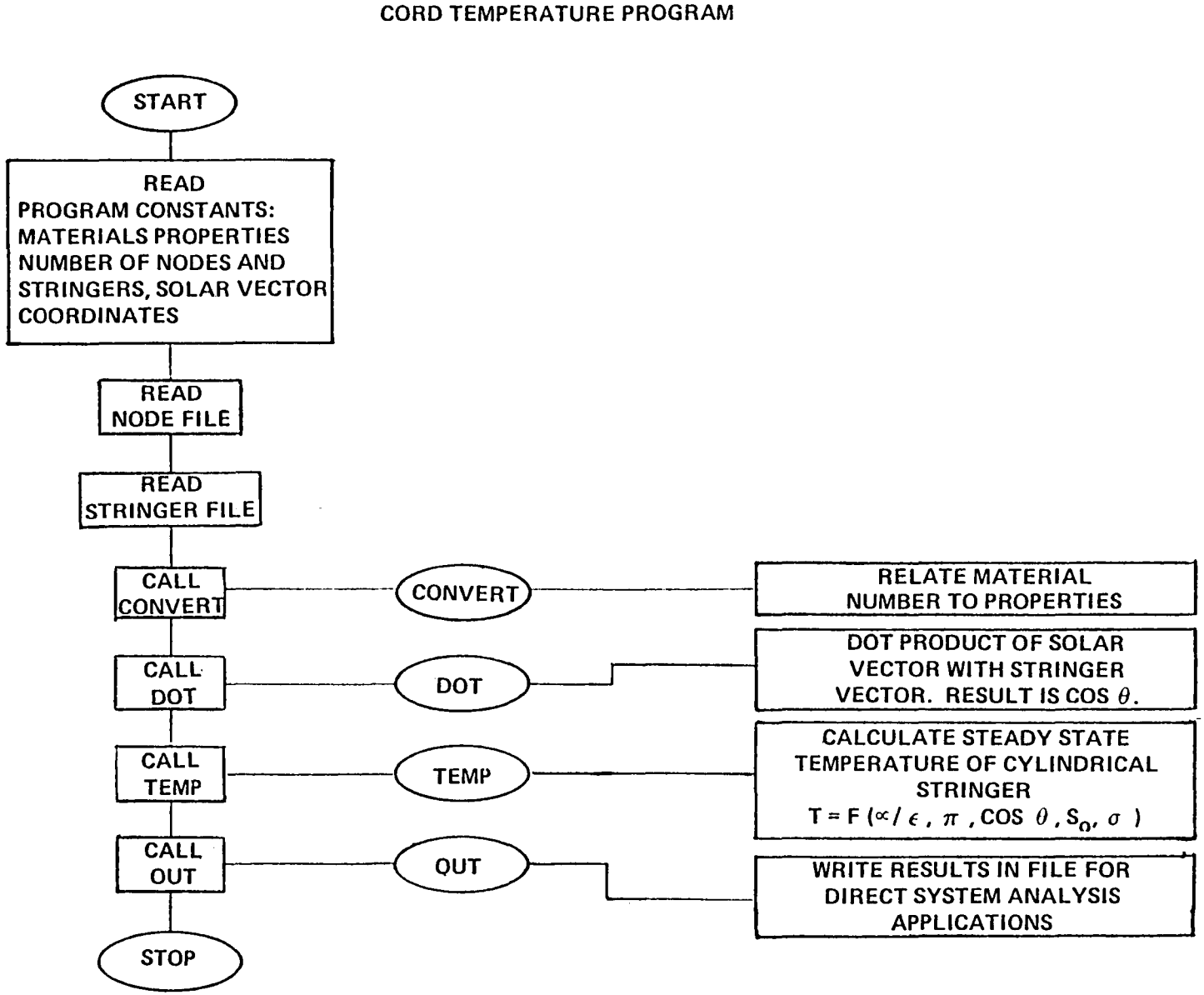

Figure 5.2.3-1. Cord Temperature Program

and writes these temperatures to a file for direct inclusion into Systems Analysis Software. This process results in increased efficiency, reduced cost, and is more accurate. Listings of the program and results are shown in Appendix B and an example of the output is shown in Figure 5.2.3-2.

5.2.4 Antenna Temperature Summary

The temperature summary from the Hoop/Column antenna thermal analysis results is presented in Figure 5.2.4-1.

ELEMENT NODE	ELEMENT PAIRS	MATERIAL NUMBER	CROSS SECTIONAL AREA	INITIAL LOAD	TEMPERATURE DIFFERENCE FROM 70°F
101	102	6	.50000+00	.47520-01	.23713+03
105	106	6	.50000+00	.47419-01	.24289+03
109	110	6	.50000+00	.47905-01	.24850+03
113	114	6	.50000+00	.82396-01	.25541+03
116	117	6	.50000+00	.75477-01	.26317+03
119	120	6	.50000+00	.75468-01	.27127+03
122	123	6	.50000+00	.75243-01	.28011+03
125	126	6	.50000+00	.75157-01	.29015+03
128	129	6	.50000+00	.92350-01	.30158+03
131	132	28	.50000+00	.16522+01	.32190+03
12	15	32	.50000+00	.54438+01	.58291+02
15	20	16	.50000+00	.27176+01	.65210+02
20	25	16	.50000+00	.27138+01	.64880+02
25	30	16	.50000+00	.27091+01	.64471+02
30	35	16	.50000+00	.27043+01	.64069+02
35	40	16	.50000+00	.26996+01	.63676+02
40	45	16	.50000+00	.26949+01	.63297+02
45	50	16	.50000+00	.26902+01	.62953+02
50	55	16	.50000+00	.26852+01	.62585+02
55	60	16	.50000+00	.26803+01	.62237+02
60	65	16	.50000+00	.26753+01	.61904+02
65	70	16	.50000+00	.26706+01	.61589+02
70	75	16	.50000+00	.26657+01	.61286+02
75	80	16	.50000+00	.26607+01	.61001+02
80	85	16	.50000+00	.26560+01	.60717+02
85	89	15	.50000+00	.40363+01	.60449+02
89	93	15	.50000+00	.40313+01	.60195+02
93	97	15	.50000+00	.40266+01	.59956+02
97	101	15	.50000+00	.40217+01	.59733+02
101	105	15	.50000+00	.40167+01	.59526+02
105	109	15	.50000+00	.40118+01	.59335+02
109	113	15	.50000+00	.40071+01	.59158+02
113	116	14	.50000+00	.62339+01	.58996+02
116	119	14	.50000+00	.62290+01	.58850+02
119	122	14	.50000+00	.62240+01	.58721+02
122	125	14	.50000+00	.62193+01	.58609+02
125	128	14	.50000+00	.62144+01	.58514+02
128	131	14	.50000+00	.62083+01	.58420+02
131	134	23	.50000+00	.64093+01	.60998+02
12	21	19	.50000+00	.16286+01	.62771+02

Figure 5.2.3-2. LSST Hoop/Column AntennaCord Temperature Program Output Example

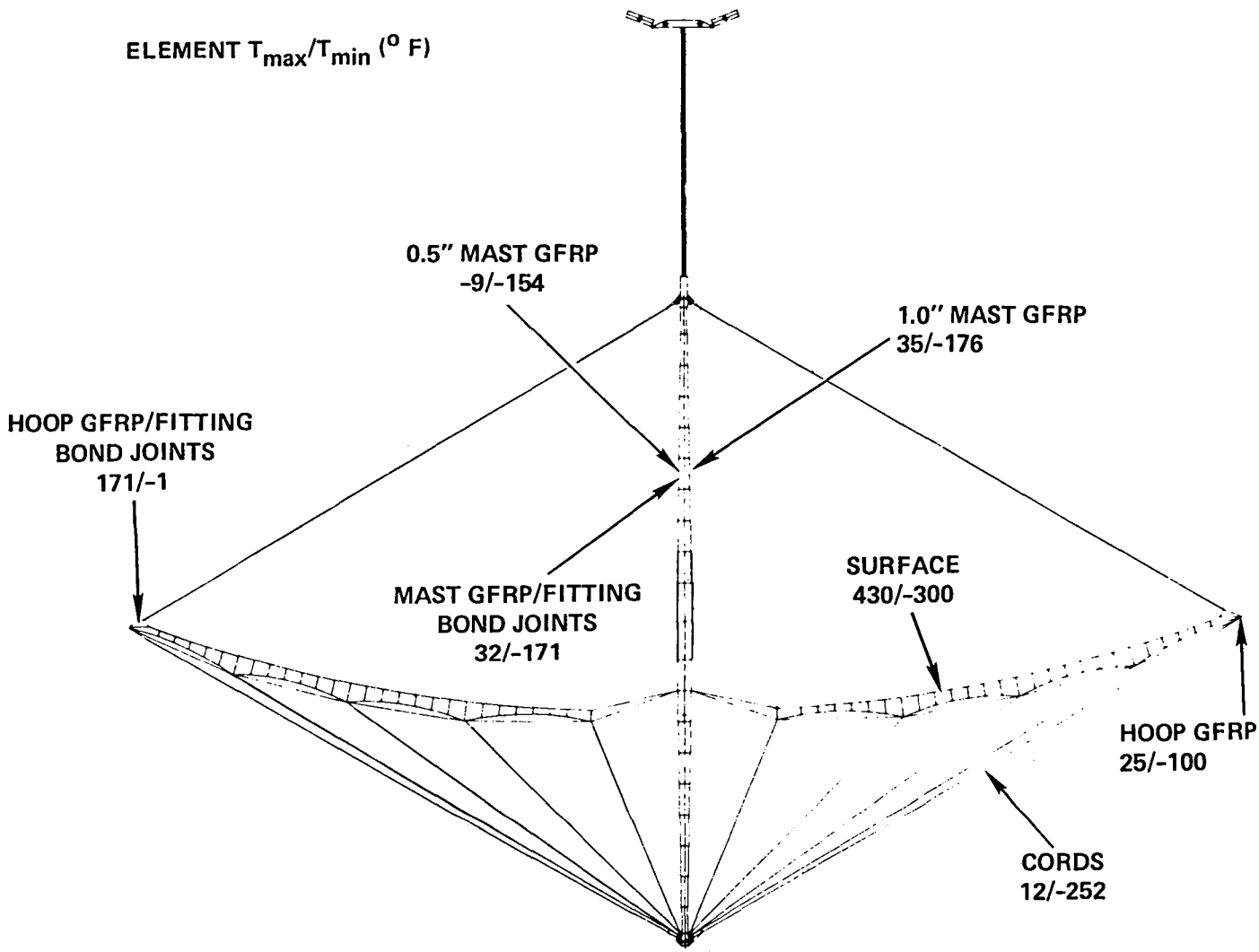

Figure 5.2.4-1. LSST Hoop/Column Antenna Thermal Analysis Temperature Summary

5.3 Contour Analysis

The primary function of contour analysis is described by the following objectives:

1. Establish and describe the point design surface countour. Specifically this includes: determining cord location and operating tension, selecting mesh pretension and stiffness requirements, provide for adjustment of the surface and for meeting surface roughness requirements.
2. Provide support analysis required to develop manufacturing processes, tolerances, and techniques.
3. Predict the operational performance of the antenna/structure based upon:

   - MANUFACTURING CONSIDERATIONS
   - MESH PILLOWING
   - THERMAL-ELASTIC DISTORTIONS
   - MATERIAL PROPERTY DEGRADATION
   - UNCERTAINTIES

For the 100-meter point design the requirements for contour of the surface are:

CONTOUR REQUIREMENTS

RF FREQUENCY	2.0 GHz
f/d	1.53, (F = 62.12 METERS)
RMS	$\leq$0.3 IN
Δ F	<10 IN

The ability to meet these requirements has been optimized through the design of the structure. The final performance of the design to meet the requirements will be based upon the following consideration:

- SURFACE DESIGN
  - PILLOW
  - MESH REFLECTIVITY
- MANUFACTURING
  - TOLERANCE CONSIDERATIONS
  - ASSEMBLING (FLAT PANEL MAPPING)
  - MATERIAL SENSITIVITIES
  - UNCERTAINTIES
- ON-ORBIT PERFORMANCE
  - ACTIVE SURFACE CONTROL
  - MECHANICAL ALIGNMENT
  - THERMAL ELASTIC PERFORMANCE
  - CORD CREEP MATERIAL AGING
  - GFRP DRYOUT
  - FOCAL POINT BIAS
  - UNCERTAINTIES

Each of these consideration will be presented in detail in this section.

5.3.1 Contour Analysis Models

The basis of the analysis of the point design is the finite element math model. Two finite element models are used in the analysis and they are:

1. One-for-one half-gore model
2. Pillow finite element model

5.3.1.1 One-For-One Half-Gore Model

The one-for-one half-gore model is a finite element model represented with one finite element for each continuous length of cord on the surface design. Node to node stringer elements represent cord junction to cord junction cord structure and triangular membrane elements represent cord junction to cord junction areas of the RF-reflective mesh surface. Figure 5.3.1.1-1 reveals the above mentioned modeling technique.

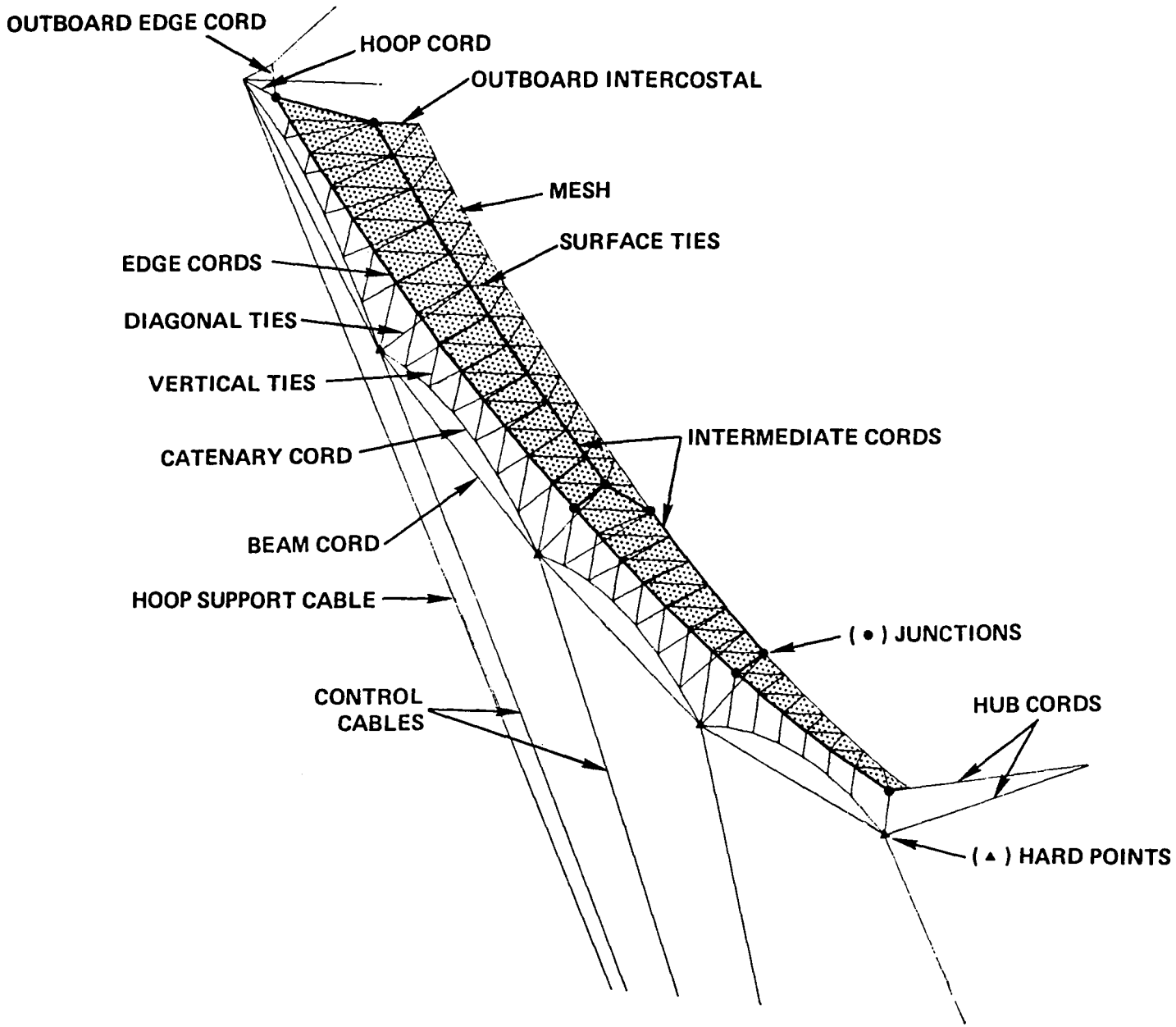

Figure 5.3.1.1-1. Element Terminology

The one-for-one half-gore model represents one half of one of the cyclic 48 gores of the LSST surface. Figure 5.3.1.1-2 reveals a single gore of the 48 gores and shows the geometric location of the half-gore model. For the single gore shown in Figure 5.3.1.1-2, a more detailed view of the gore showing only one-quarter of the entire 100-meter surface is shown in Figure 5.3.1.1-3. This view also lists the equation of the surface with Z_o and r = 0.0, being at the vertex. Shown in Figure 5.3.1.1-4 is the change in length of the vertical ties for each quadrant of the full reflector. As can be seen the tie length change is small, even at the extreme edge of the quadrant where θ = +/- 45°. Thus accurate conclusions can be justified with the use of the half-gore model. Also included in this section is cord properties and mesh material properties. They are listed in Figures 5.3.1.1-5 and 5.3.1.1-6, respectively.

The model details explaining cord tensions and the number of strands of 3000 graphite fibers used for each cord are shown in Figures 5.3.1.1-7 and 5.3.1.1-8. Varying numbers of strands are needed to maintain an operating load in the linear range on the stress-strain curve. Figure 5.3.1.1-9 shows the mesh surface material properties (D_y/D_x) and the direction and magnitude of the mesh pretensions (N_{xx}/N_{yy}).

5.3.1.2 Pillow Finite Element Model

The curvature of the reflective mesh surface is maintained by graphite cords, which form a truss network, and by the mesh stiffness and pretensions. These elements are in a force equilibrium which is maintained at the points of contact by mainly the vertical ties, the diagonal ties, and the surface ties (Figure 5.3.1.1-1). To analyze the pillowing of the mesh, a unique model is created to maintain a reasonable level of modeling effort on the half-gore model and to accurately predict the amount of bulge or "pillow" of the surface. Again, taking advantage of the symmetry of the structure, a quarter symmetric model was developed and is shown in Figure 5.3.1.2-1. Note that tie points are indicated in the lower half of Figure 5.3.1.2-1 and that the finite elements are shown in relation to the tie points.

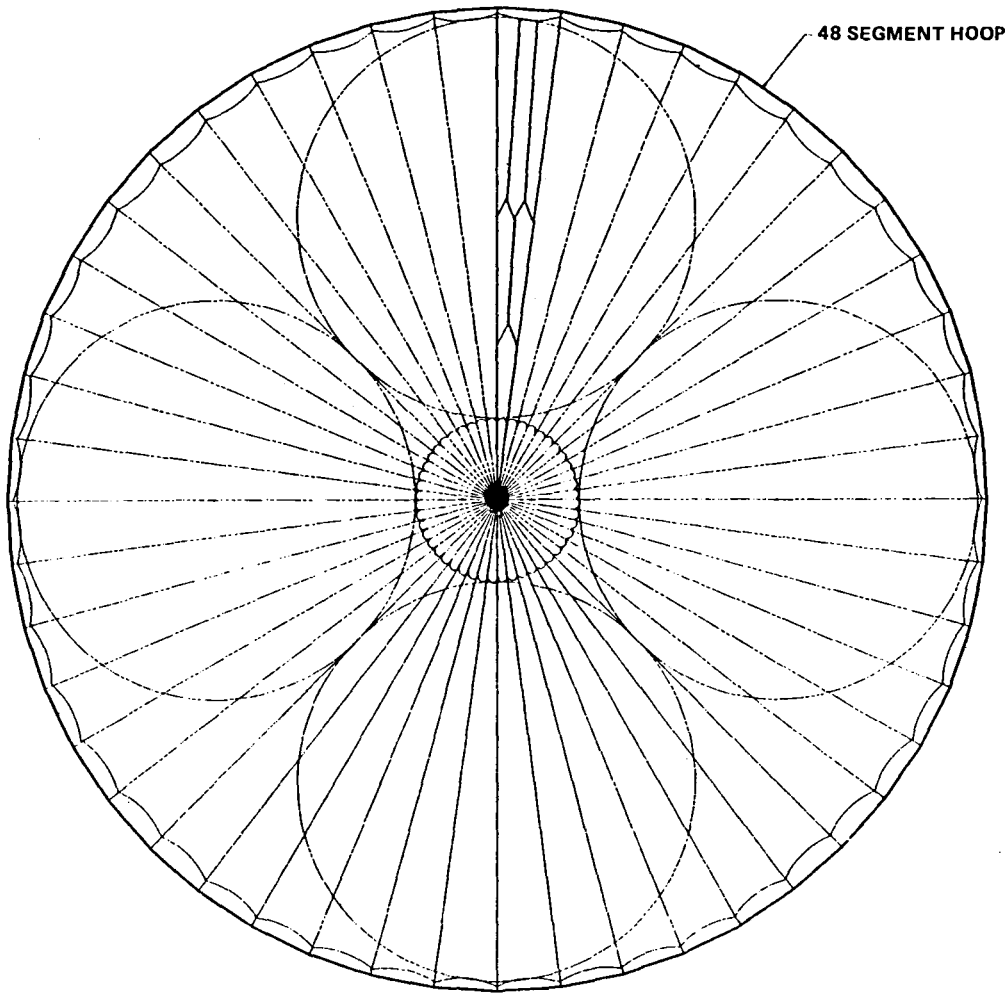

Figure 5.3.1.1-2. Analytical Model Full Gore Location

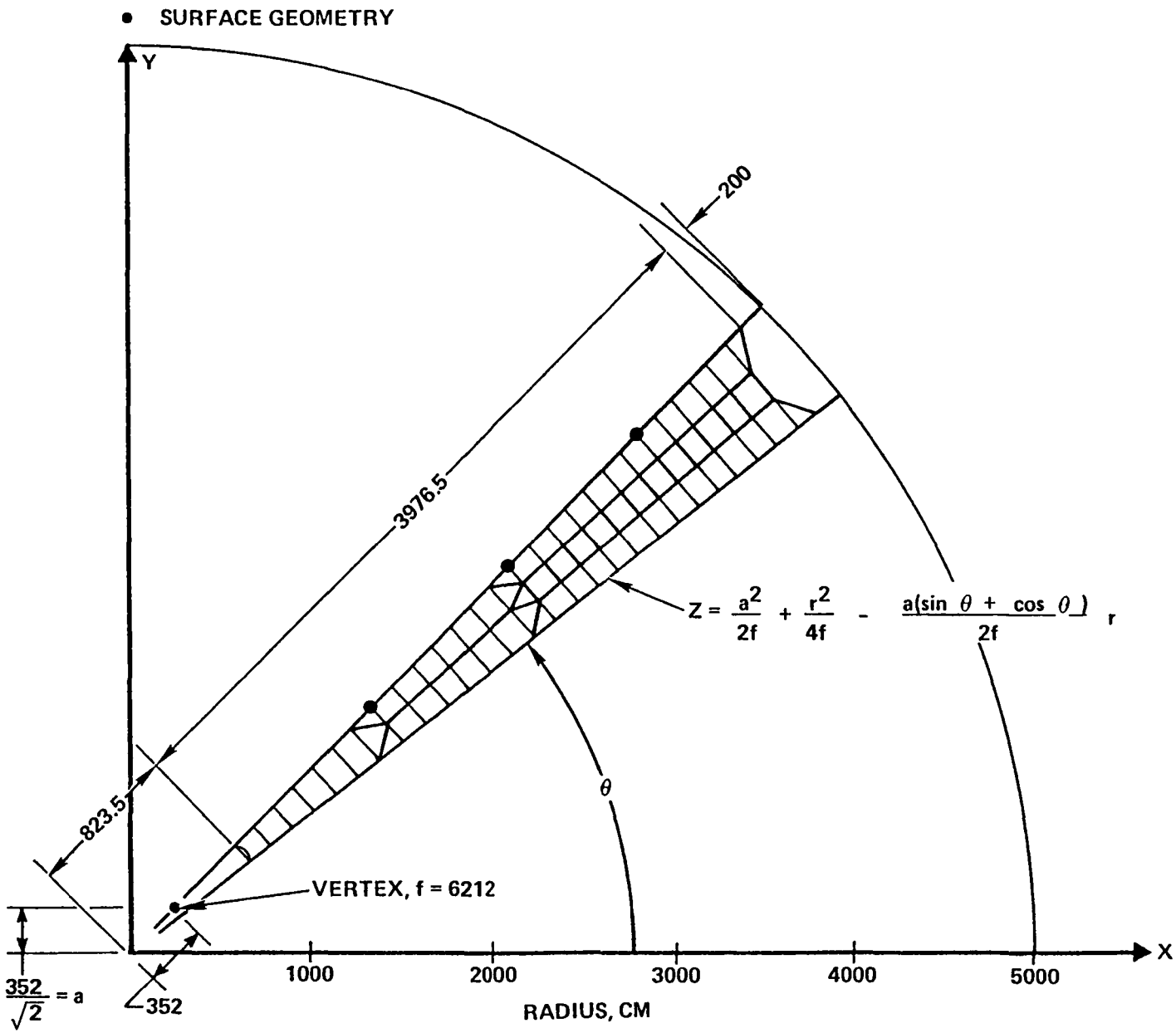

Figure 5.3.1.1-3. Surface Geometry

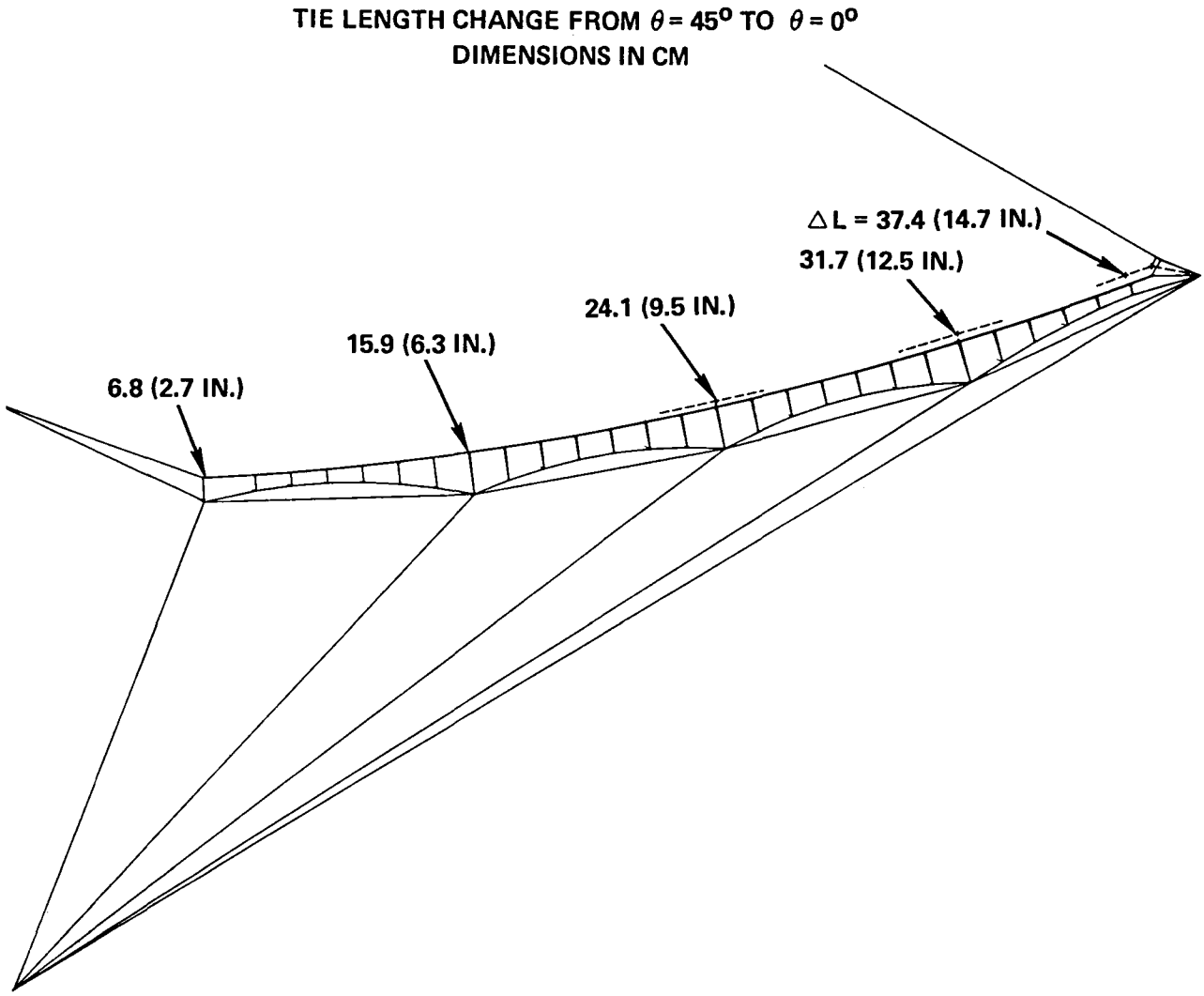

Figure 5.3.1.1-4. Tie Length Change from θ = 45° to θ = 0°
Dimensions in CM

CORD PROPERTIES (PER STRAND)

- 3000 GRAPHITE (CELION 3000) FIBERS
- EA = 4000 LB (17793.6 NEWTONS)
- CTE = $-.25 \times 10^{-6}/^{o}F$
- BREAK STRENGTH = 23 LB (102.3132 NEWTONS)
- WEIGHT = 13.024×10^{-6} LB/IN., (2.28×10^{-5} NT/CM)
- OPERATING TENSION 0.5 LB TO 1.2 LB (2.2242 TO 5.338 NT)

Figure 5.3.1.1-5. Cord Properties Per Strand

MESH PROPERTIES

- MATERIAL: TRICOT KNIT, 0.0012 IN. DIAMETER, GOLD PLATED MOLYBDENUM WIRE
- TENSION: N_x = 0.004 LB /IN. = 0.0070 N./CM.
  N_y = 0.0015 LB IN. = 0.0026 N./CM.
- STIFFNESS: LB /IN. (N./CM.)

SAMPLE	D_x	D_y	D_1	D_{xy} EST.
1	0.054 (0.095)	0.083 (0.145)	0.056 (0.098)	
2	0.062 (0.109)	0.083 (0.145)	0.058 (0.102)	
AVG.	0.058 (0.102)	0.083 (0.145)	0.057 (0.100)	0.035 (0.061)

- WEIGHT

  $\gamma = 9.97 \times 10^{-6}$ LB /IN^2 = 6.87×10^{-6} N./CM^2

- COEFFICIENT OF THERMAL EXPANSION

  $\alpha = 3. \times 10^{-6}$ CM /CM /°F

- OPENING

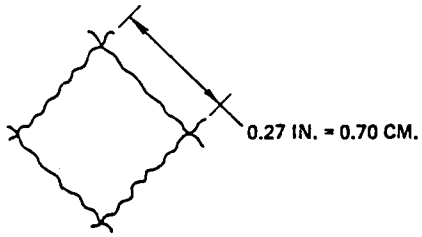

Figure 5.3.1.1-6. Mesh Properties

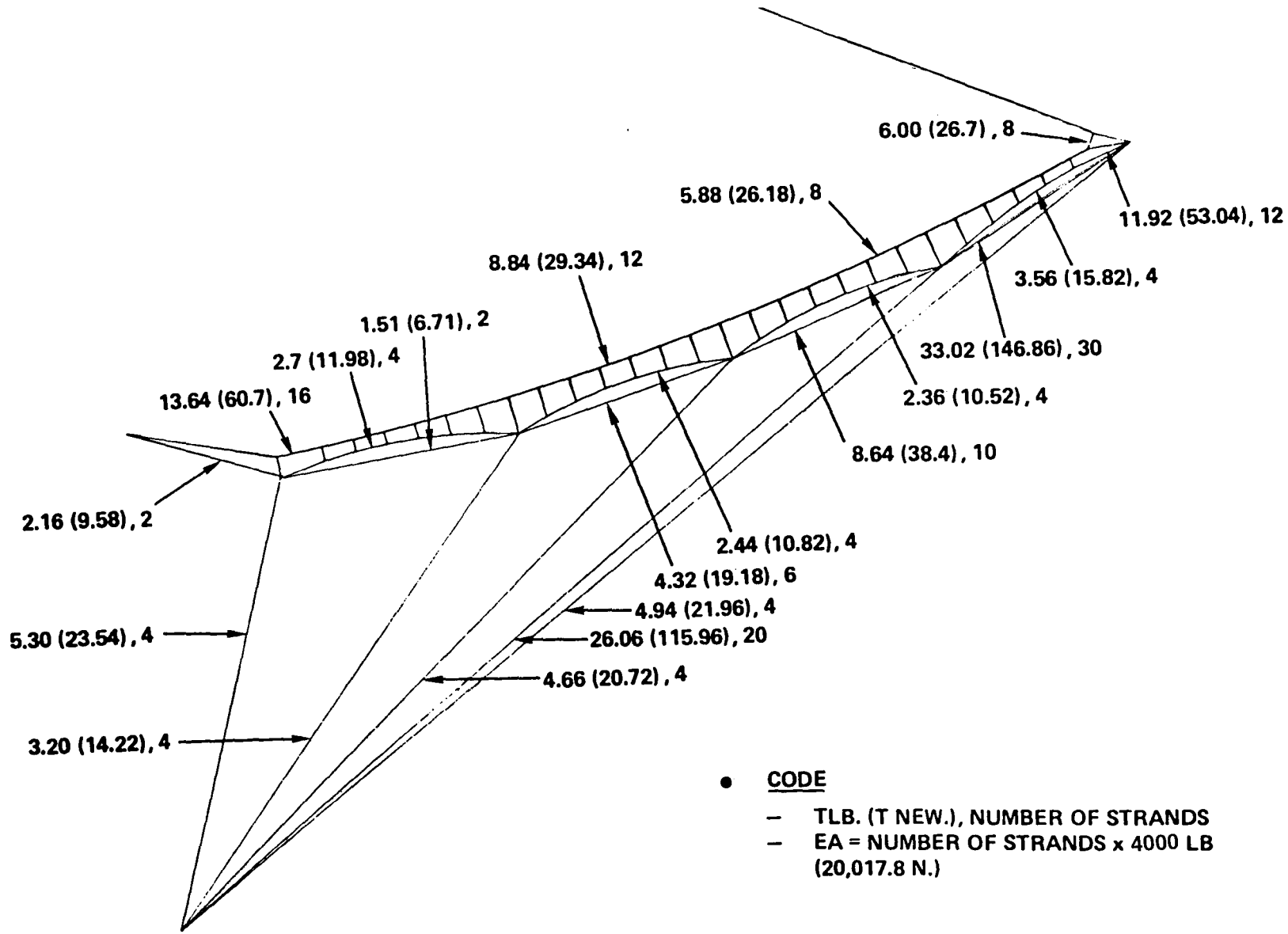

Figure 5.3.1.1-7. Surface Element Definition

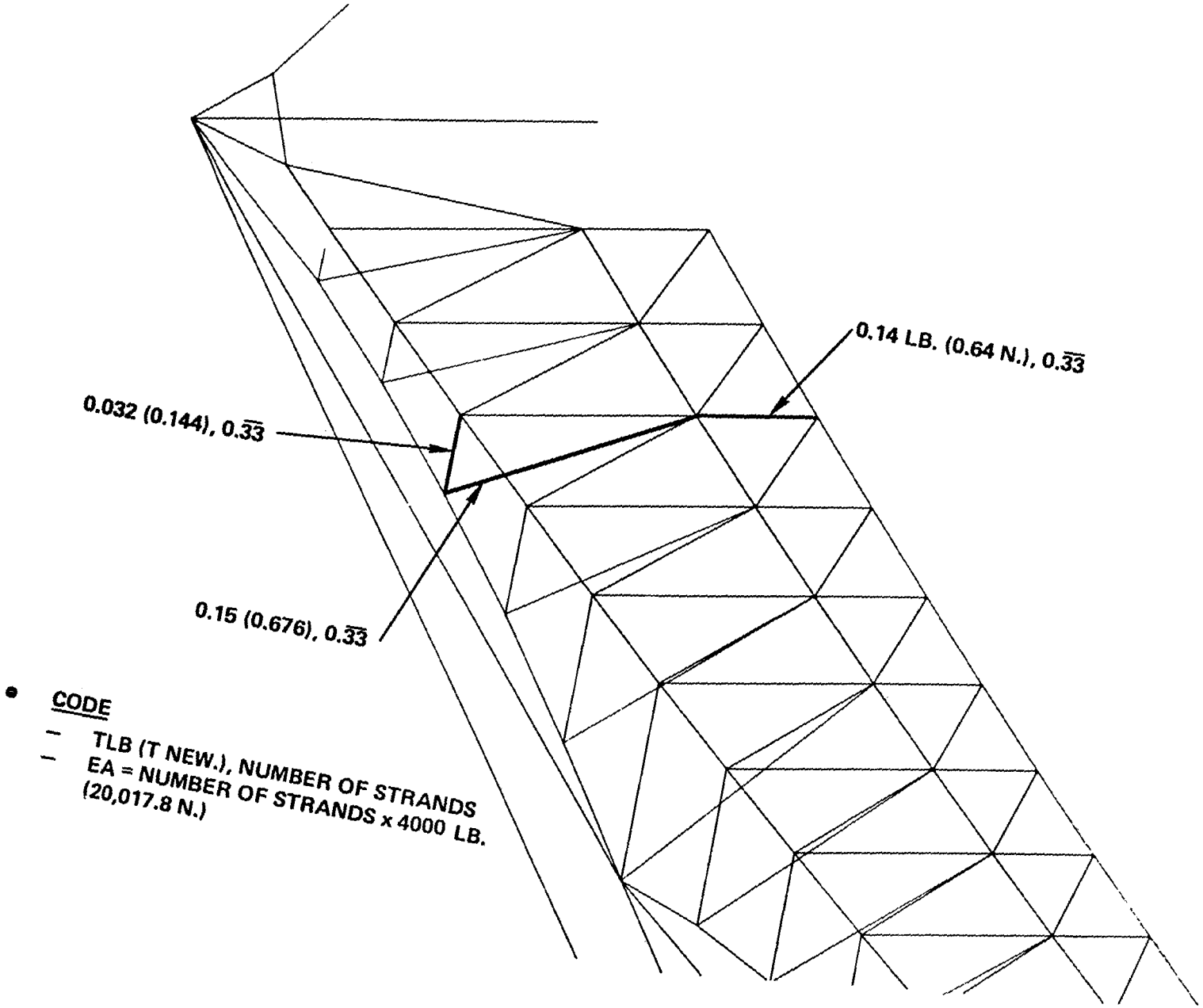

Figure 5.3.1.1-8. Surface Element Definition

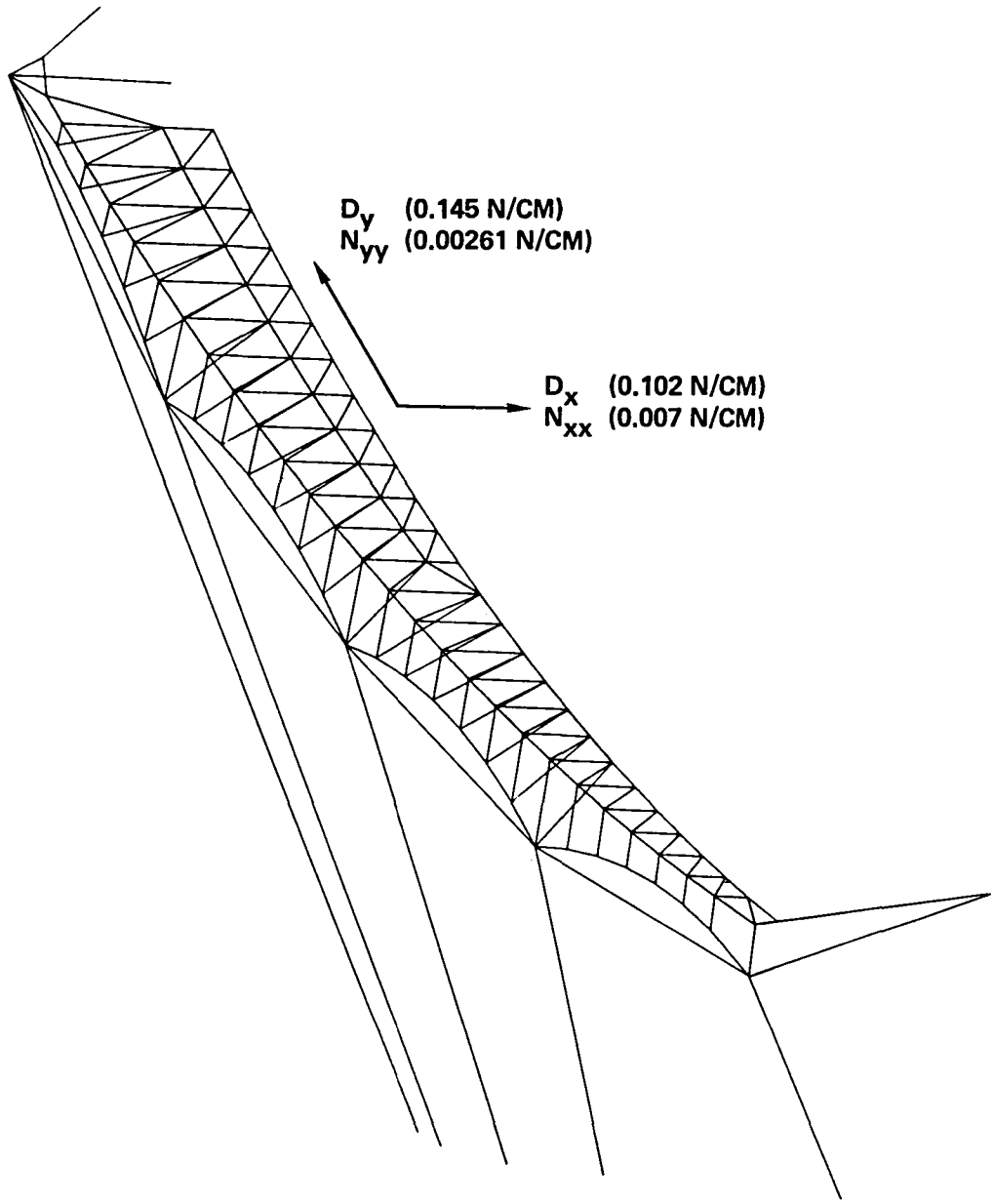

Figure 5.3.1.1-9. Half Gore Analytical Model
Material Stiffness Directions (D_x, D_y)
Membrane Preload Directions (N_{xx}, N_{yy})

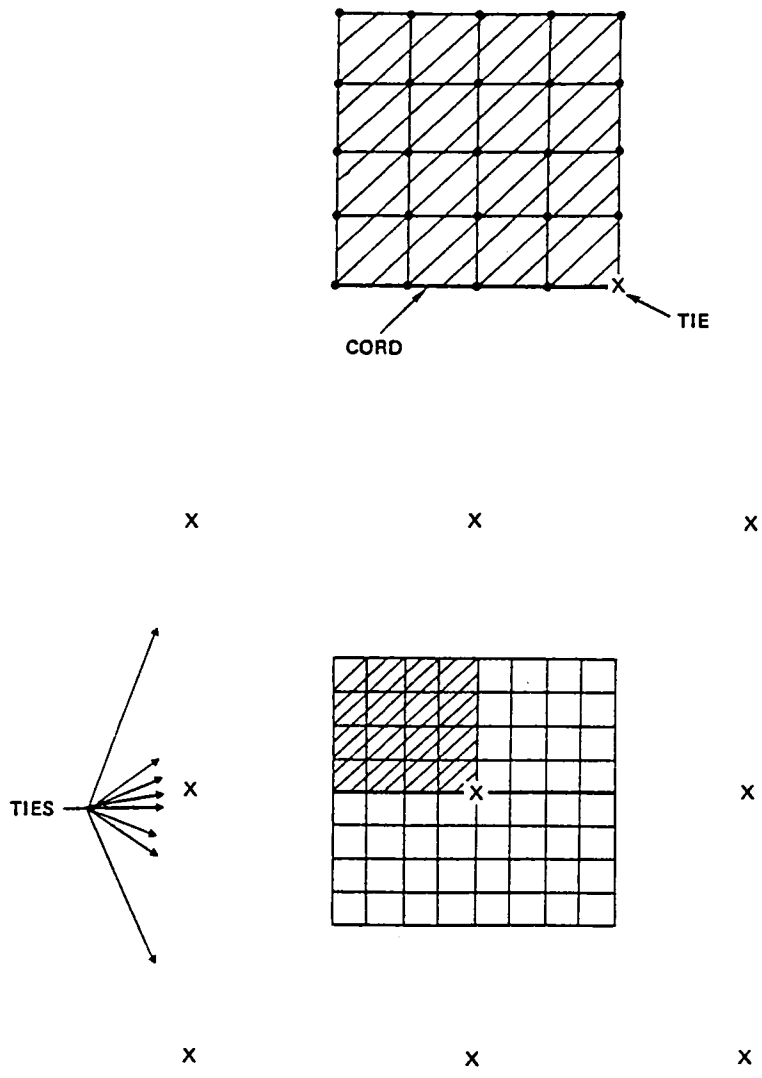

Figure 5.3.1.2-1. Pillow Model

5.3.2 Contour Analysis and Results

The operational performance of the LSST 100-meter point design is affected by many contributors. By predicting the effects of the contributors, the system can be adjusted to maximize its performance. The philosophy of accounting for the surface distortions and preadjusting the system is called biasing. This section will present the predicted changes to the surface characteristics and a subsequent section will present the biasing philosophy.

The antenna system characteristics are depicted in Figure 5.3.2-1. The results of the analysis will be presented in terms of the change in the focal length of the antenna parabola (Δ F), the change in the origin of the parabola (Δ Z) and the Root Mean Square (RMS) of the distortions of the surface, when compared to a best-fit parabola through the distorted surface.

Changes to the surface which affect operational performance can be grouped under the following subheadings:

- MANUFACTURING
- MESH PILLOWING
- THERMAL ELASTIC DISTORTIONS
- MATERIAL PROPERTY DEGRADATION
- UNCERTAINTIES

5.3.2.1 Manufacturing Effects

The manufacturing process requires that certain limits be imposed to ensure quality of the finished product and also to prevent excessive waste of time and resource due to unnecessary restrictions. Therefore, tolerances are established and expected raw material property deviations (such as cord stiffness) are incorporated into the analysis. Fortunately, past product experience has established good criteria as a basis for this subject and the affects of the manufacturing process can be controlled, as well as analyzed. The contributors are grouped under three headings and the analaysis results are listed in Figure 5.3.2.1-1.

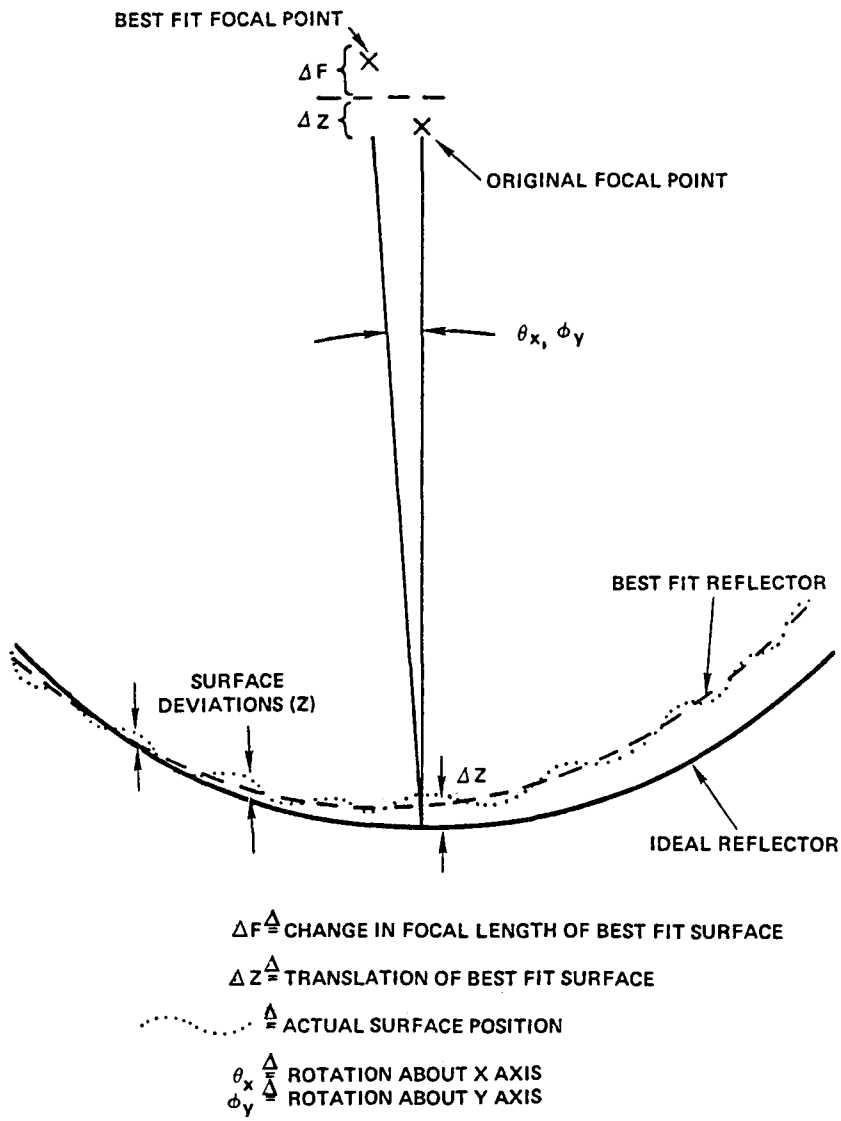

Figure 5.3.2-1. Antenna Surface System Characteristics

MANUFACTURING BUDGET PREDICTIONS
SUBTOTAL

BUDGET ARTICLE	CONTRIBUTION F (CM)	RMS(CM)
FLAT PANEL MAPPING	0.030	0.000
TOLERANCE EFFECTS 80 PPM	5.458	0.302
ASSEMBLING EFFECTS (DUE TO Δ CORD LOADS)	5.436	0.340
SUBTOTAL (RSS)	7.703 CM (3.033 IN.)	0.455 CM (0.179 IN.)

Figure 5.3.2.1-1. Manufacturing Budget Predictions Subtotal

5.3.2.2 Mesh Pillowing

Figure 5.3.2.2-1 shows the one gore represented in part by the pillow model. The pillow model was incorporated in the analysis of four different locations of the gore and these locations are indicated in Figure 5.3.2.2-1 as areas A, B, C, and D. As indicated by the results, area "A" has the largest cord spacing. This relationship is graphically illustrated in Figure 5.3.2.2-2, and was derived from the pillow finite element model for mesh tension and tie spacing as indicated.

The four areas analyzed have different amounts of roughness, however the largest value of roughness will be carried in the contour budget for surface pillowing.

BUDGET ARTICLE	CONTRIBUTION F (CM)	RMS (CM)
MESH PILLOW	0.000*	0.249 (0.098 IN.)

*BIAS ACCOUNTS FOR F

The numerical results of the worst-case pillow (area "A") are shown in Figure 5.3.2.2-3.

5.3.2.3 Thermoelastic Distortions

The distortion of the surface due to the operational environment is caused by changes from the ambient environment conditions in which the reflector was manufactured. In effect, a controlled environment of 70° F and 50% relative humidity is changed to a passively controlled moisture free environment.

The effect of the change in temperature on the surface elements is to impose a strain rate directly portional to its coefficient of thermal expansion and dependent upon the length of the element.

For the LSST Mission the two temperature extreme cases are:

1. 1.5 hour eclipse
2. Head-on Sun

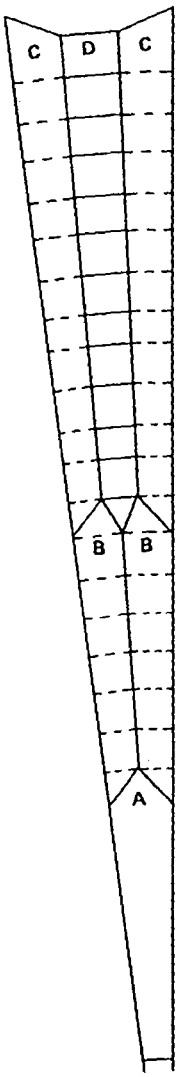

MESH PILLOW BUDGET PREDICTION

- AREA OF CONCERN

MESH PILLOWING DUE TO MESH PRE-TENSION AND DOUBLY CURVED SURFACE

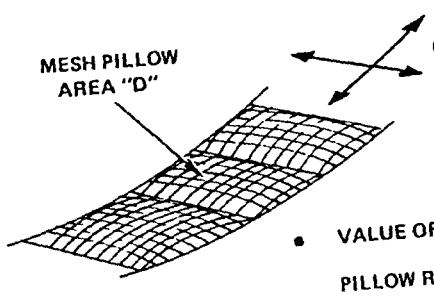

- VALUE OF 0.249 CM. REPRESENTS WORST CASE

PILLOW RMS (CM)	LOCATION
0.249	A
0.127	B
0.157	C
0.122	D

BUDGET ARTICLE	CONTRIBUTION F (CM)	RMS (CM)
MESH PILLOW	0.000*	0.249 (0.098 IN.)

*BIAS ACCOUNTS FOR F

Figure 5.3.2.2-1. Mesh Pillow Budget Prediction

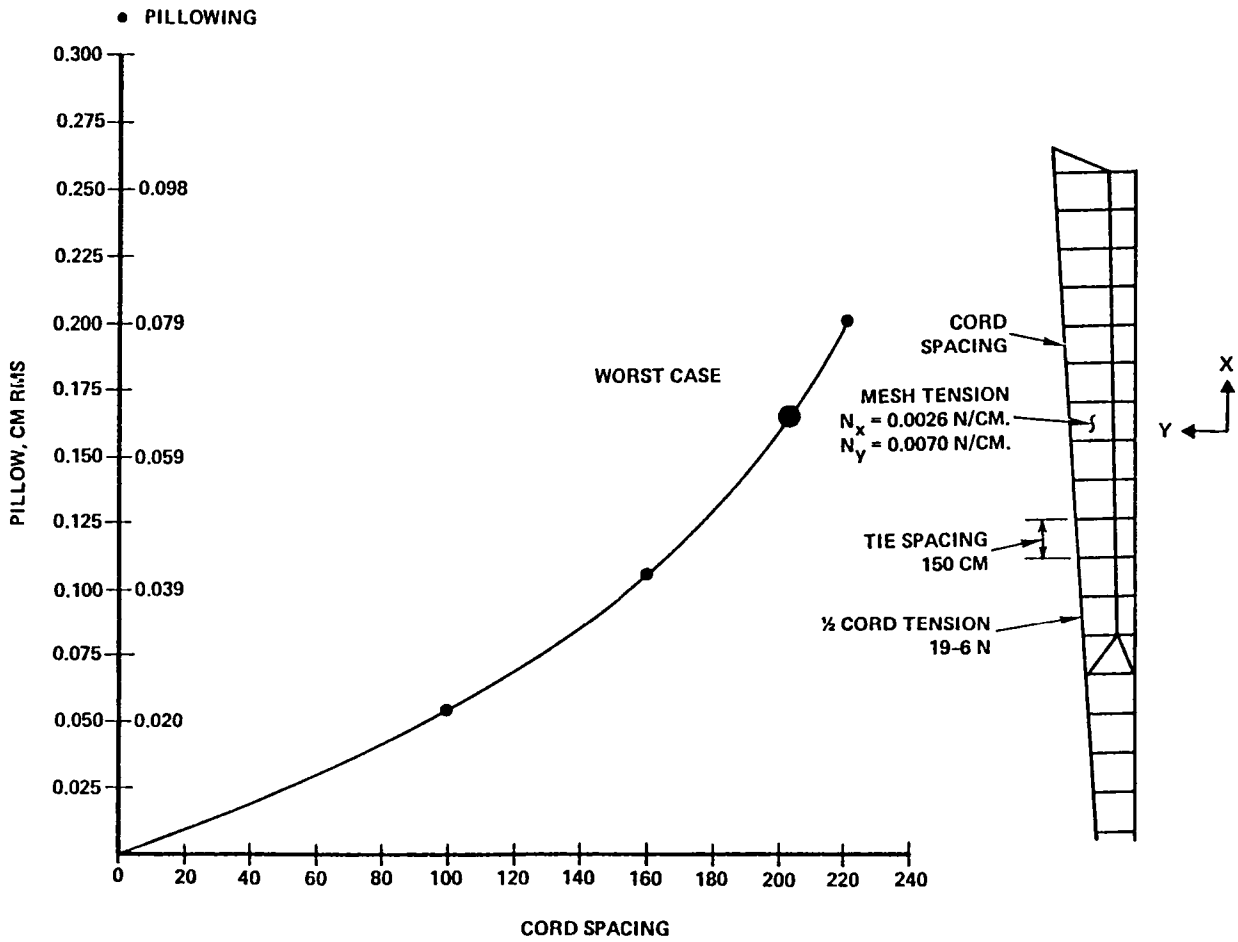

Figure 5.3.2.2-2. Relationship of Pillowing Versus Circumferential Cord Spacing

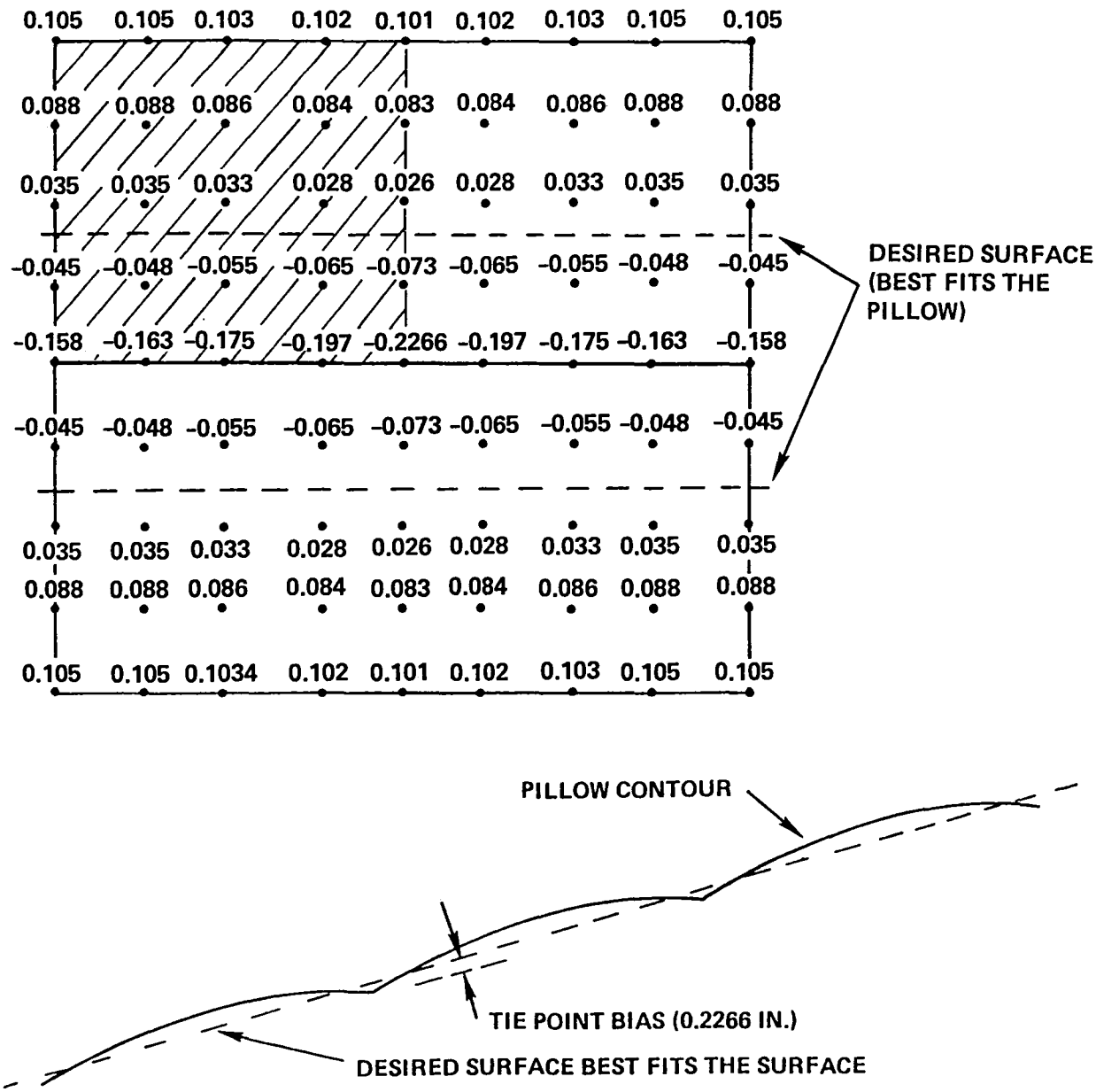

Figure 5.3.2.2-3. Contour Plot of Worst-Case Pillow

The temperatures and the coefficient of thermal expansion used are listed in Figure 5.3.2.3-1. Dielectric quartz cords were used as the upper control cords to avoid RF interference. The quartz cords show acceptable results even though their coefficient or thermal expansion is greater than graphite and is positive as opposed to the negative CTE of graphite cords.

The results of the thermoelastic distortion analysis for the two cases is presented in Figure 5.3.2.3-2. The worst-case will be carried in the contour budget.

5.3.2.4 Material Property Degradation

For the purposes of contour analysis the effect of material property degradation is changing of the element lengths. The length change is due to:

- **CORD CREEP**
- **GRAPHITE EPOXY DRYOUT**
- **GRAPHITE EPOXY MICROCRACKING**

Cord Creep

During manufacturing operations of the quartz and graphite cords, residual strain will be maintained in the cord fibers. During the operational life of the antenna, the cords are subjected to perturbations of load and temperature, and the residual strain will be relieved. The result of this phenomena is an elongation of the cords. The elongation will occur rapidly after mission start and will approach an asymptotic strain of 50.0×10^{-6} in/in. Imposing this strain on the cords gives the following contribution:

Cord Creep Contribution

	$\Delta F + \Delta Z$	RMS
50 $\mu \epsilon$	0.437 cm	0.003 cm

Figure 5.3.2.4-1 shows the cord creep effects values for different strains.

Graphite Epoxy Dryout and Microcracking

During the manufacture and assembly of the graphite-epoxy hoop segments, the epoxy resin will saturate with moisture. Based upon test data as shown in Figure 5.3.2.4-2 the graphite-epoxy hoop will absorb 0.7% of its weight in moisture, at a temperature of 75°F and relative humidity of 35%. The subsequent loss of moisture in space causes a shortening of the elements

- THERMAL PROPERTIES

COMPONENT	CTE $\left(\frac{IN}{IN\ ^oF}\right)$
MOLYBDENUM MESH	3.0×10^{-6}
GRAPHITE CORDS	-0.4×10^{-6}
HMS GRAPHITE HOOP	0.486×10^{-6}
GRAPHITE MAST	-0.385×10^{-6}
ASTRO MAST	0.0

- TEMPERATURES USED (RELATIVE TEMPERATURE USED IN ANALYSIS)

1.5 HR ECLIPSE

COMPONENT	TEMPERATURE ^oC	TEMPERATURE ^oF
MESH	-184	-300
HOOP	-43	-45
MAST	-73	-100
FRONT CORDS	-184	-300
BACK CORDS	-184	-300
INTERCOSTALS	-184	-300
TIES	-185	-300

HEAD-ON SUN

COMPONENT	TEMPERATURE ^oC	TEMPERATURE ^oF
MESH	221	430
HOOP	-29	-20
MAST	-51	-60
FRONT CORDS		
BACK CORDS		
INTERCOSTALS*		
TIES		

*TEMPERATURES VARY WITH SUN ANGLE, BUT AVERAGE AROUND 54^{o}C, (130^{o}F)

Figure 5.3.2.3-1. Thermoelastic Properties

- THERMAL ELASTIC BUDGET PREDICTIONS

BUDGET ARTICLE	CONTRIBUTION ΔF (CM)	ΔZ (CM)	RMS (CM)
HEAD ON SUN	-0.346	-0.101	0.037
ECLIPSE	-1.258	-0.054	0.077

- SUM OF ΔF + ΔZ

HEAD ON SUN	-0.447 CM
ECLIPSE	-1.312 CM

- BUDGET ARTICLE (WORST CASE)

ECLIPSE ΔF = -1.312 CM RMS = 0.077 CM

Figure 5.3.2.3-2. Thermoelastic Budget Predictions

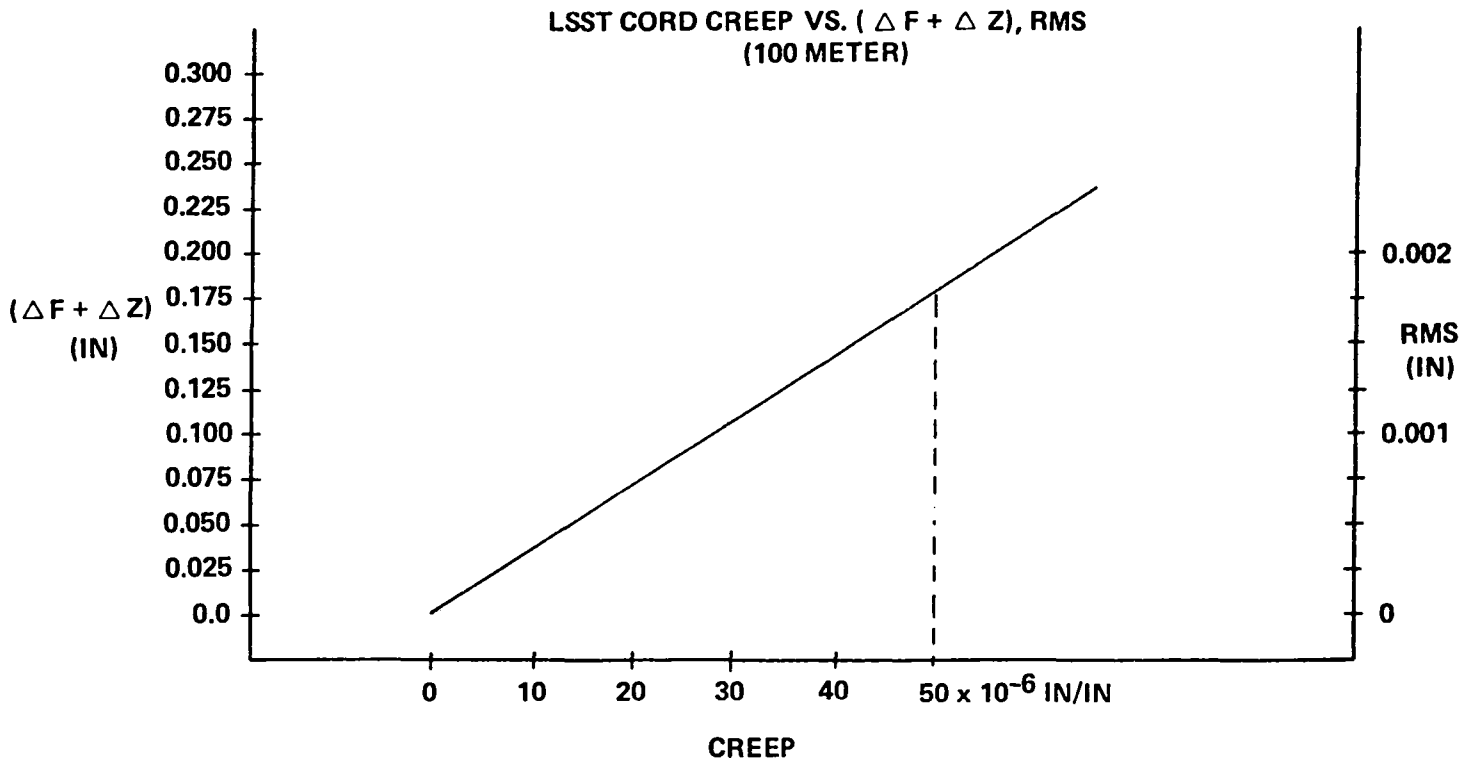

- LINEAR FUNCTION BASED UPON INTERPOLATED DATA POINTS
- MAXIMUM VALUE PREDICTED
  50×10^{-6} IN/IN (TEST RESULTS)
- PREDICTED CONTRIBUTION
  △ F + △ Z = 0.437 CM RMS = 0.003 CM

Figure 5.3.2.4-1. Cord Creep Projection

- REQUIREMENT ~ PROVIDE AVAILABLE DATA
- CAUSE ~ RESIN MATRIX ABSORBS MOISTURE AND EXPANDS
- MOISTURE CONTENT ~ FUNCTION OF HUMIDITY LEVEL

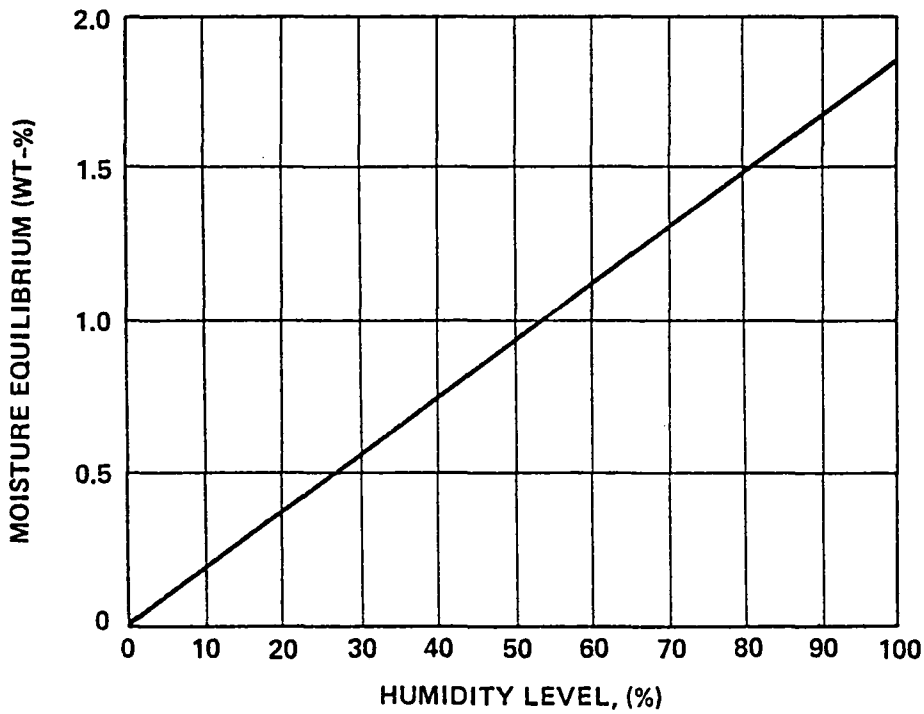

- AVAILABLE DATA
  - 3501-6/HMS (90, 0, $\pm$45) TUBE
  - 3501-5/AS (0_2, 90, 0_2) FLAT STRIP

Figure 5.3.2.4-2. Dimensional Change Due to Moisture

by a strain of -125 μ ε. However this strain is imposed at a slow rate and can be characterized by:

– **TUBE DRYOUT STRAIN RATE IN VACUUM (10^{-5} ATM) IS CHARACTERIZED BY:**

$$\epsilon = -\epsilon_F [1 - EXP (-\sqrt{t/s})]$$

IN WHICH

$$S = EXP (5893.6/T - 14.1503)$$

WHERE:

t = **TIME, HOURS**

T = **TEMPERATURE, KELVIN**

ϵ_F = **TOTAL SHRINKAGE STRAIN**

This equation is shown graphically in Figure 5.3.2.4-3 for different values of temperature. For a typical geosynchronous orbit 80% of the dryout will occur within the first 9,000 hours. Imposing the 100% dryout strain on the hoop is equivalent to a radius change of -0.625 cm on the 100-meter point design.

Another distortion contributor is graphite microcracking. This is a phenomenon which is caused by the difference between the coefficient of thermal expansion of the graphite fibers and the bonding matrix. During the post cure cooling and exposure to low operational temperatures, small cracks are formed in the epoxy matrix and a residual strain results.

Figure 5.3.2.4-4 shows the results of tests performed on a 5-inch diameter tube with a 0.025-inch wall. The layup was HMS-3501-6 (90, 0, ±45).

For a predicted temperature of -65° F the microcracking strain is 8.2×10^{-6} in/in. This is equivalent to a +0.041 cm change in the radius of 100-meter point design. Therefore, the total radius change that will occur from microcracking and the graphite dryout is:

$$-0.625 + 0.041 = -0.584 \text{ cm}$$

This radius change is equivalent to the following:

Hoop Dryout, Microcracking Contribution

$\Delta F + \Delta Z = -0.004$ cm RMS -0.120 cm

The graphite dryout on the mast is governed by the same process as for the hoop and causes a strain of -96 μ ε or a change in length of -0.333 cm from the surface intersection to the cord intersection point on the mast. The change in length will tend to decrease tension in the upper control cord, however a mast preload section will maintain cord load as designed.

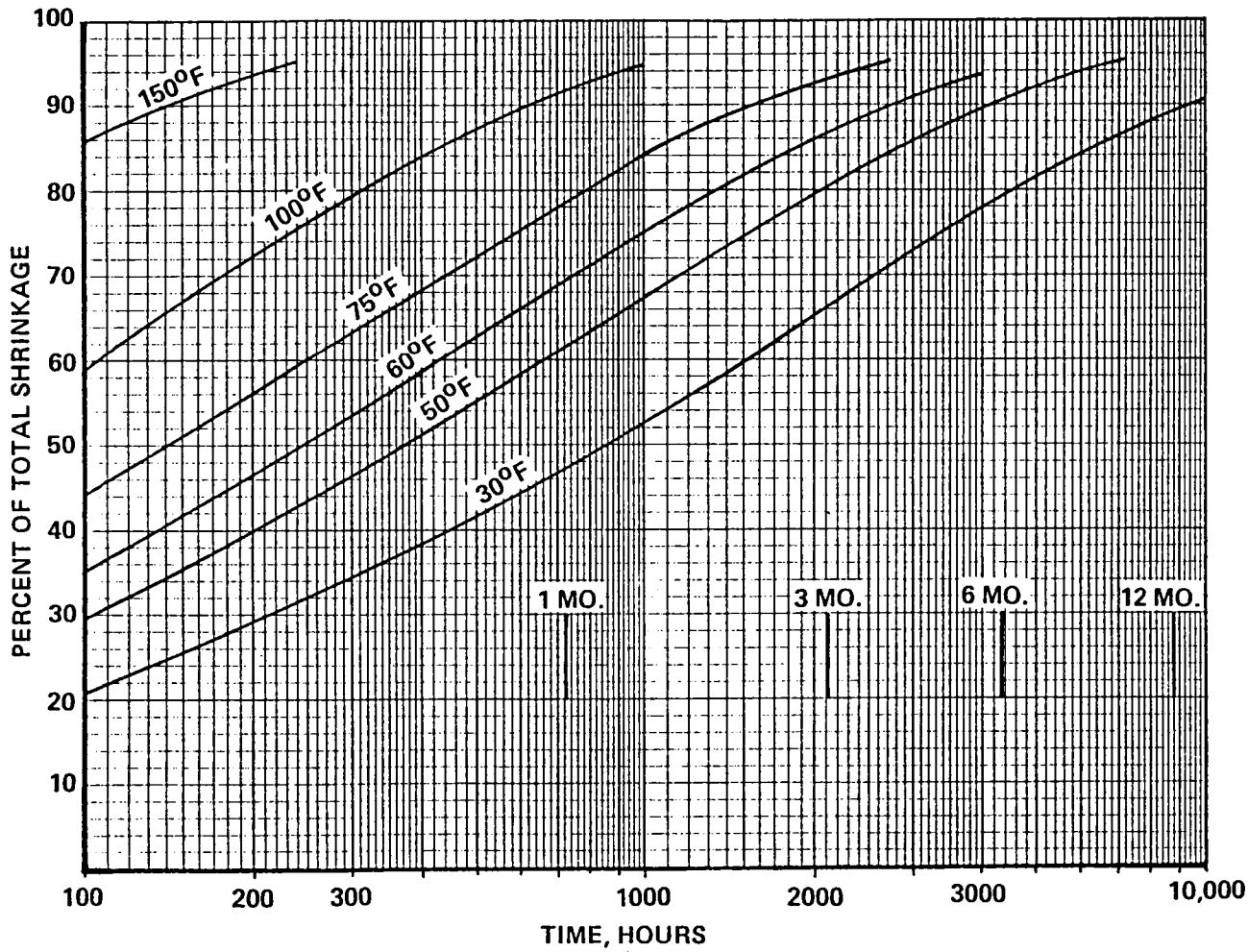

Figure 5.3.2.4-3. Dryout Versus Time

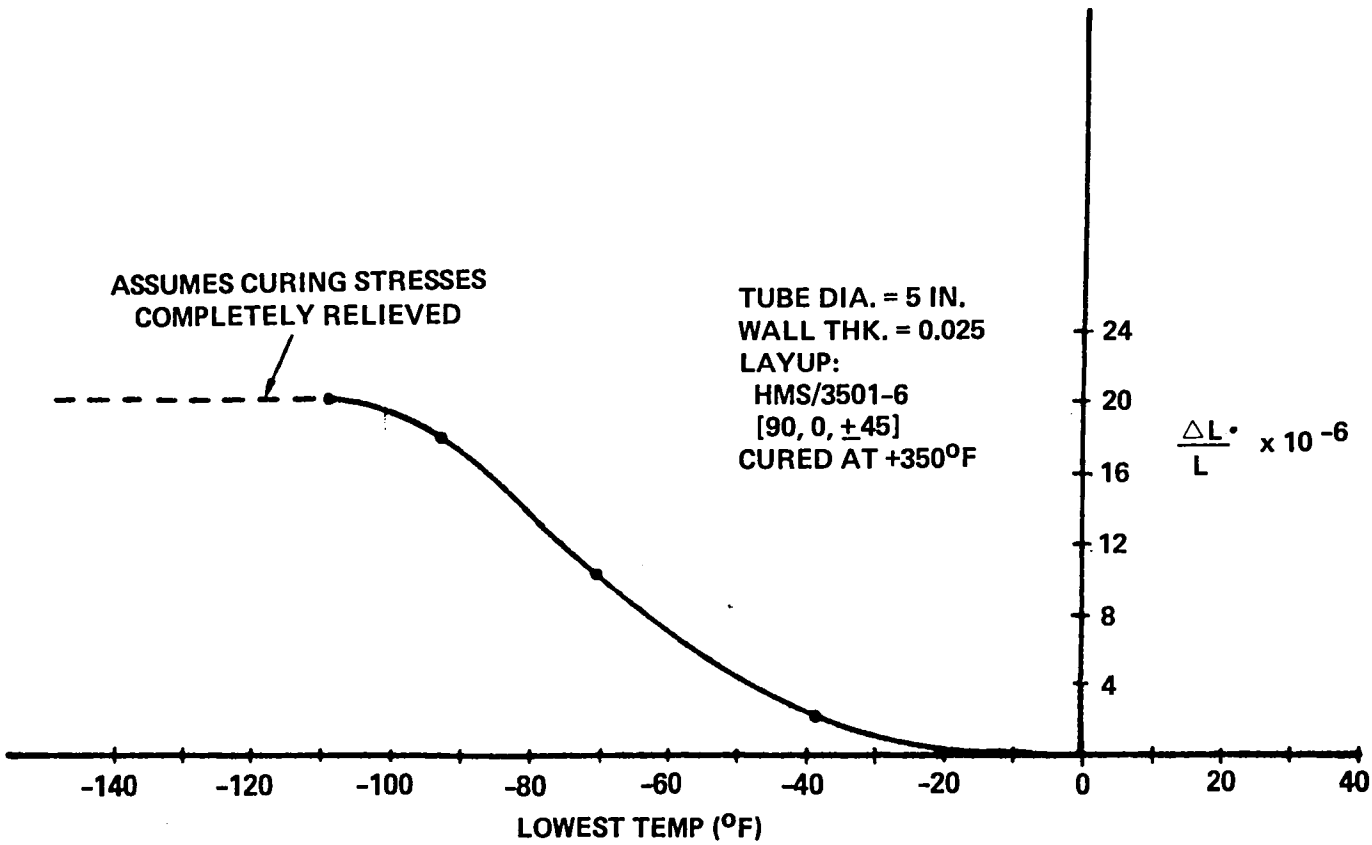

Figure 5.3.2.4-4. Supporting Test Data For Tube Microcracking Strain

The microcracking strain for a predicted temperature of -100°F is 20 $\mu\epsilon$. This is equivalent to +0.069 cm change in length of the mast. Therefore the total change in length of the mast (thus the feed position) is:

$$-0.333 + 0.069 = -0.264 \text{ cm}$$

The change in length is directly equal to a defocus of antenna/feed relationship, or

Mast dryout, microcracking contribution

$\Delta F + \Delta Z = -0.264$ cm RMS = 0.0 cm

The total contribution from material property degration is shown in Figure 5.3.2.4-5.

5.3.2.5 Uncertainties

Inherent in any analysis is the area of uncertainty. The uncertainty does not lie within the mathematical model but with the inputs to the mathematical model. Unexpected variations in the analysis parameters are accounted for to indicate sensitivities and to replace unavailable test data of actual hardware. The uncertainty values and analysis results are listed in Figure 5.3.2.5-1. The variations are based upon previous test data results from other programs.

Factors which influence the operational performance of the 100-meter point design are tabulated in Figure 5.3.2.5-2. This figure represents an initial value of degraded performance. Through the use of the anlaysis results, the feed position can be altered so that as the focal position of the reflector shifts it will temporarily coincide with the altered feed position. This is explained in the "bias" section that follows. Note that because of manufacturing and uncertainties, defocus can be either positive or negative values. The worst-case value is used in the contour budget.

5.3.3 100 Meter Point Design Budget Improved After Surface/Feed Position Biasing

The purpose of biasing the focal position is to achieve the maximum possible RF gain. By predicting the reflector focal position under certain known conditions, the position of the feed phase center can be matched to that

MATERIAL PROPERTY DEGRADATION
BUDGET CONTRIBUTION
(INITIAL)

BUDGET ARTICLE	ARTICLE CONTRIBUTION $\Delta F + \Delta Z$ (CM)	RMS (CM)
CORD CREEP	0.437	0.003
HOOP DRYOUT, MICRO	-0.004	0.120
MAST DRYOUT, MICRO	-0.264	0.000
TOTAL (SUM)	0.169 (CM) (RSS)	0.120 (CM)

Figure 5.3.2.4-5. Material Property Degradation
Budget Contribution
(Initial)

- UNCERTAINTIES CONTRIBUTION TO BUDGET PREDICTIONS (INITIAL)
- AREA OF CONCERN
  - UNEXPECTED VARIATIONS IN AS DESIGNED AND AS ANALYZED PARAMETERS, PROPERTIES, TENSIONS, TEMPERATURES AND MECHANICAL ANOMALIES

BUDGET ARTICLE		BUDGET CONTRIBUTION $\Delta F + \Delta Z$ (CM)	RMS (CM)
• MESH SURFACE			
MESH STIFFNESS	($\pm 3\sigma$)	0.046	0.0025
MESH PRETENSION	($\pm$50%)	1.240	0.017
• GRAPHITE CORDS			
STIFFNESS	($\pm$5%)	0.776	0.034
CTE	($\pm$25%)	0.381	0.002
CORD CREEP	($\pm$50%)	0.437	0.003
• GFRP UNCERTAINTY			
STIFFNESS	($\pm$10%)	0.001	0.024
CTE	($\pm$25%)	0.575	0.015
DRYOUT	($\pm$5%)	0.000	0.012
• TEMPERATURE			
ALL TEMPERATURE	($\pm 50^{o}$F)	0.975	0.015
• OTHER UNCERTAINTIES			
DEPLOYMENT			
HOOP EGGING		4.058	0.054
MEASUREMENT SYSTEM			
ETC.			
UNCERTAINTIES TOTAL		$\Delta F + \Delta Z$ = 8.116 (SUM)	RMS = 0.076 (RSS)

Figure 5.3.2.5-1. Uncertainties Contribution To Budget Predictions (Initial)

INITIAL CONTOUR BUDGET PREDICTIONS

	△F + △Z (CM)	RMS (CM)
MANUFACTURING	-7.704 CM	0.455
MESH PILLOWING	0.000	0.294
THERMAL ELASTIC ECLIPSE	-1.312	0.077
MATERIAL PROP. DEGR.	0.169	0.120
UNCERTAINTIES	-8.116	0.076
TOTAL	-16.963 (CM) (SUM)	0.565 (CM) (RSS)

Figure 5.3.2.5-2. Initial Contour Budget Predictions

focal position prior to liftoff ensuring minimum losses due to defocus. Also, with the benefit of active surface control the effect of surface position deviations can be measured, controlled, and thus minimized. RF performance can be improved by biasing which is accomplished by the knowledge of direction and magnitude of the focal position shift of the following areas:

Bias Areas

- Mesh pillowing
- Thermoelastic Performance
- Material Property Degradation

5.3.3.1 Mesh Pillow Bias

Bulges of the mesh surface can be best fit by a smooth analytical surface. This is indicated by the dashed line in Figure 5.3.3.1-1. The tie points are purposely placed 0.227 inches below the analytical surface and the mesh pillows bulge through analytical surface. This is a bias to the surface and is accounted for in determining surface position during surface adjustment.

5.3.3.2 Thermoelastic Bias

As the thermal operational environment changes the response of the surface cycles between to extreme parabolic shapes and thus two extreme focal positions. An optimum placement of the feed would depend upon the rate of response (time constant) of the system and a better knowledge of the mission profile in terms of time-temperature relationships. However, based upon the two known extreme cases, the logical position for this analysis is the average focal position.

Therefore $(-0.447 - 1.312)/2 = -0.8795$ cm

Because both extremes are negative, the negative bias of -0.8795 cm will greatly improve the effect of thermoelastic degradation on performance. Thus, the improved thermoelastic focal position shift will be about the biased position $\pm$ 0.433 cm.

Summarizing:

Old Budget (eclispse) Δ F - 1.312 cm
New Budget $(-1.312 + 0.8795) = \pm 0.433$ cm

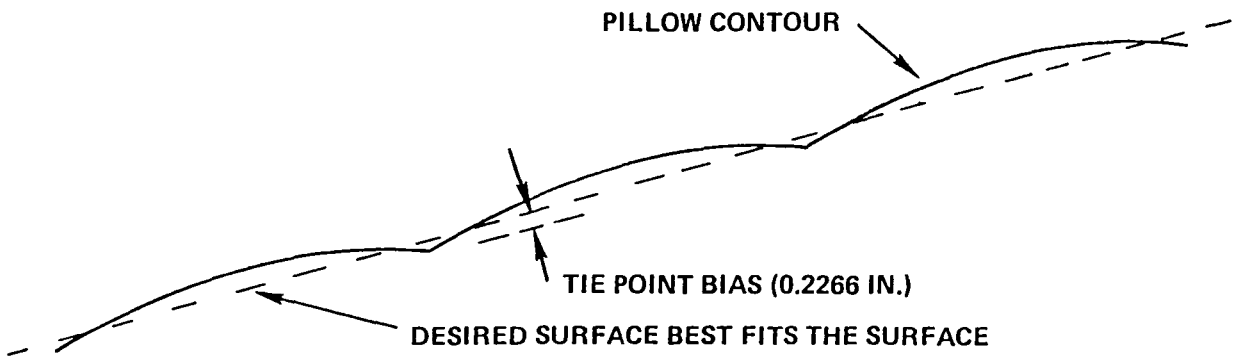

Figure 5.3.3.1-1. Mesh Pillow

5.3.3.3 Material Property Degradation

The degradation of the surface contour due to the changing material properties is a function of time and temperature. The cord creep occurs at a rapid rate and should reach an asymptotic limit within 6 months of operational life. The graphite microcracking occurs during the initial temperature cycle through eclipse temperatures. A typical geosynchronous orbit dryout rate is shown in Figure 5.3.2.4-3. The four lines each represent a different launch time. At the 12-month operational time point (9000 hours) approximately 80% of the dryout will have occurred. Based upon a surface adjustment after the first year, the bias need only be for a 1-year dryout or 80% of the mast dryout/microcracking contribution.

Thus: $\Delta F = (0.8 \times -0.264) = -0.211$ cm

Bias 50% of $-0.211 = -0.1055$ cm

The hoop dryout/microcracking contribution is small to begin with, but the same rate of dryout will occur. Thus, for the hoop dryout/microcracking:

$\Delta F = (0.8 \times -0.004) = -0.003$ cm

Bias 50% of $\Delta F = -0.0015$ cm

As stated, the cord creep occurs within the first 6 months as shown in Figure 5.3.3.3-1. A bias of 50% of the total $\Delta F = 0.437$ cm will improve on the first 11 months of performance. Thus the bias is:

Cord creep bias = 50% x 0.437 = 0.219 cm

By incorporating the above biases the material property degradation budget will be as shown in Figure 5.3.3.3-2.

5.3.3.4 Biasing Summary

Manufacturing contributions occur randomly and cannot be improved upon with a bias. Mesh pillowing is accounted for with a surface bias during surface adjustment and does not contribute to a system defocus, but does contribute a surface roughness. Thermoelastic distortion effects can be greatly improved with the bias technique and the defocus contribution changes from $\Delta F = 1.312$ cm to $\Delta F = \pm 0.433$ cm. The material property degradation is improved by changes from 0.169 cm to $\pm$ 0.112 cm. The worst-case

- CORD CREEP

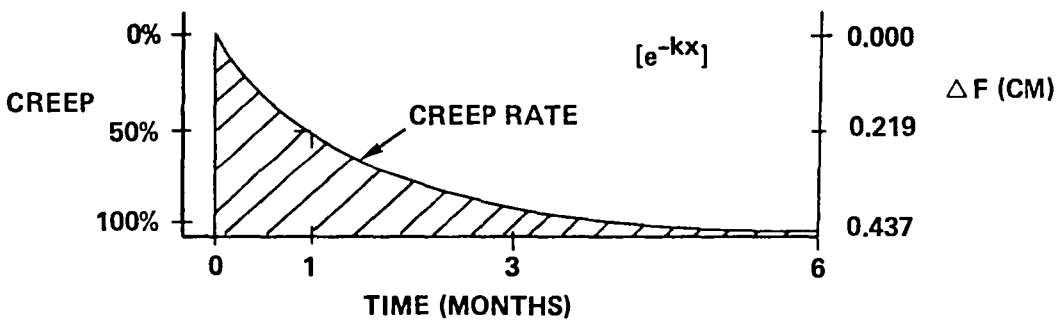

Figure 5.3.3.3-1. Cord Creep

MATERIAL PROPERTY DEGRADATION BUDGET
(AFTER BIASING)

BUDGET ARTICLE	CONTRIBUTION $\Delta F + \Delta Z$ (CM)	RMS CM
CORD CREEP	-0.219	0.003
HOOP DRYOUT, MICRO	+0.0015	0.120
MAST DRYOUT, MICRO	+0.1055	0.000
TOTAL	-0.112 CM (SUM)	0.120 CM (RSS)

Figure 5.3.3.3-2. Cord Creep Bias

contribution of +0.112 cm will be used in the budget. The uncertainties budget contribution (like the manufacturing contribution) occurs in a random process and cannot be improved upon by biasing.

As shown in Figure 5.3.3.4-1 the biasing technique will improve on the defocus contribution from $\Delta F + \Delta Z = -16.963$ cm to the improved defocus of $\Delta F + \Delta Z = 16.365$ cm.

5.3.4 Active Surface Control

Active surface control will improve upon the contour budget accuracy. Because it:

- REDUCES BUDGET CONSIDERATIONS FOR MANUFACTURING AND UNCERTAINTIES
- ALLOWS FOR MORE ACCURATE INITIAL POSITION OF FEED/ASTRO-MAST
- CORD ADJUSTMENT WILL INCREASE SIMILARITY TO ANALYTICAL MODEL, THUS INCREASE ACCURACY OF PREDICTIONS

Active surface control has the potential of eliminating all defocus contributions due to manufacturing and uncertainties. Also, the surface roughness is decreased. For the contour budget contributors of manufacturing and uncertainties, the defocus contribution is reduced by 50% because the total adjustment time required to eliminate all defocus is not cost-effective. A more thorough discussion of surface adjustment is presented in Section 9.0 (50-meter breadboard).

5.3.5 100-Meter Point Design Budget After Adjustment

Additional contour budget improvement can be accomplished by on orbit active surface additional contour budget improvement can be accomplished by on orbit active surface control/adjustment capability. The improved budget is presented in Figure 5.3.5-1.

IMPROVED BUDGET (FROM BIASING)

	△F + △Z (CM)	RMS (CM)
MANUFACTURING	-7.704 CM	0.455
PILLOWING	0 000	0.294
THERMAL ELASTIC ECLIPSE	-0.433	0.070
MATERIAL PROP. DEGR.	-0.112	0.120
UNCERTAINTIES	-8.116	0.076
TOTAL	-16.365 CM (SUM)	0.565 CM (RSS)

Figure 5.3.3.4-1. Improved Budget (From Biasing)

IMPROVED CONTOUR PERFORMANCE BUDGET
FROM BIASING AND ADJUSTMENT

BUDGET ARTICLE	CONTRIBUTION $\Delta F + \Delta Z$ (CM)	RMS (CM)
MANUFACTURING(1)	3.852	0.455
PILLOWING	0.000	0.294
THERMAL ELASTIC ECLIPSE(2)	0.433	0.077
MATERIAL PROP. DEGR.(3)	+0.112	0.120
UNCERTAINTIES(4)	4.058	0.076
TOTAL	8.445 (CM) (SUM) (3.329 IN.)	0.565 (CM) (RSS) (0.222 IN.)

(1) $\Delta F + \Delta Z = (7.704) - (3.852)$ ADJUSTMENT

(2) $\Delta F + \Delta Z = (-0.477) + (0.8795)$ BIAS

(3) $\Delta F + \Delta Z = (0.169) - (0.057)$ BIAS

(4) $\Delta F + \Delta Z = (8.116) - (4.058)$ ADJUSTMENT

Figure 5.3.5-1. Improved Contour Performance Budget from Biasing and Adjustment

5.4 RF Performance

The Quad Aperture antenna possesses broad performance applicability. The RF performance comprises of not only gain but all the requirements listed in Figure 3.0-1. Specific design parameters affecting the Quad Aperture performance must be addressed individually in the design process. These design parameters and their effects are delineated in Paragraph 5.4.1. The budgeted gain performance is presented in Paragraph 5.4.2. Lastly, areas of concern requiring further study are given in Paragraph 5.4.3.

5.4.1 Quad Aperture RF Design Parameters and Effects

The Quad Aperture antenna point design has been configured with a parent reflector of 100 meters in diameter and contains four offset reflector apertures with parallel boresight axes. Each offset aperture is 41 meters in diameter. Other design parameters of interest are given in Figure 5.4.1-1. These and other parameters result in a system performance of 219 Contiguous Spot Beams and HPBW = 0.26°. The projected aperture diameter for each of the four apertures has been nominally sized using the operating frequency, half-power beam width, -20 reflector illumination taper, and the following formula:

$$D = \frac{70}{HPBW} = 40.6 \text{ meters}$$

Parameter	Value
Number of Beams	219
Half Power Beam Width	0.26°
Beam Isolation	-30 dB
Number of Feed Arrays	4
Number of Feeds (subarrays)/Array	55
Feed Illumination Reflector Edge Taper Level	-20 dB
Number of Beams/Aperture	55
Beam Collimation for Interleveled F/D	1.53

Figure 5.4.1-1. Quad Aperture Antenna Design Parameters

This diameter provides the correct beam size in the far-field of the offset aperture. The 100-meter diameter for the point design allows for two offset apertures to be placed opposite each other (when looking along one plane of the parent reflector) with 18.8 meters open in the center. This open area allows the presence of the central support column and feed arrays without RF blockage.

The far-field beam coverage of the Continental United States (CONUS) is accomplished by interleaving the secondary beams from each aperture. The overlap of these beams is controlled by feed element placement and gimbaling to assure that the -3 dB crossover is achieved.

Several reflector and feed characteristics contribute to the beam-to-beam isolation requirement of -30 dB: side lobe levels, cross polarization levels, feed system mutual coupling, and choice of an optimum beam plan. Each of these characteristics are themselves affected by certain parameters of the design. The side lobe levels of the Quad Aperture must be below the -30 dB level to achieve the isolation requirement. The antenna aperture must possess very little blockage. The design which has been implemented on LSST by Harris contains no significant blockage. There are hoop control cables which do present some small level of primary and secondary blockage, however, even though these cables do not appear to offer a significant gain loss effect, their cross-polarization generation and defraction effects are not yet known. A small amount of analysis and measurements has revealed that the most desirable material for these cables is quartz. Further investigation during the next year will characterize the total effect. The reflector edge illumination, generated by the feed system, also determines (in a first order sense) the near-in side lobe levels. The optimum feed function has been chosen. The F/D chosen minimizes the coma lobe levels which affect beam isolation directly for the scanned beams.

Cross polarization can be minimized by reducing the surface distortions and reflector curvature. In a high F/D system the cross polarization generated is low and for the point design it is below the -30 dB level. The feed system must possess very little cross polarization.

The feed system must have low mutual coupling so that the individual feed patterns are essentially isolated. Since the feed system has not been designed, this effect has not been addressed in any detail. However,

techniques for providing low levels of feed mutual coupling have been developed. The beam plan for providing good beam isolation will utilize orthogonal polarization and multiple frequency subbands. As the design progresses, further definition of the beam plan will be developed.

The secondary beam crossover and relative alignment is crucial for maintenance of minimum gain variation due to diurnal and other effects. What is required is a stable multibeam antenna system which remains essentially unaffected by these external effects. The required 0.03° beam collimation and point specification arises from the need to maintain minimum power level variations and beam interference effects. This pointing level is one-tenth of a half-power beam width which reduces gain variations of the 0.30° beams to -0.03 dB.

5.4.2 Quad Aperture Gain and System Efficiency

The LSST Quad Aperture antenna gain is computed in Figure 5.4.2-1. The process used for computing gain is the budgeting process where individual gain detractors are identified. A broad class of gain loss mechanisms are included: feed illumination (spillover - taper efficiencies), thermal elastic structural effects, and the effects of the mesh reflector surface. The effects of each of these mechanisms, and components of each mechanism, are separable so that the individual contributions to gain loss can be analyzed independently. All mechanisms are tabulated and subtracted from the maximum area gain.

5.4.3 Quad Aperture Antenna Design Parameters Requiring Further RF Investigation

During Phase I of the LSST program, several areas of concern were identified which need further analysis efforts and RF verification. These included the effect of hoop control cables in front of the Quad Aperture, the effects of surface roughness and pillows, specific methods of implementing deployable feed arrays and corporate RF networks feeding the array elements, and the general area of control and payload integration involving the Quad Aperture design. These effects must be assessed and controlled in the following ways:

PROJECTED GAIN BUDGET

LOSS MECHANISM	LOSS (dB)
AMPLITUDE ILLUMINATION (20-dB TAPER)	1.27
PHASE EFFICIENCY	0.05
AMPLITUDE SPILLOVER	0.46
FEED BLOCKAGE	0.00
FEED OHMIC LOSS	0.15
FEED VSWR (1.2:1)	0.04
CABLE BLOCKAGE (CABLE DIA. = 0.22 IN.)	0.13
SURFACE REFLECTIVITY (MESH OPENING SIZE 0.25 IN.)	0.20
REFLECTOR ROUGHNESS (RMS ϵ = 0.22 IN.)	0.47
REFLECTOR CROSS POLARIZATION	0.01
DEFOCUS ($\triangle$ F = 6.82 IN.)	0.08
SCAN LOSS (13 BEAMWIDTHS SCAN)	0.25
TOTAL LOSSES (dB)	3.1
ANTENNA EFFICIENCY	49%
100% GAIN (dBi)	58.6
NET GAIN (dBi)	55.5

Figure 5.4.2-1. Projected Gain Budget

Hoop Control Cables

The hoop control cables obviously present a blockage effect since they are in front of the radiating aperture. They also intercept energy radiated by the feed system, hence, they produce both primary and secondary blockage. During Phase I, Harris measured the first order effect of metallic cables on gain loss. The results of this effort indicated that loss mechanism did not seem to warrant any significant concern. However, due to the extremely stringent multibeam performance requirement in the area of beam isolation, the defraction effects of these cables could be the most degrading phenomenon. Because of the unavailability of existing information in literature on this topic and since this effect defies closed form analytical evaluation, NASA and Harris have jointly decided to embark upon an "RF Verification Plan" which will quantify these effects.

Surface Roughness and Pillow

This effect also detracts from the multibeam performance. This surface roughness and pillow has been examined relative to gain loss, however, the effect on beam isolation will be examined in the "RF Verification Plan."

Deployable Feeds and Corporate Feed Networks

Specific designs and fabrication techniques in this area have not been examined. Future program planning presently does not include this study area. However, any real utilization of the Quad Aperture antenna will rely heavily on definition of deployable feed arrays and techniques for providing RF energy to these arrays.

5.5 Antenna Size Versus Stowed Envelope

Geometric constraints for several LSST Hoop/Column reflectors have been calculated and plotted. The following Figures 5.5-1 through 5.5-5 show the stowed reflector length, diameter and hoop segment diameter versus the deployed reflector diameter for 24, 36, 48, 60 hoop segments. The calculations were based on a hoop segment slenderness ratio (L/ρ) of 120. The maximum stowed length and diamter of 18.3-meter and 4.6-meter, respectively, were set by the available clearance envelope in the Shuttle's cargo bay.

The overall stowed length was taken as 1.34 times the length of a segment based on existing point design layouts.

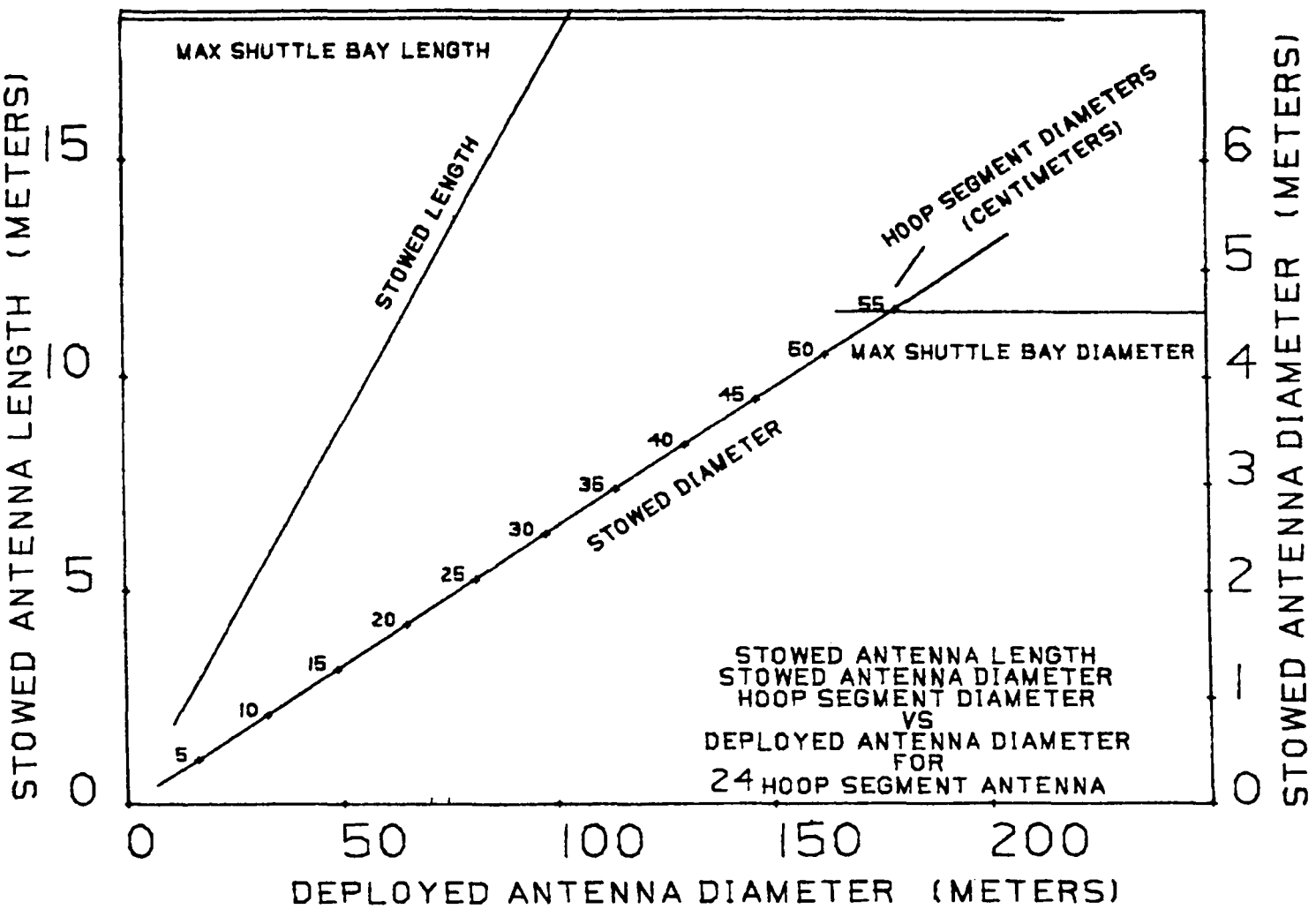

Figure 5.5-1. Deployed Antenna Diameter (Meters)

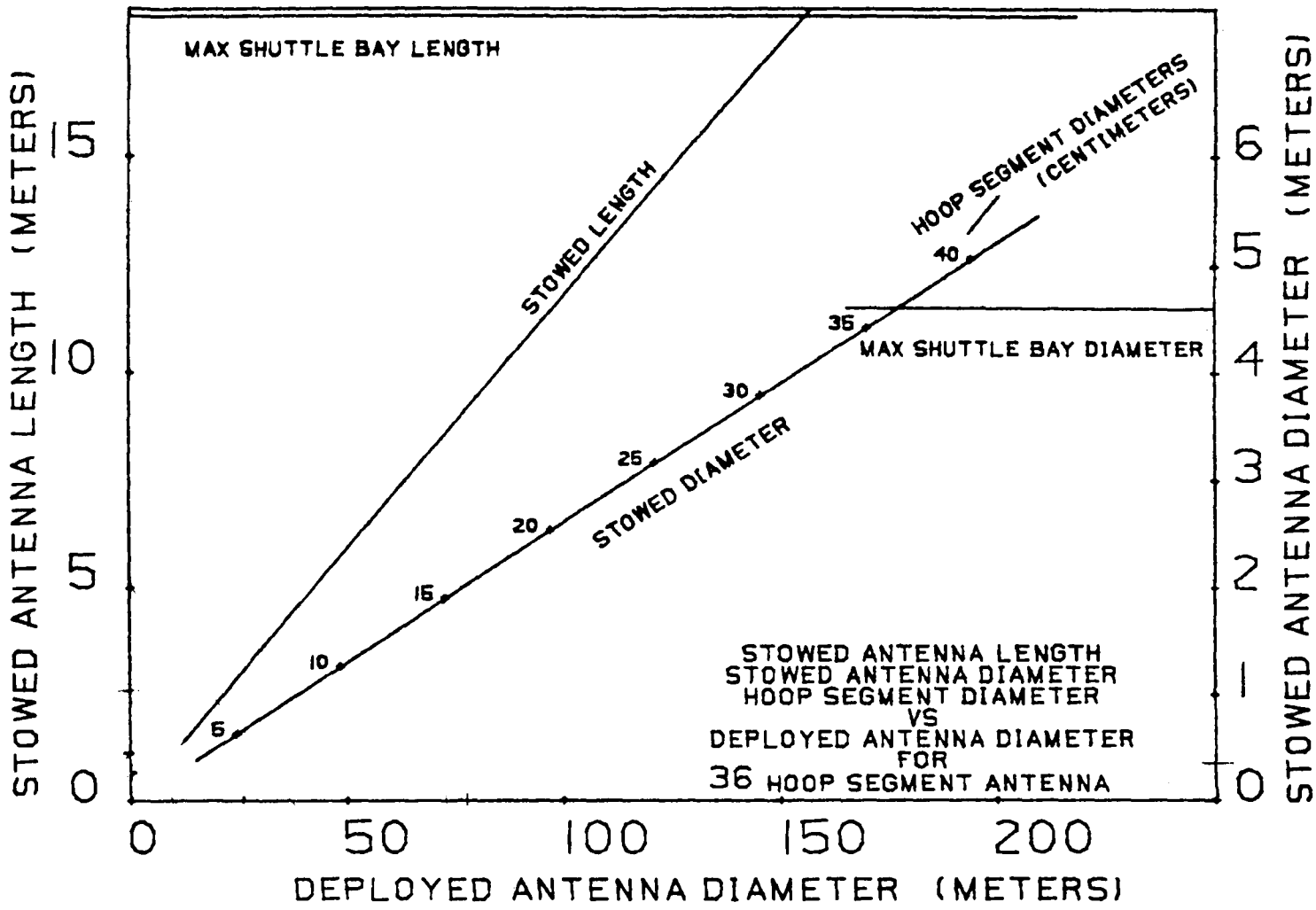

Figure 5.5-2. Deployed Antenna Diameter (Meters)

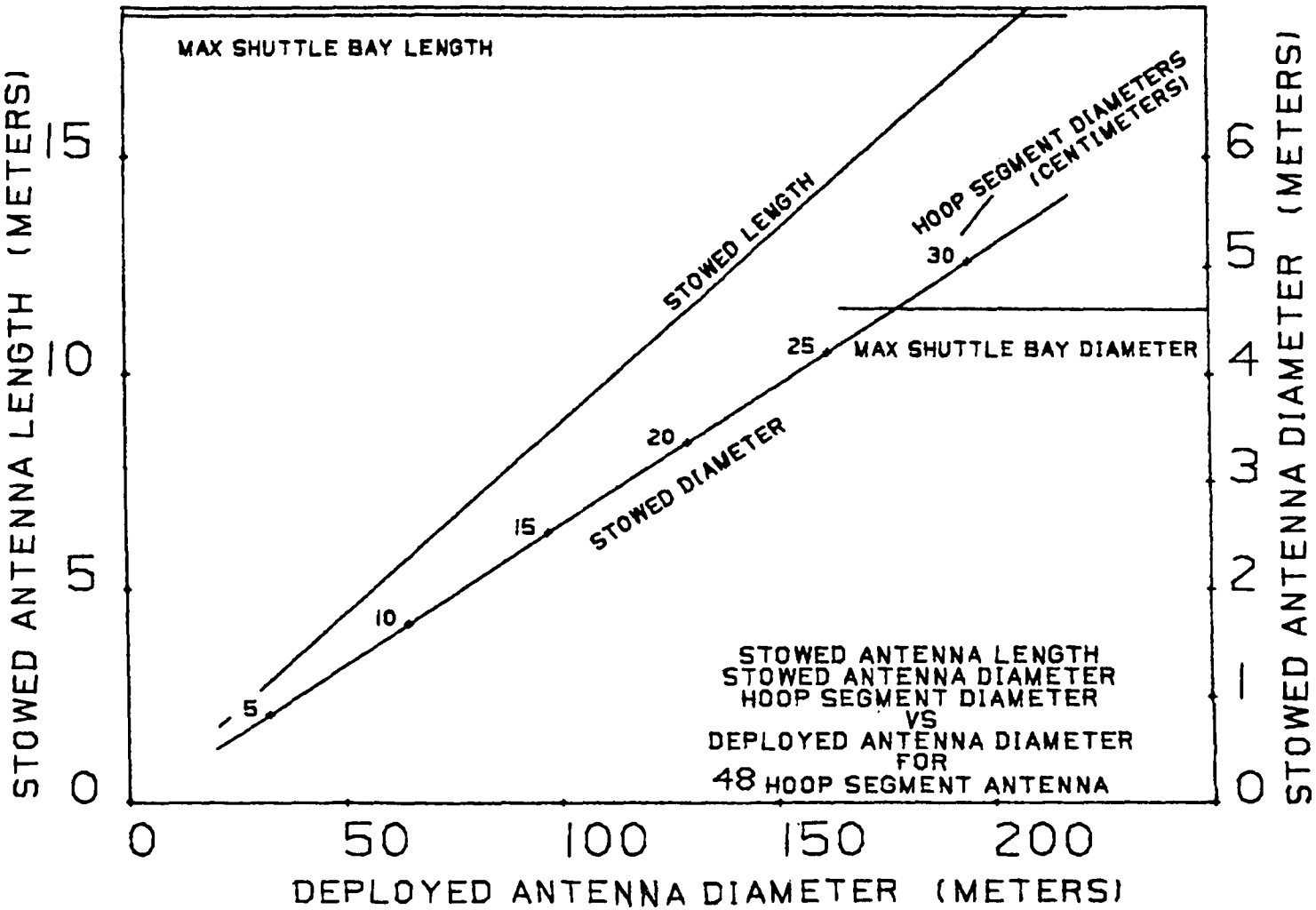

Figure 5.5-3. Deployed Antenna Diameter (Meters)

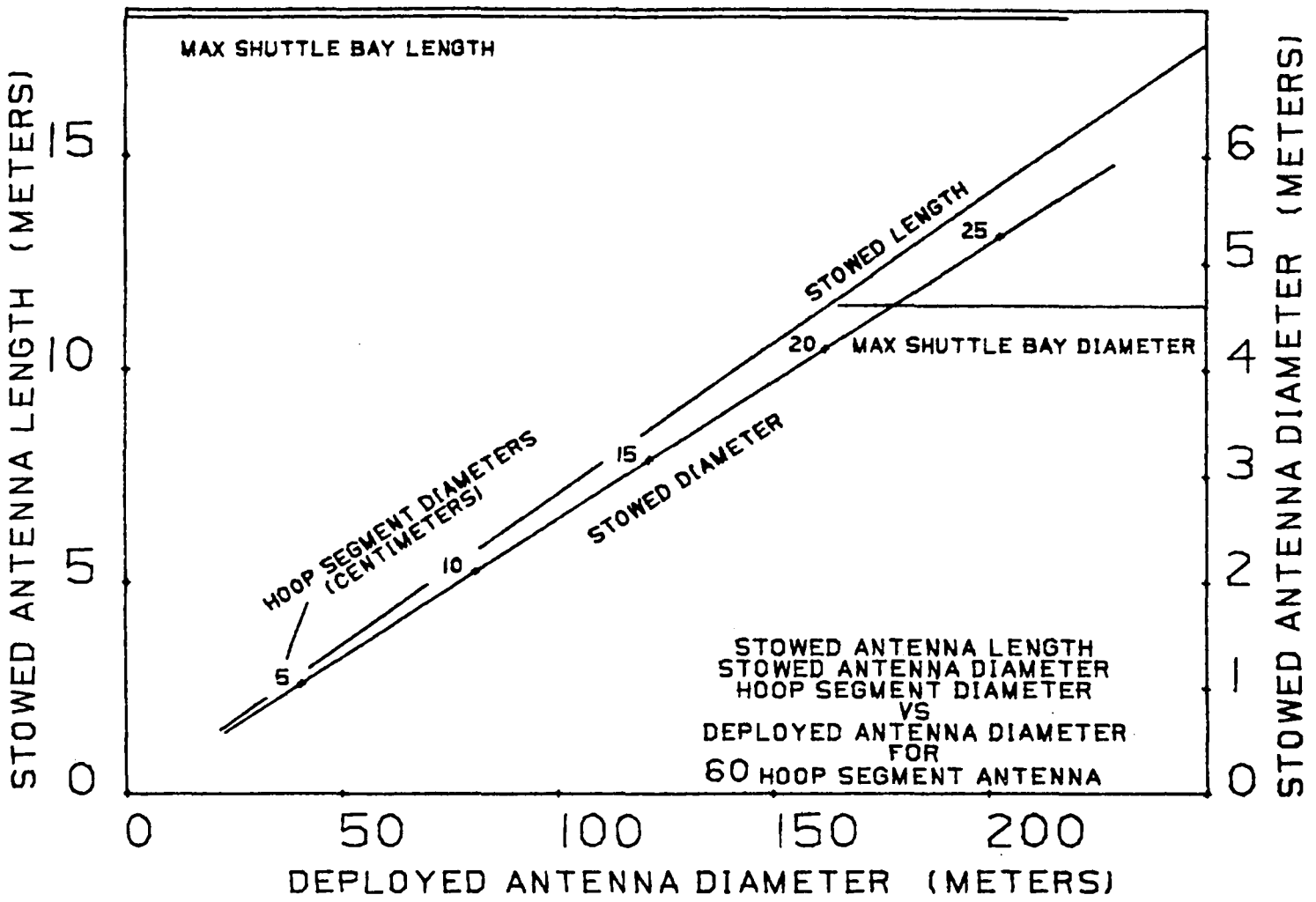

Figure 5.5-4. Deployed Antenna Diameter (Meters)

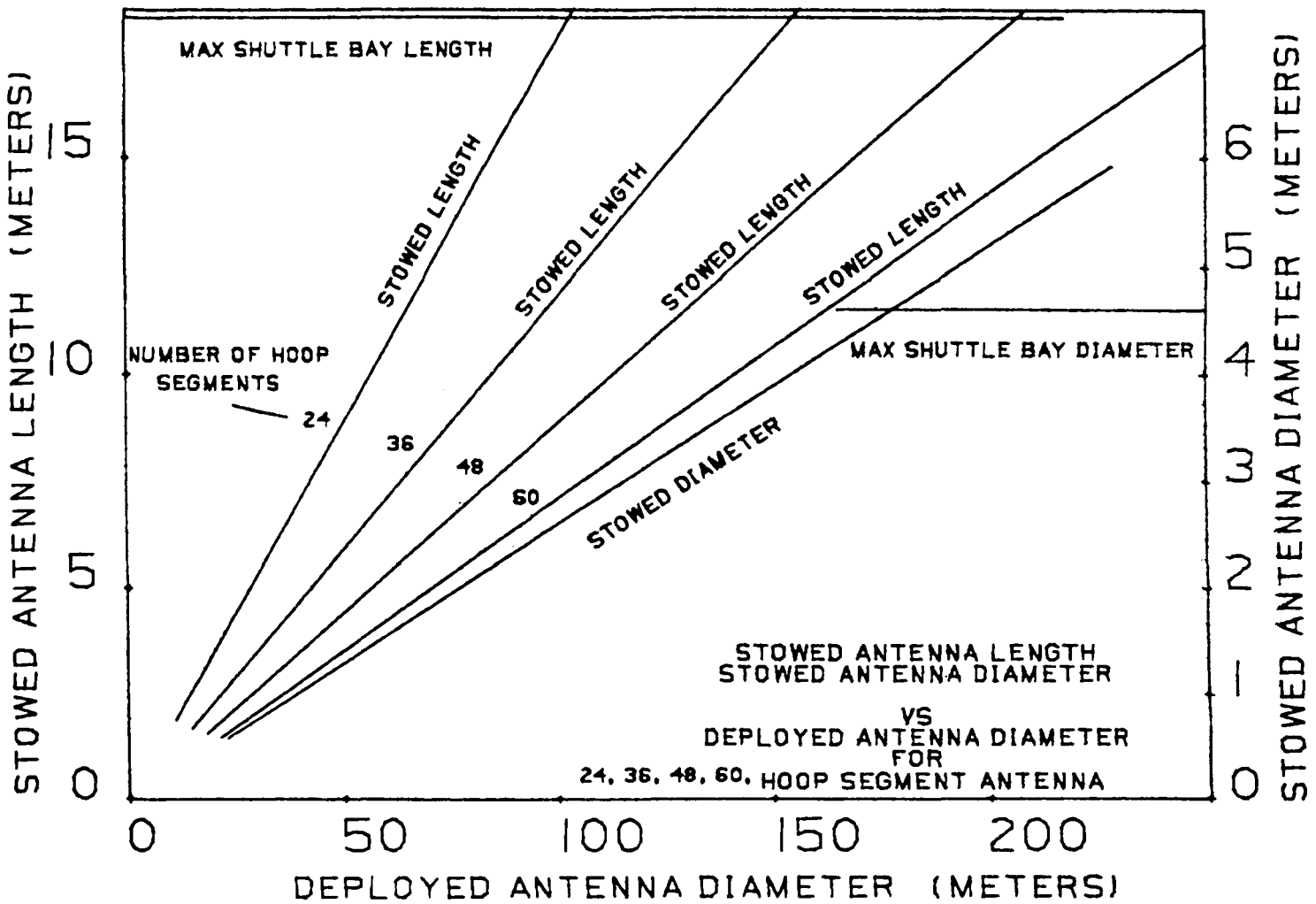

Figure 5.5-5. Deployed Antenna Diameter (Meters)

1. Report No.	2. Government Accession No.	3. Recipient's Catalog No.
NASA CR-3558, Part 1		

4. Title and Subtitle	5. Report Date
LSST (HOOP/COLUMN) MAYPOLE ANTENNA DEVELOPMENT PROGRAM	June 1982
	6. Performing Organization Code
7. Author(s)	8. Performing Organization Report No.
Marvin R. Sullivan	
	10. Work Unit No.
9. Performing Organization Name and Address	
Harris Corporation, Government Systems Group Electronic Systems P.O. Box 37 Melbourne, FL 32901	11. Contract or Grant No. NAS 1-15763
	13. Type of Report and Period Covered
12. Sponsoring Agency Name and Address	Contractor Report
National Aeronautics and Space Administration Washington, DC 20546	14. Sponsoring Agency Code

15. Supplementary Notes

Langley Technical monitor: Thomas G. Campbell
Phase I final report, Part 1

16. Abstract

The first of a two-phase program was performed to develop the technology necessary to evaluate, design, manufacture, package, transport and deploy the Hoop/Column deployable antenna reflector by means of a ground based program. The Hoop/Column concept was originated in a previous contract and consists of a cable stiffened large diameter hoop and central column structure that supports and contours a RF reflective mesh surface. NASA supplied mission scenarios for communications, radiometer and radio astronomy provided the data to establish technology drivers that resulted in a specification of a point design. The point design is a multiple beam quadaperture offset antenna system which provides four separate offset areas of illumination on a 100 meter diameter symmetrical parent reflector. The periphery of the reflector is a hoop having 48 segments that articulate into a small stowed volume around a center extendable column. The hoop and column are structurally connected by graphite and quartz cables. The prominence of cables in the design resulted in the development of advanced cable technology. Design verification models were built of the hoop, column, and surface stowage sub-assemblies. Model designs were generated for a half scale sector of the surface and a 1/6 scale of the complete deployable reflector. These models will be fabricated in Phase II of the program and will verify the 100 meter point design in terms of surface accuracy and adjustment, deployment kinematics, manufacturing techniques and analytical models correlation. An RF verification model and test was also planned for the Phase II effort.

17. Key Words (Suggested by Author(s))	18. Distribution Statement
LSST Technology Large space deployable antenna Quadaperture Cable stiffened hoop/column	Unclassified - Unlimited Subject Category 03

19. Security Classif. (of this report)	20. Security Classif. (of this page)	21. No. of Pages	22. Price
UNCLASSIFIED	UNCLASSIFIED	246	A11

For sale by the National Technical Information Service, Springfield, Virginia 22161

NASA-Langley, 1982

End of Document